

University of Nottingham
UK | CHINA | MALAYSIA

Simulation of the future home energy management system

Thesis submitted to the University of Nottingham for the degree of **Doctor of Philosophy, Oct 2023.**

Zhihao Hua, MSc., BSc.

20101269

Supervised by

Prof. Mark Sumner
Prof. David William Philip Thomas

Abstract

As global energy trends move toward electrification, managing home energy efficiently has become a key research area. This involves studying the behaviour of household devices and systems like electric heaters, ground source heat pumps (GSHPs), water heaters, and electric stoves. Reliable energy management is important to ensure consistent energy supply and reduce wastage. This research aims to create models for different household energy systems and validate their accuracy.

This research employed a range of techniques to ensure the accuracy and reliability of data and models. Firstly, the reliability of the load and PV datasets was significantly improved after applying the KNN (K-Nearest Neighbors) and SVM-GMM (Support Vector Machine and Gaussian Mixture Model) algorithms. Secondly, through the creation and validation of models for several heat energy systems like electric heaters, GSHPs, water heaters, and electric stoves, a comprehensive understanding of these energy subsystems was achieved. Thirdly, the study showcased the potential of Markov Chain simulations in accurately representing the inherent randomness of electric vehicle (EV) operations. Strategic integration of Home Energy Management Systems (HEMS) in hybrid houses with gas heating was identified to optimize energy consumption, promoting cost efficiency. The research further highlighted the implications of household appliance

electrification and EVs on domestic electricity consumption and its management. Importantly, an economic analysis underscored the feasibility of both traditional and "all-electric" residential schemes, while also bringing to light the significant environmental considerations, particularly regarding greenhouse gas emissions.

Advanced models for energy systems, including electric heaters and GSHPs, were developed and validated. Implementing Home Energy Management Systems (HEMS) in hybrid houses showed potential in optimizing energy use, reducing costs, and aiding in the electrification of household appliances. Furthermore, the study highlights the economic feasibility and environmental impact, especially concerning greenhouse gas emissions, of traditional and "all-electric" residential schemes. Lastly, the exploration of community-level energy strategies demonstrates the potential for enhanced energy utilization and economic efficiency.

This research provides a concrete foundation for future investigations in the field of household energy management. By integrating detailed energy sub-models, the study offers an conprehensive view of household energy dynamics, which can guide strategic energy management at both individual and community levels. Moreover, the insights into the economic and environmental impacts of different energy management approaches ensure a balance between economic feasibility and environmental responsibility. By addressing challenges and highlighting directions for future research, the findings contribute to global sustainability goals and evolving energy trends.

Acknowledgements

Big thanks to my supervisor, Prof Mark Sumner and Prof David Thomas. Your guidance and the way you inspired me to think differently have really opened my horizon. You are the high peak in research and I have learned so much from you.

My family has been there as basis for me in every way. Those late calls and messages really kept me going. And thanks to my girlfriend, who support me during the long journey, meant everything. They are the engine that kept me moving forward.

I cant forget my friends and colleagues. Their insights, ideas and support made my work better and the whole process more fun. Thanks to everyone for making this a real learning journey.

Contents

Abstract **i**

Acknowledgements **iii**

List of Tables **xiii**

List of Figures **xiv**

Chapter 1 Introduction **1**

1.1 Background 1

1.2 Structure of the Proposed Model 5

1.3 Aims and Objectives 6

1.4 Contributions 8

1.5 Structure of the Thesis 9

Chapter 2 Literature Review **11**

2.1 Introduction 11

2.2 Household Energy Demands and Challenges 13

2.3 Integration of Photovoltaic Systems with Home Energy Management 15

2.4 Battery Technology and Home Energy Storage 16

2.5 The Development of Electric Vehicles and the Impact on Home Energy system 18

2.6 Changes in Household Thermal Energy Demand 19

2.7 Models and Future Development of Home Energy Management 21

2.8 Conclusions 25

Chapter 3 Load Profiles and PV Generation Data for the Simulation Studies **28**

3.1 Collected Domestic Load Profiles and PV Datasets 28
3.1.1 Introduction 28
3.1.2 Datasets Description 31
3.1.3 Statistical Analysis of the Load and PV Profiles . . . 32
3.1.3.1 Seasonal Analysis 33
3.1.3.2 Weekday and Weekend Analysis 34
3.1.3.3 Load and PV Patterns by Month 35
3.2 Pre-processing of the Load Profiles 37
3.2.1 Introduction 37
3.2.2 Load Profile Imputation Algorithm 38
3.2.3 Results of Imputation 41
3.2.3.1 One Day Result 41
3.2.3.2 Analysis of the Parameters of the Algorithm 44
3.3 Feature Extraction and Generation on the PV Datasets . . . 47
3.3.1 Introduction 47
3.3.2 A Hybrid SVM-GMM Algorithm for Feature Generation of PV profiles 51
3.3.3 Results Based on the Hybrid Algorithm 53
3.3.3.1 SVM Results 53
3.3.3.2 GMM Results 53
3.3.3.3 Results of the PV Profile Generation 54
3.4 Conclusion 56

Chapter 4 Home Energy Management System and Battery Control 58

4.1 Home Energy Management System 58
4.1.1 Introduction 58
4.1.2 HEMS Infrastructure 60
4.1.3 Sub Systems in HEMS 62
4.1.4 Developments and Challenges for HEMS 64

4.2 Modelling of Batteries in Home Energy Systems 66
4.2.1 Introduction 66
4.2.2 Linear Battery Degradation Formulae 67
4.2.3 Rainflow Counting Algorithm 69
4.2.4 Non-linear Degradation of Battery Capacity 71
4.2.5 Results of Modelling of Battery Degradation 74
4.2.6 Summary of Battery Degradation Model 77
4.3 Control Algorithms and Home System Design 78
4.3.1 Introduction 78
4.3.2 System Model of the HEMS 81
4.3.3 Control Algorithms of the Home Energy Schedule . . 85
4.3.3.1 HEMS Control Using the Rule-based Algorithm 85
4.3.3.2 Genetic Algorithms 87
4.3.4 Case Study for the HEMS 90
4.3.5 Concepts for Economic Analysis 92
4.3.6 Results of the Simulation of HEMS 93
4.3.6.1 Energy Analysis 93
4.3.6.2 Algorithms Comparison 97
4.3.6.3 Economic Analysis 101
4.4 Conclusion 105
Chapter 5 Domestic Occupancy Model, EV Model and Combination 108
5.1 Introduction 108
5.2 An Occupancy Model Based on the Markov Chain Technique 110
5.2.1 Introduction 110
5.2.2 Method for Occupancy Modelling 114
5.2.3 Model Performance 118
5.2.4 Conclusion of the Occupany Model 121

5.3 EV Operation Modelling 122
5.3.1 Introduction 122
5.3.2 Methodology for the EV Operation Modelling 125
5.3.2.1 Markov Chain and EV Simulation 125
5.3.2.2 Trip Duration of EVs 130
5.3.2.3 V2G Algorithm 132
5.3.2.4 Incorporating EV and Home Battery Systems 134
5.3.2.5 Selection of Predictive EV State Curve for Simulation 135
5.3.3 Model Performance 136
5.3.4 Combination of Occupancy Model and EV Model . . 141
5.3.5 Conclusion of the EV Operation Modelling 142
5.4 Conclusion 143

Chapter 6 Modelling the Thermal Demand in Domestic Electricity Systems 145

6.1 Introduction 145
6.2 Thermal Room Heating Model 149
6.2.1 Introduction 149
6.2.2 Thermal Room Heating Model 152
6.2.3 Control Algorithm and Heating Period 155
6.2.4 Sub Model for Hysteresis Control 157
6.2.5 Parameter Estimation and Range 160
6.2.6 Optimization Techniques for Model Identification . . 162
6.2.7 Adjustment of the Thermal Parameters with Room Area 165
6.2.8 Performance of the Model 167
6.2.9 Conclusion of Room Heating Model 172
6.3 Ground Source Heat Pump 173
6.3.1 Introduction 173

6.3.2 Modelling the GSHP 175
6.3.3 Performance of the GSHP Model 179
6.4 Hot Water Usage Model 182
6.4.1 Introduction 182
6.4.2 Modelling Method of Hot Water Usage 183
6.4.2.1 Hot Water Demand Model 183
6.4.2.2 Water Tank Model 184
6.4.2.3 Combined Hot Water Usage Model 186
6.4.3 Model Performance 187
6.5 Electrical Cooking Model 189
6.5.1 Introduction 189
6.5.2 Model for Electric Cooking 190
6.5.2.1 Cooking Event Probability 190
6.5.2.2 Cooking Duration 191
6.5.2.3 Seasonality Effect on Cooking Consumption 193
6.5.2.4 The Effect of Number of Households 194
6.5.2.5 Integration of Cooking Model 195
6.5.3 Performance of Model 196
6.5.4 Conclusion of the Cooking Model 200
6.6 Combination of Occupancy and Heat Demand 201
6.7 Analysis and Comparison of Different Domestic Heating Systems 203
6.7.1 Introduction 203
6.7.2 Methodology 204
6.7.3 Results of Heating System Comparison 206
6.8 Conclusion 209

Chapter 7 Results and Discussion: Integrated Models, LCC and LCA of Electrification, and Community Level Application 211

7.1 Model Integration and Comparison 211
7.1.1 Introduction to Models, Integration, and Comparisons 211
7.1.2 Simulation Results and Comparison 215
7.1.3 Conclusion of the Proposed Integrated Home Model . 220
7.2 Models in the Traditional and the "all electric" Schemes . . 222
7.2.1 Power Profiles in Future Schemes 223
7.2.2 Battery Control Algorithms in Future Schemes 224
7.2.3 Heat Demand in Future Schemes 225
7.2.4 Vehicles in Future Schemes 226
7.2.5 Traditional Scheme and the "all electric" Scheme . . 227
7.3 Energy Analysis of the Traditional and the "all electric" Schemes 227
7.3.1 Performance of Battery Management Schemes 227
7.3.2 Energy Demand in Traditional and the "all electric" Schemes 230
7.3.3 Analysis of the Battery Charging and Discharging . . 235
7.3.4 Conclusion of the Energy Analysis 236
7.4 Comparative Economic Analysis of the Traditional and the "all electric" Schemes 238
7.4.1 Analysis of Economic Benefits 238
7.4.2 Sensitivity Analysis 243
7.4.2.1 Energy Storage 246
7.4.2.2 Investment Cost & Tariff 248
7.4.2.3 Energy Price 251
7.4.3 Conclusion of the Economic Analysis 255
7.5 Life Cycle Assessment of the Traditional and the "all electric" Schemes 256
7.5.1 Introduction of LCA Study 256
7.5.2 Goal and Scope 257

7.5.3 System Boundary 258
7.5.4 Data Acquisition 260
7.5.5 LCA Results and Economic Benefits 262
7.5.6 Conclusion of the LCA 265
7.6 Analysis and Comparison of Different Domestic Heating System 267
7.6.1 Introduction 267
7.6.2 Methodology 268
7.6.3 Comparative Results of Energy System with Different Heating Appliances 270
7.6.4 Conclusion 274
7.7 Applying Community Strategies Based on the Proposed Home Energy Management Models 276
7.7.1 Introduction 276
7.7.2 Method of Applying Community Management Strategies Based on Home Energy Models 278
7.7.2.1 Simulation Setup and System Model 278
7.7.2.2 Community Level Energy Pairing Strategies 282
7.7.2.3 Case Study of Households 289
7.7.2.4 Community & Households Sizing 292
7.7.3 Results of Community Simulation 295
7.7.3.1 Energy Analysis of the Separated Households and the Proposed Community Pairing Strategy 295
7.7.3.2 Internal Trade Tariff in Energy Community 297
7.7.3.3 Sizing Battery and PV Systems for Community Energy Management 299
7.7.4 Conclusion of Applying Model at Community Scale . 304
Chapter 8 Overall Conclusion 306

8.1 Summary 306
8.2 Main Achievements 308
8.3 Contributions 310
8.4 Proposals for Future Work 311
Bibliography **313**

List of Tables

4.2.1 The relationship between equivalent and DOD 68
4.3.1 Unit cost values for TOU purchasing tariff scheme at each time period 91
4.3.2 System parameters 92

5.2.1 Some statistical parameters of the proposed model and the original data 121
5.3.1 Annual results of the simulated data and the UK average data 140

6.2.1 Pre-estimation of parameters 161
6.2.2 List of order of magnitude matrix 162
6.3.1 List of modelling method of GSHP 173
6.3.2 Formulae for COP calculation 175
6.3.3 Manufacturer catalogue of GSHP 2500BX [259] 176
6.4.1 Flow rate summary for domestic hot water usage 184
6.7.1 Costs and GWP of different domestic heating methods . . . 206
6.7.2 Annual heat demand and energy consumption of different heating appliances (unit: kWh) 207

7.1.1 Annual simulation results in CREST model and proposed model 217
7.3.1 Calculated energy results of two schemes 235
7.4.1 Electricity tariff of Time-of-Use (TOU) 238
7.4.2 Global warming potential of different energy sources 242
7.5.1 LCA results of boilers of different phases (unit: kg CO_2e) . . 260

7.5.2 LCA results of hobs of different phases (unit: kg CO_2e) . . . 261
7.6.1 Supplement costs and GWP of different domestic heating methods . . . 269
7.7.1 Unit cost values for TOU purchasing tariff scheme at each time period. . . . 290
7.7.2 System parameters of case study . . . 290

List of Figures

1.2.1 The structure diagram of models and related chapters . . . 6

3.1.1 Minute by minute average domestic load in all, summer and winter seasons . . . 33

3.1.2 Minutely average household load for weekdays and weekends 34

3.1.3 Monthly average daily load and PV . . . 36

3.2.1 Flow chart of the proposed imputation algorithm . . . 39

3.2.2 Load power graphs of raw datasets, modified test sample, imputation result . . . 42

3.2.3 Normalized RMSE based on changing k and p . . . 45

3.3.1 Comparison of results from the SVM and GMM parts of the simulation . . . 54

4.1.1 A typical HEMS infrastructure [132] . . . 61

4.2.1 The trend curve of cycle number and capacity [166] . . . 72

4.2.2 The curve of remaining capacity ratio and operating cycles 73

4.2.3 The curve of simulation days and accumulative battery discharge cycles . . . 75

4.2.4 Comparison of proposed simulation results and test results from ITP report . . . 76

4.3.1 Flowchart of rule-based algorithms . . . 86

4.3.2 One day power graphs of load, PV, grid and battery in different seasons . . . 94

4.3.3 Average daily energy utilization in different tariff periods . 96

4.3.4 The fitness value with the iterative generation curve 97
4.3.5 Graph of power usage for the two HEMS algorithms for the same day 98
4.3.6 NPV cash flow of the HEMS system in 20 years 101
4.3.7 IRR graph with variable battery capacity and power limitation 103
4.3.8 IRR graph with different investment and tariff rates 103
4.3.9 Cash flow under different discount rate in 10 years 104

5.1.1 Structure diagram of occupancy, heat, EV model 109
5.2.1 Occupancy and activity state curve of CREST and proposed model 118
5.2.2 Occurrence of time duration for stochastic model based on TUS 120
5.3.1 Transfer process of EVs between three states 126
5.3.2 Variation of the EV state probability 128
5.3.3 Schematic diagram of probability selection 129
5.3.4 Examples of EV state simulation 130
5.3.5 Probability distribution graph of EV trip distance 131
5.3.6 Flow chart of EV battery simulation 133
5.3.7 Simulation results of EV battery 137
5.3.8 Battery and state graph for EV 141

6.2.1 Structure diagram of the “3R3C” model 153
6.2.2 Experimental measurement system for the room 155
6.2.3 Flowchart of the control algorithm 156
6.2.4 Single heating duration versus double heating duration . . 157
6.2.5 Temperature and power graph in the experiment 158
6.2.6 Room heating model with hysteresis control 159

6.2.7 Flow chart for model construction, estimation, optimization and simulation 164
6.2.8 One day simulation of optimization result of sub model . . 168
6.2.9 One day simulation of optimization result of whole model . 170
6.2.10 Simulation of one day in Dec with single duration 171
6.2.11 Simulation of one day in Dec with double duration 171
6.3.1 Structure diagram of GSHP system 174
6.3.2 Flow chart of GSHP simulation algorithm 178
6.3.3 Regression result with fixed parameters for GSHP modelling 179
6.3.4 One day simulation result of GSHP heating 180
6.4.1 Flow chart of hot water usage model 187
6.4.2 One day simulation result of hot water usage 188
6.5.1 Average time spend on cooking of UK citizen [275] 192
6.5.2 Cumulative distribution function curve for cooking duration 192
6.5.3 Seasonality effect on cooking energy consumption, by week 194
6.5.4 Annual consumption per person per family size 195
6.5.5 Probability of event trigger in workdays 197
6.5.6 Probability of event trigger in holidays 197
6.5.7 One day simulation result of cooking model 198
6.5.8 Annual average daily electricity consumption profile for electrical cooking 199
6.6.1 State graph for occupancy and room heating 202
6.7.1 Annual cost and GWP for different heating method 208

7.1.1 Structure diagram of modelling 214
7.2.1 Structure diagram of integration of the load, PV, battery, heat and EV models in both schemes 222
7.3.1 Bar graph of traditional scheme and original consumption profiles for different tariff periods 228

7.3.2 Energy bar of two schemes with different periods and usage 232
7.3.3 Detailed energy diagram of the composition of system energy 234
7.4.1 NPV graph with only electricity tariff (unit: £) 241
7.4.2 NPV graph with carbon savings benefit 243
7.4.3 IRR results based on battery capacity and power rating limitation 247
7.4.4 IRR results based on a ratio of annual cost and investment 249
7.4.5 IRR results based on ratio of electricity tariff price and investment 250
7.4.6 IRR results based on the ratio of the price of electricity and fossil fuel 254
7.5.1 Phase graph of life cycle assessment of integrated energy system 259
7.5.2 GHG emissions savings in 20 years by using the "all electric" scheme instead of the traditional scheme 263
7.5.3 NPV in 20 years by using the "all electric" scheme instead of the traditional scheme considering LCA study 264
7.6.1 Annual Energy Consumption (kWh) 271
7.6.2 The NPV value of using GSHP in "all electric" scheme in twenty years (unit:£) 272
7.6.3 20-year Net Present Value (NPV) of the GWP for the GSHP in "all electric" scheme 273
7.6.4 The NPV value of using GSHP in "all electric" scheme in twenty years with LCA study (unit: £) 274
7.7.1 Flow chart of algorithms for pairing energy supply in community scale 283
7.7.2 Energy bar of two schemes for different tariff periods . . . 296
7.7.3 Initial annual cost of households versus the savings ratio . 297

7.7.4 Energy utilization across different tariff periods for scenarios with and without a battery/PV system 300
7.7.5 NPV graph for the optimal sizing of community 301
7.7.6 Tariff savings comparison of community sizing and pairing strategy 302

Chapter 1

Introduction

1.1 Background

In the contemporary global scenario, energy plays an important role in daily activities and industrial operations. With the rise in the global population and the expansion of urban regions, there has been a significant increase in energy consumption. This growing demand for energy presents challenges, especially when considering environmental implications. Conventional energy sources, primarily derived from fossil fuels, have been identified as major contributors to environmental issues such as global warming and air pollution [1]. In response to these challenges, there is a pronounced shift towards renewable energy sources, including solar and wind power. Utilizing these sustainable energy sources not only mitigates environmental impacts but also addresses the concerns of a potential global energy crisis. Within this framework, the importance of energy management at the household level has gained prominence. The emergence of systems such as Home Energy Management Systems (HEMS) offers households the capability to transition from being solely energy consumers to also functioning

as energy producers, moving towards a sustainable energy future [2].

In recent years, the concept of managing energy within households has transformed significantly. In the previous years, households were simply consumers of energy, relying on national grids and conventional energy sources. With advancements in technology and increased awareness of environmental sustainability, however, the paradigm has shifted. HEMS have been introduced as innovative solutions to address the complexities of modern energy needs. These systems enable households to monitor, control, and optimize their energy consumption [3]. Furthermore, with the integration of renewable energy sources, such as solar panels, households have the potential to produce their own electricity, reducing reliance on external energy supplies [4]. This not only leads to cost savings for the consumers but also aids in decreasing the carbon footprint, promoting a greener and more sustainable environment. The incorporation of HEMS in modern homes symbolizes a step forward in the realm of energy management, responding aptly to the challenges of the current era [2, 5, 6].

As the global focus shifts towards sustainable energy solutions, significant technological advancements have been made in the field of home energy management. The introduction of smart meters, advanced sensors, and Internet of Things (IoT) devices have enabled real-time monitoring and efficient energy consumption within households [7, 8, 5]. These technologies provide detailed insights into energy usage patterns, allowing for the optimization of consumption based on daily routines and external factors such as weather conditions.

Moreover, the integration of renewable energy sources like solar panels and wind turbines with home systems has seen considerable innovation. More efficient photovoltaic cells and advanced energy storage solutions ensure

that households can store more energy than before [4, 9]. However, with these advancements come challenges, the intermittent nature of renewable energy sources requires sophisticated algorithms and systems to ensure a consistent energy supply. The integration of multiple energy sources and the management of bidirectional energy flow, especially in homes that produce surplus energy, necessitates advanced Home Energy Management Systems.

Additionally, there are concerns about the initial costs of setting up these advanced systems, cybersecurity threats related to connected devices, and the need for regular maintenance and updates [10, 11, 12]. Addressing these challenges is essential to ensure that the technological advancements in home energy management are not only efficient but also sustainable and secure in the long run.

Battery technologies have seen a significant evolution, especially with the rise of penetration of electric vehicles (EVs) and the need for sustainable energy storage solutions in households. Electric vehicles, equipped with high-capacity batteries, have introduced new dimensions to home energy systems. These vehicles can serve as mobile energy storage units, allowing for the energy to be stored during off-peak hours and used during peak demand [13]. This bidirectional flow of energy, often referred to as Vehicle-to-Grid (V2G) and Vehicle-to-Home (V2H) interactions, provides households with flexibility in managing their energy consumption and costs. The integration of EV batteries with household energy systems also offers potential benefits in grid stabilization, especially in regions with high renewable energy penetration. However, this integration presents challenges, such as the need for advanced management systems, concerns about battery lifespan due to frequent charging and discharging, and infrastructure requirements [14, 15].

Household thermal demands (primarily for heating and hot water) constitute a significant portion of total energy consumption. The way households meet these thermal demands has direct implications on their energy systems. Traditionally, many homes relied on fossil fuels for heating, leading to high carbon emissions [16]. However, with advancements in technology, there has been a shift towards electric heating solutions, such as heat pumps, which are more efficient and environmentally friendly. Integrating these heating solutions with other home energy systems allows for optimization of energy consumption based on thermal needs. For instance, surplus energy from solar panels can be stored for energy demand or used to power heating systems. However, meeting fluctuating thermal demands requires sophisticated control algorithms and efficient insulation to ensure energy is used with optimization [17]. Addressing these challenges is crucial to ensure that households can meet their thermal needs in an energy-efficient manner.

The realm of home energy management has witnessed increasing complexity due to the integration of diverse energy sources, advanced devices, and varying consumer behaviours. To address this complexity and design efficient energy management strategies, the application of models and simulations has become imperative [18]. Through accurate models, it is possible to replicate real-world scenarios, predict energy consumption patterns, and test different energy management strategies under various conditions.

Simulations offer a platform to analyse the performance of Home Energy Management Systems, evaluate the efficiency of energy storage solutions, and gauge the impact of renewable energy integration. They help in understanding how different components of a household's energy system interact with each other and how external factors, such as weather patterns or grid outages, might influence energy consumption and production [19, 20].

Furthermore, models and simulations play a crucial role in the design and development of algorithms that optimize energy consumption, ensuring that households can meet their energy demands in the most cost-effective and environmentally friendly manner. However, the accuracy of these models and simulations is paramount. Inaccurate models can lead to inefficiencies, increased costs, and suboptimal energy utilization [21, 22, 23]. Therefore, continuous research and refinement of these tools are essential to reflect the evolving landscape of home energy management.

1.2 Structure of the Proposed Model

Navigating through the complexities of home energy management requires a detailed, well-structured model. This research introduces a comprehensive model (Figure 1.2.1), structured around several key sub-models, each with a specific role and function in managing, predicting, and optimizing household energy usage.

The Local Household Load Data sub-model brings in crucial data about past and present energy use, laying a solid foundation for the model. The Photovoltaic (PV) sub-model predicts household solar energy output, while the Electric Vehicle (EV) sub-model manages the energy interactions between the home and the vehicle. Human activity and its impact on energy use are managed by the Occupational sub-model. Thermal energy needs, a significant component of energy management, are addressed through specific sub-models managing different aspects of heating. Finally, the Batteries and Home Energy Management Systems (HEMS) sub-model brings everything together, managing and optimizing the entire system.

Each of these sub-models is explored in more detail in the following chap-

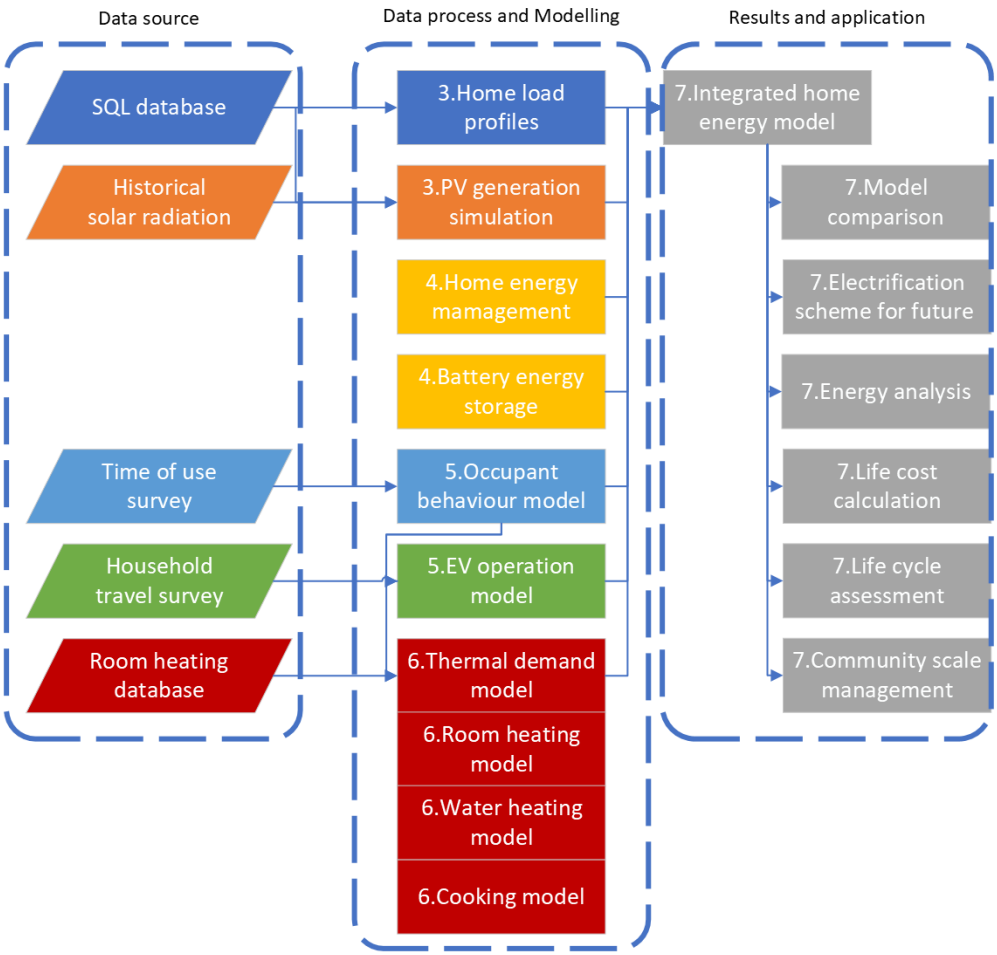


Figure 1.2.1: The structure diagram of models and related chapters

ters, providing a clear view of the entire model and its ability to manage household energy effectively.

1.3 Aims and Objectives

Navigating through the complex world of household energy management, especially in the light of technological advancements and sustainability efforts, requires a meticulous and comprehensive approach. When households evolve from simple energy consumers to potential energy producers and storers, thanks to innovations like solar panels and battery technologies, a thorough investigation into this dynamic and the associated technologies is

crucial.

In this context, this research pivots towards understanding the complex elements of household energy systems. The aim is to carve out strategies that optimize energy use and minimize environmental impacts, while also addressing the challenges and potentials offered by renewable energy integration and technological advancements in energy management strategies.

Aims and Objectives:

- Explore Energy Component Dynamics: Investigate the roles, challenges, and potentials of various energy components, such as PV systems, EVs, and HEMS in household energy management.
- Develop and Validate Optimization Strategies: Create strategies to optimize energy use while ensuring minimized environmental impacts and enhanced sustainability.
- Enhance Model and Simulation Accuracy: Improve the reliability of models and simulations in predicting and strategising household energy management, aligning them closely with real-world scenarios.
- Analyse and Compare Sub-Models: Integrate and contrast the roles and outputs of different sub-models, forging a comprehensive household energy model for efficient and optimal energy management.
- Assess Economic and Environmental Impact: Evaluate the proposed models and strategies in terms of their economic feasibility and environmental impact, balancing cost-effectiveness and sustainability.
- Apply Strategies at a Community Level: Explore the application and implications of the developed energy management strategies at a

community level, investigating the potential benefits for community energy sharing and overall sustainability.

The above aims and objectives establish the structural framework of this research, providing a focused, structured, and impactful exploration into household energy management. Through a combination of theoretical analysis, model development, and practical application, this study aims to chart a course through the intricate domain of current and future household energy management, contributing valuable insights and strategies to the field of sustainable energy use.

1.4 Contributions

This research navigates through the field of future home energy management, carving out noteworthy contributions as follows:

- Integration of Sub-Models: Development and synchronization of various energy sub-models, establishing a comprehensive model that accurately represents and predicts household energy dynamics.
- Algorithm Development: Introduction and validation of innovative algorithms, optimizing energy management with a special focus on battery operations, thermal requirements, and EV functionalities.
- Strategy Analysis: Comprehensive evaluation of energy management strategies, scrutinizing technical, economic, and environmental aspects, and providing a well-rounded perspective on their practical implications.

- Predictive Accuracy Enhancement: Refinement of models and simulations, ensuring enhanced predictive accuracy and reliability in real-world applications.
- Comparative Strategy Analysis: An in-depth comparative analysis of traditional and electrification schemes, yielding nuanced insights into their respective merits and challenges.
- Scalability and Applicability: Ensuring developed models and strategies possess broad applicability and scalability, applicable across diverse scenarios and scales.
- Community-Level Application: Extending insights to the community level, exploring potentials and challenges in community energy management and sharing.

1.5 Structure of the Thesis

Chapter 2 begins with a thorough literature review, dissecting current research and identifying gaps in home energy management, laying the foundation for the detailed analysis that follows.

When it comes to Chapter 3, load curves and PV datasets are carefully explored, emphasizing the critical role of accurate data in forecasting energy demand and solar generation. Chapter 4 focuses on the complexities of home energy management system (HEMS) and battery modelling, dissecting the subsystems and decoding control algorithms that are critical to optimal home energy management.

Chapter 5 then delves into modelling EV operations and occupancy dynamics, linking these elements to energy utilization patterns and highlighting

their critical role in household energy needs. Chapter 6 delves into the thermal dimension of home energy, building and analysing models related to individual heating aspects and weaving this together with occupancy patterns to present a comprehensive view of home thermal energy management.

In Chapter 7, the developed models are combined and reviewed, comparing the traditional and electrified scenarios through rigorous analysis. This chapter further conducts a detailed life cycle assessment (LCA) and extrapolates the findings to the community level, providing a macro perspective on the potential impact and utility of the proposed models and strategies. The Chapter 8 comes to the conclusion of the thesis.

Chapter 2

Literature Review

2.1 Introduction

Home energy management is becoming more and more important, especially with concerns about the environment and the rise of new technology. Modern homes are now able to both use and make power. This shift is thanks to systems such as Home Energy Management Systems (HEMS). These systems not only streamline energy consumption but also integrate renewable energy sources, making households both efficient and eco-friendly [24, 25]. Advancements such as the integration of Internet of Things (IoT) devices have paved the way for more dynamic and responsive HEMS, optimizing energy consumption patterns [26].

Increasingly, households are adopting solar panels for electricity generation. Such initiatives not only offer cost savings but also promote sustainable energy consumption, reducing carbon footprints [27, 28]. HEMS play a big role here by showing how much energy is being used and helping to use it in the best way [29, 30].

The adoption of Electric Vehicles (EVs) is witnessing a surge [31]. As home charging becomes essential, HEMS play a pivotal role in scheduling optimal charging times, shifting energy consumption to off-peak periods and ensuring efficient energy use [32], and the use of green energy when it is available [33].

However, there are still some problems. For example, solar panels, while efficient, may face inconsistencies in power generation due to varying climatic conditions [34]. HEMS, therefore, must possess adaptability to manage such variations, ensuring continuous energy supply [35]. Also, people have their own habits and needs. A good HEMS should be easy to use and not affect how people live [36, 37]. With many different devices in homes today, making them all work with HEMS in a safe way can be challenging [38, 39].

To sum up, HEMS offer a promising way to manage home energy, but there are still challenges to overcome. These require new solutions and understanding of how people use energy.

Nowadays, prioritizing energy conservation and environmental sustainability is crucial. Home energy management plays a central role. Modern homes are evolving to consume energy and produce it. This transformation is attributed to technological advancements, societal shifts, and environmental considerations. The integration of solar panels, electric vehicles, and advanced battery storage in households marks a significant step towards electrification, influencing energy landscapes and setting precedents for future urban developments.

This literature review investigates the home energy management. The aim is to highlight the complex interactions of technologies, strategies, and user behaviours that characterize this domain. Emphasis is placed on the

significance of effective Home Energy Management Systems (HEMS) in guiding households towards a sustainable future.

The review begins with an in-depth analysis of load profiles and EV datasets, emphasising the crucial role data holds in shaping effective energy management strategies. The attention then shifts to HEMS and battery technologies, exploring their influence on household energy dynamics. Subsequent sections delve into EVs and occupancy models, offering insights into the relationship between energy consumption patterns and resident behaviours. Thermal models are also discussed, highlighting their importance in achieving energy efficiency.

Concluding sections provide a comprehensive examination of integrated models and the life cycle assessments of electrification. A comparison is drawn between traditional energy paradigms and electrified alternatives, focusing on their economic and environmental impacts.

Overall, this literature review underscores the importance of home energy management in a rapidly electrifying global context and highlights the potential of HEMS in crafting sustainable living environments.

2.2 Household Energy Demands and Challenges

The transition in the energy landscape sees households not just as energy consumers, but also as contributors to the energy grid. This change in role is evident with the distinct differences between past and present household energy consumption and production. Especially, it is led by the increase of electronic devices, the use of renewable energy sources, and the rise of

electric vehicles [40, 13].

The energy demand in homes nowadays is undoubtedly on the rise. The introduction of smart devices, combined with the desire for comfort through advanced HVAC systems, has amplified energy usage. However, this growing demand is counterbalanced by the potential of electrification, pointing to a future with more renewable energy [41].

Photovoltaic (PV) systems in homes showcase this shift. These systems not only meet a household's energy needs but also have the potential to provide excess energy back to the grid. Additionally, with more households owning electric vehicles (EVs), there is a pressing need for home energy management systems. These systems help plan the best times to charge EVs, especially when relying on renewable energy sources [42, 13].

Using renewable energy sources like solar is not without its challenges, particularly the inconsistency due to variable weather conditions. This inconsistency demands homes to have effective energy storage solutions. This becomes even more challenging in remote areas that are not connected to the main power grid [43, 44, 45, 46]. This literature review [43] explores the use of solar home systems in Malaita, Solomon Islands, emphasising how island mode microgrids have enabled rural communities to develop a localised energy identity. [47] compares the similarities and differences between grid-forming and grid-following inverters: both types synchronize and interface with the grid, but differ in methods such as frequency droop control versus PLL, current-following voltage-forming versus voltage-following current-forming, and their respective stability issues in varying grid strengths.

Another factor to consider is the viewpoint of consumers. While there have been many advances in home energy technology, their success depends on

consumer adoption. People's willingness to invest in these systems varies, influenced by their perceived advantages, cost concerns, and other factors [48].

In conclusion, while the path to sustainable home energy management shows promise, it comes with its own set of challenges, both technical and behavioural, that need careful consideration.

2.3 Integration of Photovoltaic Systems with Home Energy Management

Photovoltaic (PV) systems have seen significant growth in recent decades. Initially utilized for specific applications, they have found their way into regular households, driven by technological advancements and decreasing costs [49]. These systems, once considered auxiliary, are now essential components of modern energy solutions.

One of the transformative facts of PV systems is their role in redefining households from mere energy consumers to potential energy producers [14]. With the integration of home energy management systems, households can efficiently utilize solar energy, optimizing consumption patterns and even contributing excess energy back to the grid.

The economic viability of PV installations has been a significant driver for their adoption in households. Over the years, the costs associated with PV installations have seen a considerable reduction, making it an attractive investment for homeowners [50]. Analysing the costs associated with PV systems, it becomes evident that not only do they offer environmental benefits, but they also provide tangible returns on investment. The decreasing

costs have been attributed to technological advancements, bulk manufacturing, and increased market competition, allowing more households to harness solar energy without incurring excessive expenses [51].

Furthermore, the versatility of PV systems extends beyond just household consumption. They are finding applications in specialized setups, including DC homes, underscoring their adaptability [21].

However, the integration of PV systems into households is not without challenges. Efficiently harnessing and managing the generated energy, especially during non-peak hours, remains an area of research and development [52]. For instance, optimizing the storage and distribution of solar energy during cloudy days or seasons with shorter daylight hours presents logistical and technical difficulties. There are also challenges where the grid is "weak". A large amount of local PV connection can cause significant local voltage variations, and this then requires innovative mechanisms for local voltage control [53]. The "sunshine tariff" is a good illustration of this challenge.

In summary, the synergy between PV systems and home energy management is shaping the future of household energy consumption, offering a sustainable and economically efficient path forward.

2.4 Battery Technology and Home Energy Storage

Battery technology has experienced substantial advancements in recent years, emerging as a cornerstone in the realm of home energy management. Traditional energy storage mechanisms have given way to more efficient

and sustainable battery solutions, ensuring that homes not only generate energy but store it effectively for later use [54].

Modern battery technologies, particularly Lithium-ion batteries, have received significant attention due to their high energy densities and longer cycle lives, making them ideal for household energy storage applications [55]. These advancements allow homes equipped with renewable energy sources, such as PV systems, to store surplus energy produced during peak hours and utilize it during periods of lower generation or adverse weather conditions [56]. These developments have been critical in ensuring that homes equipped with renewable energy sources, like PV systems, can store excess energy produced during peak hours and utilize it during non-peak hours or cloudy days.

Beyond mere storage, the integration of battery technology into home energy systems has paved the way for optimized energy consumption patterns [57]. Advanced energy management systems now incorporate battery storage solutions to balance energy demand, reduce grid reliance, and even contribute back to the grid when necessary [58].

The growing popularity of electric vehicles (EVs) has further accentuated the importance of battery technology in homes. With EVs becoming commonplace, homes now need to cater to their charging requirements, effectively transforming the household energy landscape. The synergy between home energy storage and EV charging can be seen as a two-way street – while homes need to ensure adequate energy for EV charging, EVs can also act as mobile energy storage units, potentially feeding back into the home during high demand periods [59].

However, the integration of battery technology is not without challenges. Factors like battery degradation, lifecycle estimation, and optimal inte-

gration strategies with renewable energy sources remain areas of active research [60, 61]. Additionally, for a more sustainable energy future, understanding the challenges of sustainability and the lifecycle impacts of metals used in these batteries is vital to ensure a truly sustainable energy storage solution [62].

In conclusion, battery technology has fundamentally reshaped the way modern homes approach energy management, ensuring a more sustainable, efficient, and forward-looking energy consumption paradigm.

2.5 The Development of Electric Vehicles and the Impact on Home Energy system

In recent years, the evolution of electric vehicles (EVs) has been remarkable, transitioning from niche products to mainstream transport options. This transition has been fuelled by advancements in battery technology, environmental considerations, and policy incentives [63].

The interplay between EVs and home energy is a fascinating aspect of this revolution. With increasing home electrification, integrating EVs into the home energy landscape has become paramount. Recent studies underscore the importance of plugged-in electric vehicle-assisted demand response mechanisms in managing home energy consumption [64]. Modern HEMS are now designed to incorporate EV charging, ensuring efficient charging without excessive reliance on the domestic grid [65].

The Vehicle-to-Home (V2H) concept, which also encompasses the broader Vehicle-to-Everything (V2X) paradigm [66], showcases the intersection of EVs with home energy. This allows EVs to not only draw energy from the

home but also feed energy back into the home grid during peak demand periods [67].

Moreover, combining photovoltaic (PV) systems with EV charging opens new avenues for sustainable energy consumption. Homes equipped with PV installations can utilize solar energy to meet the charging demands of EVs, further reducing carbon footprints associated with transportation [68]. Optimal integration techniques for hybrid solar-battery power systems have been proposed to further enhance this synergy [58].

However, seamlessly integrating battery technology into home energy systems is not without challenges. Managing energy flows between multiple EVs, especially in multi-household settings, remains a hot topic of research [69]. Research indicates that developing effective energy management models for such scenarios is essential [70]. Additionally, integrating home appliances into this ecosystem can further optimize energy utilization [71].

In conclusion, the proliferation of EVs plays a significant role in the dynamics of home energy consumption and management. As the lines between transportation and home energy blur, innovative solutions will be key to ensuring a sustainable and harmonious energy ecosystem.

2.6 Changes in Household Thermal Energy Demand

Modern households face evolving thermal energy demands, influenced by both external factors such as climatic changes and internal factors like technological advancements and shifting lifestyles [72]. Primarily, the thermal energy demands of households encompass heating, hot water supply, and

cooking [73]. Traditionally distinct, these elements are now converging under the comprehensive concept of home energy management.

A noticeable trend in home heating is the transition from traditional systems to more sustainable alternatives [72]. Heat pumps, solar thermal systems, and biomass heating systems offer reduced carbon emissions compared to traditional fossil fuel-based systems. It is not just about comfort, and heating also has significant implications for a home's carbon footprint [74]. For instance, the energy efficiency and carbon implications of domestic tasks like cooking have been highlighted, underscoring the importance of everyday activities in the broader energy picture [74].

Water heating, another significant energy consumer, is undergoing its own transformations. Research into the heating of water emphasized the influence between configuration of work to hydraulic resistance of water flow in boilers, focusing the pressure drop and water flow in devices [75]. Newer technologies, such as on-demand or tankless water heaters, offer energy-saving potential by providing hot water only when it is needed, reducing standby energy losses. User interaction with smart home technologies is an emerging facet of thermal demand management [76]. Engagement with these intelligent systems has been shown to enable more efficient heating [77, 78]. Moreover, the need to align user perceptions and expectations with smart home interfaces have been stressed, indicating that effective thermal management is as much about user understanding as it is about technological sophistication [77].

Various factors can shape decisions around heating systems. For example, research has indicated that events like relocating can have a profound impact on residential heating choices [79], and other studies have delved into the roles of knowledge, social norms, and habits in shaping these decisions

[80].

The study examines four national household heat transitions, including China, Denmark, Finland, and the UK [81]. The heat pump system and gas heating is widely used in high latitude areas, while the solar heating system is applied in others. The effective energy frameworks are as crucial as technical advancements in facilitating energy transitions.

In a holistic approach to home energy, an integrated strategy incorporating both electricity and gas consumption was proposed [73]. This combined method highlights the overarching theme of comprehensive home energy management, where thermal needs are balanced with other energy requirements.

2.7 Models and Future Development of Home Energy Management

The energy landscape of homes has undergone significant transformation over the past decade, and models play a pivotal role in managing these changes efficiently. Several models have been proposed to aid in Home Energy Management (HEM), and while they have paved the way for smarter energy usage, there is room for improvement.

Existing HEM models often separate energy components, lacking an integrated perspective. This segmentation fails to harness the synergies that can arise from a unified system, such as the integration of solar power, batteries, and electric vehicle charging [82]. Another challenge is the unpredictable nature of domestic energy consumption. Predicting energy needs with high accuracy has proven to be a difficult task for many of the current

models [83].

Recognizing these challenges, researchers have been working on developing more robust models. The Predictive Home Energy Management System (Predictive HEMS) is a significant advancement in this area. P-HEMS employs predictive algorithms to forecast and strategic energy usage, integrating solar panels, battery storage, and electric vehicle consumption [84]. The integration of IoT and artificial intelligence is emphasized in HEMS [29]. Such integrations enhance real-time monitoring and predictive control, ensuring the optimal energy consumption.

A model is introduced to minimize energy costs by leveraging renewable energy sources and storage [85]. The approach underscores the significance of integrating diverse energy inputs for efficient home energy management.

Centralized models, such as the one proposed by [86], utilize a predictive control strategy. By assimilating multiple energy sources, these models enable a harmonized energy flow, maximizing efficiency. Stochastic modelling methods have also emerged as a promising approach, providing a more adaptive planning based on probabilistic data [6]. The overarching aim is to create an all-encompassing energy management model that holistically considers all elements of home energy [3].

Particular models also prioritize customization. Energy consumption patterns differ from one home to another, emphasizing the need for personalized energy management strategies. To this end, researchers are working on models that can adapt to individual household needs, optimizing energy consumption schedules to be both cost-effective and energy-efficient [87].

[88] highlighted a model aimed at minimizing the total cost of home energy consumption. Its approach integrates solar power, electric vehicles, and

batteries, demonstrating the potential of holistic models in future HEM developments.

Within the UK, and specifically Nottingham, residential energy management has been the focus of various model-based studies. The CREST model [89, 90, 91] offers a probabilistic approach to estimating household electricity consumption, balancing occupancy and demand simulations. A model [89] introduces a stochastic multi-energy simulation for UK homes, providing insights into energy flow and dependencies across multiple vectors, such as electricity and natural gas. Additionally, Marín et al. investigate hierarchical energy management, aligning resources at household and community levels to enhance microgrid reliability and efficiency [92]. Focusing on integrating renewables, the research [93] navigates minimizing energy costs through a strategic alignment of solar power, electric vehicles, and batteries. Moreover, machine learning predictions with microgrid community management is studied, advocating for a dynamic, decentralized approach [94]. These studies collectively underscore the significance of integrated, predictive, and dynamic models in optimizing localized energy systems amidst the complex nature of household energy management.

In modern energy systems, the rise of communities, including residential areas, university campuses, and industrial parks, has enhanced system reliability and economic efficiency. These communities reduce transmission losses and improve system reliability through internal resource sharing in standard operations. Additionally, during extreme conditions, microgrid communities can operate independently, disconnecting from the main power grid to ensure system integrity and security [95].

Energy Management (EM) in these systems can be divided into centralized and decentralized formats, each with distinct framework topologies

and control strategies addressing specific challenges [96, 97, 98]. However, as microgrid (MG) communities grow and diversify in power electronic components, they face challenges. Complex operational strategies become computationally demanding. Issues like differing optimization goals among MGs and potential security/privacy concerns hinder centralized EM deployment [96, 97, 98].

Recent research has shifted to decentralized management approaches for MG communities, focusing on cost minimization [99, 100, 101], coalitional transactions [102, 103], and other perspectives. However, while these studies are innovative, they show limitations related to optimization goals, computational complexity, and potential security and privacy concerns in both centralized and decentralized EM schemes.

A study in the "Jono Zero Carbon Smart Community" shows that real-time pricing (RTP) reduces annual electricity costs more effectively than multistep pricing (MEP) and time-of-use pricing (TOU) [104]. The results suggest that RTP optimizes grid load and offers economic benefits, providing insights for future energy policies and HEMS enhancements.

In recent years, Microgrid (MG) communities in modern energy systems have gained significant attention. While past research has explored coordinated operation and energy management in MG communities, there are still key challenges and gaps to address. Specifically, earlier studies mainly targeted larger MG communities, using complex optimization frameworks and intensive computations, which might not suit smaller MG communities. Also, most studies did not fully address the relationship between household energy management and community-wide collaboration.

In conclusion, while strides have been made in modelling for HEM, the journey towards a seamless, integrated, and adaptive home energy system

continues. These advanced models signify a step in the right direction, ensuring that homes of the future can meet their energy demands effectively and sustainably.

2.8 Conclusions

The examination of various facets of Home Energy Management (HEM) has elucidated several pivotal findings:

- HEM goes beyond simple utilization efficiency and emphasizes the generation, storage and sharing of energy. This requires integrating different systems and technologies, including photovoltaic (PV) systems, battery storage, electric vehicle (EV) charging and smart home management systems.
- While technological developments such as Home Energy Management Systems (HEMS) and Internet of Things (IoT) technology have expanded the possibilities for HEMs, several challenges remain, including inconsistent energy generation, complexity of system integration, and user fluctuation acceptance.
- The spread of electric vehicles has changed domestic energy demand and usage patterns. By integrating with home energy systems, electric vehicles not only change household energy consumption patterns, but also bring new challenges and opportunities to HEM.
- Battery technology and energy storage occupy a central position in HEM. They provide key solutions to overcome the instability and uncertainty of renewable energy, while also creating new technical and economic challenges.

- User behaviour plays a crucial role in HEM. Understanding and predicting user behaviour, and incorporating this into system design, is critical to achieving efficient energy management.

- Various models and algorithms play an important role in predicting and optimizing HEM. They need to be continuously updated and optimized at the technical level and must adapt to increasingly complex user needs and market dynamics in practical applications.

To face the challenges in the future home energy management, the listed objectives should be achieved in the following chapters of the thesis, as:

- Data-Driven Challenges: Chapters 3 and 4 underscored the significance of detailed and accurate load profiles, PV datasets, and battery modelling to enable precise energy management. Thus, enhancing the accuracy and reliability of predictive algorithms and energy simulations is imperative.

- Behavioural Dynamics: Emphasizing chapter 5, the incorporation of human behaviour, particularly occupancy and EV usage patterns, into energy management models and strategies, is vital for achieving realistic and sustainable energy management outcomes.

- Thermal Energy Management: Insights from chapter 6 highlight the evolving thermal energy demands and the need for advanced models that effectively integrate these within the overall HEM. Addressing the challenges in integrating thermal models with other subsystems in HEMS can pave the way for more holistic energy management.

- Integrated Models and Electrification: Chapter 7 underscores the need for integrated models that encapsulate all energy vectors and

subsystems. Furthermore, exploring the Life Cycle Costs (LCC) and Life Cycle Assessment (LCA) of various electrification strategies and technologies is vital to understanding their economic and environmental implications.

Chapter 3

Load Profiles and PV Generation Data for the Simulation Studies

3.1 Collected Domestic Load Profiles and PV Datasets

3.1.1 Introduction

The rapid global shift towards renewable energy sources has been largely influenced by the alarming increase in greenhouse gas emissions and the subsequent impact on climate change. Among the various renewable energy technologies, solar photovoltaic (PV) systems have gained significant attention due to their cost-effectiveness and the abundant availability of solar energy. With the increasing penetration of solar PV systems in residential settings, a comprehensive understanding of household energy consumption

patterns and PV generation characteristics has become paramount.

Modeling and forecasting of household load curves have been an active research area. Traditional methods such as regression analysis and time series forecasting are widely employed in the literature. [105] using a Gaussian process to model and predict the half-hour electricity demand greatly reduces the computational burden. More recently, advances in machine learning techniques have provided a more sophisticated approach to capturing complex patterns in load profiles. For example, a method using artificial neural networks provides a weather-dependent national electricity load spectrum based on a large amount of data across Europe [22].

The advent of smart metering provides granular data, allowing researchers to better capture the variability and uncertainty of load profiles. Residential Load Driven by Smart Meter Data considers operational scenarios for demand response and establishes methods for defining and evaluating operational potential [106].

Recent studies on PV output power forecasting and estimation have explored three main model types: phenomenological, stochastic/statistical learning, and hybrid models [107]. Deterministic approaches use physical phenomena and software like PVSyst and SAM to predict PV plant output, but they may struggle to handle uncertainties in PV power data. In contrast, probabilistic models, such as ensembles of deterministic forecasters, can describe uncertainties but come with high computational costs [108].

Machine learning models like Neural Network (ANN), Support Vector Machine (SVM), Multiple Linear Regression (MLR), and Adaptive Neuro-Fuzzy Inference System (ANFIS) offer statistical and data-driven forecasting without prior knowledge of the system [109, 110]. They prove versatile and adaptable in various contexts and have been investigated for other re-

newable energy sources. Combining different models in hybrid or ensemble approaches can further improve prediction performance. Optimizing ANN in deterministic techniques can enhance accuracy for PV power forecasting.

Traditional research mainly focused on point forecasting for predicting the PV power generation, but due to the inherent variability of solar resources, errors can be produced, which misguide energy management decisions [111, 112]. Probabilistic forecast models offer a better alternative, providing more detailed predictions to manage risks and improve system efficiency. However, most methods rely on complete input and recorded datasets, and missing data can significantly affect model performance [113]. A range of methods have been explored to impute the missing data, including statistical methods and machine learning-based methods, have been applied to deal with this issue, although challenges persist in capturing complex patterns and handling high computational costs [114, 115].

Despite the extensive research on household load profiling and PV generation prediction, few studies integrate these two aspects using real-world data. Moreover, there is limited research exploring the use of SVM combined with Gaussian mixture models (GMM) for PV simulation. The research in this chapter aims to leverage studies that consider the integration of real-world household load profiles and photovoltaic generation datasets into comprehensive household energy models. Specifically, it addresses interpolation of missing data in load curves and PV output predictions to use better quality data for integration with subsequent models.

The first section provides an overview of the domestic load and PV datasets that were collected. It provides information about the data, including some preliminary analysis of the data's characteristics. The second section focuses on the load profiles. It begins with an introduction, proceeds with

the presentation of the algorithm used to handle missing values in the load data using k-nearest neighbours (KNN), and ends with an analysis of the results. The third section is about the photovoltaic (PV) system. It starts with an introduction, then presents an algorithm that combines support vector machines (SVM) and Gaussian mixture models (GMM) to predict PV power generation.

3.1.2 Datasets Description

This study utilized a comprehensive household load database, named as the "Meadow SQL database", containing detailed information about energy consumption at the residential level. This dataset was obtained from local smart meter collection and covers a time period from 2018 to 2021, as part of a research study undertaken at the University of Nottingham.

The database contains 27 residential households, each with their unique identifiers. These households are located in Nottingham, and from a wide spectrum of the typical UK residential power usage.

The collected data includes the power consumption of each household at one-minute intervals. The dataset presents a time-series format where each row corresponds to a specific date and time. Apart from power usage, the dataset also contains the relevant active power, reactive power, PV generation and battery usage . The additional data provides context and allows for more in-depth analysis of household energy patterns.

To ensure data quality, several pre-processing steps were undertaken. These included cleansing data, imputing missing values, normalizing for further use. This method would be mentioned in the section of the load profile process.

3.1.3 Statistical Analysis of the Load and PV Profiles

Upon analysis of the household electricity consumption data, an average daily energy use of 8.38 kWh was calculated for the examined households. This value spans a broad range from a minimum of 4.20 kWh to a maximum of 19.69 kWh, indicating significant variability in domestic electricity demands and lifestyle habits. In comparison, official data published by the UK government reports an average daily electricity consumption for UK households between 8.5 and 10 kWh, suggesting the representativeness of the sample set in this study [116].

Further examination revealed that the mean self-consumption rate from photovoltaic (PV) systems stood at 29.37%, with a span from 22.01% to 43.59%. This figure demonstrates the substantial role of domestic PV systems in meeting electricity needs. The range of this metric, however, signifies notable disparities in the efficiency and benefits of PV systems across different households. Findings from the University of Oxford indicate that UK households with solar PV self-consume 45% of their own solar generation on average, suggesting a lower PV self-sufficiency in the sample set of this study compared to the national average [117].

Overall, these analytical outcomes provide vital insights into understanding domestic energy consumption patterns and the role of renewable energy sources, such as PV, in domestic energy provision. This information bears significant implications for the formulation of more effective energy policies and the promotion of renewable energy use.

3.1.3.1 Seasonal Analysis

The Figure 3.1.1 provides a comparative representation of the average household energy consumption, broken down by minutes of the day, for three scenarios: overall average, summer average, and winter average.

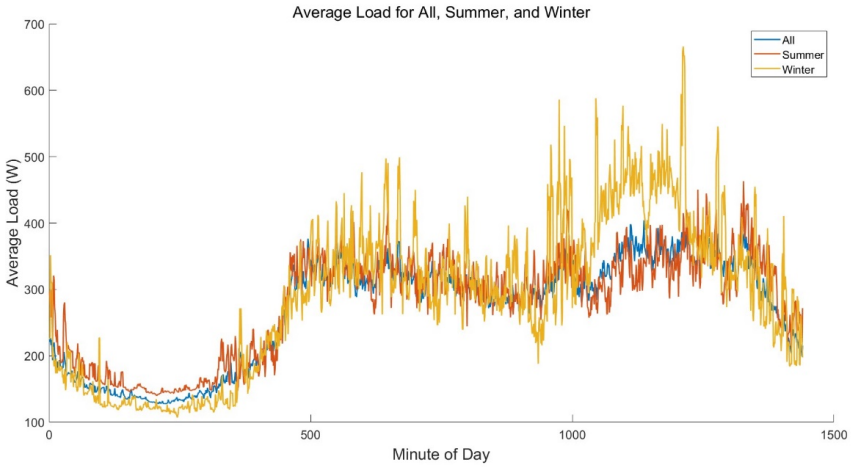


Figure 3.1.1: Minute by minute average domestic load in all, summer and winter seasons

The x-axis represents the 24 hours of the day while the y-axis shows the average load in watts. It is evident that there are distinctive patterns in the hourly energy consumption, which differ across the three scenarios.

Throughout the day, a general trend can be observed wherein the energy consumption is relatively low during the early morning hours, rises to peak during the late afternoon and early evening, and then gradually decreases towards midnight. This pattern can be attributed to typical household behaviour, with increased appliance use and activity during waking hours.

Comparatively, the summer average load curve shows lower energy consumption during the day but higher consumption during the late afternoon and evening hours. The long sunshine time leads to extended evening activities and entertainment.

On the other hand, the winter average load curve indicates higher energy consumption during the morning and evening hours. This is likely due to the increased use of heating appliances during the colder months. Interestingly, the winter curve also shows an additional peak around midnight, which is not present in the summer curve. This could possibly be explained by the use of electric blankets or heating devices during sleep hours in winter.

These findings highlight the significant role that seasonal variations play in shaping household energy consumption patterns. Understanding these variations can contribute to more effective demand response strategies, energy-efficient appliance design, and better grid management, especially with the move to the electrification of heating.

3.1.3.2 Weekday and Weekend Analysis

The Figure 3.1.2 presents a comparative analysis of the average household energy consumption patterns between weekdays and weekends, segmented by the minute of the day.

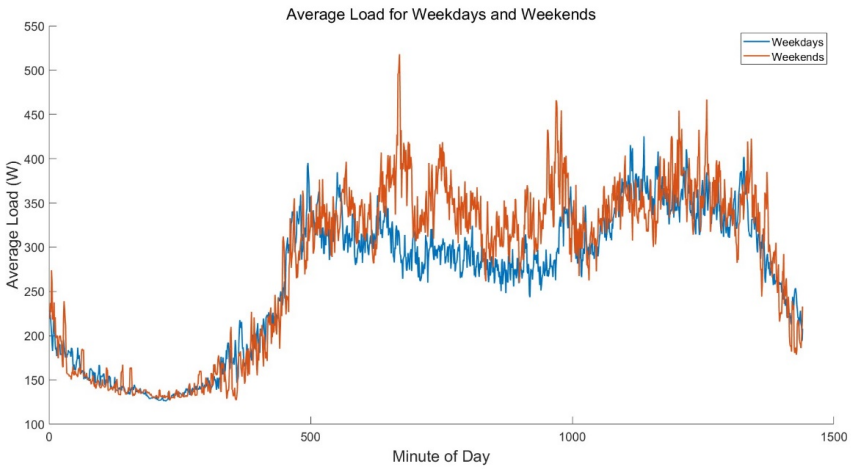


Figure 3.1.2: Minutely average household load for weekdays and weekends

The x-axis represents the 24 hours of the day, while the y-axis quantifies

the average load in watts. Two distinct lines correspond to the average energy consumption on weekdays (blue) and weekends (orange).

Overall, it can be observed that the energy consumption during weekends tends to be relatively higher during the daytime and early evening hours, compared to weekdays. This is likely attributed to increased occupancy and activity levels within households during these periods on weekends.

On weekdays, there is a noticeable peak in energy consumption in the early morning hours, potentially due to morning routines before work or school. This peak is less pronounced on weekends, suggesting a shift in routine, possibly due to later wake-up times.

In contrast, energy consumption during the late-night hours does not exhibit much variation between weekdays and weekends.

These findings underscore the importance of differentiating between weekdays and weekends when analysing residential energy consumption patterns. Such insights can support the design of time-of-use electricity pricing schemes and demand-side management strategies.

3.1.3.3 Load and PV Patterns by Month

The Figure 3.1.3 provides a monthly breakdown of the average daily energy load and photovoltaic (PV) energy production.

The x-axis represents the 12 months of the year, while the y-axis signifies the total energy in kilowatt-hours (kWh). The blue and orange bars correspond to the average daily energy load and PV generation, respectively, for each month. The peak power of PV panels ranges from 1.403 to 3.84 kW for different houses.

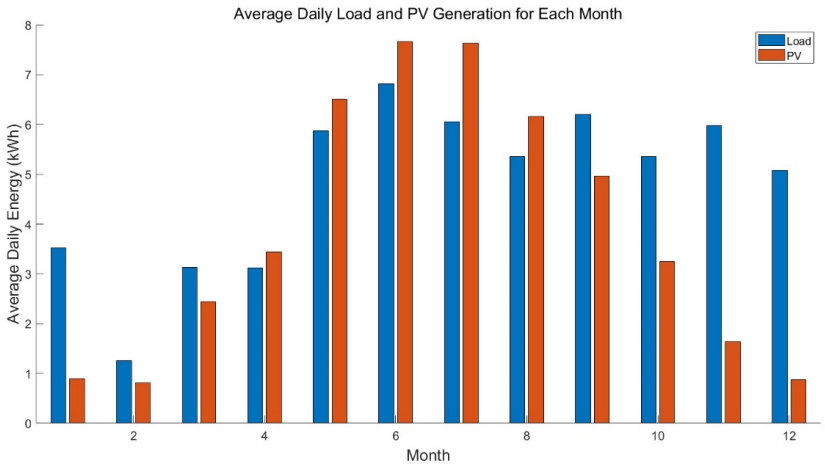


Figure 3.1.3: Monthly average daily load and PV

A clear seasonal pattern is observable in both energy consumption and PV production. The PV generation exhibits a pronounced increase from March to July, with a peak in May, mirroring the increase in sunlight hours and intensity during the summer months. This trend is conversely mirrored in the winter months, where PV production dips due to reduced sunlight.

On the other hand, energy consumption does not show a similarly pronounced seasonal pattern. While there is a noticeable increase in energy consumption during the colder months (November to February), the variation is less marked than the PV production. The daily load is low compared to the other months. This might be due to the lack of data in load profiles of February, leading to the rising demand for the high quality home profiles with pre-processing methods.

It is not surprising that the energy load exceeds the PV generation throughout the year, with the gap being more pronounced during the winter months. This underscores the need for supplementary energy sources or storage solutions to fully meet household energy demands, especially in seasons with lower solar energy production. These findings highlight the importance of considering seasonal variation in both energy consumption

and PV production when designing and implementing solar energy systems and policies.

As the trend toward full electrification of households continues, the energy consumption patterns are expected to further change. For example, with the integration of electric heating systems replacing traditional gas or oil heating, a substantial increase in electricity demand during the colder months can be anticipated. This will widen the gap between energy consumption and PV generation during the winter months. Thus, in order to accommodate the shift towards full electrification, future energy systems need to be designed with increased capacity and efficiency. This could involve larger or more efficient PV installations, increased energy storage solutions, or a combination of these and other measures. In addition, the reliance on grid energy during periods of high demand, such as the winter months, highlights the importance of maintaining robust and reliable grid infrastructure, which would be discussed in the following chapters.

3.2 Pre-processing of the Load Profiles

3.2.1 Introduction

Data cleansing and data imputation are vital parts of the data preprocessing process and are crucial across all types of data, including household load data. Implementing these steps enhances data quality, paving the way for more precise and efficient subsequent data analysis and modelling.

The primary goal of data cleansing is the elimination of errors and inconsistencies that might exist in the dataset. Erroneous data, which could be due to device malfunctions or errors during data collection, leading to

outliers or incorrect values, is a common issue. Additionally, duplication of data can introduce bias, making the analytical results inaccurate if the same event has been recorded multiple times. Lastly, inconsistencies in the data could emerge due to variations between data sources or discrepancies in formats, units, and encoding methods.

Conversely, data imputation is a process adopted to handle missing values within the dataset. Missing data can be a result of a multitude of factors during the data collection process, such as device failure or signal loss. Data imputation aims to make full use of the data, mitigating the impact of missing data on the results of the analysis. There exist a variety of methods for data imputation, including the deletion of missing data if the missing values are minimal, simple interpolation such as using the average of the data before and after the missing value, and advanced interpolation methods, like time series or regression analysis for predicting missing values.

By conducting data cleansing and data imputation, a dataset of higher quality, completeness, and consistency is obtained. This greatly aids in making the following data analysis and modelling phases more beneficial.

3.2.2 Load Profile Imputation Algorithm

The k-nearest-neighbours method is widely used for complete missing data [118]. The algorithm implements an imputation technique to fill in missing data in a year-long residential load curve. The load profile is represented as a 2D matrix with 1440 rows and 365 columns, with each cell representing one minute of load on a particular day throughout the year. Missing load data, which often occurs due to errors or interruptions in the data collection process, can be populated by borrowing information from other dates with

similar load characteristics. In this case, first of all, the algorithm will use a simple function to detect single and consecutive null values, which means that there is no data record at this point in time. This information will help subsequent algorithm processing. The flow chart of the algorithm is shown in Figure 3.2.1.

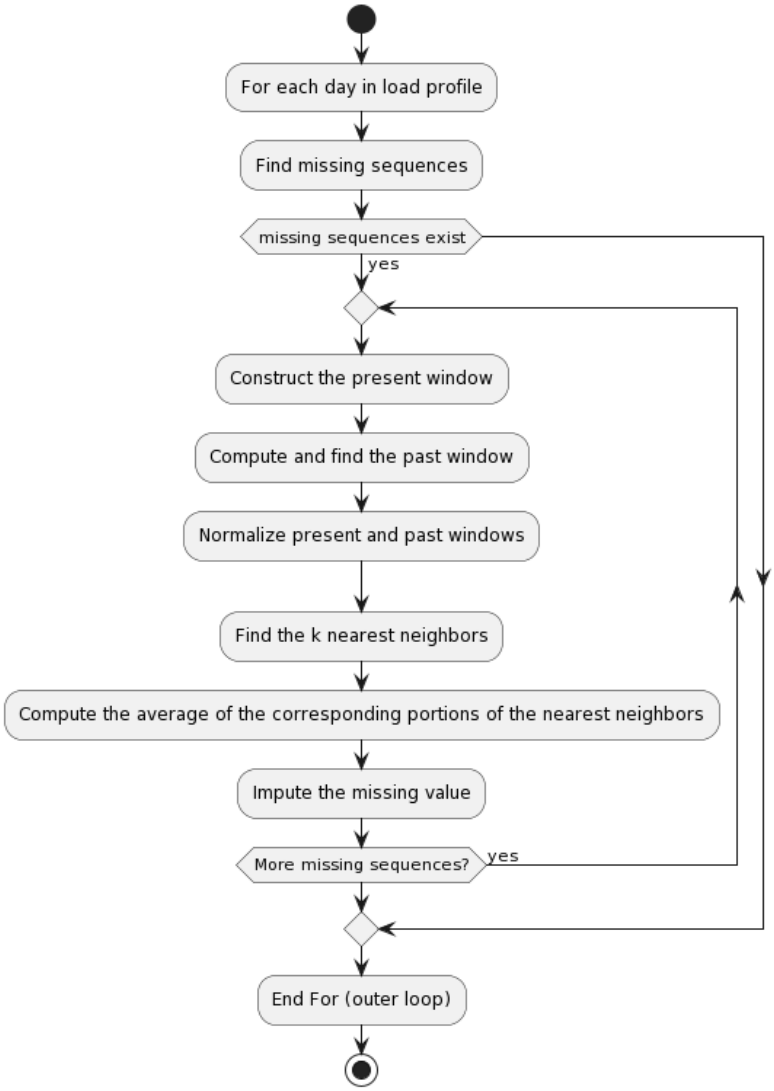


Figure 3.2.1: Flow chart of the proposed imputation algorithm

Given a certain missing portion within a day, the proposed imputation algorithm constructs a preceding window from the present day (i.e., the day with the missing portion). This window, denoted as present window, consists of the preceding p minutes' load before the missing portion.

The algorithm then compares the constructed present window with similar windows from past days. In doing so, it calculates the sum of squared differences (SS) between the present window and each past window. Here, a past window refers to the load of the preceding p minutes from a past day at the same time as the missing portion of the present day. Both the present window and past window are normalized to ensure fair comparison. The range of past days is fixed as 3 times of aimed neighbours, while weekday and weekends are treated separately.

From the computed SS values, the algorithm identifies the k past days that have the least SS with the present window, indicating they are the nearest neighbours. These neighbours essentially represent days where the load pattern before the missing portion was similar to that of the present day.

The imputation is carried out by calculating the mean load of the corresponding missing portion across the k nearest neighbours. To account for possible differences in the overall load level between the present and past days, the mean load is adjusted by a blending factor. The blending factor is the ratio of the total load of the present window of the mean total load of the corresponding windows in the k nearest neighbours.

This process is repeated for every missing portion of the load profile until all missing data are filled. The goal is to ensure the imputed data reflect similar load patterns to those in days with similar load characteristics, thereby maintaining the integrity and the pattern of the residential load profile.

In summary, this function represents an application of the k-Nearest Neighbours (k-NN) approach for imputing missing data in residential load profiles. It leverages the inherent temporal correlations in these load profiles, particularly the daily cyclical pattern, to fill in missing data. This is based

on the premise that load consumption at a given time tends to be similar across days. As such, the load data from 'similar' days can provide a reasonable estimate for missing data, resulting in a complete and more accurate load profile.

The k-Nearest Neighbours (k-NN) imputation method might face issues such as computational complexity, especially with large datasets, and challenges in determining the optimal 'k' value without inducing bias or overfitting. The algorithm may struggle with accurately predicting missing values during varied seasonal, weather, or usage conditions and may be sensitive to outliers or non-representative data. Additionally, assuming ideal energy usage across different days or households might not always be accurate, potentially leading to imprecise imputations.

3.2.3 Results of Imputation

3.2.3.1 One Day Result

In Figure 3.2.2, the imputation is operated for one-year datasets is operated, and one day power graph is shown. The raw datasets are loaded and used as a reference set. For the validation of the performance of the proposed imputation algorithm, the modified load profile is used for input, where 10% of raw one has been replaced by null. In this simulation, the k value is 3, while p equals to 360.

The first subgraph shows the 'raw load profile' (reference load) throughout the day, which serves as a benchmark or expected load profile. The 'reference load' is relatively smooth, showing typical patterns of electricity consumption throughout a day. There are two clusters of noticeable peaks in the load, which correspond to morning and evening hours, typically as-

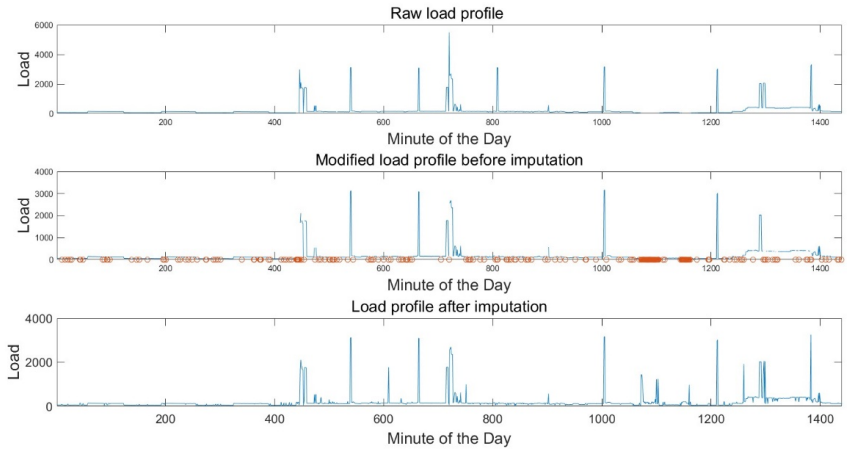


Figure 3.2.2: Load power graphs of raw datasets, modified test sample, imputation result

sociated with high electricity usage. The reference load serves as the ideal model of load consumption and is not affected by any external factors like equipment failure or data loss. The 'modified load profile before imputation' (modified load) subgraph depicts the actual electricity consumption recorded for the same day. Compared to the reference load, it has a similar pattern but with deliberately introduced gaps. These gaps represent missing or invalid data, as this series is to be used as the input for the imputation test. The overall trend, however, remains largely similar to the reference load, with peaks in the morning and evening hours.

The 'load profile after imputation' (imputation load) shows the load profile after the application of the imputation algorithm to fill the missing data points in the actual load. The most notable aspect is that it closely follows the reference load, including at the points where the actual load had missing data. This indicates that the imputation process has been successful in filling the missing data in a way that aligns well with the expected load profile. It is an affirmation of the efficacy of imputation algorithm.

The combined visualization of these three subgraphs effectively demon-

strates the performance of imputation program. It filled the missing or erroneous data in the actual load profile, making it closely follow the reference load profile. This has significant implications for load forecasting, as accurate load profiles are crucial for effective electricity supply management.

The differences between the modified load curve and the reference load curve and between the estimated load curve and the reference load curve further confirm the validity of the estimation method. Differences between the modified data and the reference data were large at some points in time, indicating outliers or missing values in the modified data, which was also manipulated for the purpose of verifying the validity of the procedure. In contrast, at most time points, the difference between the estimated and reference curves was much smaller, suggesting that the estimation process made the load curves more similar to the reference curves, illustrating that the program successfully filled with a substantial portion of missing values. In some time intervals, the imputed profile shows less divergence from the reference profile due to specific strategies such as smoothing used by the imputation method to avoid sudden peaks.

The correlation between the reference load curve and the modified load curve was found to be perfect (1.0), which is expected since the modified load curve was derived from the reference load curve with some modifications. The correlation between the reference load curve and the imputation load curve is slightly lower (0.90), indicating that the estimated data remain highly correlated with the original data, thus preserving general trends and patterns, although some are still missing. The correlation between the modified load curve and the imputation load curve was also perfect (1.0), confirming that the estimation process was imputed based on the modified load profile, and did not change the general trend of the raw

data.

The average value of the reference load curve is 172.69, while the average value of the load curve and the estimated load curve are slightly higher, 197.79 and 177.83, respectively. This is because some nodes are randomly missing in the load curve, and some wrong nodes are also washed out, such as the case where the load is less than 0. This theoretically invalid load value is due to the fact that the initial load is derived from the energy balance of the data in the database. Acquisition errors will affect the results.

The standard deviation of the reference load curve is 424.29, while the standard deviations of the load curve and estimated load curve are 450.37 and 421.09, respectively. The fact that the standard deviation of the imputed data is closer to the original data indicates that the imputation process successfully preserved the variability of the data.

In summary, the KNN interpolation method is able to replicate the global characteristics of the original load curve to a large extent. Although there are small differences in the mean and standard deviation, the overall correlation is still high. The interpolated data features are closer to the reference value than the missing load curve. However, it should be noted that while these global statistics provide useful indicators, they do not fully capture all aspects of the data, which requires a more localized analysis, such as the effect of different program parameters on the interpolation results.

3.2.3.2 Analysis of the Parameters of the Algorithm

The main objective of this analysis is to identify the combination of k and p that minimizes the RMSE, indicating the optimal parameters for the KNN

imputation. This method of selecting parameters is known as a grid search, a common approach for hyperparameter optimization. Figure 3.2.3 shows the RMSE results based on various k and p.

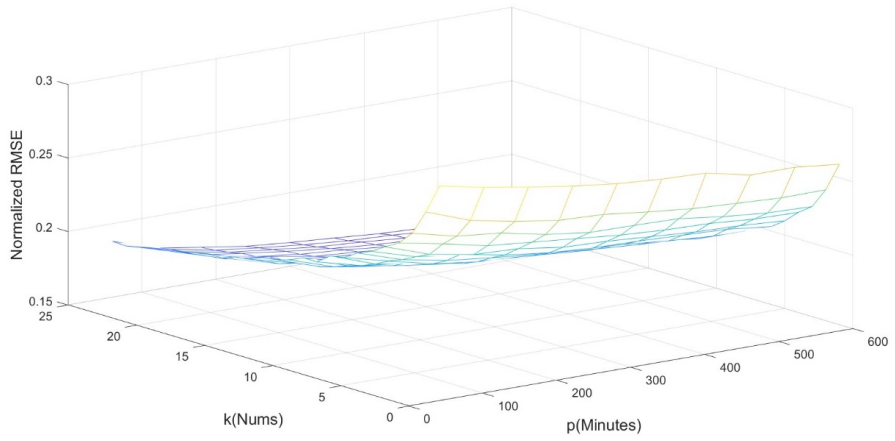


Figure 3.2.3: Normalized RMSE based on changing k and p

The generated plot is a three-dimensional scatter plot visualizing the performance of a K-Nearest Neighbours (KNN) imputation algorithm over a range of parameter settings. The parameters under investigation are the number of neighbours, denoted as k, and the length of the preceding window, denoted as p.

The x-axis represents the varying values of k, which in this case ranges from 1 to 20. The y-axis corresponds to different choices of p, which ranges from 60 to 600 with a step size of 60. The z-axis presents the Root Mean Square Error (RMSE) resulting from the KNN imputation using the corresponding k and p values. Each point on the plot represents the RMSE of the KNN imputation for a specific combination of k and p. The trend line or surface in the plot provides an overview of how RMSE changes with variations in k and p. The normalized RMSE values for the provided data range from 29.4% (0.294) to 15.7% (0.157). The fluctuation within this range depicts the error in the predicted results. Generally, as k and p values increase,

a downward trend in the model's RMSE values is observed, implying an improvement in model performance with an increase in the values of k and p.

There is a negative correlation between k and p values and RMSE, further confirming that the increase in k and p values can enhance model performance. However, such negative correlation is not universal in all circumstances. In certain specific cases, the RMSE does not significantly decrease with an increase in the p values and may even slightly increase at times. Upon closer inspection of the data, it can be seen that as the k and p values increase, the decrease in RMSE slows down. Particularly, around k values of approximately 15 to 20 and p values of approximately 300 to 400, there is a notable slowdown in the decrease of RMSE. This situation might indicate that once k and p values exceed a certain threshold, further increases do not continue to improve model performance and might even cause overfitting, thereby reducing the model's generalizability. This result shows the importance of parameter tuning, which requires finding the optimal combination of k and p to achieve the best model performance, while also avoiding the issue of overfitting.

The task of imputing missing data for consecutive days presents unique challenges. This is primarily due to the temporal variability in domestic power usage, which can differ significantly across dates or seasons. For instance, a household's energy consumption pattern of weekdays might be considerably different from that on weekends. Likewise, energy usage could vary between summer and winter seasons.

Therefore, when it is attempted to impute missing data for several consecutive days by borrowing from other days, the results may not accurately represent the actual power usage for those missing days. Although statisti-

cally the imputed data might appear reasonable, they may not realistically reflect the energy consumption pattern for the missing days.

For example, if a missing Saturday's data is filled with data from Friday, it might give a false impression that Saturday's energy consumption pattern is similar to Friday's. However, in reality, since Saturday is a weekend, people might spend more time at home, thus altering the energy consumption pattern. Similarly, when filling missing winter data with summer data, it might create a false impression that the energy consumption pattern in winter mirrors that of summer. However, in reality, winter might necessitate more energy for heating, thus altering the energy consumption pattern.

Taking these factors into account, in the data processing method mentioned above, the algorithm helps imputation with surrounding similar days (weekday to weekday, holiday to holiday).

The pre-processed datasets can provide high quality energy profiles for the home model simulation and further studies.

3.3 Feature Extraction and Generation on the PV Datasets

3.3.1 Introduction

The utilization of PV datasets in simulation serves a pivotal role in extracting unique solar generation characteristics for different households. This is imperative due to the diverse installation angles of solar panels, varying local environmental conditions, and potential shading impacts, each attributing to distinct energy output profiles per household. By meticulously

simulating and analysing these datasets, inherent features of the individual household solar output can be isolated. These features, independent from specific panel areas or configurations, provide a modular approach to simulations, enabling them to be coupled with various panel sizes or maximum power outputs as per application necessity. This methodology not only facilitates precise individualized energy predictions and modelling but also empowers scalable and adaptable solar generation simulations, essential for strategic energy management, and future solar installation planning and optimization.

The five machine learning methodologies in question, namely Linear Regression, Decision Trees, Random Forests, Support Vector Machines, and Neural Networks, each bear distinct traits and associations with photovoltaic power generation data.

As a fundamental and easily interpretable model, linear regression seeks to establish a linear relationship between features and the target variable [119]. If a linear relationship between photovoltaic power generation and features such as solar radiation intensity exists, Linear Regression would serve as a viable choice. However, it might not be optimal if the relationship is non-linear or more complex.

Capable of handling both classification and regression problems, decision trees can process non-linear relationships and are easily interpretable [120]. In cases where the relationship between photovoltaic power generation and features is non-linear, Decision Trees may be a suitable choice. However, they may overfit the data, especially when the dataset is relatively small.

As an ensemble model based on decision trees, random forests typically demonstrate superior predictive performance and are able to prevent overfitting. Nevertheless, their computational complexity might render them

unsuitable for smaller datasets [121].

Support vector machines (SVM) are models that can address both classification and regression problems [122]. They are adept at handling high-dimensional data and non-linear issues. With the use of different kernel functions, SVMs can adapt to complex non-linear relationships, which may be immensely beneficial for predicting photovoltaic power generation.

As highly potent models, Neural Networks can process complex non-linear issues [123]. However, they require substantial amounts of data, might overfit on smaller datasets, and might exhibit extended training times and poor interpretability.

The selection of Support Vector Machines appears to be a rational choice for modelling the photovoltaic power generation data under consideration. This preference is substantiated by several factors intrinsic to the dataset and the nature of the problem at hand.

Firstly, the dataset predominantly comprises continuous numerical features such as solar radiation intensity. The relationship between these features and the target variable, photovoltaic power generation, is likely to be complex and non-linear. Given these conditions, SVM, with its capability to handle non-linear relationships via the use of different kernel functions, emerges as a potentially powerful tool.

Secondly, the dataset under consideration might not be extensive. In the face of small to medium-sized datasets, SVM typically demonstrates robust performance. This is particularly relevant when the dataset size is insufficient to adequately train more complex models without overfitting, such as Neural Networks.

Lastly, the dataset is presumed to be relatively devoid of noise or outliers.

This absence of disruptive elements increases the likelihood of SVM finding a good fit for the data. In scenarios where data is embedded with substantial noise or outliers, the robustness of SVM towards these elements might be compromised, leading to sub-optimal model performance.

While Support Vector Machines (SVMs) are powerful tools for modelling complex relationships, they have limitations when it comes to dealing with very large datasets and capturing small fluctuations and uncertainties. This is particularly true for photovoltaic power generation data, which can exhibit significant minute-to-minute variability due to factors such as rapid changes in weather conditions.

SVMs tend to focus on the overall pattern in the data and may not adequately capture these small, rapid fluctuations when trained on very granular data. Moreover, training SVMs on large datasets can be computationally expensive and time-consuming.

To overcome these limitations, an approach that combines SVMs and Gaussian Mixture Models (GMMs) is used. The algorithm firstly trains an SVM on hourly data, which reduces the size of the dataset and allows the SVM to capture the overall daily pattern of power generation. Then, a GMM is trained on the changes in power generation from one minute to the next. The GMM, being a parametric model, is able to capture the statistical properties of these rapid fluctuations with a relatively small number of parameters, and it requires significantly less data compared to non-parametric models.

This two-step process, therefore, allows us to capture both the overall trend and the minute-to-minute variability in photovoltaic power generation, making efficient use of the available data and overcoming the limitations of using SVM alone.

3.3.2 A Hybrid SVM-GMM Algorithm for Feature Generation of PV profiles

Utilizing a meticulous dataset sourced from the “Meadow SQL database” detailed in this chapter, the proposed algorithm receives comprehensive inputs for PV power generation. This data, systematically stored and easily retrieved, offers a view of diverse residential solar energy profiles.

The developed algorithm comprises two primary components: a Support Vector Machine (SVM) model and a Gaussian Mixture Model (GMM). The algorithm aims to predict the per-minute power generation from solar panels while accounting for both the overall daily pattern (using the SVM) and minute-to-minute variability (using the GMM).

Initially, the power generation data from the ”Meadow SQL database” is normalized by the maximum power output of PV installation in each houses, effectively transforming the units from watts to a ratio of the actual power output to the maximum possible power output. This approach facilitates the use of a single model for all panels, regardless of their size, by eliminating the influence of the panel surface area on the power output.

Subsequently, an SVM model [124] is employed to predict the hourly power generation. The SVM model is trained on a dataset consisting of solar irradiance data for the entire year [125], the hour of the day, the day of the year, and the identifier of the solar panel. The normalized power data from the initial step is averaged for each hour, which reduces the variety and size of the dataset. This process enables the SVM model to concentrate on the overall daily pattern. The algorithm runs in Matlab, while the parameters of a function are set as: ‘KernelFunction’, ‘ref'KernelScale’, ‘auto’. 30% of the datasets are used as cross test datasets. The performance of the

SVM model is evaluated using several metrics, including the Mean Squared Error (MSE), Root Mean Squared Error (RMSE), Mean Absolute Error (MAE), and R-squared. R-squared is a statistical measure that represents the proportion of the variance for a dependent variable that is explained by an independent variable or variables in a regression model.

The algorithm's second component, a GMM, is utilized to simulate the variability in power generation from minute to minute. The GMM is trained on the differences in power output from one minute to the next for all solar panels. This data is derived by calculating the difference between the normalized power output in the first step for each consecutive minute. The GMM is a parametric model, enabling it to capture the statistical properties of these rapid fluctuations with a relatively small number of parameters, and thus requires less data compared to non-parametric models. The k value for the proposed GMM model is 2, while the regularization value is 0.1.

Upon training, the GMM can generate simulated minute-to-minute power changes. These simulated changes are added to the SVM's hourly predictions to produce the final minute-by-minute power predictions.

The effectiveness of the GMM is validated by comparing the mean and standard deviation of the actual minute-to-minute power changes with those of the simulated changes. These statistical measures provide insight into how well the GMM has captured the overall characteristics of the minute-to-minute variability in the power data.

3.3.3 Results Based on the Hybrid Algorithm

3.3.3.1 SVM Results

The Support Vector Machine (SVM) model has demonstrated a reasonable level of performance when predicting hourly photovoltaic power generation data, as evidenced by the provided metrics. The Mean Squared Error (MSE) of 0.0151 and the Root Mean Squared Error (RMSE) of 0.1229 both suggest that the model can closely predict the actual power generation with a fairly high degree of precision. Meanwhile, the Mean Absolute Error (MAE) of 0.0594 indicates that the average difference between the model's predictions and the actual values is relatively small, further confirming the model's accuracy. Lastly, the R-squared value of 0.7179 represents that the model can explain over 71% of the variance in the data, further demonstrating the model's effectiveness. A specific day for the SVM results would be shown by the GMM results in the following contents.

3.3.3.2 GMM Results

The raw datasets from the database and the generated data by algorithm exhibit identical means, both approximating zero. This suggests that the Gaussian Mixture Model (GMM) has accurately modelled the central tendency of the power change distribution. As the mean signifies the average minute-by-minute power alterations, its approximation to zero in both datasets indicates that, on average, there is no substantial power change.

However, the standard deviation of the simulated dataset is lower compared to the empirical data (0.0319 versus 0.0476, respectively). Standard deviation is a measure of data dispersion, and a lower value in the simulated dataset suggests that the modelled power changes are less volatile

compared to the empirical observations. This reduced standard deviation implies that the GMM model may be underestimating the variability inherent in the real power changes. As such, although the GMM captures the general trend of power alterations, it may not fully replicate the actual volatility observed in the solar power output.

3.3.3.3 Results of the PV Profile Generation

After the operation of the two parts of models, the feature generation results of the PV generation model over three days of PV simulation is shown in Figure 3.3.1 for further analysis.

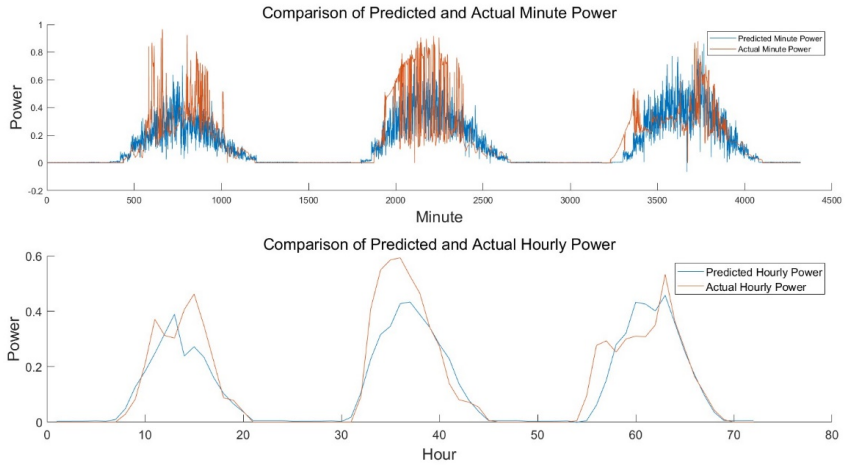


Figure 3.3.1: Comparison of results from the SVM and GMM parts of the simulation

The combined graphs represent a comparison between actual and predicted normalized photovoltaic power generation data (kW predicted power/kW max PV power output) over a span of three days. The top graph corresponds to a minute-by-minute prediction, and the bottom graph represents an hourly prediction. The predictions were obtained by a combination of Support Vector Machine (SVM) and Gaussian Mixture Model (GMM) methodologies, where the SVM was utilized for the hourly prediction and

the GMM was based on the SVM results to generate minute-by-minute predictions.

In the top graph, the blue curve illustrates the predicted minute-by-minute power generation, and the orange curve represents the actual minute-by-minute power generation data. It can be observed that the predicted power generation aligns well with the actual data, capturing the overall trends and patterns. However, the model appears to underestimate the variability of the actual data, especially during periods of rapid change. This discrepancy could be attributed to the inherent challenge in accurately modelling the minute-by-minute fluctuations in solar power due to factors such as rapid changes in weather conditions.

In the bottom graph, the hourly power generation predicted by the SVM is compared with the actual hourly power generation. The blue curve represents the SVM-predicted power, and the orange curve denotes the actual power. The model effectively captures the peak power generation during the day and the absence of power generation at night. However, similar to the minute-by-minute model, it also seems to underestimate the variability during periods of rapid change.

In conclusion, while the combined SVM and GMM model provides a reasonably accurate prediction of photovoltaic power generation trends over the course of the day, there is room for improvement in accurately capturing rapid changes and variability in power generation. Further refinement of the model, or the incorporation of additional factors such as real-time weather data, could potentially enhance its predictive accuracy.

In the integrated model, the simulated PV data, derived from the SVM-GMM methodology, not only preserves the intrinsic characteristics of the collected dataset but also adapts to various condition requirements dur-

ing simulation. This ensures that the energy management and trading strategies within a community are not only rooted in realistic PV generation patterns but also versatile and applicable under different simulation scenarios.

3.4 Conclusion

In this chapter, the insights into energy consumption and PV generation patterns offer a foundational understanding that can inform future energy policies and renewable energy utilization strategies. The demonstrated efficacy of the KNN imputation algorithm affirms its utility in managing dataset integrity, albeit with noted limitations in handling consecutive days of missing data. The SVM-GMM hybrid model exhibits potential as a predictive tool for PV generation, preserving dataset characteristics enhances the versatility and applicability of the model in various simulation scenarios.

According to the analysis and discussion of results, the conclusion can be listed as follows:

- Significant variability is observed in domestic electricity demands, aligning with documented national averages.
- Mean self-consumption from PV systems demonstrates substantial domestic PV system usage, albeit with notable efficiency disparities across households.
- Seasonal and daily variations in energy usage patterns are accentuated, underscoring the influence of temporal factors on consumption and production profiles.

- The K-Nearest Neighbours (KNN) algorithm effectively handles the imputation of missing data in power consumption profiles, with a keen sensitivity to parameter selection via grid search methodology.
- Challenges persist in imputing data for consecutive days, warranting a nuanced approach that accounts for variation consumption patterns across different days and seasons.
- A hybrid model, combining Support Vector Machine (SVM) and Gaussian Mixture Model (GMM), yields reasonable accuracy in predicting hourly PV power generation data.
- While the model adeptly captures general PV generation trends and patterns, variability, and rapid changes in power generation present predictive challenges.
- The simulated PV data, derived from the SVM-GMM methodology, maintains intrinsic dataset characteristics while being adaptable to varied simulation condition requirements.

Chapter 4

Home Energy Management System and Battery Control

4.1 Home Energy Management System

4.1.1 Introduction

A Home Energy Management System (HEMS) is an intelligent system designed to optimize and manage the use of energy in households. HEMS integrates and coordinates various energy devices and systems within a home using advanced technologies and algorithms, aiming to achieve energy efficiency, cost-effectiveness, and sustainability.

For monitoring and control, HEMS utilizes sensors, smart meters, and other monitoring devices to continuously track energy consumption and production in a home [126, 127]. It can monitor electricity, gas, and water usage, collecting relevant data. Additionally, HEMS has the ability to control the operation of energy devices in a home, such as adjusting lighting, temper-

ature control, and home appliances, to achieve efficient energy utilization and conservation.

In the view of data analysis and optimization, HEMS analyses household energy data and provides energy management advice and optimization strategies [128]. It can develop optimal energy usage plans based on factors such as user energy demands, energy costs, and energy supply-demand conditions. By optimizing energy scheduling and flow, HEMS maximizes the utilization of renewable energy sources, reduces energy waste, and lowers energy costs and carbon emissions.

When involving the domestic users, HEMS encourages user participation in energy management decisions and provides real-time feedback through visual interfaces [129]. Users can monitor energy usage, set energy preferences, and view energy costs through mobile applications or online platforms. User engagement enables a better understanding of energy consumption and behaviour, allowing users to take appropriate actions to reduce energy waste.

HEMS features intelligence and automation capabilities, automatically adjusting the operation modes of energy devices based on user preferences and environmental conditions [130, 131, 132]. It utilizes artificial intelligence, machine learning, and predictive algorithms to forecast energy demands, optimize energy scheduling, and make real-time adjustments as needed.

In summary, implementing HEMS offers several benefits to households, including reduced energy costs, improved energy utilization efficiency, decreased reliance on traditional energy sources, and providing a comfortable living environment while minimizing environmental impacts [133, 134]. HEMS is an intelligent home energy management system designed to achieve efficient and cost-effective energy utilization through monitoring, control,

data analysis, and optimization strategies. By involving users and providing feedback, HEMS empowers household members to effectively manage and control their energy usage, leading to sustainable energy management goals.

In this chapter, the battery degradation model will be established, and various HEMS control algorithms will be operated and compared. Based on this investigation, an economic sizing of the required battery and an analysis of the home energy system will also be proposed.

4.1.2 HEMS Infrastructure

The HEMS (Home Energy Management System) infrastructure is a comprehensive framework designed to support and manage the operation and optimization of residential energy systems. This infrastructure encompasses hardware, software, and communication technologies to enable energy monitoring, control, and optimization. A typical HEMS infrastructure with microgrids, ICT interface and intelligence management systems is shown in Figure 4.1.1 [135].

The HEMS infrastructure typically includes multiple sensors and measurement devices to monitor real-time energy flows and the electricity consumption of household appliances [2]. These sensors can measure the power generation of solar photovoltaic systems, the state of charge/discharge of batteries, and the energy consumption of household appliances. Accurate data collection from sensors is crucial for the operation and optimization of HEMS.

The HEMS infrastructure utilizes data collection and communication technologies to gather and transmit sensor data. This can include wireless sen-

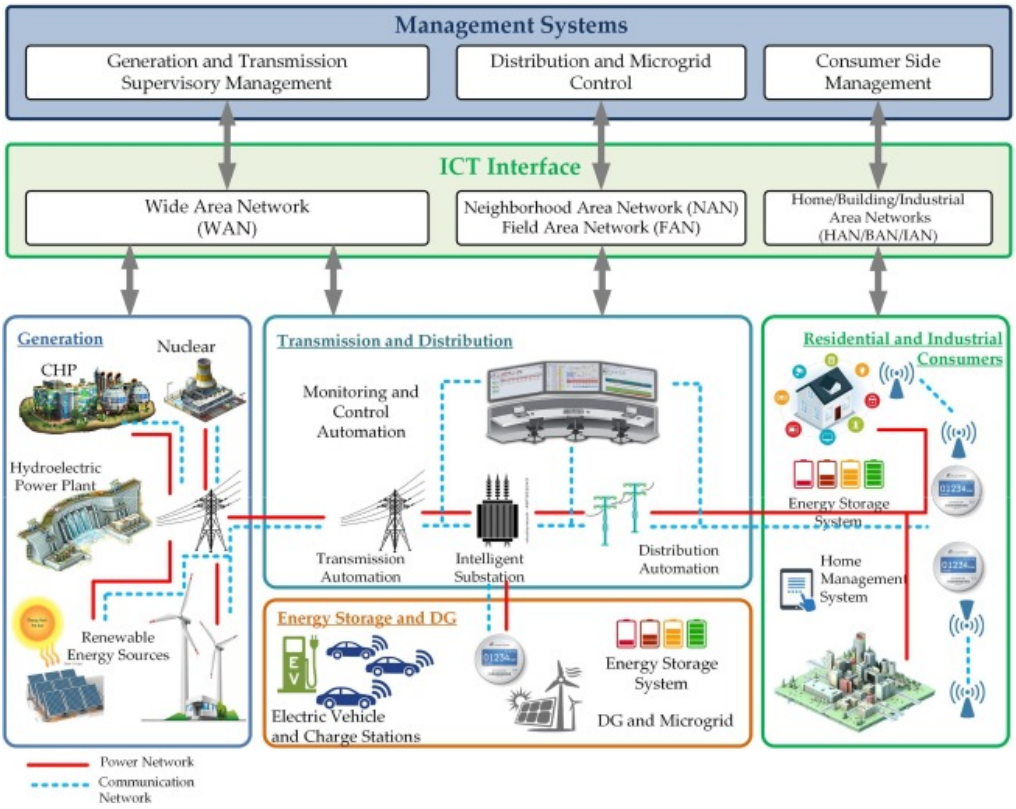


Figure 4.1.1: A typical HEMS infrastructure [132]

sor networks, Internet of Things (IoT) technologies, smart meters, among others. Data collection and communication technologies enable real-time transmission of energy data to the HEMS system, forming the foundation for energy management and optimization.

The HEMS infrastructure includes data storage and processing systems to store and manage large volumes of energy data [136]. This can be cloud servers, local storage devices, or distributed databases. Data storage and processing systems analyze, aggregate, and store sensor data to support subsequent energy management decisions and optimization.

The HEMS infrastructure requires powerful energy management software. This software typically includes modules for energy monitoring, energy optimization, and energy forecasting. The energy monitoring module provides real-time visualization of energy data, the energy optimization mod-

ule allocates, and schedules energy based on real-time data, and the energy forecasting module predicts future energy demand and supply.

The HEMS infrastructure should have a user-friendly interface and control system to allow household users to conveniently monitor and control the energy system. This can be a mobile application, a web interface, or a dedicated control panel. The user interface and control system enable household users to view real-time energy data, set energy optimization strategies, and manually control the energy system.

The HEMS infrastructure should also include mechanisms for fault detection and safety protection to ensure the stable and safe operation of the energy system. This can involve fault monitoring, alarm systems, current overload protection, battery overcharge/discharge protection, and more. Fault detection and safety protection mechanisms help mitigate the risk of system failures and protect equipment and household safety.

In summary, the HEMS infrastructure is a comprehensive framework consisting of sensors, data collection and communication technologies, data storage and processing, energy management software, user interfaces and control systems, as well as fault detection and safety protection. These components work together to enable monitoring, control, and optimization of residential energy systems, leading to improved energy efficiency, reduced energy costs, and enhanced utilization of renewable energy.

4.1.3 Sub Systems in HEMS

In a Home Energy Management System (HEMS), several subsystems play a crucial role in optimizing energy consumption and enhancing overall energy efficiency. Some of these components include:

Photovoltaic (PV) systems consist of solar panels that convert sunlight into electricity. They are commonly integrated into HEMS to generate clean and renewable energy for household consumption [137]. PV systems help reduce reliance on grid power and can even feed excess energy back into the grid through net metering.

Energy storage systems, typically in the form of batteries, are used in HEMS to store excess energy generated by PV systems or during off-peak periods [138]. Battery energy storage system can also be recharged using cheap(er) electricity. These stored energy reserves can be utilized during high-demand periods or when solar generation is insufficient. Batteries enable energy shifting and help maximize self-consumption of renewable energy.

Heating, Ventilation, and Air Conditioning (HVAC) systems are responsible for maintaining indoor comfort and temperature control [139]. In HEMS, HVAC components are often equipped with energy-efficient features and smart control algorithms to optimize energy consumption based on occupancy, weather conditions, and user preferences. This ensures efficient heating and cooling operations while minimizing energy waste.

HEMS can integrate electric vehicles as a controllable load and energy storage device [140]. EVs can be charged during periods of low electricity demand or when renewable energy generation is high, thereby reducing reliance on fossil fuel-based transportation and enabling vehicle-to-grid (V2G) capabilities. This allows EVs to serve as energy storage units and supply electricity back to the grid during peak demand.

Smart appliances, such as refrigerators, washing machines, dishwashers, and smart thermostats, are integrated into HEMS for optimized energy management [139]. These appliances can communicate with the HEMS

controller and adjust their operation based on energy pricing, user preferences, and grid conditions. They can also schedule their operation during off-peak hours to take advantage of lower energy costs.

By integrating these components into a HEMS, homeowners can achieve greater control over their energy consumption, reduce reliance on grid power, maximize the utilization of renewable energy sources, and optimize overall energy efficiency in their homes.

4.1.4 Developments and Challenges for HEMS

HEMS has gained significant attention in the research community as a promising solution for optimizing energy consumption in residential buildings. Researchers have focused on various aspects of the HEMS, including system architecture, algorithms, optimization techniques, and user behaviour analysis [2, 141, 5].

One area of research involves the development of intelligent algorithms for energy management in HEMS. These algorithms aim to optimize energy consumption by considering factors such as energy prices, weather conditions, user preferences, and the availability of renewable energy sources [142]. Techniques such as machine learning, optimization algorithms, and predictive control are used to achieve efficient energy scheduling and load management [143].

Another research direction is the integration of renewable energy sources into HEMS. This includes the integration of solar photovoltaic (PV) systems, wind turbines, and energy storage devices [15, 144]. Researchers have investigated methods to maximize the utilization of renewable energy, minimize grid dependence, and enable energy self-sufficiency within

households.

Behavioural analysis is another important aspect of HEMS research. Understanding user behaviour and energy consumption patterns helps to design effective energy management strategies. Researchers have explored techniques for monitoring and analysing user behaviour, such as occupancy detection, activity recognition, and user feedback mechanisms [145]. This information is used to personalize energy management and provide recommendations to users for energy-saving actions.

The interoperability and communication protocols of HEMS have also been studied. Ensuring seamless integration between different devices and systems within a home is crucial for effective energy management. Research has focused on developing standard communication protocols, such as Zigbee, Z-Wave, and Wi-Fi, to enable interoperability and data exchange between different HEMS components [7, 12].

Furthermore, researchers have conducted case studies and field trials to evaluate the performance and effectiveness of HEMS in real-world settings [146, 147, 148]. These studies assess the energy savings, user acceptance, and economic viability of HEMS implementations. Results from these studies provide valuable insights into the practicality and potential challenges associated with HEMS adoption.

Overall, research on HEMS is a multidisciplinary field that encompasses areas such as energy management algorithms, renewable energy integration, user behaviour analysis, communication protocols, and real-world evaluations. These studies contribute to the development and advancement of HEMS technologies, aiming to achieve sustainable and efficient energy consumption in residential buildings.

4.2 Modelling of Batteries in Home Energy Systems

4.2.1 Introduction

Battery degradation is a complex process influenced by various factors that contribute to the gradual loss of a battery's performance and capacity over time. One significant factor is calendar aging [149, 150], which refers to the natural ageing of the battery even when it is not in use. Chemical reactions within the battery can occur over time, leading to the degradation of its components and a decrease in performance. Cycling ageing is another important element of battery degradation [151]. It occurs during the repetitive charging and discharging cycles of the battery during its operation. Factors such as the depth of discharge, charging rates, and operating temperatures can impact the extent of degradation experienced by the battery during each cycle. The depth of discharge (DoD) also affects battery degradation [149]. Batteries that are frequently discharged to a high DoD may experience faster degradation compared to those that are discharged to a shallower DoD. Managing the depth of discharge and avoiding extreme states of charge can help reduce degradation.

Temperature plays a critical role in battery degradation [152]. High temperatures accelerate the degradation process by promoting increased chemical reactions and the breakdown of electrode materials, resulting in capacity loss. Controlling the temperature during battery operation is crucial for mitigating degradation and prolonging battery life. Chemical reactions and side reactions within the battery during charging and discharging processes can also contribute to degradation [153]. Over time, these reactions can lead to the formation of side products or undesired reactions that degrade

the battery's performance.

It's important to consider these corresponding factors, while the influence of these factors on battery degradation can be changed depending on the specific battery chemistry, design, and usage conditions. Managing these factors effectively through proper battery management practices can help minimize degradation and extend the lifespan of the battery. The authors of [153] proposed an iterative formulation to evaluate the effects of battery capacity degradation. Building upon this, in [154], a degradation model was proposed depending on the weighted sum of exponential functions. This model considers N degradation events and incorporates factors such as the average, or the normalized standard deviation of the state of charge of the battery, and the temperature to compute the capacity fade.

These equations allow for the representation of different situations of operations and the number of cycling loops. To analyse the cycling operation, the rainflow counting algorithm (RCA), commonly used in fatigue analysis [155], is employed.

4.2.2 Linear Battery Degradation Formulae

The depth of discharge (DOD) refers to the difference in state of charge (SOC) from the top and bottom levels within a cycle and plays a significant role in cycle aging. A cycle-counting algorithm is used to detect half-cycles under different periods of the batteries, such as charging, discharging. The algorithm detects cycles by monitoring the zero-crossings in the power-flow at the battery terminal. Whenever the power-flow reaches zero, it signifies the completion of a half-cycle. The DOD is then calculated by determining the SOC difference between the beginning and end of the counted battery

operation cycle.

In one research [156], Rosenkranz suggests that smaller DOD values result in reduced ageing compared to larger DOD values. In this project, a scaled model curve is utilized to simulate 5500 full cycles for a battery, considering a remaining battery capacity as 80% of its initial value, as reported for the Powerwall product [157]. The manufacturer value of operation cycles used in the model are provided in Table 4.2.1 [157, 158]. The values in the table mean the equivalent number of complete cycles with the corresponding DOD until the capacity drops to 80%. To determine the equivalent full cycles for each specific DOD value, piecewise cubic interpolation was employed based on the given parameter set. Commonly, 80% of the remaining total battery capacity is considered a reasonable range of use [159].

Table 4.2.1: The relationship between equivalent and DOD

DOD/%	**Reference aging**	**Strong aging**
10	14,500	8700
25	9500	5700
50	6900	4100
80	5500	3300
100	5000	3000

Considering the conditions for battery capacity ranges from full to 80% of a new one, calendar ageing represents the natural degradation of the battery over time, and its rate is influenced by factors such as temperature and state of charge (SoC) of the battery. Based on linear relationships, the life lost in capacity (L_{cal}) and the ratio of loss (r_{cal}) at a specific period i can be represented as:

$$L_{cal} = (1 - 0.8)Capacity_{battery}\frac{t_i}{t_{life}} \tag{4.2.1}$$

$$r_{cal} = (1 - 80\%)\frac{t_i}{t_{life}} \tag{4.2.2}$$

Where the 80% is lower limit as a benchmark for battery usage, $Capacity_{battery}$ means the raw capacity of a new battery which is brand new and unused. t_{life} is the time period for the lifespan of battery degraded to 80% limit, which is 15 years according to manufacturer [157]. t_i is the length of the specific time for calculation.

$$L_{cyc} = (1 - 80\%)Capacity_{battery}\frac{DoD_i}{DoD_{life}} \tag{4.2.3}$$

$$r_{cyc} = (1 - 80\%)\frac{DoD_i}{DoD_{life}} \tag{4.2.4}$$

Where the 80% is lower limit as a benchmark for battery usage, $Capacity_{battery}$ means the raw capacity of a new battery which is brand new and unused. DoD_{life} is the number of discharge cycles of battery degraded to 80% limit, which is 5500 according to the table. DoD_i is the number of cycles during specific time t_i.

In general, as the time period and total cycles for fixed capacity is stable, the corresponding number of discharge cycle depends on the time period that used in the calculation. For instance, when the time period is when a new battery was firstly used, the capacity would be higher than the later time with the same duration, while the number cycles are therefore less.

4.2.3 Rainflow Counting Algorithm

In the calculation of capacity loss of batteries, the depth of discharge, as well as the discharge cycles are crucial. In battery storage systems, differ-

ences of full cycle and half cycle are of great importance [160, 161]. The rainflow counting algorithm is a method used to analyse cycle loads[162].

The principle of the rainflow counting algorithm involves gathering load data, identifying peaks and valleys, and counting stress cycles by their amplitude and duration [163]. One of the advantages of the rainflow counting algorithm is its intuitive reliability [155, 164]. However, the rainflow counting algorithm requires data preprocessing, including filtering, sampling, and interpolation, and large datasets or smaller cycles might lead to counting errors.

Rainflow counting has significant applications in simulating battery degradation due to cycling, temperature, and aging[165]. This algorithm helps monitoring degradation patterns of the charging and discharging cycles of the battery [166].

By applying a rain flow counting algorithm, prediction of the remaining battery life would be possible when the battery capacity performance will drop[167]. This information is crucial for optimizing battery usage, scheduling maintenance or replacement, and ensuring the reliability of energy storage systems. Moreover, the algorithm enables the evaluation of different operational conditions and their impact on battery degradation [168], aiding in designing strategies for battery management.

In summary, the application of the rainflow counting algorithm in battery degradation simulation provides valuable insights into the cyclic loading patterns experienced by batteries.

In this project, considering the long duration of the simulations, a variable that varies within a stable range is much more suitable for operation under the rainflow counting algorithm. As the battery capacity changes due to

loss, the SOC is the input that is used for the algorithm. Afterwards, the results of the number of equivalent full cycles and half cycles will be the output.

4.2.4 Non-linear Degradation of Battery Capacity

In the previous work, the influence on degradation of time and discharging during use is analysed, and the method of calculation is also shown. The total degradation ratio can be presented as Equation 4.2.5.

$$r_{total} = r_{cal} + r_{cyc} = (1-80\%)\left(\frac{t_i}{t_{life}} + \frac{DoD_i}{DoD_{life}}\right) = (1-80\%)(1+k\frac{d_{DoD}}{d_t})\frac{t_i}{t_{life}} \tag{4.2.5}$$

Where k is the ratio between a lifetime period and the corresponding cycles. And the differential $\frac{d_{DoD}}{d_t}$ is the proportion of change over time, which is quite small. In situations where all cycles are identical, the state of charge (SoC) within a single cycle remain consistent with the overall operation. The calculated results of this method are close to the linear equation.

Contrary to the assumptions made by the calendar and cycle ageing models, observations from lithium-ion battery degradation experiments reveal a non-linear degradation rate in relation to the number of cycles. The results from battery ageing tests (Figure 4.2.1 [169]), which shows different stages of battery use and ageing, demonstrate that during cycling operation, the degradation rate is notably higher when the number of cycles is small, compared to the larger numbers. Upon initial operation of a new battery, there is a consumption of a specific quantity of active lithium ions required to establish a protective film [170], which is called Solid Electrolyte Interphase

(SEI) film. The rate of film formation gradually decreases once a stable film has been established [171, 172].

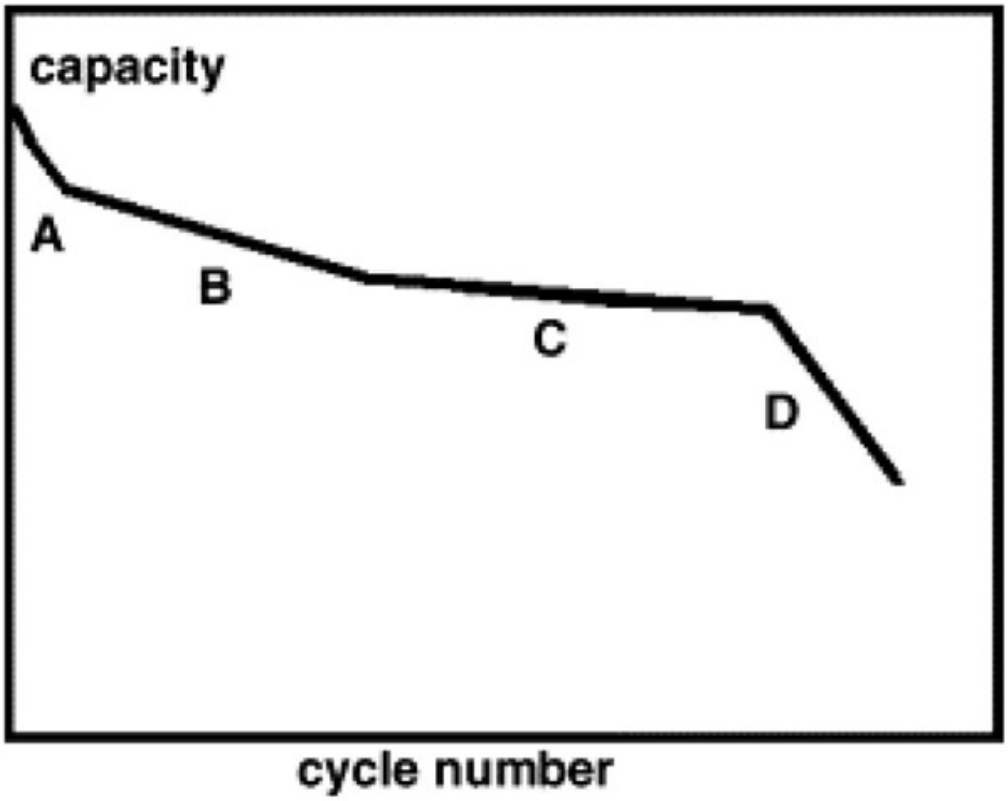


Figure 4.2.1: The trend curve of cycle number and capacity [166]

Additionally, the degradation rate accelerates rapidly as the battery approaches its end of life (EoL). These findings indicate that the degradation rate of lithium-ion batteries is dependent on the remaining capacity ratio, rather than remaining constant throughout the cycles as assumed by the models. Hence, the relationship between battery life cost and actual degradation rate can be expressed as:

$$f_L\left(L_{total,i}, r_{total,i}\right) = \frac{d_L}{d_{cycle}} = \left(1 - L_{total}\right) r_{total,i} \tag{4.2.6}$$

When the battery life cost L is presented on one side, the equation would be:

$$L = 1 - e^{-r} \tag{4.2.7}$$

Based on this, the simulation result for the battery degradation is shown in Figure 4.2.2.

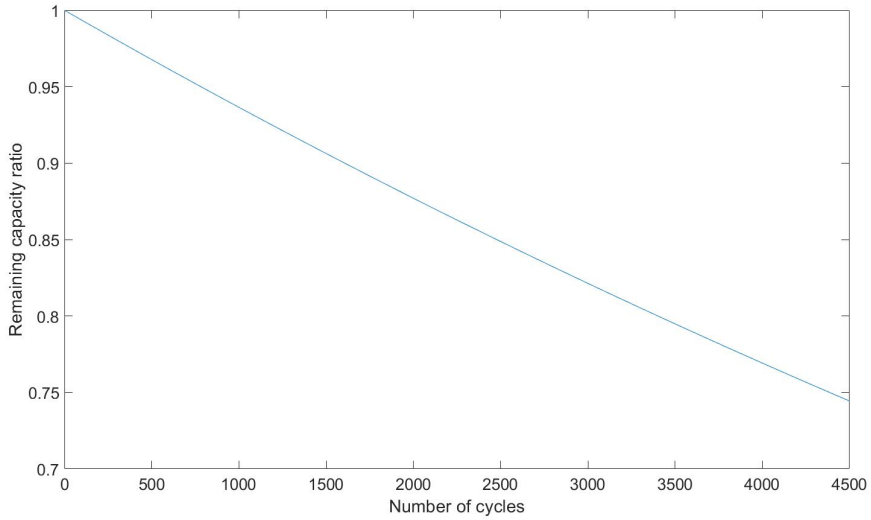


Figure 4.2.2: The curve of remaining capacity ratio and operating cycles

However, this existing correlation does not capture the rapid degradation in the initial cycles, while the SEI films are mentioned in the previous section. The simulation result for the simple exponential equation leads to a steady line for the declining battery capacity. The assumption is made that a specific fraction of the active material in the battery contributes to the SEI film. Its rate of formation is inversely related to the amount of existing SEI film, and it ceases once a fixed SEI film has been established.

Assuming α_{sei} represents the fraction of the consumed battery capacity that is used for film formation, the normalized battery capacity can be divided into the SEI portion α_{sei}, and the remaining portion $(1 - \alpha_{sei})$.

$$L = 1 - \alpha_{sei} e^{-r_{sei}} - (1 - \alpha_{sei}) e^{-r_{total}} \tag{4.2.8}$$

According to studies conducted by researchers [173, 174], it has been determined that $\alpha_{sei}$is dependent on factors such as the conditions of layer

formation and the specific surface area of the graphite ranging from 3% to 8%. Since the SEL film formation is also impacted by the temperature and utilization, r_{sei} is assumed as being proportional to r_{total} :

$$r_{sei} = \beta_{sei} r_{total} \tag{4.2.9}$$

Hence, the equation can be rewritten as one with a single dependent variable, as:

$$L = 1 - \alpha_{sei} e^{-\beta_{sei} r_{total}} - (1 - \alpha_{sei}) e^{-r_{total}} \tag{4.2.10}$$

Applying existing experimental profiles of battery from a database or test centre [175], the fixed parameters that adapt to different brands of batteries can be obtained.

4.2.5 Results of Modelling of Battery Degradation

In the simulation of battery degradation, with the change of power and SOC as inputs, the rainflow algorithm is one of the key functions which is aimed at obtaining the operation cycles of battery discharge. At the end of every day of simulation, using cycle numbers from the one-minute battery power simulation results with the rain flow counting algorithm, the accumulated cycles in one year are calculated and shown in Figure 4.2.3.

The X-axis is the number of days, which ranged from day 1 to day 365. For the Y-axis, it is the total discharge cycle, which changes in every day. Comparing to the time step of one day in the graph, the input SOC value, which is used for calculating cycles through the rainflow counting algorithms, is based on the resolution of one minute. Then the result of cycles from rainflow counting algorithms is calculated by day and shown in the

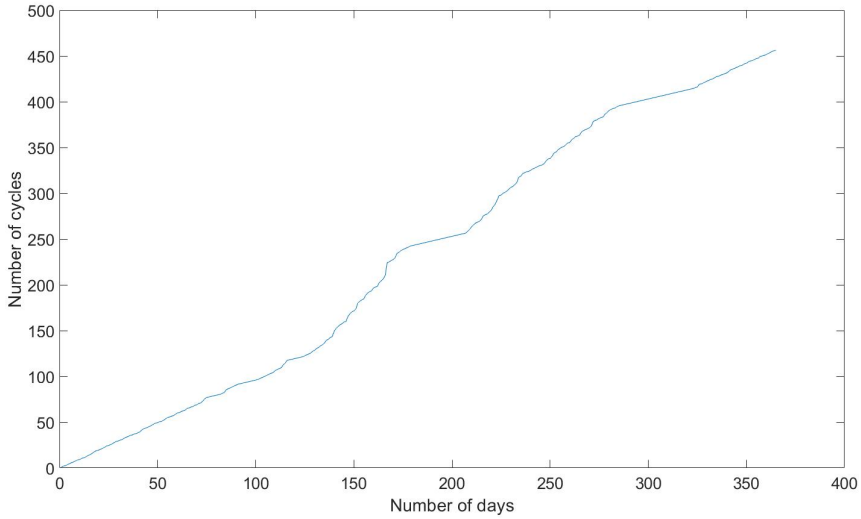


Figure 4.2.3: The curve of simulation days and accumulative battery discharge cycles

graph. The curve of the number of cycles is monotonically increasing along with the number of days, as would be expected.

The trend of the curve is very close to a straight line, where the rate of ascent is higher in summer. This is due to the higher solar irradiance in summer, which brings more fuller usage of the battery system. For instance, in most home battery storage systems, the local consumption of generated PV energy is important. The more solar irradiation in summer leads to more PV generation, thus more energy is charged and discharged to and from batteries, with the number of cycles growing. The sum of the number of cycles is 471.5 in one year with a new battery, which is reasonable compared to 5500 cycles in 15 years [158]. On average every day, the average value of the number of cycles is about 1 to 1.5, which is in line with reality.

The result of the number of cycles is affected by the input SOC, and both in reality or in simulation, the SOC is affected by the load, solar power generation, hardware configuration, control algorithm and other aspects. Even

if the battery capacity of the first year and the second year are different, if the same SOC is input, the same cycle number result will be obtained, so it is meaningless to control a single variable for comparison. On the other hand, if the battery capacity is slightly smaller or much smaller than the actual user demand, the battery will be fully used daily, so the change in the cycle number result is very small.

Based on the effective rainflow counting algorithm, the change of battery capacity can also be obtained by the non-linear calculation method. In order to ensure the validity of the calculated parameters, the results of the theoretical model and the experimental results must be as close as possible, so the parameters (α , β) are adjusted based on minimizing the variance. The comparison between iteration simulation results and test results from ITP Renewables [175] based on minimum deviation is shown in Figure 4.2.4.

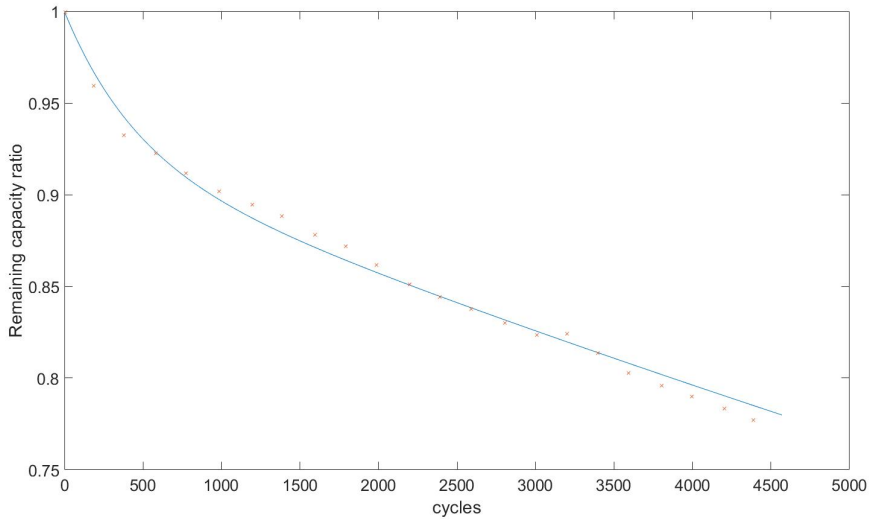


Figure 4.2.4: Comparison of proposed simulation results and test results from ITP report

In order to obtain more intuitive results, the x-axis is no longer the number of days but the number of cycles. Meanwhile, the y-axis is the ratio of the

remaining effective battery capacity of the initial capacity. In the figure, the blue curve is the result based on simulation calculations, while the x-shaped points are from the experimental results of the battery test centre.

The capacity ratio curve declines rapidly at first, and the downward trend gradually decreases after the ratio is 0.95. At about 0.88, the change of the descending slope tends to stop, after which it is closer to a stable straight line. This phenomenon of battery capacity change is not only consistent with previous research results, but also in line with the expectations of the calculation method design. The optimization result of searching parameters is that α is 0.0791, β is 60.95. These values are in line with previous research and within the expectations that are consistent with reality.

4.2.6 Summary of Battery Degradation Model

In this section, the modelling and degradation of batteries within domestic energy systems are addressed. Factors contributing to battery degradation, such as calendar aging, cycling aging, and depth of discharge (DoD), are delineated. The rainflow counting algorithm is introduced as a method to accurately capture the stress cycles experienced by batteries throughout their lifecycle.

The primary objective is the integration of these battery degradation models into domestic energy management and battery control algorithms. By doing so, predictions related to battery lifespan and performance can be enhanced, facilitating optimized strategies for domestic energy system management. Linear and non-linear battery degradation models are detailed, providing methodologies for calculating battery capacity loss. Furthermore, the application of these models within energy management strategies aims

to ensure optimized battery utilization and longevity.

In conclusion, the battery degradation models and algorithms offer a comprehensive approach to understanding and managing batteries within domestic energy systems, thereby promoting efficient energy utilization and system reliability.

4.3 Control Algorithms and Home System Design

4.3.1 Introduction

HEMS systems have garnered significant attention in recent years within the research community. In one study [176], priority levels were assigned to different electrical appliances in order to optimize costs and ensure the provision of necessary services. Another approach [177] involved scheduling appliances based on their preferred time of use, taking into account limited power consumption during specific time periods. Furthermore, the integration of energy storage in HEMS offers benefits beyond load shifting. It plays a significant role in managing power consumption and voltage levels, particularly during peak and off-peak hours [178].

To manage total demand and decrease peak energy consumption, a binary backtracking search algorithm was employed, resulting in a more than 20% reduction in peak-hour demand [179]. However, this study did not specifically analyse electricity costs. Another research study [180] focused on the combination of scheduling of smart appliances and a shared HEMS among multiple households, aiming to minimize peak energy consumption and

electricity costs. Additionally, a system incorporating floating pricing and accounting for uncertainties in a PV energy generation was presented, effectively minimizing costs of energy through strategic electricity purchase, sale, and storage [181]. However, long-term economic analysis was not addressed in this approach.

One of the key challenges in the economic benefit of HEMS is sizing of BES in terms of battery capacity and power ratings [182]. An efficient and economical strategy of sizing appliances involves meeting entire system demand while minimizing operation costs [183, 184]. For instance, a study [185] investigated a stand-alone system consisting of PVs, and a battery system and wind turbines, with the objective of minimizing costs by determining the optimal settings.

In home energy management systems (HEMS) with batteries, several commonly used control algorithms exist, each with their own advantages and disadvantages.

The Rule-based control is an approach where predefined rules and strategies are used to control the operation of the energy system. This algorithm is often simple to implement and has lower computational costs, offering real-time performance. However, rule-based control may lack adaptability to dynamic environments and changing demands, as the rules are relatively fixed [186].

The Model Predictive Control (MPC) is an algorithm that utilizes mathematical models to predict future energy demands and battery states, optimizing control decisions based on these predictions [187]. MPC is capable of considering the constraints while optimizing, allowing for flexibility in addressing different operational requirements and goals. However, MPC requires high computational power and longer computation time, making

it less suitable for real-time applications that demand quick responses.

The Optimal Power Flow (OPF) algorithms optimize the power flow allocation in the energy system to achieve optimal control [188]. Taking into account factors such as electricity prices, battery state, and other constraints, OPF minimizes energy costs or maximizes energy utilization efficiency. OPF algorithms provide globally optimized solutions but are computationally complex and require accurate system parameters and models.

The Genetic Algorithm (GA) is an optimization algorithm inspired by biological evolution principles [189]. It can be used to optimize control parameters or strategies for energy systems. By simulating the processes of natural selection and genetic mutation, GA searches for the best control solutions. Genetic algorithms have good global search capabilities but may be less efficient in terms of computational speed, when it is compared to other HEMS control algorithms.

Each algorithm has its own strengths and weaknesses and is applicable to different scenarios and requirements. The selection of a suitable control algorithm depends on factors such as system complexity, computational resources, real-time requirements, and the need for optimization performance and robustness. Additionally, the effectiveness of the control algorithm also relies on the selection of algorithm parameters and the accuracy of the system simulation. Therefore, in practical applications, a comprehensive consideration of various factors is necessary, and the most suitable control algorithm should be chosen based on the specific circumstances.

4.3.2 System Model of the HEMS

The control algorithm incorporates a battery-PV system model to establish the operational boundaries of the battery and maintain energy balance within the whole system. In the real-time simulation, the energy is balanced under each time step hence is based on the unit of power, and system constraints are expressed through the following equations:

The total power balance equation in the system can be represented as:

$$PG_{import}(t) - PG_{export}(t) + P_{BESS}(t) = \quad P_{load}(t) - P_{PV_gen}(t) \tag{4.3.1}$$

The equation illustrates the power flow dynamics within the system, where $PG_{import}(t)$ denotes the power imported from the main electricity grid during time interval t (measured in kilowatts, kW), $PG_{export}(t)$ denotes the power exported to the main electricity grid during time interval t (in kW), $P_{load}(t)$ represents demand of the home load energy during time interval t (in kW), $P_{PV_gen}(t)$ represents the electrical power generated by the PV system installed at the residence during time interval t (in kW), and $P_{BESS}(t)$represents the net electrical power discharged or charged by the battery energy storage system (BESS) during time interval t (in kW).

The simplified model utilized for the BESS in this research is expressed as:

$$E(t) = E(t-1) - \frac{\Delta T \times P_{bat\ disch}(t)}{\eta_d \times \eta_{Conv}} - \Delta T \times \eta_c \times \eta_{Conv} \times P_{bat\ charge} \tag{4.3.2}$$

$$SOC(t) = \frac{E(t)}{C_B} \tag{4.3.3}$$

The power discharged by the battery during time interval t is denoted as $P_{bat\ disch}(t)$ and is measured in kilowatts (kW). It represents the electrical

power released from the battery to meet the system's demand. On the other hand, the power charged by the battery during time interval t is denoted as $P_{bat\ charge}$ and is also measured in kilowatts (kW). It represents the electrical power supplied to the battery for recharging. Additionally, the energy stored in the battery at time intervals t and t-1 is represented by $E(t)$ and $E(t-1)$, respectively, and is measured in kilowatt-hours (kWh). These variables quantify the amount of electrical energy stored in the battery at specific time points. To account for the efficiency of the battery system, η_d and η_c are used to represent the discharging and charging efficiencies, respectively.

The state of charge (SOC) of the battery at time interval t is denoted by $SOC(t)$. Binary constraints (Equation 4.3.4 to Equation 4.3.6) are included to prevent simultaneous charging and discharging of the battery energy storage system. These constraints ensure that either the battery is charged or discharged at any given time, but not both.

$$0 \leq P_{bat_disch}(t) \leq \quad \phi(t) \times {P_{BESS}}^{rated} \tag{4.3.4}$$

$$0 \leq P_{bat_{charge}} \leq \quad (1-\phi(t)) \times {P_{BESS}}^{rated} \tag{4.3.5}$$

$$\phi(t) = \begin{cases} 1, & \text{if discharge} \\ 0, & \text{if charge} \end{cases} \tag{4.3.6}$$

where ϕ (t) is a binary variable.

Constraint represents the maximum power limit for charging or discharging the battery for energy storage in the system at each time interval, ensuring

that the power flow remains within the allowable limits. It sets an upper bound on the electrical power that can be charged or discharged from the battery energy storage system (BESS) at time interval t.

$$-P_{BESS\ max} \leq P_{BESS}(t) \leq \ P_{BESS\ max} \tag{4.3.7}$$

Constraint establishes the upper and lower limits of the state of charge of the battery energy storage system.

$$SOC_{\min} \leq SOC(t) \leq \ SOC_{\max} \tag{4.3.8}$$

where $SOC_{\max}$ and $SOC_{\min}$ represent the upper and lower limits, respectively, for the state of charge of the battery energy storage system in percentage (%). These constraints play a crucial role in safeguarding the battery energy storage system (BESS) against overcharging and deep discharge, which are detrimental to the battery's longevity. By preventing these conditions, the constraints contribute to maximizing the lifespan of the battery. Overcharging and deep discharging can have a substantial negative impact on the overall durability and performance of the battery.

Regarding the investment and operation costs, they can be calculated using the following formula:

$$C_{investment} = IC_{energy} \times C_B + IC_{power} \times P_{BESS}{}^{rated} + C_{Installation} \tag{4.3.9}$$

$$C_{operation} = \sum_{\text{day 1}}^{\text{day 365}} \{F_{buy}(t) \times \Delta T \times PG_{import}(t) - F_{sell}(t) \times \Delta T \times PG_{export}(t)\} \tag{4.3.10}$$

$$\text{Total cost} = C_{investment} + \sum_{i=1}^{\text{years}} C_{operation} \times (1 + r\%)^i \tag{4.3.11}$$

The equation given represents various cost factors and parameters involved in the analysis of the battery energy management system. $C_{investment}$ represents the cost of investing in the battery system and related equipment, while $C_{operation}$ denotes the annual operating cost of the entire system. $PG_{import}(t)$ and $PG_{export}(t)$ represent the power imported from and exported to the main electricity grid at time interval t. The electricity tariff for purchasing power from the grid is denoted as $F_{buy}(t)$, and $F_{sell}(t)$ represents the tariff for selling excess power to the grid. The cost of installation, $C_{investment}$, is determined by the rated cost, with the size of battery capacity and power limitations IC_{energy} corresponds to the investment cost per unit of BESS energy rating (£/kWh), and IC_{power} represents the investment cost per unit of BESS power rating (£/kW). The parameter r corresponds to the inflation rate, which signifies the rate at which the general level of prices for goods and services is increasing and, consequently, the purchasing power of currency is decreasing over time.

The goal is to find the optimal battery size by considering the yearly fluctuations in load consumption and PV generation patterns. The objective is to minimize the overall annual energy costs for the household, which includes investment and operational expenses, while simultaneously maximizing the utilization of self-generated PV power. An extensive analysis is conducted from a long-term perspective to assess the economic implica-

tions of implementing a HEMS, enabling the determination of key financial metrics such as the internal rate of return, as well as payback period.

4.3.3 Control Algorithms of the Home Energy Schedule

4.3.3.1 HEMS Control Using the Rule-based Algorithm

A rule-based control algorithm is proposed for the management of a battery energy storage system within a home energy management system. The algorithm operates on in the resolution of one minute, taking into account a time-of-use (TOU) tariff. To evaluate its performance, historical consumption and photovoltaic (PV) generation data are utilized with the rule-based algorithm for a the whole year. Each day, at the conclusion of operations, the battery's capacity is adjusted based on the degradation model's predictions, ensuring the algorithm remains adaptive to the battery's changing performance. The assessment is based on changing capacity of BES and power ratings of converter to assess the impact on electricity cost savings and system cost.

The control strategy, illustrated in Figure 4.3.1, integrates both tariff considerations and battery degradation insights. In situations where the solar generation surpasses the demand of home load, the surplus energy can be stored in the battery or freely exported to the grid. Additionally, during the low tariff period at night, the battery can be charged while it is discharged during the high tariff period. During peak tariff periods, this strategy aims to shift energy consumption, thereby minimizing or eliminating the necessity to procure electricity from the grid during high tariff periods.

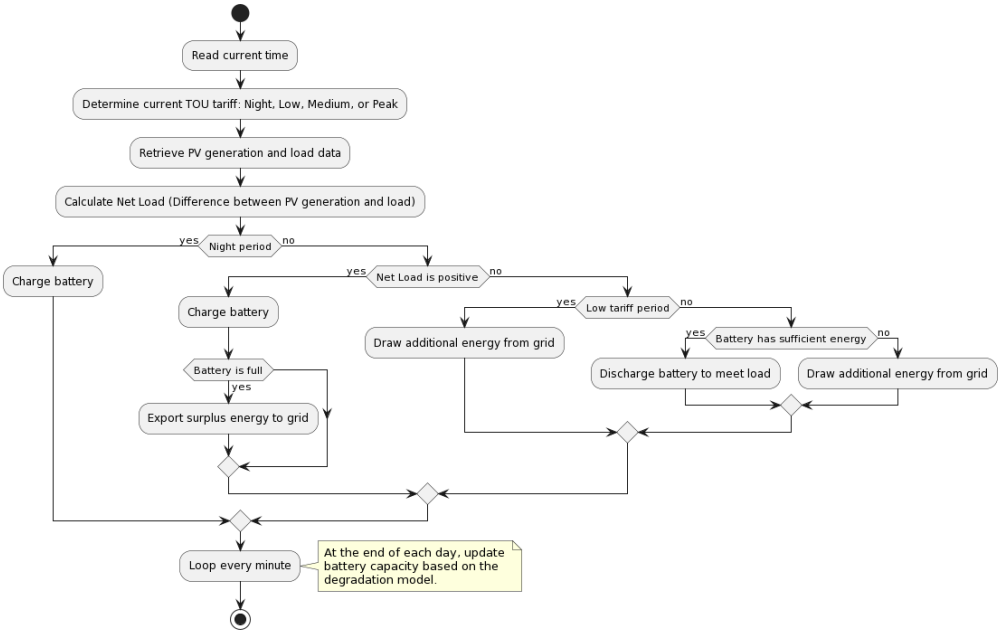


Figure 4.3.1: Flowchart of rule-based algorithms

Based on the time step of one minute for each time, a loop is executed for system control, and the algorithm employs conditional statements to determine the appropriate actions. If it is a low tariff period, e.g., the beginning of each day, the algorithm maximizes the utilization of grid electricity, with any required load energy sourced from the grid. During the low tariff period, the battery is charged for later use, known as the overnight charging period. However, if it is not the low tariff period, the control algorithm prioritizes power requirements. If the load is less than the PV generation, the surplus energy can be stored in the battery directly. If the battery is already fully charged, the energy would be exported to the grid. Charging the battery takes priority over exporting to the grid.

When the PV generation is insufficient to meet the load demand, the system requires additional energy to maintain balance. In such cases, a conditional statement is used to decide whether the energy should be supplied by the battery or the grid. The stored energy would not the be discharged from the battery in the first medium tariff period, as it is primarily reserved for use

during peak hours. Therefore, the energy difference is directly sourced from the grid. However, during the peak tariff periods, the battery can be freely discharged, and the stored energy can be utilized. This also makes sense in the second medium tariff period. Through this rule-based algorithm control, the energy demand during peak hours and even medium electricity rate periods can be successfully shifted to low-price periods, which can be met with stored energy during low-price periods. Otherwise, the remaining energy needed is fulfilled by the main electricity grid.

4.3.3.2 Genetic Algorithms

In Home Energy Management Systems (HEMS), a genetic algorithm is a commonly used as an optimization method for finding the optimal energy management strategy. This algorithm simulates the process of biological evolution and searches for the best solution through iterative optimization. In a HEMS workflow which uses a genetic algorithm, the first step is to define the objective function to be optimized, such as minimizing energy cost, maximizing self-consumption ratio, or minimizing carbon emissions. Then, the variables that affect the energy management strategy are identified, and an appropriate encoding method, such as binary encoding, real-valued encoding, or discrete encoding, is selected to represent these variables as chromosomes.

Next, a set of initial individuals is randomly generated as the population, and the fitness value of each individual is calculated based on the objective function to measure the quality of their solutions [189, 190]. Selection operators, such as roulette wheel selection or tournament selection, are used to probabilistically choose individuals with higher fitness as parents. The selected parent individuals undergo crossover and mutation operations to

generate offspring individuals. The current population is updated based on the offspring individuals generated from the selection, crossover, and mutation operations. The algorithm continues until a termination condition is met.

After the algorithm terminates, the individual with the highest fitness value is selected as the optimal solution, representing the best energy management strategy. The genetic encoding of the optimal solution is transformed into an executable energy management strategy, and relevant results, such as energy cost savings, increased self-consumption ratio, etc., are output.

Through the genetic algorithm, the HEMS can find the optimal energy management strategy to achieve efficient energy utilization and cost minimization. In practical applications, parameter settings, fitness function design, and crossover/mutation operations should be adjusted based on the specific problem to achieve better optimization results. Additionally, other factors and constraints such as energy market prices, load demand, energy storage capacity, etc., should also be considered to meet the requirements of different application scenarios.

In the simulations operated with GAs, the fitness function, which is also called the objective function, is still the cost function, which is based on TOU tariffs. Using the energy balance and power, it is only necessary to evaluate the charge and discharge of the battery, and then the energy input and output requirements of the household system and the grid can be determined. Another critical input parameter in the algorithm is the numbers of variables. Since the charge and discharge values at each time node are actually independent, this number is related to the time length and step size of the algorithm. For example, if the resolution is one hour, then only 24 relatively independent variables are needed for the optimization

of one day. However, if the resolution is one minute, then there are 1440 minutes in one day of the simulation, and this is the number of variables.

In addition, there are functions such as population size, number of iterations, and fitness, which affect the iteration width and depth of the algorithm. Of course, from a data point of view, household load, photovoltaic power generation, and electricity price data are always needed by the algorithm to help the model run.

The pseudocode provided below encapsulates the GA's workflow. It commences by defining the datasets, objective function, and the GA's parameters. The population is initialized, and a series of genetic operations—selection, crossover, and mutation—are performed iteratively. These operations aim to evolve the population, ideally improving its fitness with each generation. The algorithm iterates until a termination criterion, such as a maximum number of generations or a convergence threshold, is met. The end product is the best-found energy management strategy, optimized for the defined objectives. Following is the pseudocode detailing the GA's structure and operations:

Begin

Datasets: import load, PV, tariff profiles

Fitness function: Objective function $C = F(P_{battery})$

Determine decision variables based on time granularity: Variables = Time duration / Time step Set GA parameters: Population size, Number of generations, Crossover rate, Mutation rate, Iteration limitation (termination criteria)

Initialize population

Evaluate initial population using fitness function

While Iteration limitation

Perform selection Perform crossover

Perform mutation

Evaluation of solutions using fitness function

Creation new generation

End while

Return best solution

End

In practice, the efficacy of the GA hinges on the fine-tuning of its parameters, the design of its fitness function, and the specific genetic operations employed. Moreover, real-world considerations, like energy market dynamics, load demands, and storage capacities, interject additional complexity, necessitating the integration of these factors within the algorithm for a holistic and practical energy management solution.

4.3.4 Case Study for the HEMS

In this chapter, the primary focus is on a residential house located in the UK. The house is equipped with various home appliances, a PV generation system, and a battery energy storage system. It is also connected to the main electricity grid, which enables the house to import additional energy from the grid when the PV system cannot meet the demand. Moreover, the system allows for the export of surplus PV energy back to the grid.

For the analysis, the household load profiles are derived from real measurements taken in the UK, providing a one-year dataset with a one-minute

resolution [191]. The annual electricity consumption of the house under study amounts to 4104 kWh, which closely aligns with the average consumption of 4200 kWh for medium-sized users in the UK [192]. These load profiles are combined with actual PV generation data obtained from a 3.8 kW rooftop PV system located in the UK [193]. The PV generation profiles are adjusted to match a 1.4 kW peak system, which is considered reasonable for the house in this study, reflecting a common installation in Meadows. However, generally installations are likely to be higher up to the 4 kW permitted without special application limit. These were then employed with the HEMS algorithms to determine battery usage and energy shifting for a one year period.

Regarding the electricity tariff schemes, the research takes into account two specific schemes. Firstly, there is the Time of Use (TOU) tariff scheme, which determines the cost of purchasing electric energy from the utility. Secondly, there is a fixed feed-in tariff scheme, which determines the revenue obtained from exporting electricity to the main grid. For the TOU tariff scheme, the research refers to Table 4.3.1, which provides the tariff values for purchased electricity. These values are sourced from the Green Energy Company in the UK [194]. As for the fixed feed-in tariff scheme, the research utilizes a value of 5.24 pence/kWh. This value is obtained from an up-to-date website that provides information on feed-in tariffs in the UK [195].

Table 4.3.1: Unit cost values for TOU purchasing tariff scheme at each time period

Time (h)	Tariff	Unit cost (pence/kWh)
23:00 to 06:00	Off-peak	7.5
06:00 to 16:00	Mid-peak	16.44
16:00 to 19:00	Peak	32.55
19:00 to 23:00	Mid-peak	16.44

Following the simulation, a thorough economic analysis was performed.

The simulation results, along with other essential parameters such as system specifications and tariff values, were taken into account for this analysis. The specific system parameters and tariff values utilized in the simulation can be found in Table 4.3.2, sourced from reputable references [196, 197, 198]. By considering these factors, a comprehensive understanding of the optimal BESS size and its economic viability was achieved.

Table 4.3.2: System parameters

Parameter	**Value**
IC_{energy}	£135 /kWh
IC_{power}	£95 /kW
Battery Capacity (C_B)	13.5 kWh
Battery power limitation (P_{BESS}^{Rated})	3.5 kW
SOC_{min} - SOC_{max}	20 % - 90 %
Converter efficiency (η_{Conv})	98 %
Battery charging & discharging efficiency (η_d, η_c)	90 %
Inflation rate	2 %

4.3.5 Concepts for Economic Analysis

The net present value (NPV) provides an assessment of the cash flow's value over different periods, considering the time interval and discount rate. It quantifies the equivalent interest value that would have been earned if the same amount of money had been invested in more conventional investment accounts.

$$NPV = \sum_{Yr=1}^{Yr} \frac{Cash_t}{(1 + r)^{Yr}} - Cash_0 \tag{4.3.12}$$

In Equation 4.3.12, the NPV is calculated by summing the net cash inflows $Cash_t$ for each period (Yr) and discounting them using the factor of $(1 + r)^{Yr}$. The discount rate is set as 2% for the home system [199]. The resulting sum is then reduced by the initial investment cost ($Cash_0$).

The anticipated rate of return on the investment in future years, known as

the internal rate of return (IRR), is a metric used to assess profitability. It is determined by finding the discount rate at which the present value of future cash flows matches the initial investment. A higher IRR value signifies a more favourable return on investment.

$$IRR = a + [\frac{NPV_a}{NPV_a - NPV_b} (b - a)] \tag{4.3.13}$$

Equation 4.3.13 outlines the calculation of the IRR. It involves determining the discount rate (a) at which the NPV is positive and (b) at which the NPV is negative. The IRR is then calculated as the value of a plus the ratio of NPV at rate a to the difference between NPV at rates a and b, multiplied by the difference between rates b and a.

By analysing the NPV and IRR, it is possible to assess the financial viability and profitability of the investment. These metrics provide valuable insights into the long-term economic prospects of the investment.

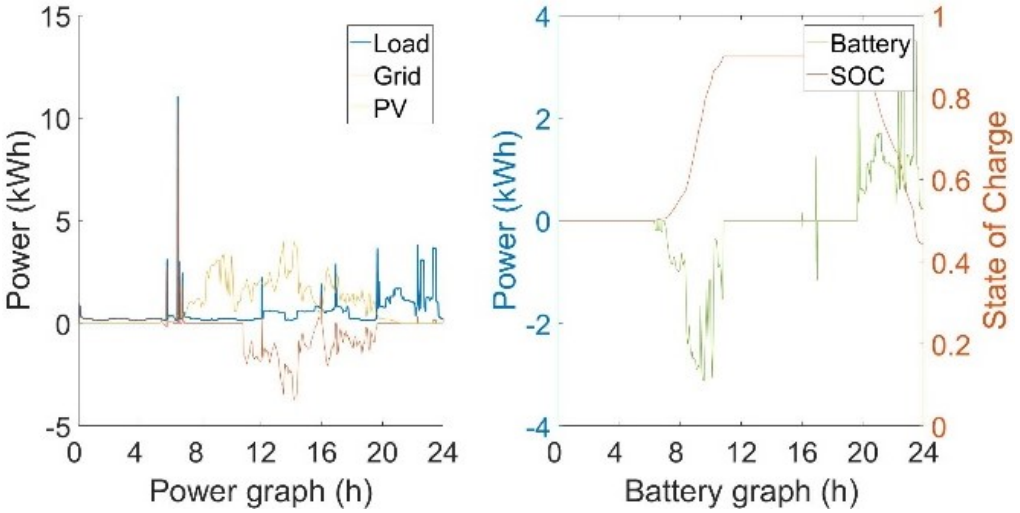
4.3.6 Results of the Simulation of HEMS

4.3.6.1 Energy Analysis

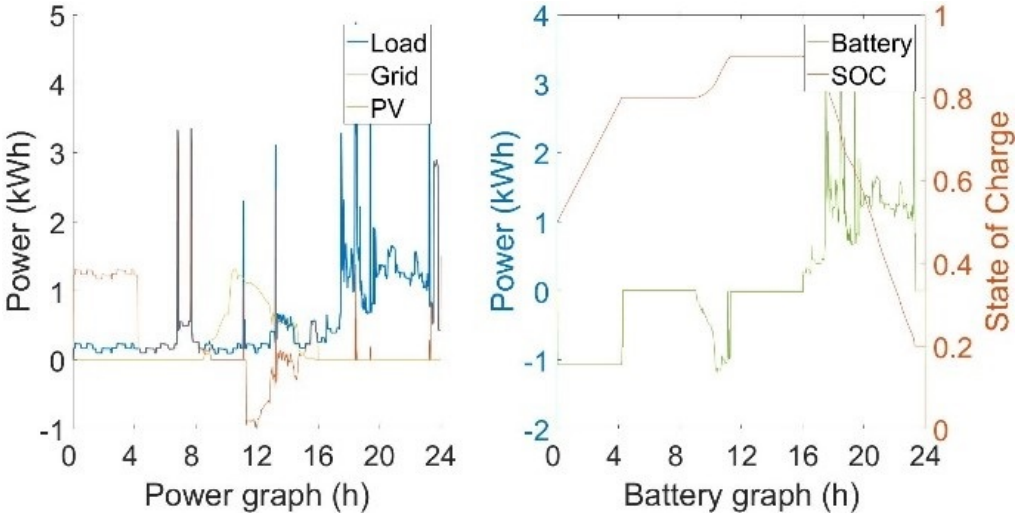
To determine the optimal size of the Battery Energy Storage System (BESS), a comprehensive simulation process was conducted using the MATLAB software. The simulation incorporated minute-by-minute data for both the household load and PV generation, while net power and battery storage were integrated into the simulation, ensuring a detailed analysis.

Applying the rule-based algorithm, the home energy system has been simulated for a duration of one year, allowing for an analysis of its performance

during both summer and winter seasons. Figure 4.3.2 illustrates the results for a typical summer day (represented by graph (a), with July 1st as an example) and a typical winter day (represented by graph (b), with December 1st as an example).



(a) Summer



(b) Winter

Figure 4.3.2: One day power graphs of load, PV, grid and battery in different seasons

In the first subplot, the load profiles are depicted by the blue curve, illustrating the energy demand of the entire system. The yellow curve represents the PV profiles, showcasing the power generated by the PV system. The orange curve corresponds to the simulation results of the net grid power.

Positive power values indicate energy being imported from the grid, while negative power values indicate energy being exported from the system.

The second subplot displays the green curve, representing the power flow of the battery. When the curve falls below zero, it indicates energy being transferred from the system to the battery, representing the charging process. The orange curve represents the state-of-charge (SOC) of the battery.

Throughout the summer season, the SOC of the battery consistently remains above 0.4 (40%). Conversely, during winter, the SOC can reach the minimum SOC limitation of 0.2. This indicates that the battery capacity is fully utilized during periods of high load demand in winter. These results emphasize the efficient utilization of the Home Energy Management System (HEMS) in conjunction with the battery system throughout the entire year.

Furthermore, an economic analysis was conducted based on the results obtained over the course of one year. The daily dynamic battery degradation due to cycling is also integrated. This analysis considered different tariff periods and compared the energy consumption before and after the implementation of the battery system and its control.

Figure 4.3.3 presents the total energy bought from the grid during various tariff periods over one year.

This figure visualizes the average daily energy import and export during different tariff periods, including low, medium, and high tariff periods, as well as the exported electricity under the sale tariff. The blue bars represent energy utilization before the implementation of the battery system, while the yellow bars represent the results achieved with the battery energy management system. The four pairs of bars represent energy consumption

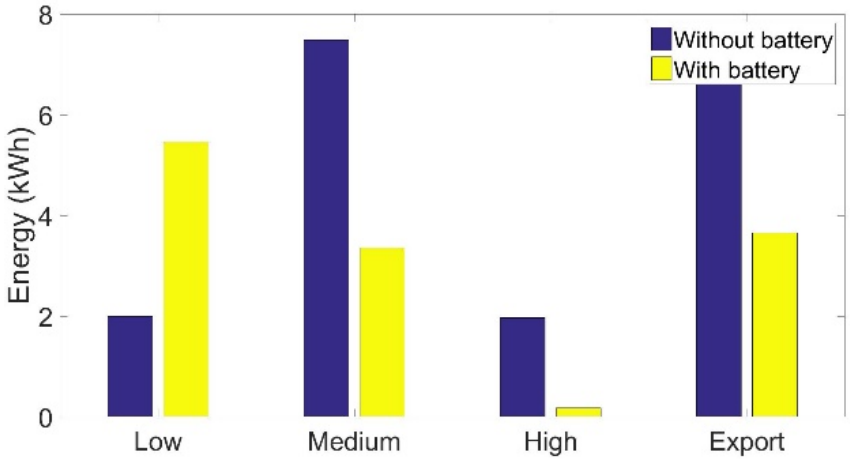


Figure 4.3.3: Average daily energy utilization in different tariff periods

in the Off-Peak, Mid-Peak, High-Peak tariff periods, and exports, respectively.

The implementation of the battery system leads to significant reductions in energy consumption during the medium peak and high peak tariff periods. More than half of the energy consumption during the medium peak period and the majority of the consumption during the high peak period has been moved. Consequently, the amount of electricity that needs to be purchased from the grid during these expensive periods is substantially reduced.

Additionally, a larger proportion of the required electricity can be imported during the low tariff period, enabling the shifting of energy peaks, and contributing to overall cost savings. Furthermore, with the implementation of the battery system, there is a more efficient utilization of the energy generated from the PV system. Instead of exporting the excess energy generated during peak sunlight hours, a significant portion of it is now stored in the battery for later use. And the seasonality of solar radiation leads to the better self-consumption in low PV generation days. The average daily export is reduced from 7 kWh to 4 kWh.

4.3.6.2 Algorithms Comparison

In the previous section, the rule-based algorithm was applied to the simulation, and the short-term and long-term energy performance was obtained, which shows the effectiveness of the algorithm. As a comparison, the genetic algorithm is also introduced into the calculation and compared. For the genetic algorithm, the real-time usage of the battery is a very large data set that needs to be optimized, so the efficiency of the algorithm has been of great concern. Shown in Figure 4.3.4, is the iterative generation curve for the optimization results over the duration of the simulation for one day.

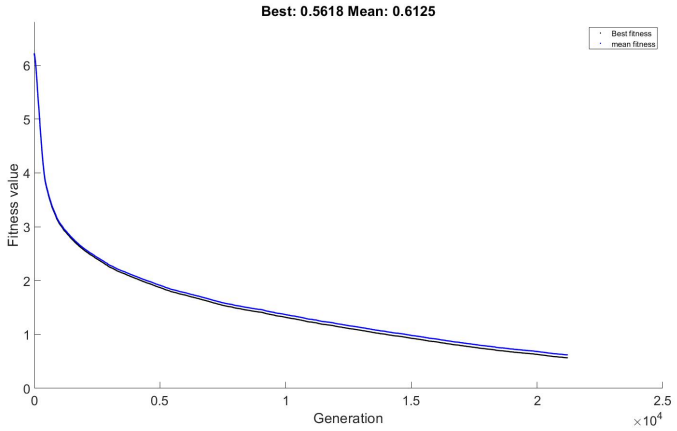


Figure 4.3.4: The fitness value with the iterative generation curve

In the figure, the x-axis is the evaluation of the iterations, and the y-axis is the fitness result based on the real-time battery power. As is mentioned in the previous sections, the cost function of the GA operation, $C = F(P_{battery})$, is the calculation tariff result which relies on system power as Equation 4.3.10. In the iteration, the genetic algorithm was applied for more than 21,000 generations, and the fitness result dropped from greater than 6 to the optimal 0.56. In the first thousand generations, the fitness result dropped very fast, by more than half. After that, the decline rate

began to slow down with the increasing numbers of generations, suggesting that the extremely unreasonable energy plan results were quickly eliminated, and the rest was remaining for further optimization. The end, the algorithm obtains both a value for the fitness result, and the real-time usage of a large battery power.

Substituting the real-time battery power array into the model for simulation, the results of this typical weekday with the energy usage results of the rule-based algorithm can be compared, as shown in the Figure 4.3.5.

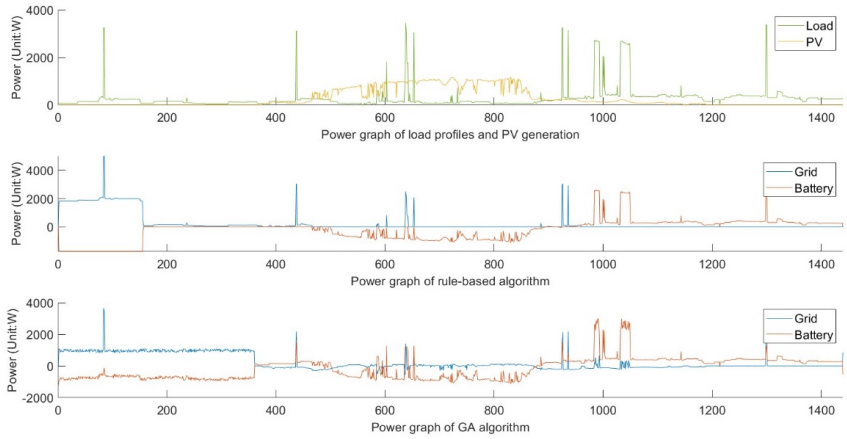


Figure 4.3.5: Graph of power usage for the two HEMS algorithms for the same day

As shown in the Figure 4.3.5, this is a power comparison chart of the simulation results for the rule-based algorithm and for the genetic algorithm. For the convenience of comparison, the power change curve is split into three graphs. Their common x-axis is minutes, and a day is 1440 minutes. The top subplot shows fixed parameters for that day, including household load and solar generation, shown in green and yellow, respectively. This is the composition of a typical household electricity consumption profile, with obvious energy consumption peaks during active mealtimes, and continuous energy consumption during the period from returning from work to sleep.

The photovoltaic pattern is also a typical continuous power generation and reaches the maximum pattern at noon. Within a day, the household load was 6.69kWh, while the photovoltaic power generation was 6.29kWh, both reasonable vales. The sub-picture in the middle is the power consumption of the grid and the battery controlled by the rule-based algorithm, where the grid is blue, and the battery is orange. When the battery power is less than 0, it means it is charging, otherwise it is discharging. This is similar for the grid, where greater than 0 means the grid is supplying power to the home system. The sub-picture at the bottom is the power consumption of the grid and the battery and the grid controlled by the genetic algorithm simulation, where the grid is blue, and the battery is orange.

Whether it is the rule-based algorithm or the numerical-based automatic optimization genetic algorithm, it is not difficult to see that they all exhibit several key characteristics in terms of macro trends, such as charging the battery at night, absorbing additional PV energy supply, and providing energy at peak times for home use. This is determined by the relationship between the amount of electricity energy required at different times and the associated tariff values. The macroscopic picture of the results obtained by the two algorithms is similar, and they are also affected by common parameters, such as the load and the photovoltaic power generation. Of course, there are many subtle differences between the two. For example, during the charging period at night, the rule-based control will allow the battery to be charged at a power of 2kW. Because there is a long period of low electricity price, this value is about 1kW for the GA, and it fluctuates up and down. In two consecutive time nodes, first 1.1 kW and then 0.9 kW, there is no direct difference from maintaining a stable value of 1 kW. However, this oscillation appears in the results of the GA algorithm. These oscillations observed in the GA results can be attributed to the inherent

nature of genetic algorithms. GAs work by exploring a broad solution space and often make small adjustments to potential solutions in the quest for an optimal result. These adjustments, or mutations, can lead to slight variations in the outcomes.

There are some noticeable differences between the behaviour of the two control algorithms at about 450 minutes, (7:30 in the early morning time), the rule based control does not allow the battery to discharge, whereas the battery controlled by the GA algorithm is already providing energy for the home system. After that, both controllers showed a certain consistency in storing the energy of photovoltaic power generation. When comparing the excess power between the 600-minutes and 800-minutes, apart from a small oscillation for the GA curve, a small part of the energy is often not absorbed and instead output to the grid. In the rule-based control algorithm, several peaks of the household load are met by the grid outside the high electricity tariff period and whereas they are supplied by the battery during the high electricity tariff period. For the GA control, it is during peak tariff periods energy is supplied, sometimes from the grid, sometimes from the battery, and sometimes mixed, the two long periods of large-scale power consumption around 1000 minutes are the best examples.

According to the results shown, if the battery system is not used, the original electricity cost for the day is 1.319 pounds. This number is small but reasonable given seasonal variations and reliable energy consumption figures. The grid supplied electricity costs £0.658 with the rule-based control and battery system. When the control algorithm is the GA, the grid supplied electricity cost is 0.640 pounds. The electricity bill is less than half of the original household load cost. For the rule-based control algorithm, the self-consumption of solar energy of the home system is 3.54kWh, and the corresponding value for the GA is 3.25kWh. That is, the self-consumption

rate of 56.28% and 51.67% is an expected result for the home energy management system. The speed at which the algorithm executes is also important. The rule-based control is a single-threaded real-time operation, which executes quickly. But the GA requires tens of thousands of generations and multiple iterations of intergenerational crossing for real time operation and requires considerably more computational powers, which indicates the higher demand on operation time and hardwares.

4.3.6.3 Economic Analysis

According to the results from the previous analysis, in the economic analysis, the default values of 13.5 kWh and 3.5 kW have been used as the starting point for the battery capacity and battery system power rating respectively. The daily dynamic battery degradation due to cycling is also considered. Using the rule-based control algorithm for simulation, as well as the economic method mentioned in the previous section, the NPV cash flow graph over twenty years has been calculated and is shown in Figure 4.3.6.

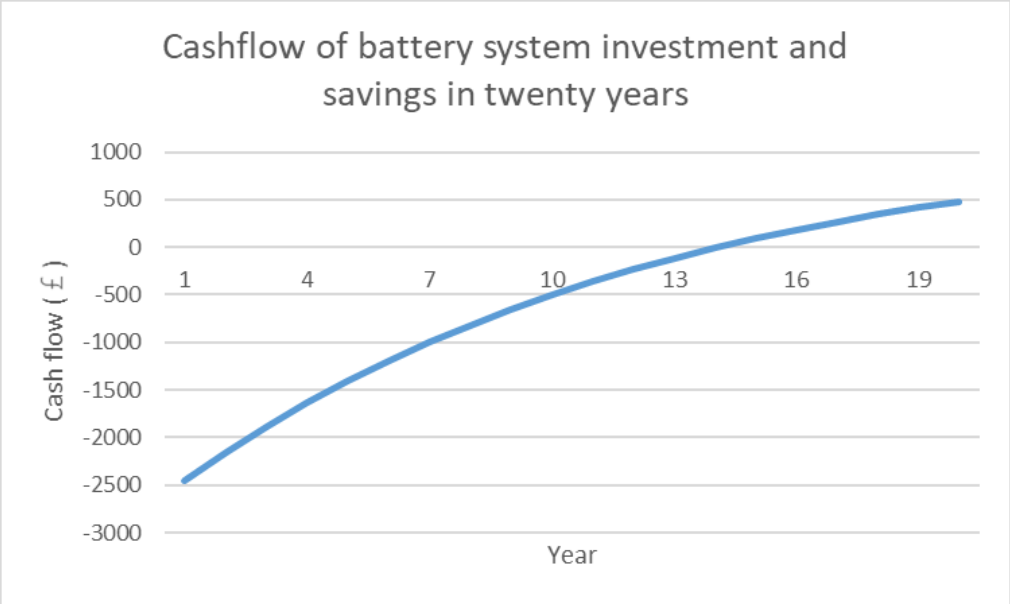


Figure 4.3.6: NPV cash flow of the HEMS system in 20 years

To evaluate the financial performance of the investment, the future value is discounted to obtain its present value for each period. A higher Net Present Value (NPV) after a specific number of years indicates a better rate of return for the investor. After ten years of operation, the system's NPV is -£504.62, indicating that the investment costs £504.62 more than the estimated benefit over the ten-year period. The payback period is another important metric that defines the number of years required to reach the balance point of the investment. A shorter payback period implies a quicker cost recovery. In this case, the payback period is 15 years, as the net present value changes from negative to positive in the fifteenth year. The Internal Rate of Return (IRR) is another key indicator of the investment's profitability. After twenty years, the IRR is 11%, while the IRR after ten years is 4.4%. These values provide insights into the expected return on investment over the respective time periods.

To determine the most suitable size for the battery system, particularly focusing on achieving a payback within 10 years, a further analysis has been conducted. The simulations mentioned earlier are repeated for different sizes of battery systems, considering their capacity and power limits. Figure 4.3.7 illustrates the IRR after ten years for these varying battery system sizes.

Figure 4.3.7 illustrates some interesting observations. When the power limit reduces below 2 kW, the Internal Rate of Return (IRR) decreases significantly, reaching a minimum value of 3.06% (15 kWh, 0.5 kW). This indicates that a low power limit severely limits the system's ability to capture PV energy and charge adequately during overnight periods. On the other hand, when the power limit exceeds 2 kW, the IRR shows changes, ranging from 9% to 14%. In order to maximize the economic benefit, it is desirable to achieve the highest IRR value. The optimal configuration is

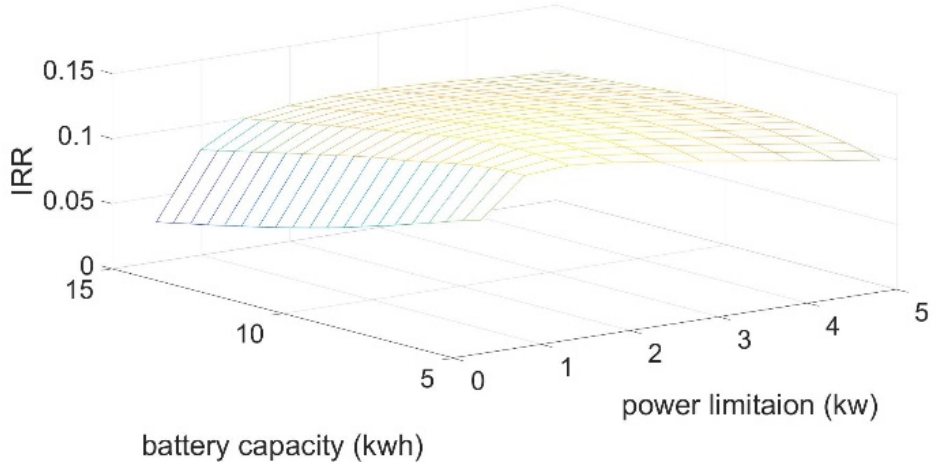


Figure 4.3.7: IRR graph with variable battery capacity and power limitation

achieved with a battery capacity of 7 kWh and a power limitation of 2 kW, resulting in a maximum IRR value of 13.14%.

Furthermore, a sensitivity analysis has been conducted by fixing the battery capacity and power limit at 7 kWh and 2 kW, respectively, while varying the tariff rate and investment rate. The investment rate and tariff rate are represented as simple multiplying factors applied to the default initial costs specified. For instance, a value of '1.1' indicates that the new tariff for calculation is 1.1 times the original tariff values.

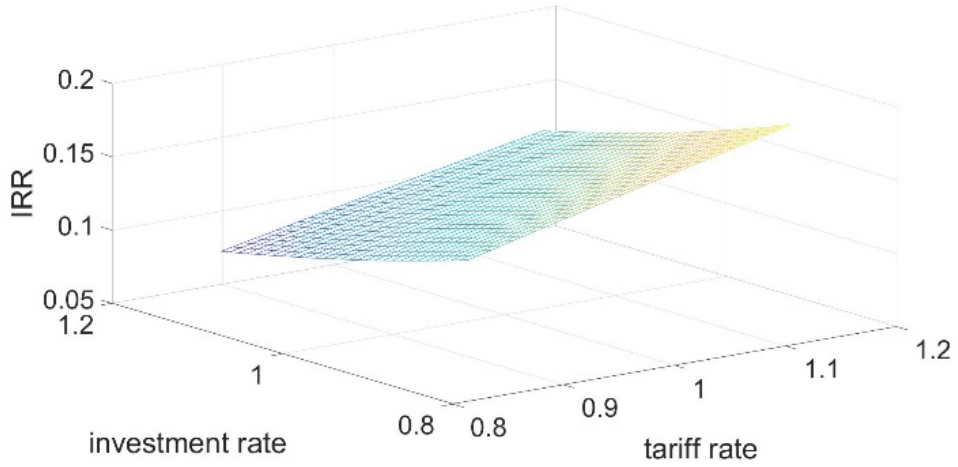


Figure 4.3.8: IRR graph with different investment and tariff rates

The analysis in Figure 4.3.8 reveals that the maximum Internal Rate of Return (IRR) is 18.40%, achieved when the investment rate is 0.85 (85%) and the tariff rate is 1.12 (112%). This result is expected as it indicates lower initial investment costs for the system and higher monetary savings from reducing peak tariff consumption.

Considering the progress in technology and equipment innovation, it is important to explore the impact of the discount rate. Figure 4.3.9 displays the cash flow of the entire system over a period of 10 years, considering different discount rates while keeping other parameters at their original values.

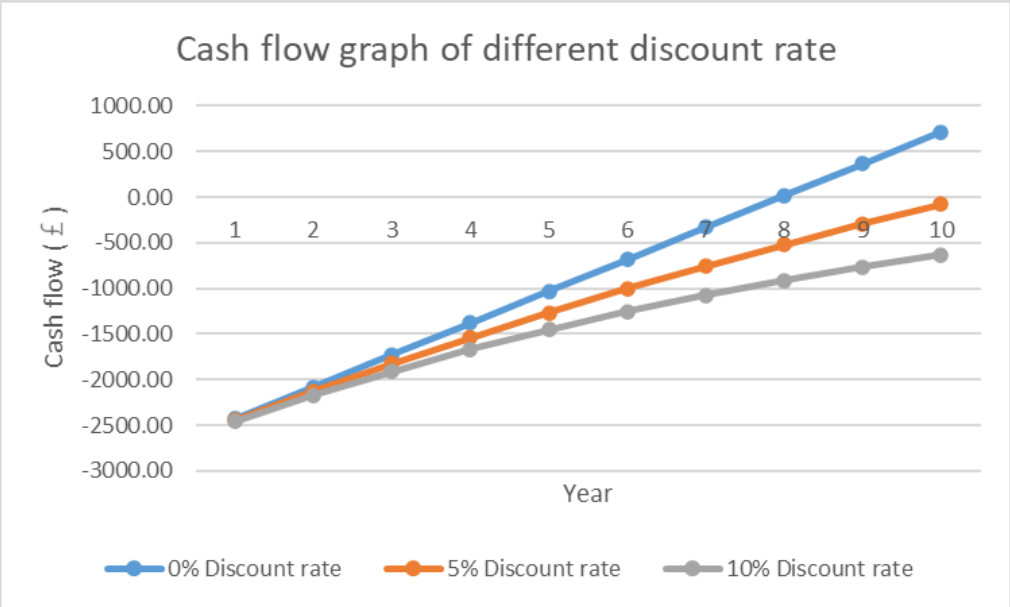


Figure 4.3.9: Cash flow under different discount rate in 10 years

As shown in Figure 4.3.9, the net present value (NPV) is a measure used to determine the value of future cash flows in today's terms. It helps in evaluating the profitability of an investment by accounting for the time value of money. The NPV over 10 years with no discount rate is £715.9, indicating a high financial return. However, when the discount rate is set to 10%, the NPV in 10 years becomes -£630.9. This high discount rate makes

it challenging to recover the costs. On the other hand, when the discount rate is 5%, the NPV in 10 years reduces to -£79.9. This value is very close to zero, suggesting the possibility of recovering the investment within 10 years if the overall discount rate remains below 5%. In conclusion, while the HEMS project seems profitable without discounting, a discount rate of 5% or lower would make this investment more appealing from a financial perspective.

4.4 Conclusion

In conclusion, the simulation results and analysis presented in this study provide valuable insights into various aspects of battery degradation, energy analysis, algorithm comparison, and economic sizing in the context of battery energy storage systems.

Regarding battery degradation, the simulation results showed a monotonically increasing trend in the number of cycles as the days progressed, with a higher rate of ascent during the summer season due to increased solar irradiance and fuller usage of the battery system. This consistent utilization during peak solar periods ensures the efficient operation of the HEMS, maximizing the benefits of solar energy. The accumulated cycles over one year were found to be reasonable compared to the expected lifespan of the battery. Additionally, the change in cycle numbers was found to be small when the battery capacity deviated slightly from the actual usage demand. This has significant implications for the economic sizing of HEMS. A battery that degrades slowly ensures consistent energy savings over time, enhancing the system's overall return on investment.

The energy analysis demonstrated the effectiveness of the Battery Energy

Storage System (BESS) in optimizing energy utilization. The simulation process incorporated minute-by-minute data for household load and PV generation, allowing for a detailed analysis of the system's performance during different seasons. The results highlighted the efficient utilization of the Home Energy Management System (HEMS) in conjunction with the battery system, with the SOC of the battery remaining above 0.4 during summer and reaching the minimum SOC limitation of 0.2 during winter. The implementation of the battery system resulted in significant reductions in energy consumption during medium peak and high peak tariff periods, contributing to cost savings and a decrease in daily exported energy.

The comparison of algorithms, specifically the rule-based algorithm and the genetic algorithm, showcased their effectiveness in optimizing battery power usage. The genetic algorithm demonstrated its efficiency in optimizing real-time battery power usage over thousands of generations, resulting in improved fitness values and power consumption patterns. The macroscopic trends observed in the results of both algorithms were similar, with the charging of the battery at night, absorption of additional PV energy supply, and provision of energy during high-demand periods. However, there were subtle differences in the details and economic benefits, with the rule-based algorithm exhibiting more stable power values without oscillating and faster computational speed compared to the genetic algorithm.

Finally, the economic sizing analysis considered the financial performance of the battery system over a 20-year period. The analysis included metrics such as Net Present Value (NPV), payback period, and Internal Rate of Return (IRR). The results indicated a negative NPV over ten years, suggesting higher investment costs compared to the estimated benefits during that period. The payback period was determined to be 15 years, indicating the time required to reach the balance point of the investment. The IRR

values of 4.4% after ten years and 11% after twenty years provided insights into the expected return on investment over the respective time periods.

Overall, the findings from this study contribute to a better understanding of battery degradation, energy optimization, algorithm selection, and economic considerations for battery energy storage systems. These insights can inform the design, operation, and decision-making processes related to the implementation of such systems in various applications.

Chapter 5

Domestic Occupancy Model, EV Model and Combination

5.1 Introduction

Occupancy rates play an important role in informing energy management in households. The Markov Chain technique is widely used in occupancy models for understanding domestic occupancy and energy use.

The electric vehicle is a device which has increased in use over recent years. The increasing concentration of EVs is due to the improvement of technology and the reduction of price, but also the developing integration concept of EVs. The Markov Chain method was applied in this research to predict the state of EVs in the domestic environment. Based on this predicted EV state, the battery of the EV was charged and discharged accordingly. The proposed control algorithm can store energy in the EV battery during low tariff periods and supply a lack of energy during peak tariff periods, saving energy import and cost.

The relationship between occupancy model, EV model and the thermal demand model which would be proposed in the next chapter can be seen in the Figure 5.1.1.

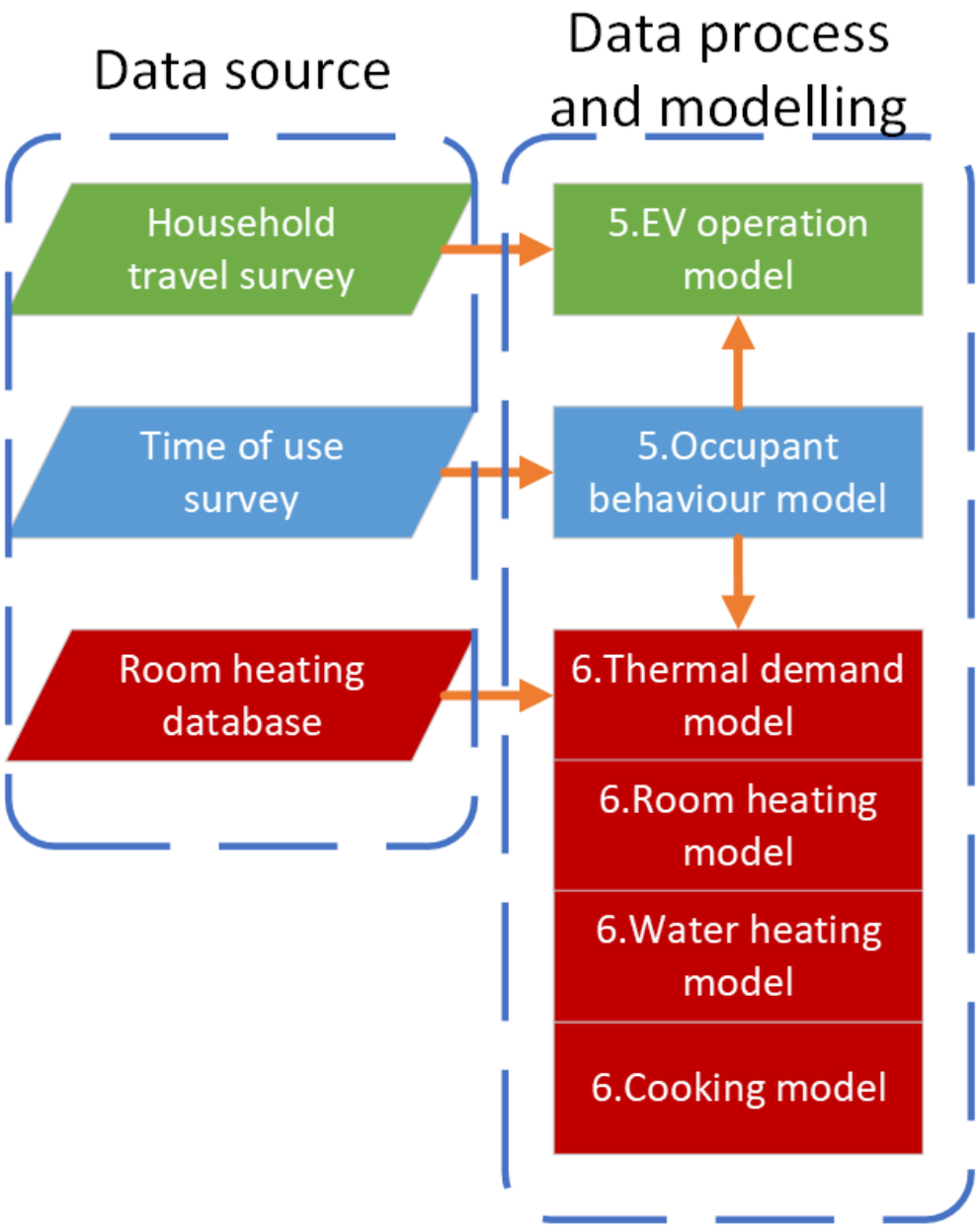


Figure 5.1.1: Structure diagram of occupancy, heat, EV model

In the ideal model of this project, the occupant behaviour model would provide occupancy information to the heat demand model, as well as electric vehicles (EV) model. Although the water would be kept hot (in a

tank) while the occupant is not at home, the demand for room heating and cooking, as well as usage of hot water would be affected by inhabitants' behaviour. This heat demand would lead to a great difference in energy consumption profiles. Electric vehicles nowadays cater for short distance trips, and closely integrated with users. The relationship between occupancy, heat and EV model should therefore be examined.

In this chapter, the following functions are considered using the occupancy model: (1) occupant behaviour should be connected to normal electrical appliances, (2) the impact of occupancy on domestic heat demand should be embodied, (3) the occupancy information and the state of EVs should be determined for appropriate management of the EV battery.

5.2 An Occupancy Model Based on the Markov Chain Technique

5.2.1 Introduction

When considering the domestic energy demand, the behaviour of dwelling inhabitants has a big influence on the activation of electrical appliances, including the state of electric vehicles in domestic environment [200]. As one objective of this work is to create a home energy consumption model when considering future energy demand, an appropriate occupant behaviour model integrating novel low carbon technologies is essential. Compared to previous occupancy models reported in the literature[201, 202, 203, 204], a key feature of the work presented here is the relationship between the occupant behaviour model, domestic heat demand and electrical vehicle state, as these will become much more influential on domestic dwelling energy

costs in the near future.

When modelling the influence of human beings' behaviour on energy consumptions in houses and buildings, four layers are commonly presented [23]. For modelling techniques, the deterministic models and stochastic models are the two main modelling types. Space-based granularity, as well as person-based granularity, are seen as two types of output level.

For deterministic models, determined rule sets and fixed schedules are included. A number between 0 to 1 represents the diversity factor, (also known as "schedules"). This number influences the consumption of appliances on different days, such as weekdays and weekends, based on a mixture of monitored datasets and engineering methods [201]. It offers a comprehensive analysis of energy consumption patterns across thousands of households, emphasizing the role of seasonal variations and unique household behaviours in determining this diversity factor. The datasets for occupant behaviour comes from various publications. [205], [206] present standard programs to obtain building energy demands by calculation. [8] introduces a versatile algorithm that factors in building orientation, window placements, and insulation materials to deliver accurate energy demand projections. Some literature also proposes the schedules of appliance usage [207], [208]. Specifically, [207] delves into the peak usage times for various household appliances, highlighting the influence of cultural and socio-economic factors on consumption patterns. [208]provides a detailed breakdown of hourly appliance usage rates, emphasizing the significance of understanding individual household behaviours to optimize energy consumption strategies. Based on the datasets and rule sets, the occupant behaviour can be modelled, with the assumption of a direct relationship between typical domestic actions of the inhabitants.

Stochastic occupant behaviour modelling is different from deterministic modelling, as it obtains samples from the distribution of statistics, in order to predict the occurrence of typical actions. In either the space or the clock time, there are accounts correlations between specific actions and occupant behaviour. Commonly, the Markov Chain method is widely applied to stochastic models, especially first-order models. The first-order Markov Chain is favoured because it 'memoryless' property ensures that future states depend only on the current state, simplifying the modelling process. Based on inhomogeneous time steps, a Markov Chain Monte Carlo method was applied in the active occupancy models [209, 210], where time of use survey data plays an important role. The researchers specifically highlighted the significance of the Markov Chain Monte Carlo method in effectively capturing the dynamic and unpredictable nature of active occupancy, emphasizing its advantages in providing a more realistic representation of real-world scenarios. In a domestic environment, inhabitants actions can be connected directly to the power demand of appliances [204], such as lights. In this way, residential electricity load, gas and water usage can be generated [211] for occupancy profiles, and these can be created for a number of households. The actions that change in a domestic environment are generated using stochastic methods, while datasets which then provide energy problems are obtained through sensors or home surveys [203], [20]. According to the latest research [212], the reliability of an estimation of general behaviour datasets is of more importance than modelling technologies on occupant behaviour, which is one of the most important reasons why the stochastic method has been applied in occupant behaviour modelling in this project.

The efficiency of such Markov Chain models, however, hinges on the quality and relevance of the underlying data. Time-use surveys, especially those

conducted at national or regional scales, serve as key data sources. For instance, one low-carbon technology, PVs, is considered when the stochastic model was established by Swedish time use survey [210]. Similarly, the demand side management solutions are proposed for lower energy consumption in the occupancy model which utilizing Spanish time use survey [209], underscoring the significance of region-specific data in shaping energy consumption strategies.

In the occupancy model developed by CREST (Centre for Renewable Energy Systems Technology) model [213], the utilized datasets is from the United Kingdom Time-use survey 2004. In addition to the occupancy state, which indicates at home or not (changing from 0 to 1), the activity state is created as well [200]. Inactive occupant behaviour is taken into consideration, which would have different actions and environmental influence associated with it, such as asleep, resting, or sick in bed. The model was programmed in MS Excel.

In this chapter, the occupancy model which is based on up-to-date UK time-use survey (2014) is proposed. The updated 2014 datasets can improve the simulated occupant behaviour to better represent modern life. At the same time, the similar UK time-use surveys provide the possibility of combining this research to CREST model, where its modelling of electrical appliances, illumination energy consumption can still be useful and appropriate. Moreover, in the CREST model, the heat demand is separated while EVs have not taken into consideration. In this work it proposed that the occupancy model would provide a confluence interface for occupant behaviour, room heat supply and EV usage.

5.2.2 Method for Occupancy Modelling

The proposed model in this section applies a first-order Markov-chain technique, using data from the UK time-use survey 2014 [214]. This survey data is updated compared to previous ones and consists of all day around diaries the year round, with a time interval of 10 minutes. The occupancy model also has a 10 minute resolution, but thus can be changed for interacting with other models.

Compared to the general Markov Chain method for solving the modelling problems, there are three challenges that are associated with the database. The 2014 survey includes six "dictionaries", such as individual, households, etc., to reflect actions from different points of views. Additionally, each data element comprises of more than a dozen of items, which makes it concise but also complicates the extraction of the required data.

The first problem is the identification of respondents. In the survey, there is much information about respondents, for instance, the ages of children occupy the house, and also the relationships in one household. This kind of information would not be needed when processing the data, as the stochastic model is assumed to include distinct composition of households, and the model simulation results would demonstrate any possible differences.

The second issue concerns the actions. In the survey, the actions are recorded in detail and that there are up to three actions during one single period. After detailed analysis of the datasets, there is always a first action, but the second or third actions are sometimes 'null'. Hence, only the first action is taken into consideration. As the actions are not easily marked as 'at home / not at home', a manual classification is essential. The survey results are more like answering questions than selecting existing options,

which also complicates data processing.

The third problem is related to the blanks in the survey results. For some periods in the questionnaire, the action has been recorded as 'cant remember what was done at that time'. For that period, it will be defaulted to be the same action as the previous period.

In the data preprocessing phase, special attention was given to converting the intricate details from the UK time-use survey 2014 into a format suitable for Markov Chain analysis. The richness of the survey data, while invaluable, posed challenges in its conversion. For instance, the multi-dimensional nature of the actions recorded, with up to three actions within a single period, required distillation. Through a systematic process, only the primary action was selected for further analysis, ensuring simplicity and coherence in the subsequent modelling. The survey's descriptive style, rather than a more straightforward binary representation, demanded a comprehensive mapping strategy. Each described action was meticulously classified into one of the two categories: 'at home' or 'not at home'. This categorical simplification was crucial to maintain the integrity of the Markov Chain model. Additionally, for periods marked as 'can't remember', a continuity-based approach was employed, defaulting such instances to the immediate preceding period's action. This strategy ensured that the dataset was devoid of any gaps, readying it for a seamless integration into the Markov Chain framework.

The Markov process, for stochastic occupancy simulation or other building energy calculation, is usually in a discrete form with fixed time steps, 10 minutes in this section as mentioned. The state of the Markov Chain is manually set as it is not correlated with environmental variables. It is based on the pre-processed of survey database. The key assumption to

model the first-order Markov Chain is that only the instant previous state has an influence on the present state of the occupant (called Markovian property).

Assuming the final occupancy state is S=$\{s_1, s_2, \ldots s_n\}$, the probability of changing state at any time interval k (less than n) can be defined. The occupancy status oscillates between two values: 0 and 1. A value of 0 at any time interval s_i implies the household space is unoccupied, while a value of 1 indicates that it is occupied. For modelling purposes, it is crucial to understand the likelihood or probability of transitions between the two occupancy states across these time points. When choosing any two consecutive time intervals s_i and s_{i+1}, the probability P defines the transition from the state at s_i to the state at s_{i+1}. This transition matrix and the associated probabilities are foundational to the Markov Chain modelling of occupancy dynamics. The probability (P) of changing from state i to state j can be written as:

$$P_{i,j}\ (k)\ =\ P\ \{\ State(k) = j\ |\ State(k-1) = i\ \} \tag{5.2.1}$$

It represents the probability of transitioning from state i to state j at a given time k. Specifically, if it is known that the system is in state i at time k-1, then the probability that it transitions to state j at time k is denoted as $P_{i,j}\ (k)$. As the time steps are continuous, it also follows that:

$$\begin{aligned} P\left\{\text{State}(k) = j \mid \text{State}(1), \text{State}(2), \ldots, \text{State}(k-1)\right\} \\ = P\left\{\text{State}(k) = j \mid \text{State}(k-1)\right\} \end{aligned} \tag{5.2.2}$$

Equation 5.2.2 emphasizes a core property of the Markov chain, known as the 'memoryless property'. It signifies that the probability of the system

being in state j at time k, given the prior state at time k-1, depends solely on the state at k-1 and is independent of all preceding states. In this proposed model, the state can only equal 1 (at home) or 2 (not at home), the probability (P) matrix would lead to the transition of state during simulation. The P matrix, which stacks together of 2×2 matrices, can be written as:

$$P = \begin{bmatrix} P_{0,0}(1) & P_{0,1}(1) \\ P_{1,0}(1) & P_{1,1}(1) \\ P_{0,0}(2) & P_{0,1}(2) \\ \cdots & \cdots \\ P_{1,0}(n) & P_{1,1}(n) \end{bmatrix} \tag{5.2.3}$$

In the proposed model, the transition probability matrix P encapsulates the probabilities of all potential state transitions. Specifically, each element $P_{i,j}(k)$ defines the probability of transitioning from state i to state j at time k. For instance, $P_{0,1}(1)$ delineates the probability of moving from state 0 (not at home) to state 1 (at home) within the first-time interval. The matrix P furnishes a holistic view, illustrating how the system might transition from one state to another at diverse time points. This is pivotal for simulating the behaviour of the occupants, as it offers a mechanism to predict their likelihood of being at home at a given point in time.

Given the nature of the raw dataset, state transitions are characterized over a 10-minute interval. To adapt this to the targeted model that operates on a per-minute basis, a foundational assumption is made: the dynamics of state transitions derived from the 10-minute interval data remain consistent when applied to each minute within this interval. In essence, if the probability of transitioning from State i to State j over a 10-minute span is found to be 0.2, it is posited that this transition probability remains uniformly at 0.2 for every individual minute within that 10-minute period. This approach

offers a streamlined model process, albeit with an acknowledgment that potential intricacies arising on shorter time scales might be overlooked. This simplification, however, is deemed appropriate given the constraints of data granularity and the overarching objective of maintaining model tractability.

The simulation operates on a minute-by-minute granularity within a 24-hour framework. This mandates the initialization at the beginning of each day. Analysing the dataset reveals that the probability of individuals being absent from home at the start of the day is less than 5%. Given this empirical evidence, the logical approach is to initialize the simulation with the state set to '1', indicating 'at home'.

5.2.3 Model Performance

The proposed stochastic model was established with a 10 minute resolution according to the survey and compared with data from CREST model. The average occupancy and activity state of both models is shown in Figure 5.2.1.

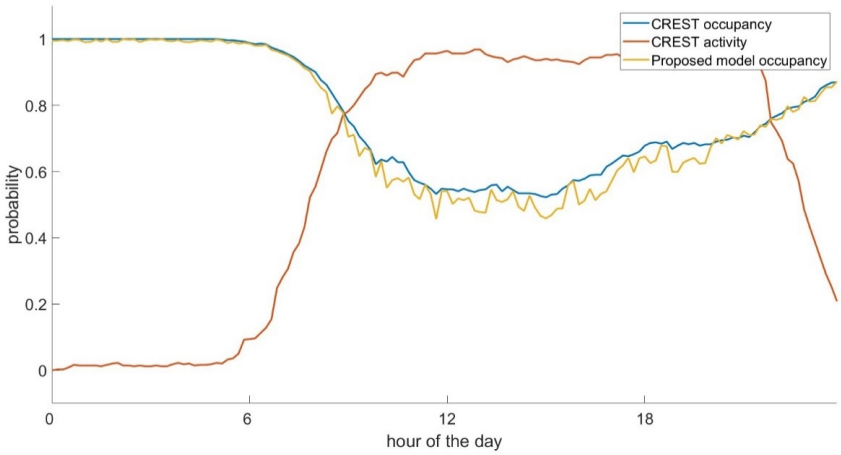


Figure 5.2.1: Occupancy and activity state curve of CREST and proposed model

In Figure 5.2.1, the graph of the average results from the models are presented. The X-axis shows the hour of the day, while the Y-axis is for the state. The blue and orange curves are the average state of the occupancy and the activity respectively. The yellow curve shows the average value of occupancy state of the proposed model. For occupancy, 1 means at home and 0 means away from home. Hence, when the value is closer to 1 at a time slot, it means there it is likely that people are staying at home. For activity, 1 means active and 0 means inactive.

From about midnight to 5.00 a.m., the occupancy is always around 1, while the activity is about 0. This phenomenon indicates people are asleep during this period. After 5.00 a.m., the occupancy decreases, while the activity increases dramatically, as some people get up. The lowest occupancy is about 15.00 p.m. At that time, people were more likely to be away from home. Afterwards, the occupancy increases again, as inhabitants finish their work at daytime and start to return home. Conversely, the peak of activity lasts from 11.00 a.m. to 19.00 p.m., meaning that people are experiencing various events and taking actions. In spite of the general trends, when comparing the CREST model and the proposed model, one key difference is the source data. The data comes from National Time Use Survey for different years. The average occupancy values are close to each other during sleep time. During the daytime, however, the value of the proposed model is always lower than the CREST model, which means people are more likely to be away from home due to changing times. When it comes in the night, the value of the proposed model and the CREST model vary in their value. Generally, the results of the proposed stochastic model of occupancy are close and reliable.

To validate the results of proposed model and Markov Chain method, Figure 5.2.2, the time duration of staying at a particular occupying state is

counted.

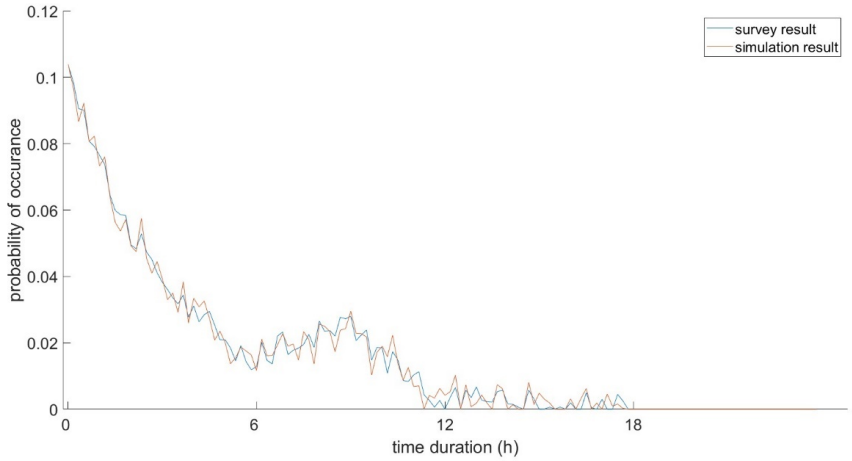


Figure 5.2.2: Occurrence of time duration for stochastic model based on TUS

In this graph, the X-axis is the time duration on occupancy state lasts. To be brief, it can be also understood as the single time period of staying at home. The Y-axis indicates the probability of its occurrence. The blue curve comes from the result of processing survey datasets, while the orange curve comes from a simulation of the proposed model. From 0 to 6 hours, the probability decreases, as this time span is commonly seen for people staying at home. Moreover, another peak of the curve is around nine hours. This indicates the regular life for the inhabitants. For instance, going back home until leaving in the next day. When the time duration exceeds 12 hours, there are very few slots for probability, corresponding to those rare cases.

Having constructed and applied the stochastic occupancy model based on the UK time-use survey data from 2014, it is paramount to evaluate its performance. By comparing the output of the proposed model with the original survey data, the accuracy and reliability of the proposed simulated results can be evaluated.

Table 5.2.1: Some statistical parameters of the proposed model and the original data

Metrices	**Original Data**	**Modelled Data**
Mean	0.77044	0.74616
Standard Deviation	0.17819	0.19621
Mean Squared Error (with respect to Original Data)	–	0.03882

Table 5.2.1 shows the mean and standard deviation value of both original and modelled data, as well as their mean squared error, to evaluate the performance of occupancy modelling. The model closely emulates the general occupancy trends observed in the original dataset. The original data showcases a mean occupancy rate of 0.77044, while the model yields a slightly lower rate of 0.74616. Such discrepancies can be attributed to the inherent variability in human behaviour and certain model assumptions. The standard deviation, a measure of data dispersion, offers insights into the model's robustness across diverse scenarios. A standard deviation of 0.17819 in the original data compared to 0.19621 in the modelled data highlights the model's sensitivity to time intervals. It suggests potential areas where the model might be overreacting or underreacting to certain patterns. The Mean Squared Error (MSE) stands as a testament to the model's overall accuracy. An MSE value of 0.03882, though relatively low, underscores the precision of the model. However, it also reminds us of the importance of regular validation, especially if the model is slated for high-stakes applications or predictive tasks.

5.2.4 Conclusion of the Occupany Model

This section presented a stochastic occupancy model based on the 2014 UK time-use survey data. Using the Markov Chain methodology, the model ef-

fectively simulates occupant behaviour in the context of energy consumption. Results indicate a close alignment between the predicted results of model and the original survey data, validating its accuracy and reliability. Discrepancies, though minimal, provide avenues for further refinement and optimization. The compatibility of the model with the CREST model highlights its versatility, setting the stage for its integration into broader energy consumption frameworks. As energy demands continue to evolve, robust and precise models like the one presented will play a critical role in guiding energy management strategies and policies.

5.3 EV Operation Modelling

5.3.1 Introduction

As mentioned in introduction and literature review, the increasing penetration of renewable energy sources into the electricity system may reduce the its robustness, and thus may be exacerbated by the increasing uptake of electric vehicles [215, 216]. Therefore, the prediction of EV operation (state) and power consumption may be useful for increasing the stability and flexibility of the electrical system, as well as effectively utilizing renewable energy.

Various methods have been proposed in the literature for accurate prediction of EV state and charging requirements, including ant colony algorithms, support vector regression, energy equivalent, Monte Carlo, etc. A high resolution probability model based on the ant colony algorithm was presented in [217]. In this model, the charging load curve was described by power, duration and start time for each charging process. However, this

model had not considered the randomness of EVs. A model based on a genetic algorithm (GA) was proposed in [218]. This algorithm can obtain parameters with a stochastic feature, while a charging strategy for EVs is presented based on the aggregation model to reduce the fluctuations of the grid caused by electric vehicle charging. But the charging load may change suddenly due to uncertainties in the number of EVs, and its scheduling did not take the SOC (state of charge) of users into consideration. A forecasting method for the daily load of electric bus charging stations based on support vector machine was presented in [124], comprehensively considering the effects of temperature, weather and similar daily load patterns. The prediction is based on some small samples for similar days, and require huge real-time computing power. In [219], a Markov Chain Monte Carlo (MCMC) simulation was applied to generate weekly EV patterns with half hourly resolution. One unlikely assumption in this particular simulation was that the driving period per journey was fixed to be 30 min, which is due to the lack of self-transition status of driving, and this limits the generation of continuous vehicle driving states.

A Markov process is a stochastic process that satisfies the Markov property [220]. It is a process for which predictions can be made regarding future outcomes based solely on its present state. The changing of state of an EV is highly random. The Markov Chain has better performance in solving the uncertainty issues in the random processes, comparing to other methods. As a result, this research proposed in this thesis applies a Markov Chain model to the EV state prediction, for further investigation and simulation of integrating EVs into the electricity system. Vehicle driving state profiles were described by Markov Chain models in [221], comprising a discrete-time Markov model and the state transition matrix wherein the size and resolution of the time under consideration and the vehicle states are pro-

portional to each other. However, the related applications are restricted to the two vehicle states of "driving" and "not driving", and no charging location is assigned. Another Monte Carlo simulation is proposed in [222]. Three key variables were collected from a transportation database, containing travel distance, as well as arrival and departure times of the vehicles. In summary, various methodologies have been explored for predicting EV state and charging requirements, each presenting its own advantages and challenges. While techniques like ant colony algorithms, support vector regression, and genetic algorithms offer unique perspectives, they may face challenges in addressing the inherent randomness of EV operations or in computational demands. Markov Chain models stand out due to their aptitude in managing randomness. However, existing applications may be limited in their state representation or detailed charging locations. Given the increasing integration of EVs into home energy systems, having a precise and efficient model for EV operations becomes crucial. It not only aids in optimizing individual household energy usage but also ensures the resilience and efficiency of the broader energy grid. Therefore, in the larger context of home energy systems, refining and applying a robust EV model can contribute significantly to holistic energy management solutions.

In this thesis, an EV state prediction method based on the Markov Chain is introduced. This approach aims to offer enhanced accuracy in predicting EV usage patterns and charging needs. By understanding these patterns more comprehensively, it is anticipated that this research will contribute to optimizing energy consumption and efficiency in household settings. Additionally, an algorithm for simulation of EV battery in a domestic environment is presented. The simulation of EV battery is operated, and the results are discussed.

5.3.2 Methodology for the EV Operation Modelling

The application of the Markov Chain method aims to predict the EV state. Based on the changing EV state curve, the modelling and simulation of EV charging are an important part of modelling home energy management simulation.

5.3.2.1 Markov Chain and EV Simulation

For the estimation of the state of an EV state, in the states of the EV at each period are predicted based on the Markov Chain method. This prediction provides state information, i.e., the drive or park state of the EV, as this would influence charging/discharging decisions for the battery of EV, and also changes its SOC. The simulation of the battery would be part of the battery control algorithm. The home load and PV generation are integrated into a simulation, forming a home energy management system. The scheduling of charging/discharging an EV in this simulation can then be optimized, focusing on some measurable units, such as total energy cost.

The main use of private cars on workdays is for commuting to work whereas the main uses during of holidays and weekend are leisure and entertainment, visiting relatives and friends. According to the daily travel situation, private cars usually stay on their owner's drives or the car park of work areas on weekdays, on holidays or weekends, private cars usually stay on the owner 's drives. Therefore, the state of the EV is divided into 3 conditions, as state 1, 2 and 3. These three states are defined as:

- State 1: vehicle parked at home
- State 2: vehicle on the road

- State 3: vehicle parked at another place

State 1 means the vehicle is at home, while the state 2 means vehicle on the road. Other cases, such as parking at work or some other place are marked as state 3. The transfer process of EVs at a certain moment is shown in Figure 5.3.1.

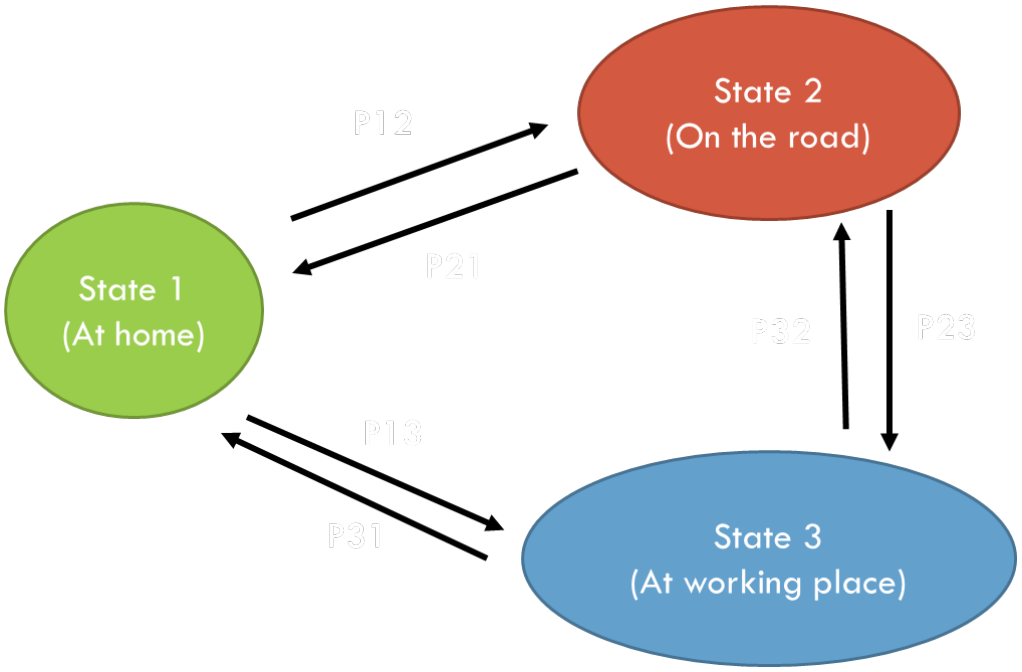


Figure 5.3.1: Transfer process of EVs between three states

This graph shows the relationship between the three states of an EV. An EV may switch from one state to any other state at any time, and the probability of switching is indicated by the transition probability. At each time interval t, the transition probability $P_{i,j}$ (t) defines the probability of changing from state i to state j. The probability can be also presented in Equation 5.3.1:

$$P_{i,j}\ (t)\ =\ P\ \{\ State(t) = j\ |\ State(t-1) = i\ \} \qquad (5.3.1)$$

where the array $State(t)$ stored the state information for different states,

and State(t)=i means the EV is in state i at time interval t. Subsequently, the sum of the probability of switching to three states equals to 1, as Equation 5.3.2.

$$\sum_{j=1}^{3} P_{i,j}\ (t) = 1 \tag{5.3.2}$$

As the states of the EV switches between 1,2 and 3, there are totally 9 (3 times 3) sets of $P_{i,j}$ (t) for each time interval t. For effective data storage and reading, the probability factors would be formed as one matrix. Hence, at time interval t, the state transition probability matrix of the electric vehicle can be expressed as Equation 5.3.3.

$$P(t) = \begin{bmatrix} P_{1,1}(t) & P_{1,2}(t) & P_{1,3}(t) \\ P_{2,1}(t) & P_{2,2}(t) & P_{2,3}(t) \\ P_{3,1}(t) & P_{3,2}(t) & P_{3,3}(t) \end{bmatrix} \tag{5.3.3}$$

In this matrix, the sum of each row is always 1, as the state of EV can only be kept or switched to the other states. This matrix makes sense at every time interval t, while there are a total of 1440 minutes in one day, leading to the 1440 series for the matrix. One example of a matrix is shown as below:

$$P(643) = \begin{bmatrix} 0.9967 & 0.0033 & 0 \\ 0 & 0.9444 & 0.0556 \\ 0 & 0 & 1 \end{bmatrix} \tag{5.3.4}$$

The time interval t is 643, which means it is the matrix for 10.43 a.m. At that moment, the transition probability $P_{1,1}(643) = 0.9967$, indicating the high possibility of the EV's staying at home. $P_{2,3}(643) = 0.0556$, in the middle of the day, the EV has a low probability changing from state 2 to state 3. This indicates the possibility for the EV to park at another place, after leaving home and travelling on the road). For each line, its sum equals

to 1, following Equation 5.3.2.

Applying these series of matrices, a probability of state distribution graph for EVs can be obtained and shown in Figure 5.3.2. The initial state is set at state 1, considering the high possibility of staying home at 0.00 p.m. The state transition probability values are extracted from the NHTS (National Household Travel Survey) [223]. The NHTS was chosen as the data source due to its comprehensive collection of nationwide travel data, which provides a robust and accurate representation of vehicle usage patterns. Furthermore, its high granularity, with a resolution of 1 minute, ensures detailed insights into short-duration vehicle activities, making it a prime choice for such simulations.

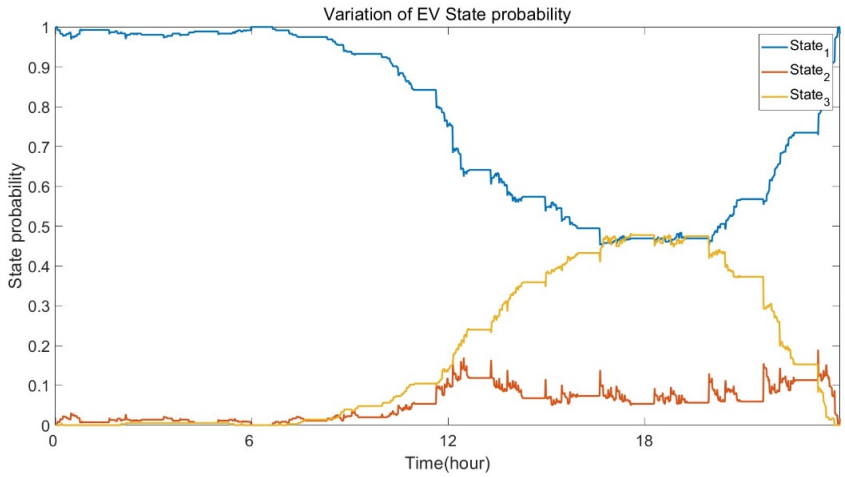


Figure 5.3.2: Variation of the EV state probability

In the Figure 5.3.2, the probability of the EV being at state 1 is close to 1 before 8.00, indicating the EV would always stay at home overnight. After 8.00, the probability of state 1 decreases, achieving the lowest value of 0.5 at about 18.00. Conversely, at 18.00, the probability of state 3 achieves its peak. During the daytime, the EVs are more likely to be driven away from home and parked at other places. Compared to the low probability of state 2 before 8.00, it is around 0.1 from 8.00 to 24.00, ensuring there is a high likelihood of state switching.

During the prediction and simulation of the EV state, the decision of the EV state is based on the time interval t, current state i, and a random number. Additionally, t and i are already known, three probability factors would make sense, and their sum is 1. The random number is randomly obtained from 0 to 1 and compared with probability, to decide what will be the next state. The schematic diagram is shown in Figure 5.3.3.

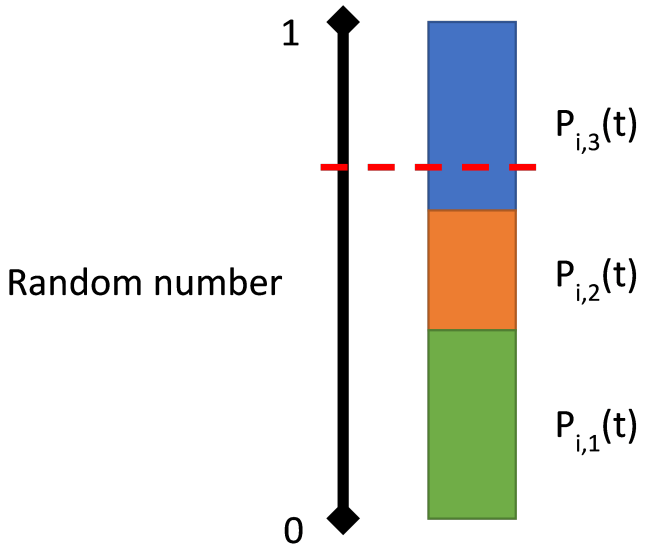


Figure 5.3.3: Schematic diagram of probability selection

Applying the Markov Chain method to the prediction of the EV state as mentioned in previous sections, the state graph shows the estimated motion of EVs. For instance, two examples of prediction results are shown in Figure 5.3.4.

In Figure 5.3.4, the given data provides a granular view of an electric vehicle's (EV) activities throughout a 25-hour period. At the onset of the day, from 00:00 to approximately 06:00 a.m., the EV remains predominantly at home. This behaviour aligns with typical nocturnal resting hours when vehicles are often stationary.

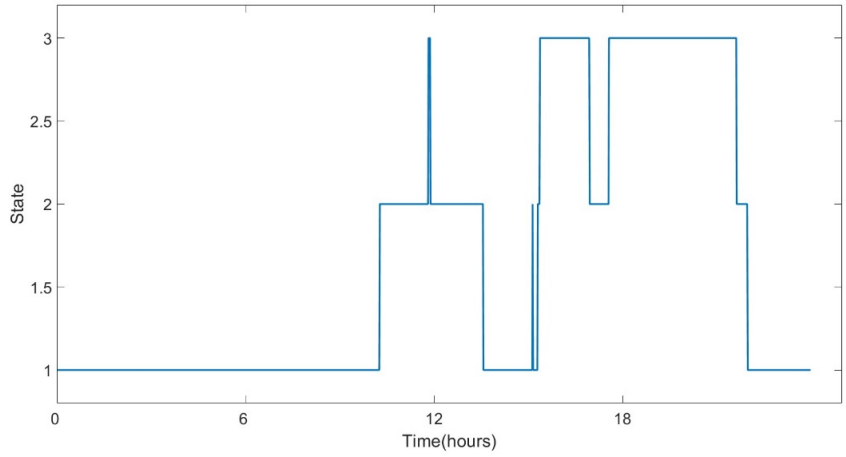


Figure 5.3.4: Examples of EV state simulation

By 06:00 a.m., a shift is observed in the vehicle's status, indicating it is being mobilized. This movement lasts for a few hours before the EV returns home, potentially representing a morning commute. However, post 15:00 p.m., the vehicle once again departs, but this time it remains away from home for an extended duration, suggesting a longer engagement, possibly work-related or leisure driven. Such trends are crucial as they shed light on the EV's daily utilization patterns, which, in turn, can inform optimized charging strategies.

Understanding the patterns of how and when an electric vehicle (EV) is used can help manage the power grid better. When it is known when most people are likely to charge their EVs, electricity can be prepared at those times. This is especially important when using sources like solar or wind power, which don't always produce electricity all the time.

5.3.2.2 Trip Duration of EVs

Another random number ranged from 0 to 1 is used for estimating the trip duration. Since there is a direct correlation between journey distance and journey duration, it is reasonable to use this correlation in combination with

the value of the journey duration obtained from the mobility state profile to estimate the journey distance. Based on datasets [223], there are 34 trip duration bins with a 10-minute width, followed by further 300 distance bins, where each width is 1 mile. Figure 5.3.5 shows three examples of journey distance cumulative probability distribution for journeys of 10 - 20 minutes, 50 - 60 minutes and 150 - 160 minutes. It becomes evident that

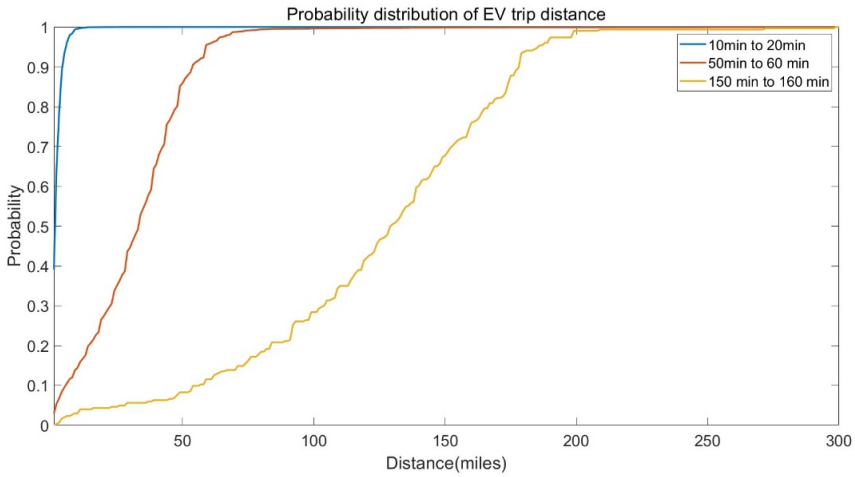


Figure 5.3.5: Probability distribution graph of EV trip distance

the cumulative probability distributions of journey distances for distinct durations provide invaluable insights into the driving behaviours of EV users. For instance, within a 10-20 minute duration, the probability that an EV travels a shorter distance is notably higher than covering a longer stretch. This directly correlates with the energy consumption patterns and, by extension, the subsequent depletion of the battery's SOC.

The longer the distance travelled, the greater the battery's energy expenditure. Consequently, for journeys lasting between 50-60 minutes, a broader spread in the distance distribution can be observed, indicating varied energy consumption patterns. For even longer durations, such as 150-160 minutes, the probability skews towards more extended distances, suggesting a more significant reduction in the SOC by the journey's end. The impact of trip distance on energy balance would be mentioned in the fol-

lowing algorithms.

During the simulation of the SOC of the EV battery, the TOU (Time of Use) tariff is applied, for the decision making for charging/ discharging the battery of EV. The control algorithm would attempt to charge EV battery during night, when the electricity tariff is the cheapest in the whole day. The loads formed by the home appliances would be integrated into the home energy system, to form a domestic environment for energy management. The load profiles come from load measurement data. The PV generation is also considered. To summarize, the input datasets of this simulation include EV states based on Markov Chain, as well as load and PV profiles. The output of this simulation is the changing SOC and power of the battery of EV.

5.3.2.3 V2G Algorithm

An example of how the EV model can be used as part of a home energy management scheme is shown in the flowchart of Figure 5.3.6. In this step, there is no domestic battery.

In the Figure 5.3.6, the main loop of the control algorithm is based on time interval t, i.e., each minute of the project, where transition probability matrix P (t) is updated. The changing power arrays in the loop includes power of the load (P_{Load}), power of the PV (P_{PV}), power of the EV (P_{EV}) and power of the grid (P_{Grid}). At any time, this power variable follows energy balance in the system, as:

$$\begin{cases} P_{\text{Grid}} + P_{\text{PV}} = P_{\text{Load}} & (\text{EV state} \neq 1) \\ P_{\text{Grid}} + P_{\text{PV}} + P_{\text{EV}} = P_{\text{Load}} & (\text{EV state} = 1) \end{cases} \tag{5.3.5}$$

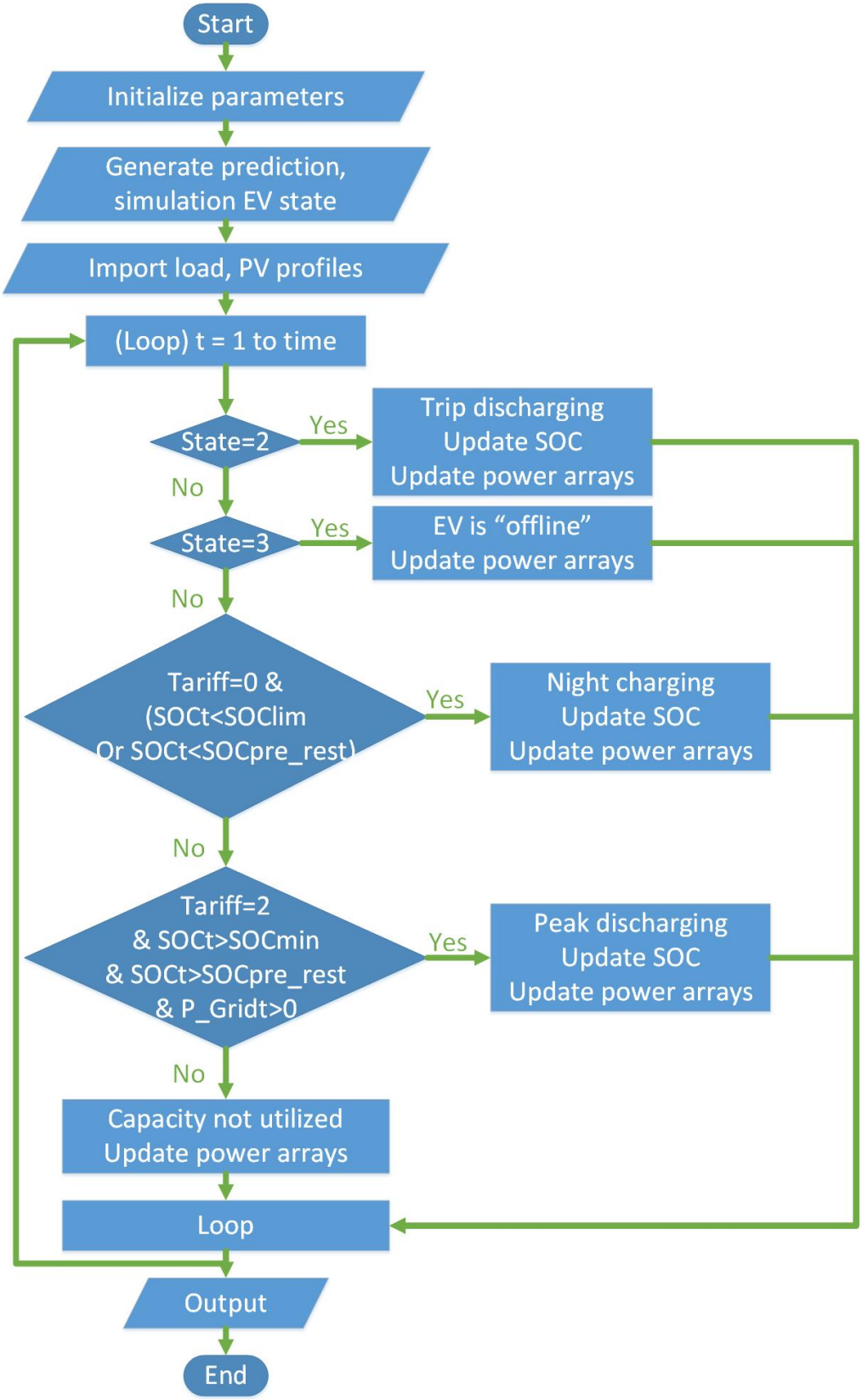


Figure 5.3.6: Flow chart of EV battery simulation

Only when the state of EV equals to 1, as the electric vehicle is parked at home, can the vehicle be connected to home system. When EV is at home, P_{EV} is valid only when EV is charging. Or it is considered invalid when it is not charging, and the value of 0 does not affect other parts

In the loop, if the state equals 2, the EV is on a journey. During the journey, the battery of the EV would be discharged to provide energy for the EV on the road. The energy consumption of the battery discharging for the trip can be calculated as Equation 5.3.6.

$$E = D \times E_{con} \tag{5.3.6}$$

where E is the energy consumption, D is the trip distance. E_{con} is the energy consumption rate, assumed as 0.34 kWh/mile [224]. Secondly, if the EV state is 3, the EV is parked at another place. It is assumed for this work that the EV battery would be neither charged nor discharged. Thirdly, the EV state can be only 1, indicating the EV has returned home. When the tariff period is 0 (low tariff period), and the current SOC is less than its maximum value or the estimated requirement for the whole day, the battery of the EV is under night charging mode, to store enough energy in the battery at low grid tariff. Finally, if the tariff period is 2, (high tariff period), and the current SOC can meet the predicted requirements for the following day, the battery of the EV would be controlled to discharge for domestic utilization during peak periods.

5.3.2.4 Incorporating EV and Home Battery Systems

In the proposed integrated energy management framework, both the EV and home batteries play distinct yet complementary roles. The synergy

between these two storage entities ensures optimal energy utilization, with the EV battery often boasting a larger capacity while the home battery offers rapid charge and discharge capabilities.

Energy derived from renewable sources, such as PV panels, is initially directed towards the EV battery when charging, owing to its larger storage potential. The home battery, designed for swift energy transactions, becomes the secondary recipient once the EV battery is adequately charged or if the EV is not available. Conversely, during periods of energy consumption, the home battery takes precedence in supplying the house. If its reserves are insufficient to meet the demand, the EV battery seamlessly supplements the power needs, always ensuring that the EV's subsequent journey requirements are not compromised.

Incorporating the home battery into the existing simulation entails modifying energy balance equations. Both batteries' state of charge, charge/discharge rates, and degradation profiles are pivotal parameters. Decision algorithms will be recalibrated, taking into account both states of batteries, their efficiency curves, and anticipated consumption trends. The predictive model for the state of EV remains a linchpin, informing the system about the optimal charging periods and maintaining the EV's transportation readiness.

5.3.2.5 Selection of Predictive EV State Curve for Simulation

Simulation fidelity hinges on the accuracy of the employed predictive models. In this research, the emphasis is on achieving a robust simulation rather than a pure prediction. Consequently, the same Markov Chain-based state transition matrix, previously described, underpins both the simulation and prediction of the EV state. When the electric vehicle is parked at home,

its charging needs are considered. During peak times, there is the possibility of the vehicle's battery discharging into the home system, based on the relationship between the battery's charge and the estimated future demand. For the operating simulation, a reference EV state curve, already factored into energy calculations, serves as the benchmark. Leveraging the consistent state transition matrix, multiple state curves are iteratively generated. The objective is to unearth a curve that, within the timespan of the completed simulation, mirrors the reference with an error margin below 10%. Such a curve is then designated as the predictive state curve for that interval.

To account for evolving real-world scenarios and the inherent variability in user behaviours, this predictive curve is updated at half-hourly intervals, ensuring the simulation remains aligned with the dynamic energy landscape.

5.3.3 Model Performance

The simulation result of EV charging as part of home system for one day is shown in Figure 5.3.7.

The presented figure consists of four sub-graphs, each highlighting a specific aspect of energy dynamics over a 25-hour period.

The first sub-graph displays the Load, Grid, and PV Power curves. The Load curve represents the household energy demand over the course of a day, showing typical diurnal variations. The PV curve illustrates the energy generated from photovoltaic panels, with a peak corresponding to the solar noon. The Grid curve indicates the net power interaction with the grid, which is either drawn from or fed into the grid based on the balance

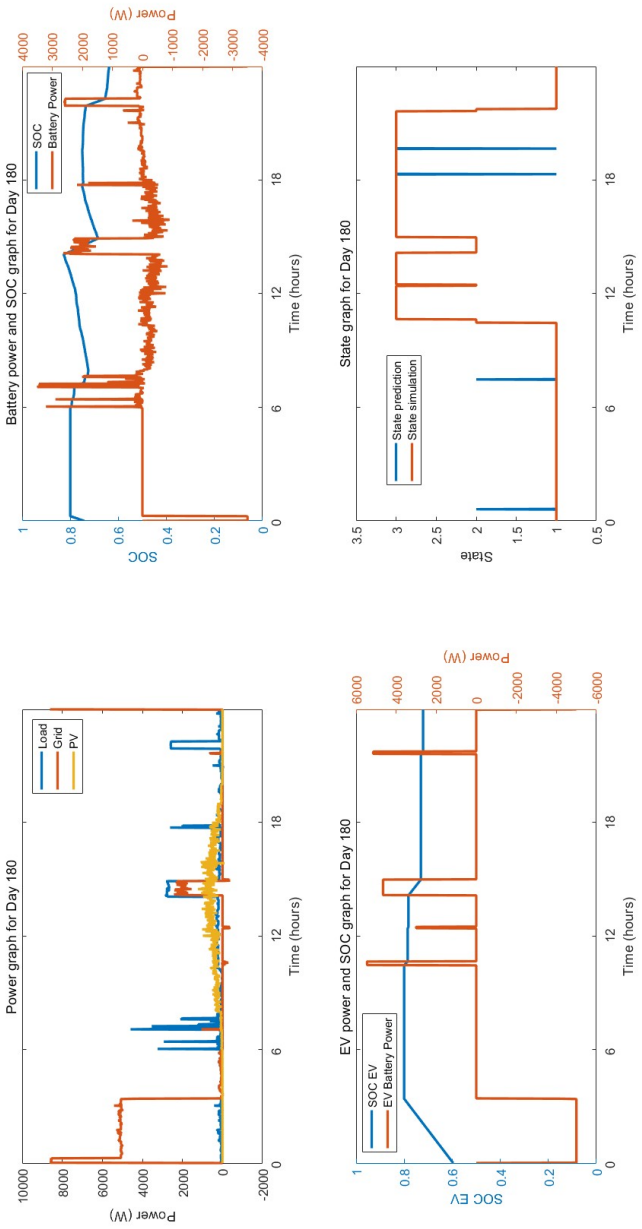


Figure 5.3.7: Simulation results of EV battery

between energy demand and supply. In the second sub-graph, the focus is on the home battery's power and state of charge (SOC). The power curve fluctuates between charging and discharging modes, determined by the energy demand and the available PV power. The SOC curve ranges between

0 and 1, indicating the battery's charge level throughout the day. The third sub-graph provides insights into the electric vehicle (EV) battery, detailing its power consumption and SOC. The power curve showcases the vehicle's energy utilization patterns, influenced by driving requirements and home energy management decisions. The SOC curve traces the EV's battery charge level, crucial for efficient EV operations. The fourth sub-graph contrasts the predicted and actual states of the electric vehicle, offering an evaluation of the prediction model's accuracy over the observation period.

The load curve exhibits two distinct peaks, likely corresponding to morning and evening residential consumption. This bimodal pattern is characteristic of typical household energy use. On the other hand, the PV generation curve shows a unimodal pattern, peaking around midday when solar irradiance is at its highest. It is notable that during midday, PV generation occasionally exceeds the load, resulting in a surplus of energy. This surplus is evident when the grid power curve dips below zero, indicating that excess energy is fed back into the grid. Conversely, during early morning and late evening, when the solar generation is minimal or absent, the household draws power from the grid, causing the grid curve to spike upwards.

The SOC (State of Charge) of the battery remains between the optimal limits, suggesting efficient power management. There are instances where the battery discharges to support the household load, evident from the Battery Power curve dipping into the negative region. Conversely, when the curve is above zero, it signifies the battery is in a charging state, absorbing excess energy from the PV or the grid. The EV's power curve displays intermittent dips, representing periods when the vehicle is in operation and consuming energy. The associated decrease in SOC during these periods reinforces this observation. The negative values in the EV power curve denote charging episodes, likely occurring during periods of PV surplus or

when grid electricity is cheap.

During periods when the solar PV output reaches its peak, the power from the grid is observed to be negative. This indicates that the solar power generation surpasses the household's load demand. Such excess solar energy is potentially utilized to charge the home battery or the EV battery, instead of being fed back to the grid. Conversely, during sunrise and sunset, the solar PV output diminishes while the household's load demand might persist, leading the household to rely more on grid supply or stored battery power.

Patterns in the EV's State of Charge (SOC) suggest certain charging and consumption periods. These patterns may correlate with the user's daily commute or travel routines. For instance, the vehicle might be stationed at a workplace during the day and undergo charging at home during the night. Sharp declines in the EV's SOC curve might represent short-distance travels, offering insights into daily commute lengths and subsequent charging needs. A critical observation is the modest consumption of the EV battery over a single day. The vehicle's limited travel distance on this particular day is a plausible cause for this minimal drain.

The battery's charging and discharging strategy appears to be influenced by Time of Use (TOU) pricing. During peak periods, when the electricity rates are higher, there's a tendency to rely more on battery power, mitigating costs. In contrast, during off-peak times with reduced rates, there's an inclination to draw power from the grid and prioritize charging. It's noteworthy that even though the battery possesses the capability to feed back to the grid during peak periods, the vehicle's absence from the household during these times potentially restricts this action.

For further discussion, the Table 5.3.1 presents a side-by-side comparison

of the simulated data against the UK average.

Table 5.3.1: Annual results of the simulated data and the UK average data

Metric	**Simulated Data**	**UK Average Data** [225]
Total Annual Distance (km)	9514 km	11909 km
Total Annual Energy Consumption (kWh)	2041.07 kWh	1762 kWh
Battery Cycle Count	2190	N/A

The first point of comparison lies in the annual distance travelled. The simulated electric vehicle covered a total of 9514.00 km throughout the year. In contrast, the average distance travelled by electric vehicles in the UK stands at approximately 11909.54 km. This difference suggests that the usage pattern of the EV in the proposed simulation is slightly below the UK average.

A notable observation emerges when analysing energy consumption. Despite the simulated EV travelling a shorter distance than the UK average, it consumed a higher amount of energy, registering at 2041.07 kWh compared to the UK average of 1762 kWh. Such a discrepancy may be attributed to factors such as the EV's energy efficiency or specific driving conditions encountered in the simulation, like frequent short trips or terrains demanding higher energy expenditure.

Delving into the operational behaviour of the EV battery, the simulated data reports a battery cycle count of 2190 over the year. While there is not a direct UK average to compare this against, this metric is instrumental in understanding the battery's charging and discharging patterns.

5.3.4 Combination of Occupancy Model and EV Model

The interaction between EV operations and occupancy patterns can be crucial for energy optimization. When an EV is in use, and the residence is unoccupied, there is an opportunity for strategic charging. This can aid in peak-shaving and makes use of off-peak rates, ensuring efficient grid operations.

The occupancy model can be linked to the EV model as shown in this section. When people left home, one could select electric vehicles for commuting for times. Also, one may just walk to some nearby places, while the EV is still parked at home. Hence, the key issue of the combination of the occupancy and the EV model is to get the state in synchronization, making it reasonable. During simulation, the EV simulation would be repeated, to make sure that the occupancy state equals to 0 (not at home) when the EV is also not at home. The Figure 5.3.8 shows the matching of two models in one day.

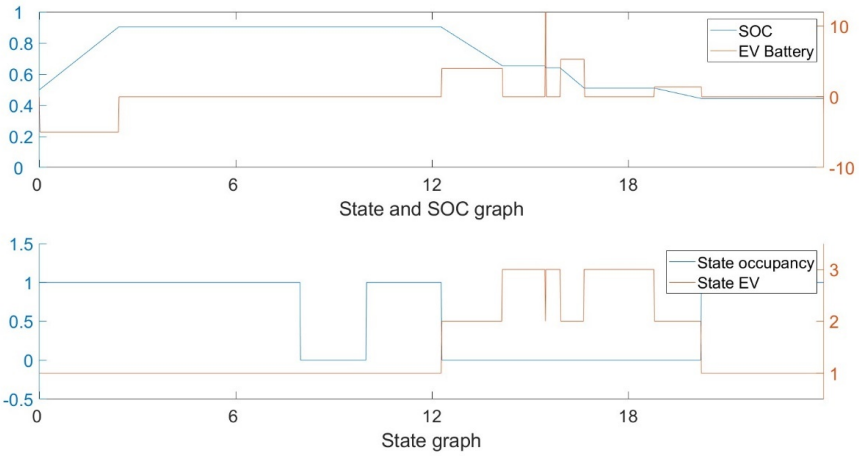


Figure 5.3.8: Battery and state graph for EV

In Figure 5.3.8, the upper graph shows the detailed information about the battery of the EV. The blue curve is the SOC of battery, while the orange

curve is the power rating of the battery. In the lower graph, the blue curve means the state of occupancy, and orange one means that of the EV. As shown in the power graph, the EV was charged from midnight, then parked at home with no energy exchange during the morning. After 12 p.m., the EV departed and parked at other places during that period. At that time, the energy of battery is consumed fast. In the view of states, the occupancy indicates that people are not at home during the afternoon, which is consistent with the driving of the electric vehicle. Additionally, from about 8.00 a.m. to 10.00 a.m., the occupancy state equals to 0 and the EV state is 1. This means people were away from home but the EV was still parked at that time.

5.3.5 Conclusion of the EV Operation Modelling

With the proliferation of renewable energy sources and the growing adoption of electric vehicles, the prediction of EV operation has emerged as a crucial factor. Accurate predictions can aid in enhancing the stability and flexibility of the electricity system, optimizing energy consumption, and maximizing the utilization of renewable energy sources.

The inherent randomness of EV operations makes it particularly apt for the Markov Chain method. The study underscored its efficacy over other techniques. Its strength lies in its ability to predict future outcomes based solely on its present state, making it particularly apt for predicting the highly random state transitions of EVs. The proposed model segmented the state of the EV into three conditions: parked at home, on the road, and parked elsewhere. This granular representation offered a detailed view into the day-to-day operations of the EV.

The simulation established an energy balance that accommodated photovoltaic generation, home loads, and the state of the EV. Understanding the interplay between these factors becomes vital for optimizing energy consumption and costs. The decision algorithms were designed to prioritize charging the EV battery due to its larger capacity. However, during periods of energy consumption, the home battery becomes the primary source, with the EV battery providing a supplement as needed.

The simulation results offer a microscopic view into the intricate dynamics of energy consumption, generation, and storage. Patterns emerge, providing insights into daily EV use, battery charging and discharging strategies, and their implications for overall energy management. Compared to the UK average, the simulated data presented intriguing observations. While the annual distance of the simulated EV was lower than the UK average, its energy consumption was higher, underscoring the influence of factors such as energy efficiency and specific driving conditions.

In summary, this study offers a holistic approach to predicting and simulating the operations of EVs within a home energy environment. The insights derived from the simulations provide valuable perspectives for homeowners, policymakers, and energy managers, paving the way for more sustainable and efficient energy management solutions in the future.

5.4 Conclusion

This chapter presents a model derived from the 2014 UK Time-Use Survey data, aimed at predicting occupant behaviour in relation to energy consumption within homes. By integrating this model with thermal demand and electric vehicle (EV) usage data, a comprehensive understand-

ing of household energy consumption patterns emerges. This integration offers potential avenues for optimizing energy consumption, aligning it more closely with actual household needs. This chapter also provides a model of the state and trip duration of the electric vehicles. The significance of accurately predicting EV charging and usage patterns, especially considering the integration of renewable energy sources like solar panels is emphasized. Both proposed models in this chapter are of great importance in the domestic energy system modelling, as the models are directly related to inhabitants ' behaviours in simulation, and thus the energy consumption in different time steps. In essence, the chapter provides an approach to effectively gauge and manage home energy consumption. The insights from the model can benefit homeowners, policymakers, and energy sector professionals.

Chapter 6

Modelling the Thermal Demand in Domestic Electricity Systems

6.1 Introduction

Along with the improving studies on energy conservation and GHG emissions reduction, the energy saving on building thermal management has significant potential. About 40% of energy consumption are in the form of thermal management in buildings worldwide[226], while 70% of electricity consumption in the US is in residential and commercial buildings [227]. In the UK, the average heating setpoint temperature is 20.9 degree, and the average weekday and weekend day heating periods were 9.5 h and 11.2 h respectively. If only dwellings with a single heating duration are taken into consideration, the heating period is 6.2h, while it is 5.6h for the double heating duration [228].

As long as the integration of renewable energy, such as solar and wind power, their intermittency leads to a novel challenge to electricity systems. Hence, stable energy supply and flexible storage are essential to decrease energy consumption and avoid net risk. Integrating large heat pumps into the energy network will absorb up to 40% of fluctuating renewable energy [229].Additionally, excess electricity can be converted into heat by heat pumps, which can be used later [230]. For instance. It can act to some extent as energy storage.

As shown in several studies [231], operational performance of heat pumps can be improved by more accurate models. However, the diverse types of models demand various levels of the order of the model, the magnitude of the data, as well as the power of computation. Therefore, the choice of model is important depending on the purpose of applying the heat pump model. In addition to groud source heat pump, the study of Air Source Heat Pumps (ASHPs) focuses on defrosting management, system management, and smart grid demand response [232]. It highlights available ASHP data for researchers and identifies future research directions to optimize ASHP efficiency and usage.

Clearly, one of the key issues in modelling a heat pump is properly accounting for its performance variation under different operating conditions. With heat pumps, the COP (coefficient of performance), which equals to the ratio of heat and power, is one of the most important definitions for analysing its performance. It varies at different condensation and evaporation temperatures. Incorporating heat pumps into the modelling process of energy dynamics simulations can be difficult for technologically innovative solutions.

In the energy utilization for buildings and domestic environments, hot water

usage plays an important role. In the residential sector, about one-fifth of total energy consumption is hot water production in the USA, while it accounts for 14% in the European Union [233].

When it comes to the distribution of water used in a domestic environment, almost 70% of hot water is consumed through baths and showers in the UK, while the rest is mainly used in basins and sinks [234]. In the US, half of hot water volume is consumed for showers, when baths, dishwashers and wash machines account for 23%, 10%, 16% respectively [235]. Moreover, the volume of hot water usage could also be affected by climate, season, as well as cultural factors [236].

In addition to applying electricity to supply domestic heating demand, the electrification of cooking appliances can lead to a future of energy savings and carbon reduction. In previous decades, electrical cooking only means a resistive element hot plate placed in the pan. Meanwhile, specific cooking appliances were dominant products in the market, such as toastie machines and rice cookers. Based on previous induction technology, such as traditional resistance element hot plates, it is generally agreed that electricity is the most expensive energy for cooking [237], as costs are higher than for traditional gas stoves [238].

However, with the improvement of technology and the increasing demand for green homes, novel efficient appliances utilize the features of insulation, pressurisation, and automation. In addition to the reduction of energy consumption, the consumer experience is also improved by novel electrical cooking appliances [239]. The progress and application of new techniques on electrical cooking not only focuses on equipment, but also on commercial activities. In order to overcome the cost barriers of modern cooking fuels, electricity, mobile payment and sharing appliances for domestic cooking

have been explored [240].

Considering the importance of energy conservation and its implications in domestic environments, this chapter presents a detailed exploration of various components contributing to household energy consumption. It is an undeniable fact that energy management in buildings, especially in domestic environments, is of paramount importance, given the global emphasis on sustainability and green energy solutions.

The initial focus of this chapter is about the intricacies of the thermal room heating model. This model is pivotal, considering the significant energy consumption associated with heating in households, especially in colder regions. The dynamics of control algorithms, hysteresis control, and the importance of accurate parameter estimation are discussed in depth.

Transitioning from room heating, the chapter investigates the field of ground source heat pumps (GSHP). The emphasis here is not just on the operational mechanism of GSHPs but also on their performance metrics. Given the potential of GSHPs in efficient energy utilization, understanding their working is crucial. Another significant contributor to household energy consumption is hot water usage. This section provides a dual perspective: firstly, the demand side, focusing on the patterns of hot water consumption, and secondly, the supply side, considering the mechanics of the water tank model. The combined model aims to present a holistic view of hot water consumption in households. The final section of this chapter addresses the evolution of electrical cooking appliances. While traditional perceptions might regard electrical cooking as energy-intensive, technological advancements have ushered in a new era of efficient and sustainable cooking solutions. From understanding the probabilities of cooking events to the effects of seasonality and household size on consumption, this section

provides a comprehensive overview. After a look into the various models and mechanisms, the chapter concludes with the integration of occupancy and an analytical comparison. Drawing insights from real-world data, the simulation results are juxtaposed against empirical findings, validating the models and methodologies presented.

This chapter serves as a guide to understanding the different aspects of energy consumption in domestic environments. By investigating each component, from heating to cooking, it aims to provide readers with a clear picture of the current landscape, challenges, and potential solutions in household energy management.

6.2 Thermal Room Heating Model

6.2.1 Introduction

To achieve better thermal management in buildings, a reliable and convenient thermal model needs to be established. There are two main methods that help with thermal simulation. The first type is physical models, which are established based on thermal dynamic equations, to simulate building thermal conditions [241], [242]. This type of model, which is also known as 'white-box-model', has good performance and accuracy, but the parameters require specific setting by an expert in thermal modelling. In addition, this model is fixed and unable to simulate any changes during operation. As a result, this method cannot be widely applied in daily life or this project. The other commonly used method is a data-driven approach [243], [244]. Combining the time-series analysis and improved learning algorithms, the indoor temperature can be predicted, basing on collected datasets and self-

trained models. This method requires accurate time-series datasets, as well as smart meter appliances for measurement. This type of model is defined as a 'black-box-model', and obtains detailed and accurate thermal simulation results using a high computing power. In this research, a suitable model should consider the reasonable thermodynamic building information, as well as reduced computing power, to be able to be employed as a real-time simulation model. As an alternative approach as a compromise, the 'grey-box-model' was proposed in [245, 246, 247, 16].

A grey-box-model is a combination of white box modelling and black box modelling, aiming at taking the advantages of both sides. The model structure is constructed using system knowledge, while the parameters are estimated, basing on collected datasets and typical constants. The thermal resistance (R) and capacity (C) are used in the grey box model to represent different components (similar to an electrical network). Different models of indoor temperature prediction were compared in [248], showing that a model order of more than 3 would not have an obvious improvement on the model performance. The performance of models with different orders was also evaluated in [249], indicating that the prediction of both indoor temperature and heating power can be accurate enough in a second order model. [250] studied the capacity problems in the grey box model, and found that in a residential building, a model with only one thermal capacity is effective to predict the indoor temperature.

In this project a grey box thermal model, which can effectively simulate the thermal performance of an electrical heater in the domestic environment is proposed. This thermal model, which is under combined hysteresis and timing control, can maintain required room temperature and reasonable model energy requirement.

In this section, the methodology of the room heating model is proposed. Modelling energy at the room level is essential for understanding a home's complete energy dynamics. Considering that electric heaters are often compact and designed for individual rooms, it's imperative to examine their impact on a room-by-room basis. By focusing on one room, a standard model can derived which can be applied across multiple rooms in a residence.

This room-based approach can reveal details that might be missed in broader models. It aids in identifying specific energy patterns, allowing for better optimization and adjustment. With architectural trends moving towards modularity, seeing a building as a collection of individual rooms, each with its energy profile, makes the modelling process more systematic and adaptive.

Furthermore, as individual room heating solutions might become more common due to their efficiency and adaptability, room-level insights are vital for future energy management. Starting from the room level and then expanding to the entire building ensures a comprehensive approach to energy modelling.

The objective of the modelling in this project is to simulate the real time electricity consumption for room heating demand. The construction of the structure of the model, the estimation of physical properties, the optimization of thermal parameters, as well as simulation of combined control is introduced in this section.

6.2.2 Thermal Room Heating Model

The aim of room heating model is to simulate the real time energy consumption of electrical heaters in a domestic environment. This can then be used in conjunction with a model of a direct electric radiator or a ground/air source heat pump to determine electricity consumption. Figure 6.2.1 shows the four components in the thermal model and the heat exchange between these parts. The four components in this model are: (a) electrical heater, (b) indoor air, (c) wall, (d) outdoor atmosphere. Four temperatures are related to these four components, which are marked as T_h (heater), T_i (indoor), T_w (wall), T_o (outdoor). The thermal resistances between each component and thermal capacities of each component are shown as well. The electric heater transforms electricity from the grid into heat energy, to satisfy the heat demand of the room. In this model, the wall is considered as a double-layer wall, which is commonly applied in the UK domestic environment for better heat insulation. As a result, the external and internal parts of the wall have separated resistances. Conversely, the indoor air and outdoor atmosphere are assumed as homogeneous substances, which have single parameter sets. For convenience, this model is named as the "3R3C" model in the following pages.

In this Figure 6.2.1, T denotes temperature; subscripts o, w, i and h indicate outdoor atmosphere, wall, indoor air and heater, respectively; R_{wo} is the thermal resistance between building envelope/ wall and outdoor atmosphere, R_{wi} is the thermal resistance between wall and indoor air, R_{ih} is the thermal resistance between indoor air and electrical heater. Thermal resistance indicates the ability of heat transfer between different objects, and its unit is K/W. C_w is the thermal capacity of wall, C_i is the thermal capacity of indoor air, C_h is the thermal capacity of heater. Thermal capac-

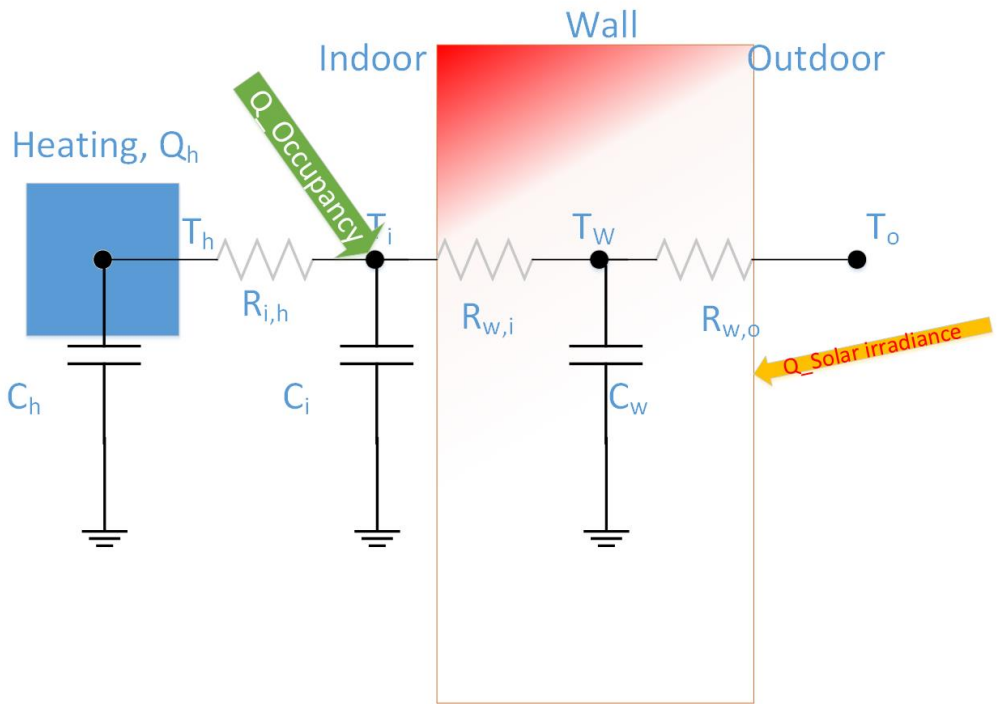


Figure 6.2.1: Structure diagram of the "3R3C" model

ity defines the amount of heat that can be absorbed by a single object, and its unit is J/K. $Q_{heating}$ is the heat transformed from electricity by the electrical heater to this system. Similarly, the heat from solar irradiance and indoor inhabitants are named as Q_{solar} and $Q_{Occupancy}$. T_o and Q_{solar} comes from historic weather datasets [125]. Based on this graph, three formulas of heat transfer and temperature change can be written as Equation 6.2.1 to Equation 6.2.3 :

$$dT_w = \left(\frac{T_o - T_w}{R_{w,o}C_w} + \frac{T_i - T_w}{R_{w,i}C_w} + Q_{solar} \right) dt \tag{6.2.1}$$

$$dT_i = \left(\frac{T_w - T_i}{R_{w,i}C_i} + \frac{T_h - T_i}{R_{h,i}C_i} + Q_{Occupancy} \right) dt \tag{6.2.2}$$

$$dT_h = \left(\frac{T_i - T_h}{R_{h,i}C_h} + \frac{Q_{heating}}{C_h} \right) dt \tag{6.2.3}$$

These equations involve three variable types. Thermal resistance (R) and capacitance (C) are physical parameters, which are tuned during running optimization, and fixed for simulation. The value of temperature sets for different components comes from measurement datasets or real time simulation. The last type is thermal energy (Q), the heat from electrical heater and the inhabitants are commonly in a limited range, while the heat from solar radiation to the room components is determined according to:

$$Q_{solar} = \alpha A I_{solar} \tag{6.2.4}$$

Where α denotes the absorptance of surface for solar radiation, A is the area of the irradiance surface, and I_{solar} denotes the global solar radiation. In this set of equations, system parameters such as thermal resistance and capacity are fixed before operating the simulation. Different temperature sets are variables which change with time. Outdoor atmosphere temperature is obtained from local long-term measurement, used as inputs of this model. Conversely, the wall and indoor temperature are outputted variables calculated from simulation.

Figure 6.2.2 shows the general approach to capturing data experimentally for use in grey-box thermal modelling. It can be seen that wireless sensors and data acquisition equipment are required.

Figure 6.2.2 contains an actuator, a heater, three temperature sensors, as well as a raspberry pi and a computer for data collection in this area. The actuator is connected to the electrical source and the heater at the same time, to measure the power rate of electrical heater. Meanwhile, two sensors [251] are set in 10cm and 20cm away from heater on the ground, while another one is set in another area in the room. Additionally, these

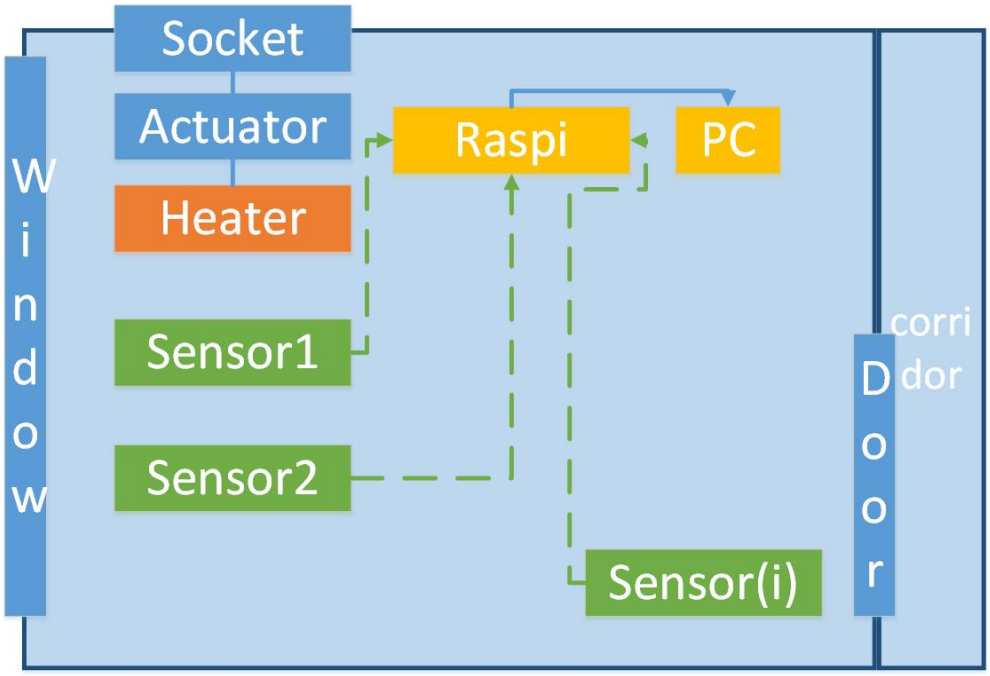


Figure 6.2.2: Experimental measurement system for the room

electronic appliances are IoT items, sending telegrams to a Fhem system [252] in the raspberry pi using Enocean radio standard [253].

6.2.3 Control Algorithm and Heating Period

The control of the heater combines hysteresis control based on local temperature measurement and timing control, and the flow chart for control algorithm is shown in Figure 6.2.3. In control systems, hysteresis can be used to filter signals so that the output reacts less rapidly than it otherwise would by taking recent system history into account. To manage the temperature in a thermal model, a thermostat controller may switch the heater on when the temperature drops below the lower reference temperature, but not turn it off until the temperature rises above a higher reference temperature. In this simulation, the set reference temperature is 20 degrees, while the set temperature difference is 0.5 degrees.

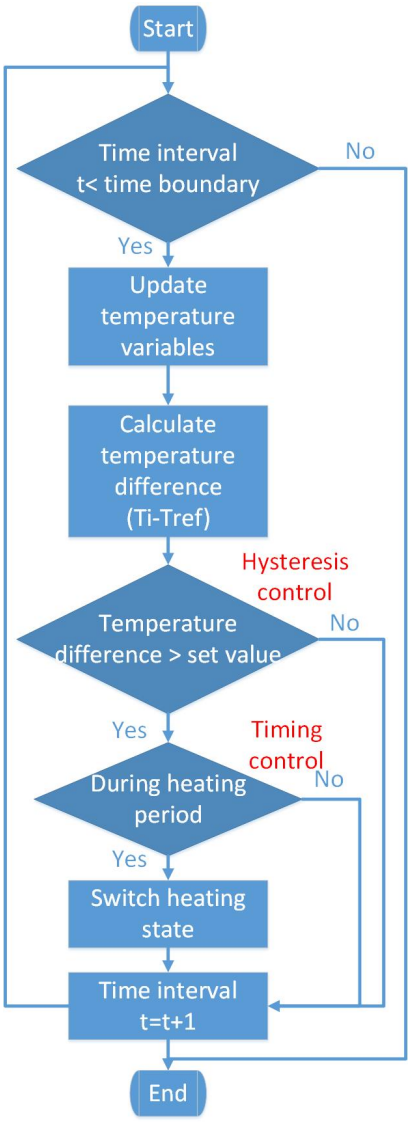


Figure 6.2.3: Flowchart of the control algorithm

At the same time, the control of system also follows the set timing pattern. Single heating duration and double heating duration are commonly used in room heating. Single heating duration means only a single period of using a heater for room heating in one day. Sometimes, the single heating duration is directly applied for 0-24 in one day. The double heating duration indicates two different heating periods in one day. In this research, double heating duration applies to 6-10 in the morning and evening for heating. Only when the required statements are true for both hysteresis control and timing control, will the electrical heater be switched by the controller.

Figure 6.2.4 shows the detailed difference between single and double.

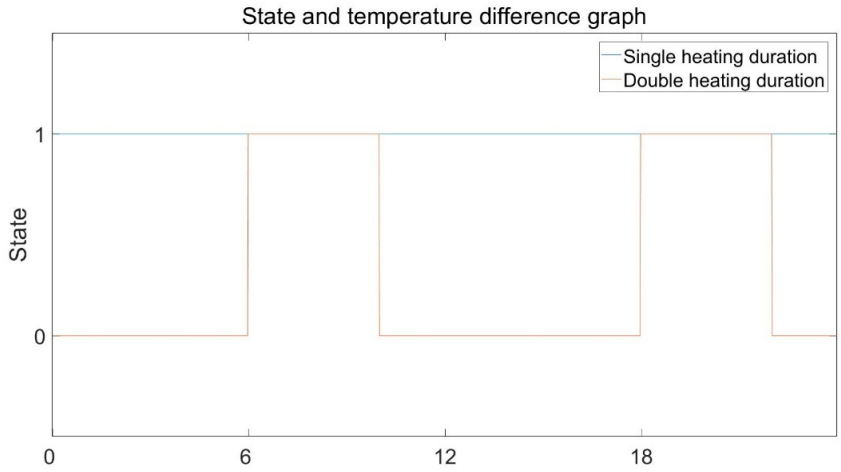


Figure 6.2.4: Single heating duration versus double heating duration

6.2.4 Sub Model for Hysteresis Control

The hysteresis control, which is widely applied in room heating systems including air conditioners, underfloor heating systems, room heating appliances, is widely investigated and proven effective in maintaining indoor temperature. For hysteresis control, the measurement of the indoor air temperature is the most critical variable. In central heating systems, such as central air conditioning systems, central underfloor heating systems, or central room heating systems, the sensors for measurement can be placed in different parts of the interior, while the heated fluid comes from other areas. Alternatively, for a small scale single domestic electrical heater, its sensor is integrated in the appliances and close to heat source.

During the operation of this domestic electric heater, several sensors are set close to the heat source at different distances, while others are utilized for measurement of indoor air temperature at other places in the room. Figure 6.2.5 shows the temperature, and power curve for a one-day ex-

periment. Three curves are based on temperature measurement in various places in the room, while the other one curve is from a smart meter which is connected to the electrical heater. The red curve of temperature is for indoor air, while the green and red indicate the temperature measured 10 centimetres and 20 centimetres away from the electrical heater respectively. The orange curve ranging from zero to about 1000 W shows the on and off state of the electric heater.

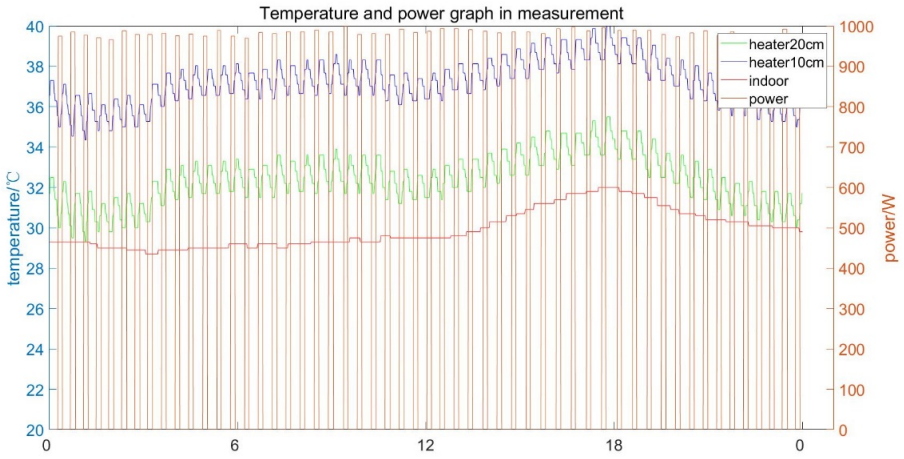


Figure 6.2.5: Temperature and power graph in the experiment

The indoor air temperature changed slightly and was kept around 30 degrees for all of the day, which is a little higher than the optimum temperature for humans. This long-term trend took place in both indoor temperature and temperature around the heater. The temperature of the air close to the heater, however, changed dramatically with small perturbations every half an hour. The peaks of these small perturbations of these temperature curves match the operation of electrical heater. By contrast, the impact of turning on and off on the electrical heater did not lead to a direct increase or decrease in indoor air temperature. Hence, for the simulation of hysteresis control of room heating with a domestic electric heater, the temperature difference between the indoor air temperature and set temperature cannot correctly reflect the on/off condition of the heater. The

temperature of air around heat source, which is measured by the heating appliance and ultimately affects the control of heaters, does fluctuate.

To reflect this phenomenon in simulation and ensure reasonable switching of the control system, a sub model is essential to the hysteresis control system. The sub model should estimate the measured temperature of the domestic heating appliance, and thus guarantee the operation of the control system. In Figure 6.2.6, the R-C room heating model with the proposed sub model is shown.

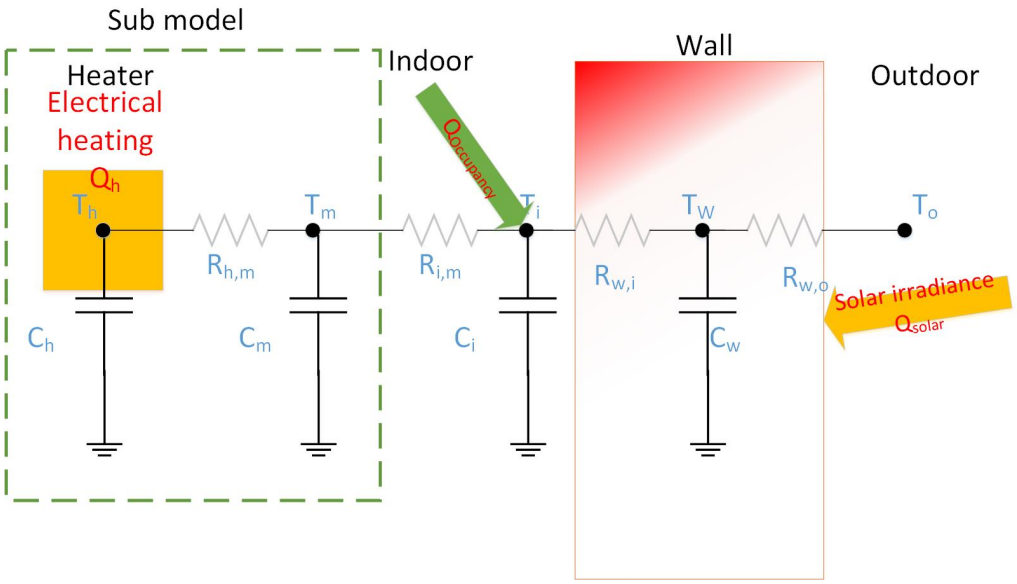


Figure 6.2.6: Room heating model with hysteresis control

In addition to the 3R3C room heating model, a new temperature point is added, which is in the middle of the temperature of the heater and that of the indoor air. As the medium layer, this point is marked as Tm. As a physical definition, this temperature point indicates the air close to the domestic electrical heater, which is measured by the sensor integrated in the appliance for control. Owing to the new temperature point, several thermal resistances and capacitances are also modified. The new thermal capacitance C_m is for the air around electrical heater, with a value similar to that of room air, considering the difference of mass. There is no R_{hi} in

this new model, compared to the 3R3C model. As replacements, thermal resistances R_{hm} and R_{mi} denote the resistance between heater, medium and indoor air. Hence the equations for energy balance can be written as:

$$dT_w = \left(\frac{T_o - T_w}{R_{w,o}C_w} + \frac{T_i - T_w}{R_{w,i}C_w} + \frac{Qsolar}{C_w} \right) dt \tag{6.2.5}$$

$$dT_i = \left(\frac{T_w - T_i}{R_{w,i}C_i} + \frac{T_m - T_i}{R_{m,i}C_i} + \frac{Qocc}{C_i} \right) dt \tag{6.2.6}$$

$$dT_m = \left(\frac{T_i - T_m}{R_{m,i}C_m} + \frac{T_h - T_m}{R_{h,m}C_m} \right) dt \tag{6.2.7}$$

$$dT_h = \left(\frac{T_m - T_h}{R_{h,m}C_h} + \frac{Q_{heating}}{C_h} \right) dt \tag{6.2.8}$$

6.2.5 Parameter Estimation and Range

In this grey-box model, the physical thermal structure of the room is combined with reasonable RC parameters for the room heating simulation. To ensure that the RC values not only follows the physical principle, but also are tuned to the simulation results, the RC values should be pre-estimated. The pre-estimation of the range of parameter values, can save computation time for the optimization. The data source for the estimated RC values can be various, including the components' physical properties, building surveys and previous grey-box model investigations.

For instance, the U-value, which is also defined as the thermal transmittance, is the rate of transfer of heat through a structure. The U-value is widely used in building issues to describe the thermal properties of external and internal walls. The thermal resistance of walls can be estimated as Equation 6.2.9:

$$R = \frac{1}{AU} \tag{6.2.9}$$

Where R,U are the thermal resistance and transmittance respectively, and A is the corresponding area of the walls. The thermal capacitance (C) can be calculated based on the heat capacity from diverse sources, such as [254, 18]. Its unit is commonly Wh/K or J/K. The pre-estimation of the thermal parameters of the room investigated is shown in Table 6.2.1.

Table 6.2.1: Pre-estimation of parameters

Parameter	C_w	C_i	C_m	C_h
Value (Wh/m^2K)	2000	250	5% C_i	50
Parameter	R_{wo}	R_{wi}	R_{mi}	R_{hm}
Value (K/W)	0.17	0.06	0.06	0.01

With the estimated RC values, the search range during optimization can be regulated by a lower boundary and an upper boundary. In this project, the range is set as 10% to 200% of initial estimation.

Due to the different physical properties of different components, the orders of magnitude of the RC parameters have large differences. This difference would lead to a poorly scaled problem in building thermal dynamics, and the cost function has different sensitivity to different parameters. Therefore, the order of magnitude matrix is introduced to balance the resolution of various parameters, as shown in Equation 6.2.10.

Table 6.2.2: List of order of magnitude matrix

OM1 10^3	OM2 10^2	OM3 10^1	OM4 10^1
OM5 10^{-1}	OM6 10^{-2}	OM7 10^{-2}	OM8 10^{-3}

$$\begin{bmatrix} C_w \\ C_i \\ C_m \\ C_h \\ R_{wo} \\ R_{wi} \\ R_{mi} \\ R_{hm} \end{bmatrix} \begin{bmatrix} OM1 & \cdots & 0 \\ \vdots & \ddots & \vdots \\ 0 & \cdots & OM8 \end{bmatrix}_{8\times 8} = \begin{bmatrix} c_w \\ c_i \\ c_m \\ c_h \\ r_{wo} \\ r_{wi} \\ r_{mi} \\ r_{hm} \end{bmatrix} \tag{6.2.10}$$

The values in the order of magnitude matrix are listed in Table 6.2.2, according to the pre-estimation of thermal parameters.

The thermal parameters would be pre rescaled before the operation, as they would be in a similar order for the optimization function. During the operation of the function, these parameters would be rescaled again to their raw value.

6.2.6 Optimization Techniques for Model Identification

After the pre-estimation of the RC parameters, the optimization of the parameters in the grey-box model can be performed. Searching for the optimal values of the undetermined parameters in a grey-box model is a

nonlinear optimization process.

The optimization library of Matlab was used as the framework for the model identification process. As the thermal parameters have a great influence on simulation results, the GlobalSearch algorithm of Matlab is used to increase the chances of finding a global minimum independently of the initial values. During the real room experiment, datasets of both indoor air temperature and electrical heater consumption were collected.

In this project, the optimization is classified as two steps. In the first step, the optimization would be operated for the sub model, which focuses on the combined control system. In this step, the simulation state for the heater under hysteresis control and timing control is the key result. The medium temperature, which is directly connected to the hysteresis control, would be calculated based on the measured indoor room temperature. Thermal model equations for the heater temperature and the medium temperature are applied in this step for state changing. Hence, four parameters (C_h, C_m, R_h, R_{mi}) are involved in this step of the optimization.

The optimization objective is the square of the error of heating state between measured and simulated results, which can be calculated as:

$$J = \sum_{i=1}^{Time} \left(State_i^{measuement} - State_i^{Simulation}\right)^2 \tag{6.2.11}$$

With the optimization of this sub model, four parameters (C_h, C_m, R_h, R_{mi}) can be obtained and fixed for a second step. In the second step, the remaining parameters (C_i, C_w, R_{wi}, R_{wo}) would be searched for. In this step, the key issue is the simulation of the indoor air temperature, which plays one of the most important roles in the room heating system. The whole thermal model would be applied in simulation during this step,

and datasets of solar irradiance, outdoor temperature, occupant would be used as inputs for this system. The optimization objective of this step is the square of the error of indoor air temperature between measured and simulated results, which can be calculated as:

$$J = \sum_{i=1}^{Time} (T_i^{measuement} - T_i^{Simulation})^2 \tag{6.2.12}$$

To show the steps of the optimization process more clearly, the flow diagram of the estimation and optimization of this thermal model is shown in Figure 6.2.7.

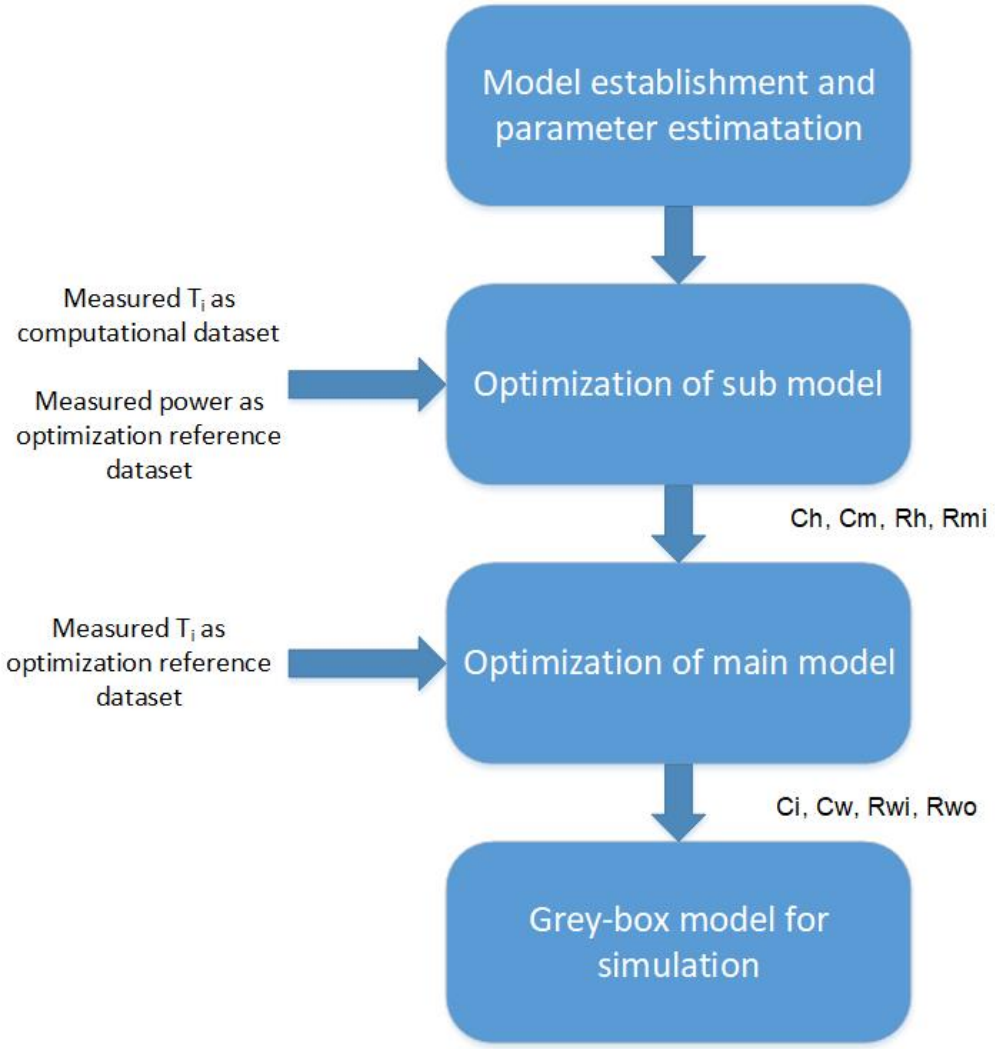


Figure 6.2.7: Flow chart for model construction, estimation, optimization and simulation

For the whole thermal model, the indoor air temperature is the simulation variable, while thermal parameters are unknown thermal parameters in the grey-box model. In the first step of the sub control model, not the measured indoor temperature instead of the simulated one is utilized, to obtain reasonable parameters for the sub model for heating state controlling. In the second step of the whole thermal model, the measured indoor air temperature is now utilized as the reference datasets for the optimization objectives.

6.2.7 Adjustment of the Thermal Parameters with Room Area

In building energy simulations, room thermal models often incorporate parameters such as thermal resistance (R) and thermal capacitance (C) to predict the thermal behaviour of the room. While these parameters are typically derived from material properties and initial room dimensions, it's imperative to adjust them when the room size deviates from a default or reference size. This ensures that the model remains accurate across various spatial scales.

The thermal capacitance of a wall is directly proportional to its area. As the wall's surface area increases or decreases, its ability to store heat changes in direct proportion. The adjusted wall thermal capacitance can be represented as:

$$C_w' = C_w \times \left(\frac{\text{Area}}{\text{Default_area}} \right) \tag{6.2.13}$$

Here, C_w' is the adjusted wall capacitance, C_w is the original capacitance, and Area and Default_area are the new and reference room areas, respectively.

The thermal capacitance of the interior components (like air) is not just dependent on the area but also the volume of the room. As the room size increases, the volume scales up faster than the area, leading to a more substantial increase in thermal capacitance. This relationship is captured by:

$$C_i^{'} = C_i \times \left(\frac{\text{Area}}{\text{Default_area}} \right)^{1.5} \tag{6.2.14}$$

Where $C_i^{'}$ is the adjusted interior capacitance, and C_i is the original capacitance.

The thermal resistance of a structure is inversely proportional to its surface area. As the wall's area scales, the path for heat transfer changes, leading to adjustments in resistance values. For both wall-to-outsideR_{wo} and wall-to-interior R_{wi} resistances, the relationships are:

$$R_{wo}^{'} = R_{wo} \times \left(\frac{\text{Default_area}}{\text{Area}} \right) \tag{6.2.15}$$

$$R_{wi}^{'} = R_{wi} \times \left(\frac{\text{Default_area}}{\text{Area}} \right) \tag{6.2.16}$$

Where $R_{wo}^{'}$ and $R_{wi}^{'}$ are the adjusted resistances for wall-to-outside and wall-to-interior, respectively.

After introducing the area scaling methodology, it's essential to highlight some assumptions and considerations. The scaling approach for parameters based on area inherently assumes a cubic geometry for the rooms. This cubic assumption implies that as the area of the room changes, the height, width, and depth of the room adjust proportionally, following a cube-root relationship. While this offers a simplified model for scaling, it might not accurately represent all building shapes and configurations. Therefore, the

cubic geometry hypothesis could introduce discrepancies when applied to rooms or buildings that deviate significantly from this shape.

Moreover, while the methodology provides a framework for scaling parameters with the area, it is imperative to treat it as an approximation. Ideally, experimental or empirical data should be used to fit and validate models for different room sizes and configurations. However, in the absence of such data, this scaling method can serve as a useful starting point.

6.2.8 Performance of the Model

Based on the optimization of the sub model, four parameters, as Ch,Cm,Rhm,Rmi are obtained. To evaluate the effectiveness of the thermal model, a definition of duty cycle is introduced. A duty cycle or power cycle is the fraction of one period in which a signal or system is active. A period is the time it takes for a signal to complete an on-and-off cycle. As a formula, a duty cycle (%) may be expressed as:

$$D = \frac{PW}{T} \tag{6.2.17}$$

Where D is duty cycle, PW is pulse active time and T is the total period.

In Figure 6.2.8, a one-day simulation result of the sub model in the grey-box system is presented, with an electric heater of 1.5 kW [255]. In the upper subgraph, the blue curve indicates the measured indoor air temperature, while the orange curve and yellow curve show the change of temperature of the electric heater and the medium air separately. The medium temperature is the value which leads to the switching on the electrical heater based on its difference with set the reference temperature. In the lower

one, the switch state of electrical heater is shown. State 1 means switching the heater on, and state 0 means the heater is turned off. The blue curve is based on the measurement of electricity consumption, while the orange curve shows the state during simulation.

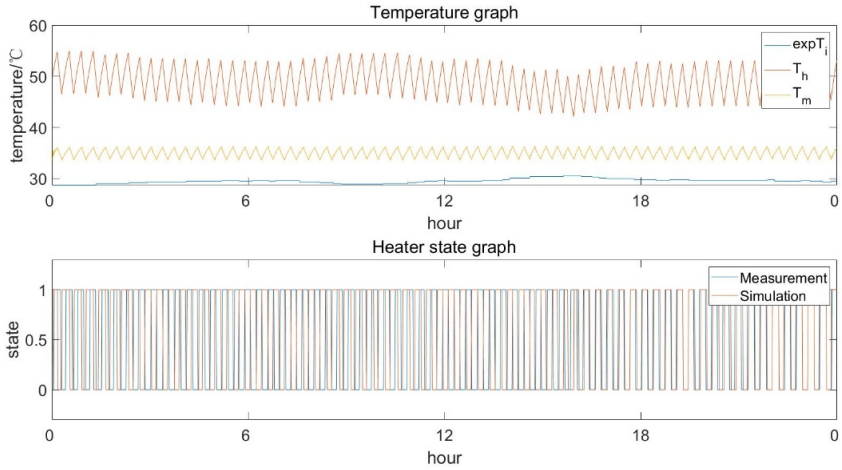


Figure 6.2.8: One day simulation of optimization result of sub model

Ideally, the control algorithm of this thermal model can maintain the indoor air temperature around reference temperature, offering a comfortable environment for the inhabitants. The measured indoor air temperature is kept around 30 degrees, which is slightly higher during the middle of the day. Due to the changing of state, the temperature of electrical heater is dramatically changed to around 50 degrees, while that of medium temperature is around 35 degrees. When the medium temperature is 0.5 lower than the reference temperature, the electrical heater would be turned on for room heating. After a period of heating, if the medium temperature is 0.5 degrees larger than the reference temperature, the heater would be turned off. In the simulation results, the temperature difference is fluctuating around 0 as assumed, but it achieves more than +2 degree or less than -0.5 degree, which is out of bounds for the set difference (0.5). This is due to the delay effect of heat transfer, as the medium and indoor air temperature cannot directly change to the set value immediately. When

the heater is turned off, although the grid would not provide the thermal system with extra energy, the temperature of the heater is still high, and can still transfer heat to indoor components, leading to the continued increase of indoor air temperature. The heating time of the simulation in this single day is 782 minutes, which is close to that of the measurement (744 minutes). In the other words, the duty cycle is 51.6% for measurement, and 54.3% for simulation. This difference, which is less than 5%, indicates its accuracy is acceptable.

The other parameters can be obtained during the optimization of the main model. In Figure 6.2.9, a one-day simulation result of the grey-box thermal model is presented. In the upper subgraph, the curves of the heater, and medium are shown based on the sub model, and also the recorded outdoor temperature is plotted with the yellow curve while the measured indoor temperature is indicated by blue dots. The indoor air curve in orange and the temperature of wall in purple are based on the simulation of thermal model. In the lower one, the switch state of electrical heater is shown. State 1 means switching the heater on, and state 0 means the heater is turned off. The blue curve is based on the measurement of electricity consumption, while the orange curve shows the state during simulation. The initial points for the one day figure is based on the assumption of steady indoor state, as the room has already been heated for some while.

In addition to the sub model, the temperature of the indoor air and wall were also simulated. The temperature of the indoor air is about 30 degrees, and changes slightly due to the influence of room heating and the wintry weather outside. Along the curve of the simulated indoor temperature, the measured indoor air temperature is closely distributed as marked dots. It indicates the superior performance of grey-box simulation model with a hysteresis control sub model. The heating time for the simulation in this

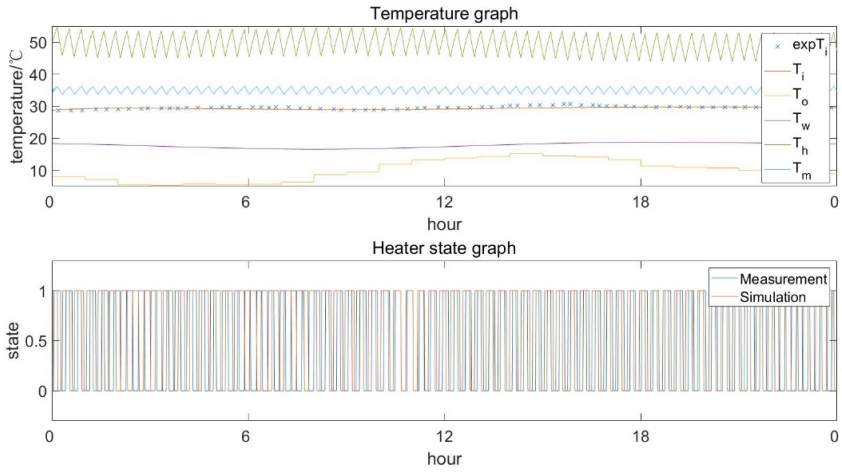


Figure 6.2.9: One day simulation of optimization result of whole model

single day is 801 minutes, which is close to that of the measurement (744 minutes). In the other words, the duty cycle is 51.6% for measurement, and 55.6% for simulation. This difference, which is less than 5%, indicates its accuracy is acceptable. In this thermal model with a sub model for hysteresis control, both the indoor temperature and the power consumption of the simulation results have a satisfactory performance, which represent the working condition of the electric heater and its impact. For the temperature of the wall, its peak is at about 5p.m., while that of the outdoor atmosphere is at 2p.m. This delay is due to the thermal properties of walls, as heat insulation is emphasized in buildings in the UK.

The simulation results for a single day in December are shown in Figure 6.2.10 and Figure 6.2.11. For comparison, the first graph is based on the simulation of single heating duration, while the second graph is based on double heating duration.

In the upper subgraph, the blue curve indicates the key value, indoor air temperature, while other temperatures are also shown. In the lower one, the blue curve shows the state of electrical heater.

In the simulation based on double heating duration, the indoor air tem-

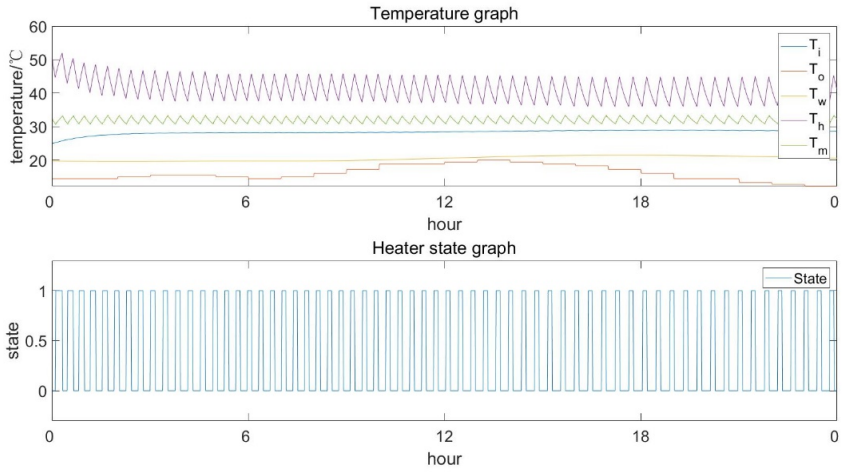


Figure 6.2.10: Simulation of one day in Dec with single duration

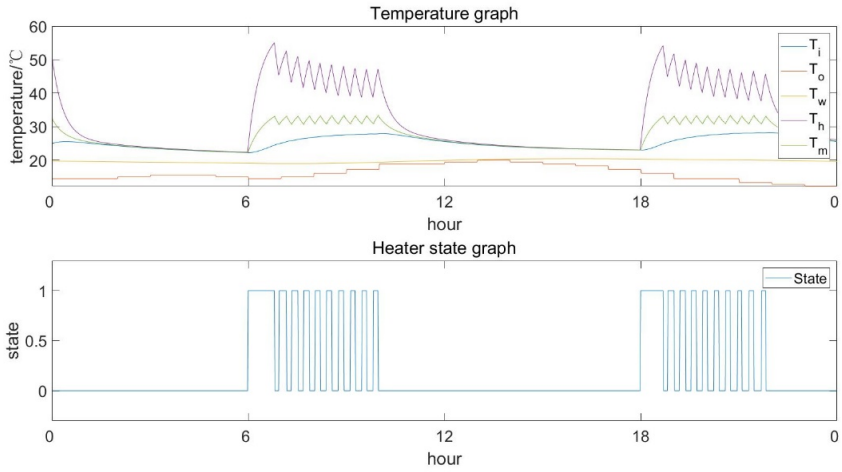


Figure 6.2.11: Simulation of one day in Dec with double duration

perature is increased to 25 degrees during heating periods. After 10 a.m., the end of first heating duration, the indoor air temperature decreases dramatically due to the lack of heat source. This phenomenon takes place in each beginning and end of heating duration. In summary, even if the model can lead to a large decrease of heating hours and heat preservation, it cannot make up for the lack of heat sources based on heating duration. Considering human behaviour, the change of timing control can still reduce heating hours and energy consumption, as well as providing a comfortable thermal environment.

6.2.9 Conclusion of Room Heating Model

The room-level model gives a detailed view of how energy is used in individual spaces. This is very important when looking at electric heaters, which often work on a room-by-room basis. Using the 'duty cycle' helps us better understand how these heating systems work. The close match between the real-world heating data and the model's predictions (less than 5% difference) shows that the model is accurate.

The model also provides insights into different temperatures inside the room, like the air, heater, and wall temperatures. An interesting observation is the delay in the highest wall temperature. This tells us about the material of the walls and how they react to heat.

The model's ability to simulate different heating times, both once and twice a day, is also very useful. These tests show that even if walls keep heat for longer, they can't replace a continuous heat source. But if considering how people use their heaters and when they turn them on or off, it can save energy and still keep the room comfortable.

In summary, this room heating model is a great tool for understanding how an electric heater works in a room. As aiming to save energy and live in a greener way, such models will be important to help us design better homes and use energy more wisely.

6.3 Ground Source Heat Pump

6.3.1 Introduction

The usual methods for modelling a heat pump are summarized as four main types [256], including balanced-state, steady-state, fitted, and dynamic-state models, as shown in Table 6.3.1. Both balanced and fits models are widely used to evaluate the seasonal or annual performance of a heat pump, and have different confidence levels and computational demands. The theoretical steady-state model, as well as a dynamic-state model, are more commonly used in the sizing and control of heat pump systems.

Table 6.3.1: List of modelling method of GSHP

Method	Basis	Confidence	Typical application	Computational need
Balanced energy	Theoretical/ Empirical	Low	Seasonal energy use and economics	Negligible
Steady state	Theoretical	Moderate	Design and sizing	Low
Fitted models	Empirical	Conditionally high	Seasonal energy use and economics	Low
Dynamic state	Theoretical	High	System integration and control	High

By gathering the data for performance of the heat pump based on operational and experimental data, the regression-fitted model can be obtained. Using evaporator and condenser temperatures as the inputs, the simple regression model can be established, which outputs the COP value. In terms of confidence, the regression model has a good fit, but requires lots of measured data to obtain.

In order to provide energy for space heating and cooling, a GSHP system can be applied in a building as one heat source solution [257]. Compared to traditional air conditioning (A/C) systems, GSHP technology can provide higher energy efficiency for air conditioning because the subterranean environment provides higher heating and lower cooling temperatures which are proportional to changes in ambient air temperature, rather than temperature fluctuations.

As with most of the heat pump types, the GSHP unit consists of an evaporator and a condenser, as well as other components including an expansion valve, and a compressor. A diagram of the structure of a typical heat pump unit is shown in Figure 6.3.1 [257].

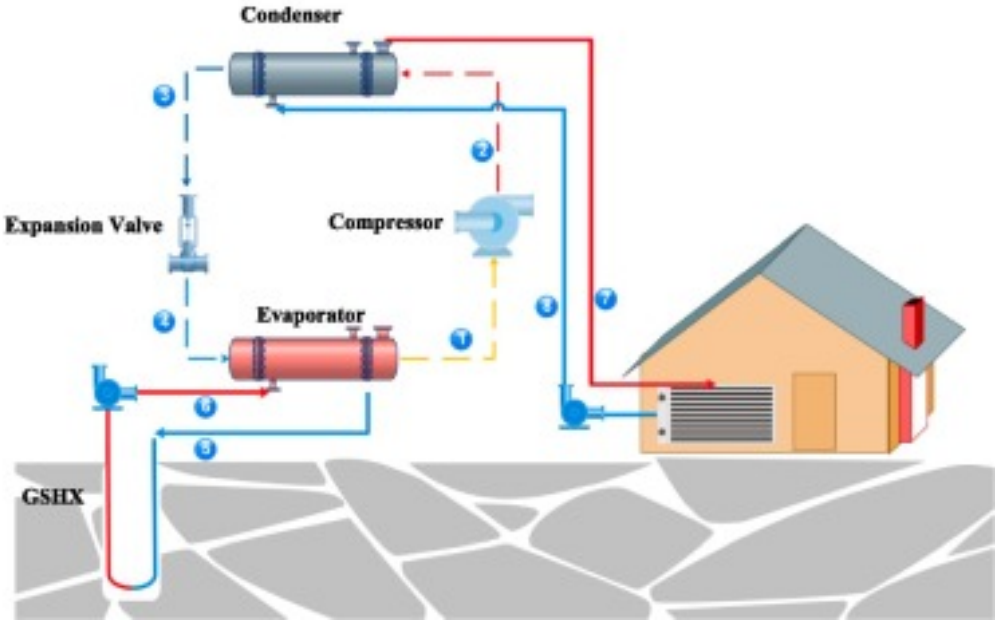


Figure 6.3.1: Structure diagram of GSHP system

The underground side is commonly also named the primary side, which uses refrigerant fluid for the loop. The other side is the secondary side, which uses water for transferring heat from the GSHP unit to a room.

When considering the various modelling approaches for GSHP performance,

the Fitted Model stands out for several compelling reasons. Firstly, its data-driven nature ensures it accurately captures real-world GSHP behaviours, making it highly reliable. Additionally, its adaptability allows it to adjust to different operational conditions with ease, ensuring the model remains up to date. From a computational standpoint, Fitted Models offer efficiency, especially beneficial for real-time applications and long-term simulations. Moreover, its intuitive design aids in clear communication of GSHP metrics. Given these advantages, the Fitted Model was the logical choice for the research.

6.3.2 Modelling the GSHP

In previous research [258, 259, 260, 261, 262], there are various empirical formulae which are proven to be effective for regression models, which contains not only COP of GSHP, but also the outlet temperature of both evaporator and condenser. These formulae are listed in Table 6.3.2.

Table 6.3.2: Formulae for COP calculation

Formulae for COP calculation
$$\mathrm{COP} = (a + bT_{\mathrm{feo}}) \times (c + dT_{\mathrm{wco}})$$
$$\mathrm{COP} = A + BT_{\mathrm{feo}} + CT_{\mathrm{wco}} + DT_{\mathrm{feo}}T_{\mathrm{wco}}$$
$$\mathrm{COP} = \left(a + bT_{\mathrm{feo}} + cT_{\mathrm{feo}}^2\right) \times \left(d + eT_{\mathrm{wco}} + fT_{\mathrm{wco}}^2\right)$$
$$\mathrm{COP} = A + BT_{\mathrm{feo}} + CT_{\mathrm{wco}} + DT_{\mathrm{feo}}T_{\mathrm{wco}} + ET_{\mathrm{feo}}^2 + FT_{\mathrm{wco}}^2 + GT_{\mathrm{feo}}T_{\mathrm{wco}}^2 + HT_{\mathrm{feo}}^2T_{\mathrm{wco}} + IT_{\mathrm{feo}}^2T_{\mathrm{wco}}^2$$

In this research, the second formula is applied, as it does not require com-

plex multiplicative relationships. It can be written as:

$$COP = A + BT_{fo} + CT_{wo} + DT_{fo}T_{wo} \tag{6.3.1}$$

where T_{fo} is the outlet temperature of the fluid side, while $T_{wo}$is that of the water side. COP is the coefficient of performance. A series of data are required for regression formulae, which are always obtained from experimental data or a manufacturers' catalogue. In this study, the catalogue comes from the catalogue file of CIAT [263], a manufacturer in the UK. Considering the thermal demand of a typical domestic environment, the device type used and its associated data are shown in Table 6.3.3 [263]. The GSHP model selected aligns perfectly with household requirements in terms of power capacity, ensuring it meets the energy demands of a typical home without being overly robust or insufficient. Furthermore, the comprehensive data provided in the user manual by the manufacturer facilitates a thorough understanding and analysis of its performance characteristics. This combination of appropriate power specifications and abundant technical information makes this GSHP model an ideal choice for residential applications.

Table 6.3.3: Manufacturer catalogue of GSHP 2500BX [259]

LW LWP	Evaporator water outlet °C		CONDENSER WATER OUTLET TEMPERATURE °C																	
			35			40			45			50			55			60		
			Pf kW	Pa kW	Pc kW	Pf kW	Pa kW	Pc kW	Pf kW	Pa kW	Pc kW	Pf kW	Pa kW	Pc kW	Pf kW	Pa kW	Pc kW	Pf kW	Pa kW	Pc kW
2500BX	Glycol water necessary	-8	**320**	112	432	**303**	121	424	**278**	134	412	**255**	145	400						
		-6	**350**	113	463	**330**	123	453	**304**	135	439	**278**	147	425						
		-4	**389**	115	504	**364**	125	489	**337**	137	474	**306**	150	456	**278**	165	443	**249**	182	431
		-2	**422**	116	538	**396**	127	523	**369**	139	508	**333**	153	486	**306**	168	474	**273**	184	457
		0	**456**	118	574	**429**	129	558	**401**	142	543	**369**	156	525	**336**	171	507	**301**	188	489
		2	**493**	120	613	**465**	131	596	**435**	144	579	**402**	158	560	**366**	174	540	**328**	191	519
	Pure water	5	**560**	124	684	**529**	136	665	**493**	148	641	**455**	163	618	**415**	178	593	**378**	196	574
		7	**588**	126	714	**571**	138	709	**535**	151	686	**494**	166	660	**453**	182	635	**412**	199	611
		10	**670**	132	802	**636**	143	779	**600**	156	756	**556**	170	726	**509**	186	695	**468**	205	673
		12	**719**	135	854	**682**	146	828	**645**	159	804	**601**	173	774	**544**	189	733	**506**	208	714
		15	**795**	141	936	**758**	152	910	**716**	164	880	**673**	178	851	**622**	195	817	**568**	214	782

In this table, at the start of the lines and the rows, the outlet temperature

of the condenser and evaporator are marked. Under different temperature series, the required electrical power for the pump and the energy produced are listed, which has been measured from long-term operation by the manufacturer. Hence, the COP under various operating conditions can be obtained.

Based on the successful modelling using regression fitting method, the numerical relationship between the COP and the temperatures can be obtained from the fitted parameters using the experimental formula. The key value COP reflects the relationship between heat gained (Q) and electricity consumption (W) of the pump, while their difference can also be presented in the water loop side, according to the physical principles [264].

$$COP = Q/W \tag{6.3.2}$$

$$mC_p(T_{fi} - T_{fo}) = Q - W \tag{6.3.3}$$

where m is the mass of water fluid and Cp is the specific heat capacity. T_{fi} is the temperature of water after the heat exchange with indoor air. In this study, the assumption of a full heat exchange has already been made. In each time interval t, the unit of gained and consumed power is Watts, hence the mass per unit time can be the multiplication of flow rate and density of water. Moreover, in the proposed model of GSHP, as a reasonable size of HP has been selected, the GSHP can produced heat to its working limitation. The heat load at time interval t in a domestic environment (under limitation) results from a low indoor temperature which can be obtained from the 3R3C model that mentioned previously, as:

$$Q = \frac{T_w - T_i}{R_{w,i}} \tag{6.3.4}$$

Based on Equation 6.3.1 to Equation 6.3.4, the two unknown values of COP and T_{fo} can not be directly calculated. However, an iteration approach can lead to the closest value based on the numerical relationships. Moreover, the GSHP can be used as a heat source for the 3R3C model, i.e., using the GSHP for room heating. In summary, the flow chart of GSHP simulation is shown in Figure 6.3.2.

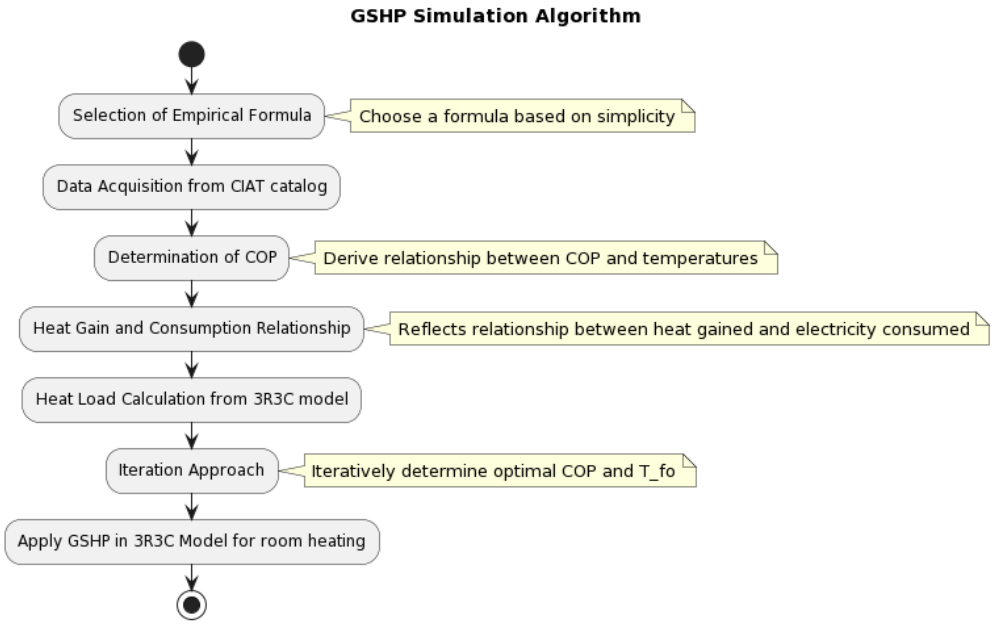


Figure 6.3.2: Flow chart of GSHP simulation algorithm

This flowchart delineates the simulation process when utilizing a GSHP. The process initiates with the import of household energy demand and photovoltaic generation data, following which the GSHP model is initialized based on parameters from the manufacturer's catalog.

The simulation first calculates the indoor temperature and, using the 3R3C model, determines the heat load resulting from a low indoor temperature. The GSHP serves as a heat source to warm the room. To accurately simulate the GSHP's performance, the process involves an iterative loop where both the COP and outlet temperature are continuously computed until stable values are achieved.

The final step of the process involves updating the GSHP's performance parameters based on the COP and temperature values of outlet flow, after which the model outputs the heating results and overall performance metrics.

6.3.3 Performance of the GSHP Model

Based on the assumption of infinite energy from ground heat, as well as one hundred percent efficiency heat supply from the GSHP unit, the catalogue data can be applied for regression. The catalogue data utilized are the evaporator outlet temperature (T_{fo}), the condenser outlet temperature (T_{wo}), and the COP. The results of the parameters based on the regression are listed, while the regression results and catalogue data are compared in Figure 6.3.3.

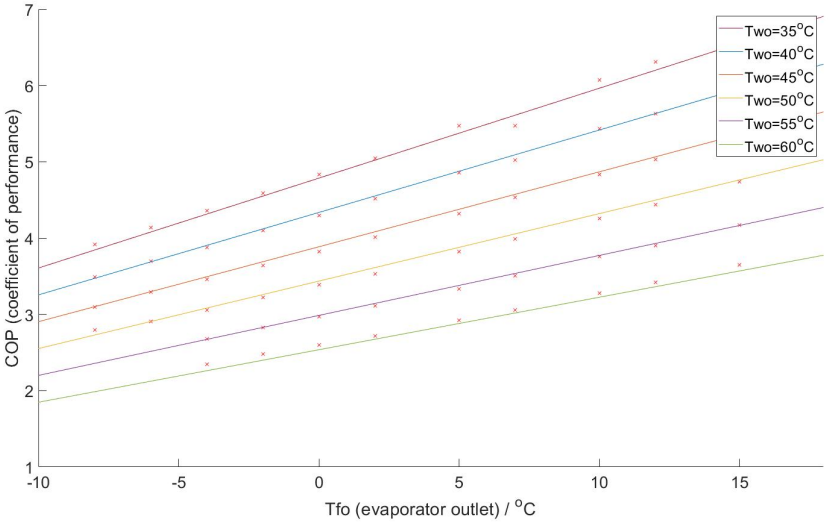


Figure 6.3.3: Regression result with fixed parameters for GSHP modelling

In this graph, the X-axis is the evaporator outlet temperature and Y-axis is the COP. The temperature of the condenser is indicated by different colour of curves. The dots are collected data from the catalogue. The

related simulation parameters in regression formula are 7.9339, 0.18640, -0.08996, -0.00196 respectively. In this graph, most of the dots are close to the corresponding curves. The simulation result of the regression model fits the datasets from manufacturer's catalogue, with RMSE of 1.41 degree, proving the effectiveness of regression model.

Using the formula from the regression model, a one-day simulation of a GSHP for room heating is shown in Figure 6.3.4.

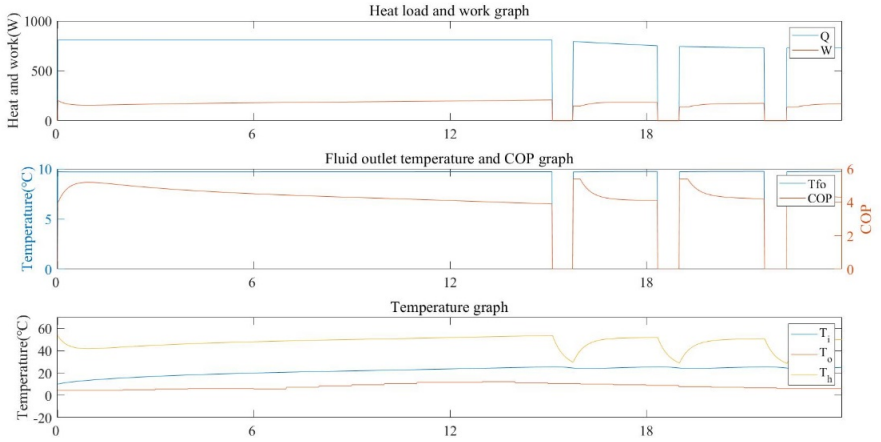


Figure 6.3.4: One day simulation result of GSHP heating

This simulation graph of Figure 6.3.4 consists of three sub graphs, showing a 24-hour period (a single day) with a resolution of one minute. The first subgraph shows the electricity consumption (w) and the gained heat of the GSHP (Q). In the second sub graph, two variables obtained from the iteration process are plotted, which are unknown in the formulae. In the last sub graph, the temperature of the GSHP, and the indoor and outdoor temperature are shown.

In this single day, the GSHP provided heat for maintaining the indoor temperature at the reference one. There are four heating periods: the indoor temperature does not require room heating for the rest of time. The power and electricity decrease slightly, as the energy demand for maintaining the

temperature of the room in the inhabited comfort zone is less than that required for increasing temperature at the beginning of each heating period.

Moreover, the COP of the GSHP achieves a peak at 1 a.m. in the first heating period, when the outlet temperature of the evaporator (fluid loop) increases. This is due to the delay phenomenon of heat transfer, considering the impact of the indoor temperature on the thermal system. The COP value at the beginning of each heating period is the highest among of the simulation. At that moment, the GSHP system has been switched off for hours before being restarted and the temperature of the output, as well as the working state of pump unit are at their boundary conditions. The COP, however, keeps at around 4 for almost all the simulations, this value follows the characteristic of GSHPs, as well as the design of this particular type of pump for simulation.

For the full day, the power consumption is 3.92 kWh, and the heat gained is 17.37 kWh. If using an electrical heater instead of a GSHP, the energy produced by the heater for room heating is 16.05 kWh. The value of producing heat from the GSHP and electrical heater are close to each other because the heat load of the household is decided by the environment temperature and the physical properties of the environment. The saving in the power consumption of the GSHP is due to the principle of heat pumps, which is an outstanding advantage of heat pumps among energy appliances. Additionally, the values of heat gained from both heating appliances are a little less than the calculated heat load values for the full day (20.5 kWh for the GSHP and 18.76 kWh for the heater). This is due to the limits of the appliances themselves and the delay of heat transfer. Neither the GSHP nor the electrical heater cannot supply energy for the peak demand of the household immediately.

6.4 Hot Water Usage Model

6.4.1 Introduction

There are various methods that can be applied to construct a domestic hot water usage model, which can be summarised as: technical standards models, stochastic models, time series models, and data-learning models.

In the models based on technical standards, typical profiles and water flow rates are defined, depending on type and occupancy of buildings, to build a domestic hot water usage pattern [265]. It is found that the accuracy mainly depends on the calculated input design values, and a better simulation performance is can be achieved using methods with regional specific standards for the measurement [266].

Stochastic models are based on monitoring datasets and behaviour survey, and can be applied to build hot water usage pattern in a domestic environment. The distribution of probability of inhabitants' behaviour, as well as the related heat and energy consumption profiles can be derived from the datasets, which is the basis of stochastic methods [267]. The stochastic methods have a higher resolution than other methods, but the resulting pattern profiles always have a similar trend [268].

The third type of method is the time series model, where history datasets are monitored and analysed to predict future behaviour in forecasting. For example the auto regressive integrated moving average (ARIMA) model is a kind of typical time series method [269].

For forecasting of water usage in a domestic environment, data learning methods such as artificial Neural Networks (ANN) models can be applied for high accuracy, and are influenced by family income, number of inhabi-

tants, occupation [270]. However, these data-mining methods cannot overcome issues with uncertainty [271].

6.4.2 Modelling Method of Hot Water Usage

The proposed model is assumed to simulate hot water consumption and related energy demand in real time. As a result, the hot water usage model can be divided into two main parts: the hot water demand model and the water tank model.

6.4.2.1 Hot Water Demand Model

In the hot water demand model, the volume consumption of hot water consumption as a function of time is simulated. The Harmonised European Time Use Surveys (HETUS) which conducted in European countries are national surveys concerning the time and duration of different activities [272]. Based on HETUS database, the probability of water usage activity can be abstracted with the resolution of every 10 minutes, which indicates the possibility of using hot water. For every 10 minutes, based on the comparison between probability and a random number, a hot water usage event is judged to be triggered (or not) in the simulation. Once the water usage event is activated, its water flow rate and time duration are then determined. The flow rate, time duration and events per day of hot water consumption are collected in Table 6.4.1, sourced from a related household survey [273, 274].

Based on the surveys about household hot water usage events, for hot water simulation in this project, the flow rate of a shower/bath event is assumed to be 8-16 L/min, while its duration is 5-15 min. Similarly, the values for

Table 6.4.1: Flow rate summary for domestic hot water usage

Parameter	European households			US households		
	Shower	Bath	Sink	Shower	Bath	Sink
Flow rate (L/min)	8	14	1	8	16	2
Duration (min)	5	10	1	7.8	5.7	0.6
Events per day	2	0.14	28	1.7	0.3	32.9

a sink event are 1-3 L/min and 1 min respectively.

6.4.2.2 Water Tank Model

The real time flow rate for hot water usage can be obtained from the hot water demand model, which is essential for the simulation of a water tank. In the water tank model, the outlet hot water and inlet cold water are considered, as the temperature of the water tank needs to be simulated, leading to the calculation of energy consumption of the hot water system. For this calculation in the water tank model, the formula of the specific heat capacity is applied, which determines the quantitative relationship between volume and energy, shown as:

$$Cm\Delta T = P\Delta t \tag{6.4.1}$$

where C is the specific heat capacity, (for water is 4200 J/KgK). m is the mass of the water, (it can be converted to volume by $m = \rho V$). $P\Delta T$ is the difference between the temperature before and after heating. $P\Delta t$ means that heating power times heating time, which unit is J (WS).

The temperature change in the water tank model includes three types. Firstly, after some hot water is used, the supply cold inlet water would enter water tank. Mixing cold inlet water and existing hot water in the water tank, the temperature of new mixture would be changed, based on

specific capacity formulae, as:

$$Cm_1(T - T_1) = Cm_2(T - T_2) \tag{6.4.2}$$

$$T_{new} = (V_1T_1 + V_2T_2)/(V_1 + V_2) \tag{6.4.3}$$

where the temperature of the new mixture is T_{new}, calculating based on the volume and temperature of cold inlet water and water in tank.

In this simulation the inlet flow rate of cold water is set to 10 L/min, while the tank storage capacity is 100L.

Secondly, there is heat loss in the water tank system, due to the temperature difference and heat transfer with the external environment. The most significant heat loss is from the storage tank, followed by short draw-offs tube loss. The temperature change of the water tank can be calculated from Equation 6.4.4, as:

$$\Delta T_{\text{loss}} = \frac{Q_{\text{loss}}}{Cm} \tag{6.4.4}$$

where T_i and T_{i-1} indicate tank temperature in time interval i and i-1. Meanwhile, the heat loss can be calculated as:

$$Q_{\text{loss}} = \Lambda(T_{\text{tank}} - T_{\text{amb}}) \tag{6.4.5}$$

where T_{tank} and T_{amb} indicate tank temperature and ambient temperature, when Λ is the heat insulation coefficient (1 W/K) [275].

Thirdly, considering the electrical water heater in this system, the water in the tank would be heated when the temperature of the water goes below a set reference.

$$\Delta T_{\text{heat}} = \frac{Pt}{Cm} \tag{6.4.6}$$

Where the heating power, P, is assumed to be 4kw (for domestic electrical water heater, 1-5kw) [276]. Finally, the tank temperature T_i can be expressed as the sum of the temperature changes from all three stages:

$$T_i = T_{new} + \Delta T_{\text{loss}} + \Delta T_{\text{heat}} \tag{6.4.7}$$

6.4.2.3 Combined Hot Water Usage Model

Combining the two sub models, a comprehensive hot water usage model can be simulated as Figure 6.4.1.

The flowchart represents the process of hot water demand modelling and the subsequent water tank model. The process begins with importing data from the Harmonised European Time Use Surveys (HETUS) and household surveys. The hot water demand model determines whether a hot water usage event is triggered within a 10-minute interval based on probability. If an event is triggered, the flow rate and duration of water usage are determined.

Following the hot water demand model, the water tank model is initiated. The real-time flow rate of hot water usage is calculated. If outlet hot water is used, cold inlet water is integrated, and the new mixture temperature is calculated. The heat loss from the tank is then determined, and the tank's temperature is updated based on this heat loss. If the water temperature falls below a predetermined set value, the electric water heater is activated, and the water in the tank is heated.

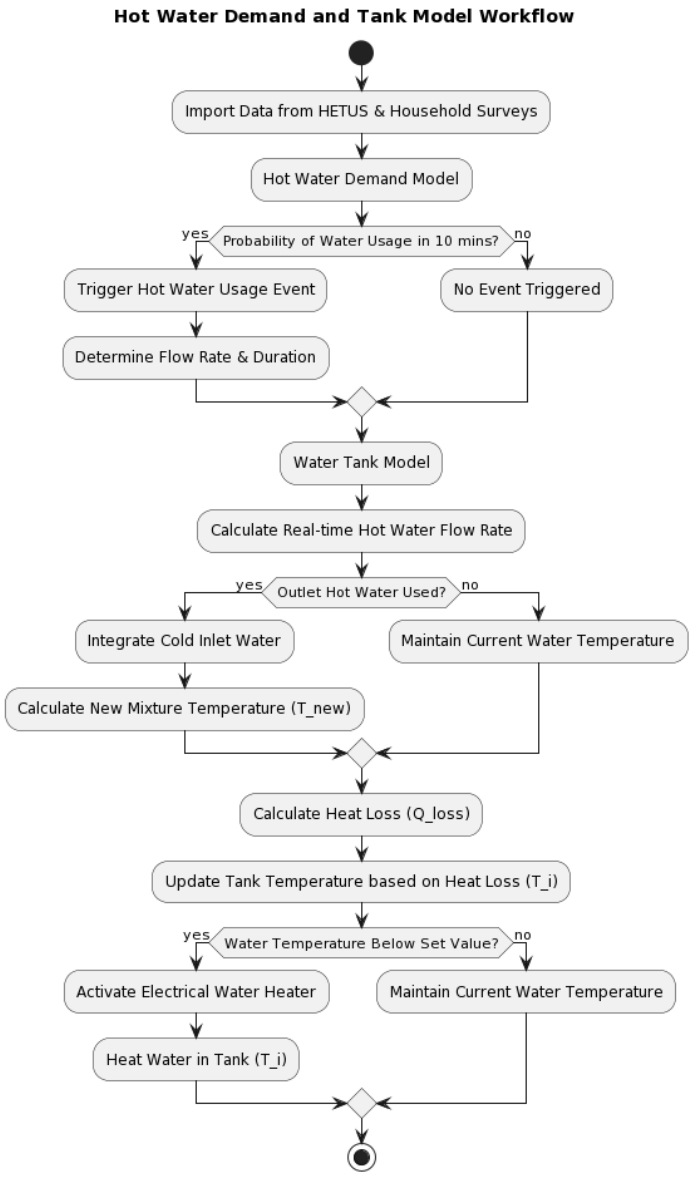


Figure 6.4.1: Flow chart of hot water usage model

6.4.3 Model Performance

The simulation results for the how water usage model are shown in Figure 6.4.2. It shows a simulation of the hot water demand, as well as the temperature and volume of water tank in a single day. In this typical house, the number of inhabitants is set as two, with a 100 L water tank and reference temperature of 55 degrees. The maximum power of electrical water heater is 4 kW.

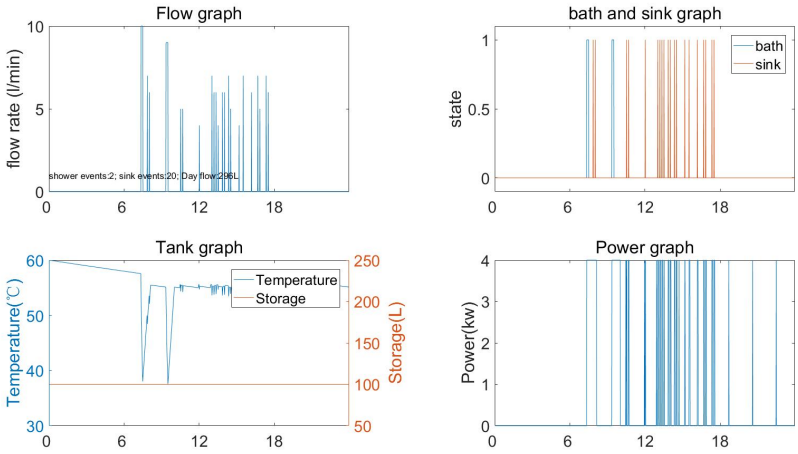


Figure 6.4.2: One day simulation result of hot water usage

In the first subgraph, the X-axis represents the time of day, while the Y-axis indicates the hot water flow rate for domestic usage. The Y-axis in the second subgraph shows the state of bath and sink water usage. A value of '1' indicates that hot water usage is active at that time, while '0' means hot water is not being used. The third subgraph displays the temperature and volume of water in the tank. Lastly, the fourth subgraph relates to the electrical power consumption associated with the water tank model.

Two shower/bath events occurred around 7 a.m. and 9 a.m., while sink hot water usage happened 20 times throughout the day. Despite no hot water usage in the early morning, the tank temperature still decreased. This reduction can be attributed to heat loss arising from the temperature difference between the tank and the ambient environment. Around 7 a.m., due to the hot water demand from the shower and the influx of cold inlet water, there was a significant drop in the tank's water temperature. Since the temperature fell below the set value, the electric heater was activated to heat the water in the tank. Upon the conclusion of the shower event, the temperature rose swiftly due to the heater's operation. This scenario repeated during the second shower event around 9 a.m. In the absence of shower events, the heat loss caused by temperature differences and sink

usage was swiftly compensated for by the electrical heater.

In this simulation, the total hot water consumption reached approximately 150L, with sink usage is about 47 L. This amount is notably higher than the typical household average (122L for total and 38L for sink) [277]. Such high consumption may impact energy use and costs. The difference between this result and industry averages suggests that the model parameters may need further refinement. For future simulations, incorporating more detailed household hot water usage data or mechanisms to adjust water consumption in real-time might be considered.

6.5 Electrical Cooking Model

6.5.1 Introduction

Electrical cooking, as an integral component of daily household activities, significantly contributes to overall energy consumption. Understanding its patterns and dynamics is crucial for a holistic approach towards energy efficiency and conservation. While several studies have explored the nuances of electrical cooking, there is a need for detailed simulations that accurately capture the intricacies of real-world consumption patterns.

This section investigates a simulation model for electrical cooking, focusing on key parameters like appliance choice, cooking duration, and frequency. The proposed model aims to closely mimic real-world cooking behaviour, making it a valuable tool for future energy planning and management. Drawing data from national surveys and integrating it with the model's predictions, this chapter presents insights into the average cooking patterns and their implications for energy consumption.

Throughout the section, the focus remains on ensuring the model's practicality, relevance, and accuracy, to understand how cooking appliances can be effectively modelled for better energy management strategies.

6.5.2 Model for Electric Cooking

The parameters which should be considered when developing a cooking model include : when the occupant turns on the appliance; how often the appliance is used; the length of time the appliance is turned on, the choice of power mode or cycle program; and the use of different types of devices for cooking. The approach for modelling can be summarized as three key issues: the probability of different cooking periods, the length of the time durations and the type of cooking appliance used.

6.5.2.1 Cooking Event Probability

In the Household Electricity Survey 2014 [278], the UK Government carried out a major survey of the use of household electrical appliances in homes, which included the energy consumption profile of different types of cooking appliances. Among those types of cooking appliances, the oven, the induction hob and the microwave, have been selected as they are widely used in domestic cooking. Considering these devices, in the survey, a series of annual electricity consumption profiles for each hour of the day can be obtained, which are classified by both appliance and day. The datasets are classified as weekdays and holidays, which is assumed to include weekends. Based on the annual consumption data for all households that surveyed, as well as the typical power rate of ovens, hobs and microwaves, the prob-

ability of appliances use by the hour can be obtained as Equation 6.5.1.

$$Prob_{device}(t) = E_{device}(t)/P_{device}\Delta t \tag{6.5.1}$$

where the $Prob_{device}(t)$ is the probability for the cooking device usage, and $E_{device}(t)$ is the energy data in the national survey at time interval t. P_{device} is the typical power rate of ovens, hobs and microwaves.

Moreover, the resolution of this simulation model is 1 minute, while that of probability datasets is 1 hour. In order to have high resolution simulation, the transmission between hourly probability and every minute event trigger should be operated. The minute value can be calculated based on the equation of no cooking behaviour in a single hour, i.e.:

$$1 - Probability_{hour} = (\ 1 - \ Probability_{minute})^{60} \tag{6.5.2}$$

6.5.2.2 Cooking Duration

In addition to the probability of event of cooking, the time duration of a single cooking event should be also considered. The survey of average time spent on cooking is shown in Figure 6.5.1 [279].

The cumulative distribution function is the accumulation of probability distributions, as :

$$F(x) = P(X <= x) \tag{6.5.3}$$

To generate a continuous cumulative distribution function (CDF) from the discrete data points and obtain a probability of cooking duration for every minute, the method opted for cubic spline interpolation. Compared to other interpolation methods, cubic spline interpolation provides a smooth

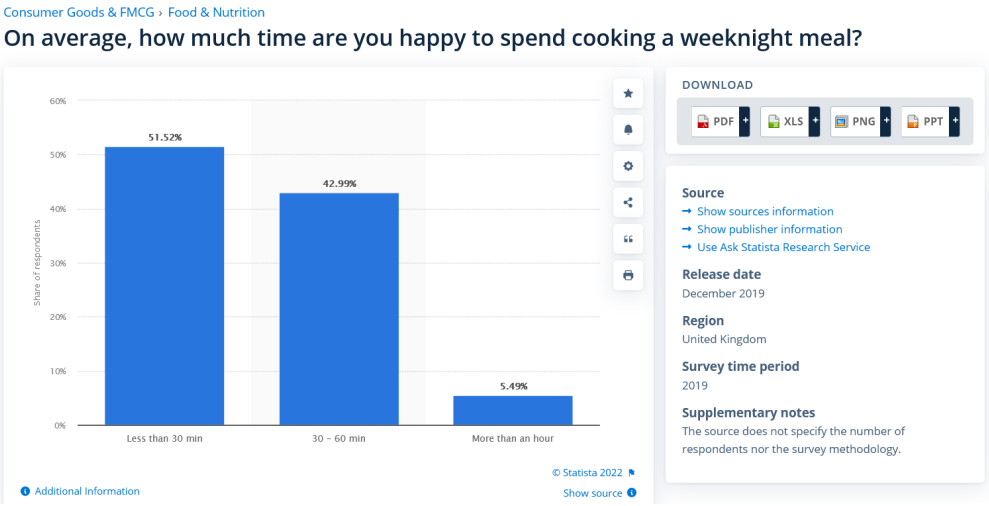


Figure 6.5.1: Average time spend on cooking of UK citizen [275]

and continuous curve while avoiding unwanted oscillations beyond the data points. This method estimates values between each pair of data points using a cubic polynomial, ensuring the entire curve is both continuous and smooth across all data points. This offers a more refined and continuous perspective, aiding in a more accurate simulation and prediction of household cooking behaviour. Based on the data, the curve of cumulative distribution function is shown in Figure 6.5.2.

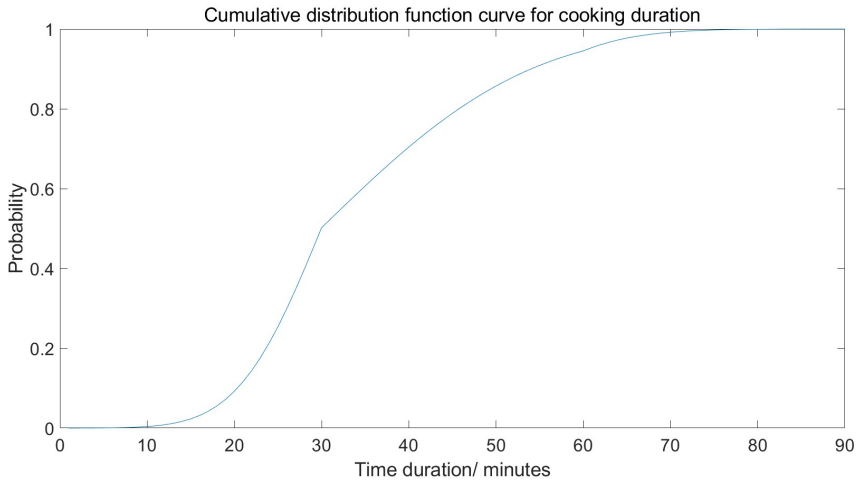


Figure 6.5.2: Cumulative distribution function curve for cooking duration

In this graph, the X-axis is time duration of a cooking event, while the

Y-axis is the value of the cumulative distribution function. The blue curve indicates the correspondence of the time duration and the probability of the cooking time to take a value less than or equal to it. In the first 20 minutes and last 30 minutes (60-90), the function curve changed slightly, as there is seldom cooking behaviour (for meals) that lasts for less than 20 minutes or more than 60 minutes [279]. As the time is closer to 30 minutes, the curve changes more dramatically with a higher slope of the curve. This phenomenon is due to the cooking duration and is generally because events are centralized around 30 minutes. At the same time, the proportion of cooking less than 30 minutes is 53.52%, being close to the medium value of cooking duration of the survey. If a random value ranging from 0 to 1 is introduced for the Y-axis, the point on the curve can be fixed, and the corresponding time duration value can be obtained from the X-axis. For instance, if the random value r is 0.5, the related cooking time duration is about 30 minutes.

6.5.2.3 Seasonality Effect on Cooking Consumption

Additionally, there are other factors that influence the cooking electricity consumption profile, including the date changing and the number of inhabitants in a single house. The 2014 survey [278] summarized the influence of season on electricity consumption profile, and the effect graph is shown in Figure 6.5.3.

In this graph, the X-axis shows the week numbers of the year, while the Y-axis is the seasonality factor of different weeks. The average value of this factor is 1, as this difference would not change the result of annual consumption. For the daily profile, however, the ratio of consumption changes with seasons. The bottom of this effect factor curve is at around

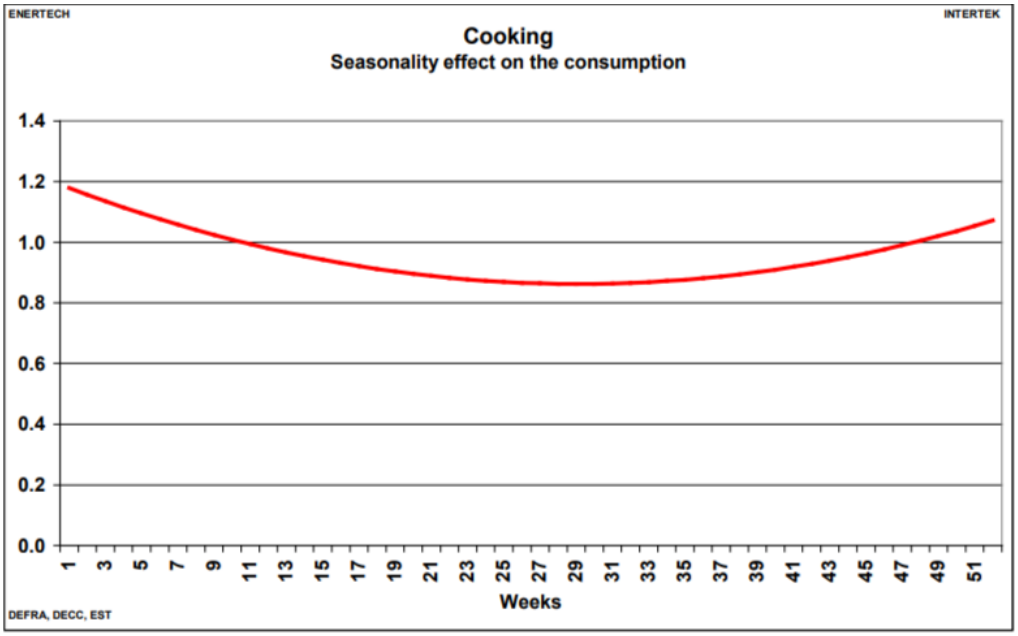


Figure 413 Cooking – Seasonality effect

Figure 6.5.3: Seasonality effect on cooking energy consumption, by week

30 weeks, as 0.85, which is the hottest day of the year. In contrast, the value of the effect factor is 1.2 in the first week of year, when there is more electricity demand for food, such as demanding hot food on cold days.

6.5.2.4 The Effect of Number of Households

The number of inhabitants also impacts on the electricity consumption of cooking in households. Figure 6.5.4 shows the average annual energy consumption for cooking.

In this graph, the annual consumption is 460 kWh for a person living alone. When the number of people increases to two, the average consumption is 235 kWh per person, a little larger than half of a single person. Along with the increasing of number of people, the average consumption decreases. Hence, the total annual cooking consumption for households of one, two or three persons, is almost the same. However, when the number of people is more than 4, the consumption is around 100 kWh per person, i.e., the total

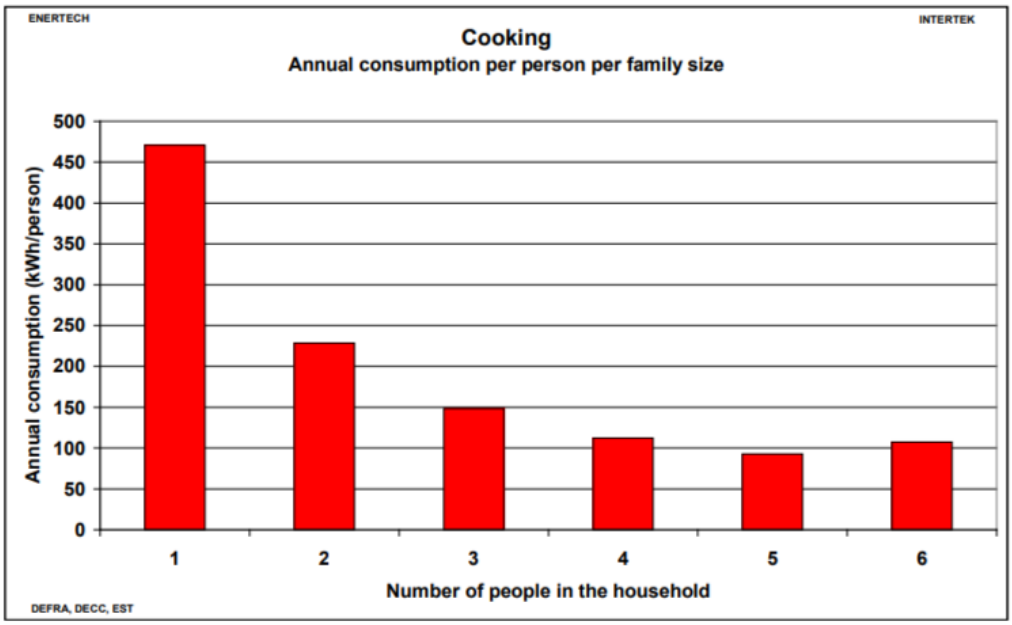


Figure 419 Cooking – Annual consumption per person per family size

Figure 6.5.4: Annual consumption per person per family size

consumption increases. The ratio of different numbers of people to the average annual consumption, can indicate the effect of number of inhabitants to the cooking electricity consumption for households.

6.5.2.5 Integration of Cooking Model

To capture the intricacies of cooking behaviour in households, a multi-layered approach was adopted. At its core lies the cooking event probability, determining the likelihood of a cooking event occurring at any given time. Once an event is deemed to occur based on this probability, the cooking duration model is then invoked, defining the length of the event based on a probabilistic assessment in conjunction with a randomly generated number. This base model is further refined using the seasonality effects and the effect of the number of household members. These act as correction factors, adjusting the base probability from the cooking event model, ensuring the simulations are reflective of real-world scenarios and adaptable to diverse

household configurations. The fixed probability can be given by:

$$\Pr ob_{total}(t) = Prob_{device}(t) \times F_{season}(t) \times F_{member}(n) \quad \textbf{(6-5-4)}$$

$Prob_{total}(t)$ represents the likelihood of utilizing a specific cooking appliance (such as an oven, hob, or microwave) at time t, derived from annualized data. $F_{season}(t)$ is a seasonality correction factor, reflecting the propensity to cook at different periods or seasons throughout the year. It varies with the number of weeks. $F_{member}(n)$ stands for a household members' correction factor, contemplating the influence of the number of individuals in a household on cooking patterns.

6.5.3 Performance of Model

According to the proposed method in the last subsection, the average base probability for cooking events can be calculated. As the utilized cooking energy dataset from survey [278] is based on national investigation, the corresponding cooking appliance power should also be the average values for matching. The power rate values of using oven, hob and microwave are 2.5, 1.5 and 0.8 kW respectively. And their average cooking duration is 40, 30, 5 minutes[280]. The calculation result is shown in Figure 6.5.5 and Figure 6.5.6.

In Figure 6.5.5 and Figure 6.5.6, the bar chart of probability series for weeks and holidays are shown separately, and contain the values for oven, hob, and microwave. The X-axis is for 24 hours of the day, while the Y-axis is the probability of an event taking place.

During the weekdays, the probability graph has three peaks, corresponding to breakfast, lunch, and dinner. Some of the inhabitants would not take

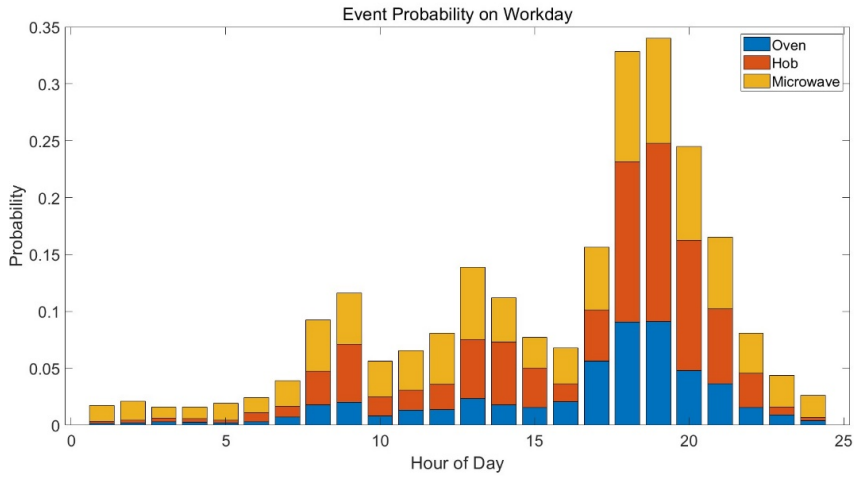


Figure 6.5.5: Probability of event trigger in workdays

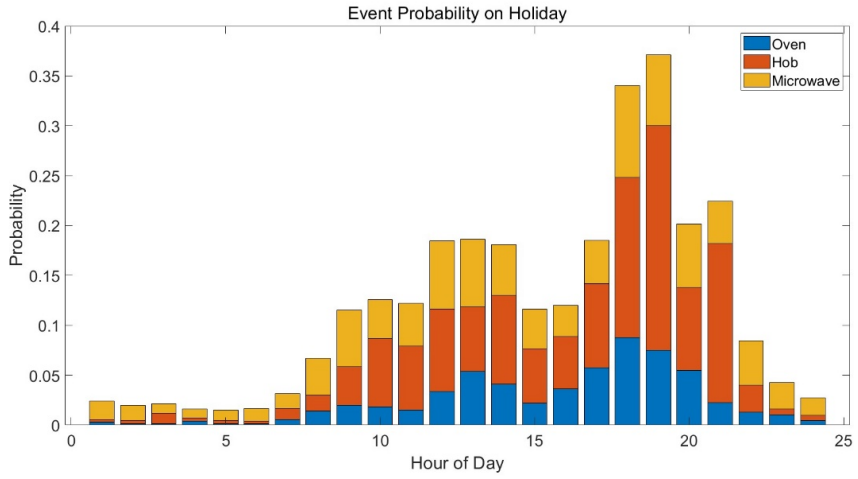


Figure 6.5.6: Probability of event trigger in holidays

breakfast or dinner at home due to weekday works. The peak of dinner is much higher than the other two meals. At the same time, there are two peaks in the graph for holidays, while brunch is nowadays popular due to fast modern life. The probability of using microwaves is the most, followed by hobs. Considering the ratio of workdays and holidays is approximately 5:2, the average mathematical expectation of using ovens probability is 0.543 per day. The average value is 1.01 for hobs and 0.93 for microwaves. These mathematical expectation values, according to the UK energy follow-up survey 2011 [281], are 5.0, 7.9 and 6.3 times for using the cooking appliances per week. In other words, the values are 0.71, 1.12, 0.9 for

ovens, hobs, and microwaves. Considering the time factor of the survey data, this difference is acceptable. In addition, although the mathematical expected values of ovens and microwaves vary slightly between working days and holidays, the two values for hobs are 0.88 and 1.13, with a larger difference. This reflects the differences in user behaviour on different days.

A simulation for single day based on the proposed cooking model is shown in Figure 6.5.7.

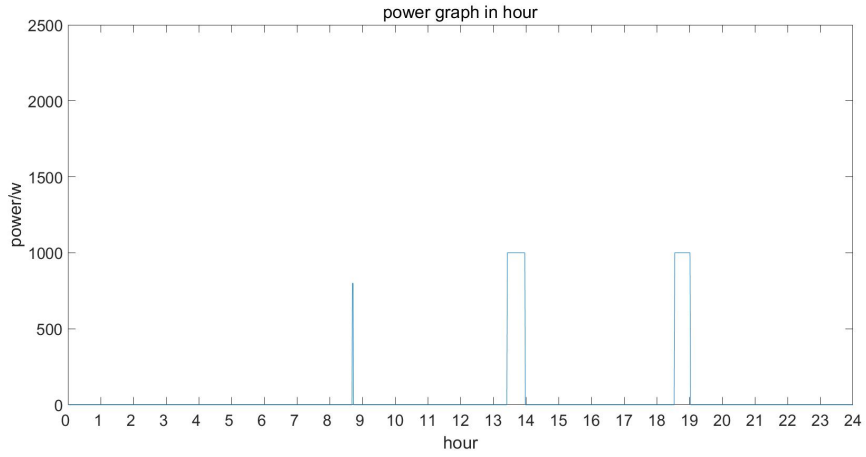


Figure 6.5.7: One day simulation result of cooking model

In the Figure 6.5.7, the time span of a day is represented on the X-axis, with the power rate captured at minute intervals on the Y-axis. Throughout the day, three prominent cooking events are observed. The first event, peaking at 0.8 kW, is consistent with the typical power usage of a microwave, suggesting a brief cooking or reheating task that spans only a few minutes. In contrast, the latter two events, registering at around 1 kW, align with the power signature of an induction hob. Each of these hob events endures for an extended period, exceeding half an hour, indicative of more comprehensive cooking sessions. Notably, these events are timed around traditional meal hours, implying breakfast, lunch, and dinner preparations. The absence of a 3.4 kW peak suggests that the oven was not utilized on this day. The data underscores the prevalence of the induction hob for

prolonged cooking and the microwave for quick tasks, providing insights into daily cooking energy consumption patterns.

Additionally, repeated year-round simulation is operated, to gain an average annual daily electric cooking profile as Figure 6.5.8.

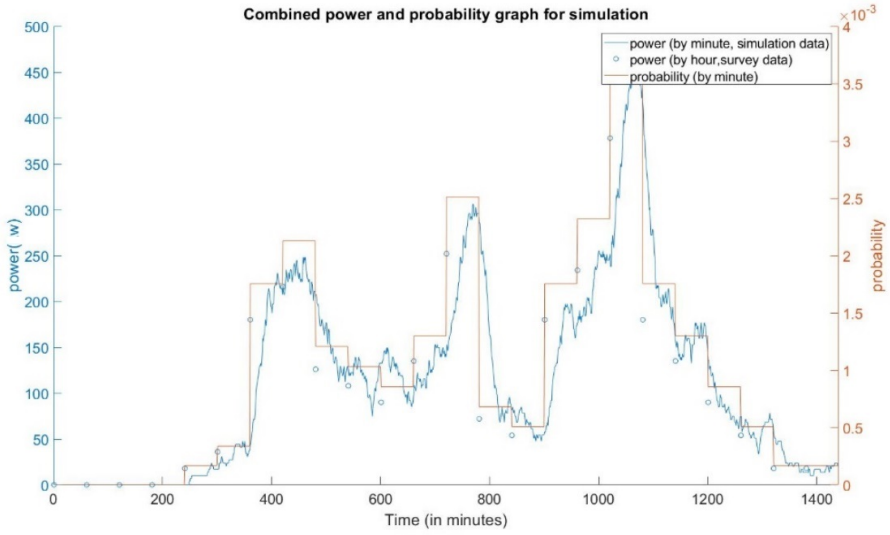


Figure 6.5.8: Annual average daily electricity consumption profile for electrical cooking

In the Figure 6.5.8, the average power utilization for cooking activities is depicted over an annual timeframe. The X-axis delineates the 24-hour daily cycle, whereas the Y-axis quantifies both the power rates in watts and the associated probabilities of event occurrences, sampled at minute intervals. The data visualization clearly manifests three salient peaks, congruent with the typical meal preparation times: breakfast, lunch, and dinner. The most pronounced surge in power consumption occurs at 18:00, registering a value of 110W, indicating that dinner preparation is typically the most energy-intensive culinary activity of the day, a conclusion corroborated by real-world observational data.

The data shows that even between primary meal times, there is a high use of power, indicating that residents cook at different times and in dif-

ferent ways. The simulation predicts yearly electrical cooking use to be 360 kWh. However, the actual survey data shows it is 497 kWh. This difference could be due to the survey covering many households that use different cooking appliances. The simulation only considers three types of appliances. Furthermore, the simulation assumes only one appliance works at a time and does not account for back-to-back cooking. This might be why the simulated energy use is lower than the actual use.

Furthermore, when comparing the simulation's predictions, the actual data, and hourly energy use, they all show similar trends. This means the simulation method is reliable and accurate.

6.5.4 Conclusion of the Cooking Model

This study provides a detailed simulation of electrical cooking consumption in homes. The model captures typical cooking times and matches them with common meal periods, making it relevant to real-life scenarios.

Clear patterns emerge, highlighting when and how different cooking appliances are used. While there are some differences between the model's predictions and actual survey data, the overall trends are closely aligned. These discrepancies can be attributed to the model's assumptions and the varied nature of the data sources.

In short, the model offers a practical way to understand and predict daily cooking energy use. This can be valuable for energy planning and promoting more efficient home energy use.

6.6 Combination of Occupancy and Heat Demand

In this section, the proposed occupancy model, is operated together with the proposed thermal model. The occupancy state is another extra input signal for thermal models, including the heating model and the cooking model. For instance, in order to achieve improved control of a room heating system, the combination of occupancy model and room heating model is presented. It also shows the potential of energy saving.

The energy required for heating or cooling a home is closely tied to occupancy. A non-occupied home might not require as much energy, leading to potential savings. Using occupancy data in tandem with heating controls can result in more efficient energy use.

Traditionally, the control system of room heating is based on hysteresis control, a combination of control using time and using temperature feedback. In the heating model, two heating periods were assumed as the timer allows the heater to be turned on during 6.00 a.m. to 10.00 a.m., as well as 18.00 p.m. to 22.00 p.m. The temperature difference hysteresis for turning on and off is set as 1 degree, while the reference temperature is 25 degrees. When it is combined with the proposed occupancy model, the state of occupancy would influence the result of heating usage, where two aspects dominate. One is the 'not at home' state would not allow the heater to be turned on. The other aspect is that the heat radiation from an inhabitants' body, which is different from no one at home and value cannot be ignored. Figure 6.6.1 shows a typical set of states for the temperature model in a typical day.

The X-axis is the time of the day, while the Y-axis is for the states. In the

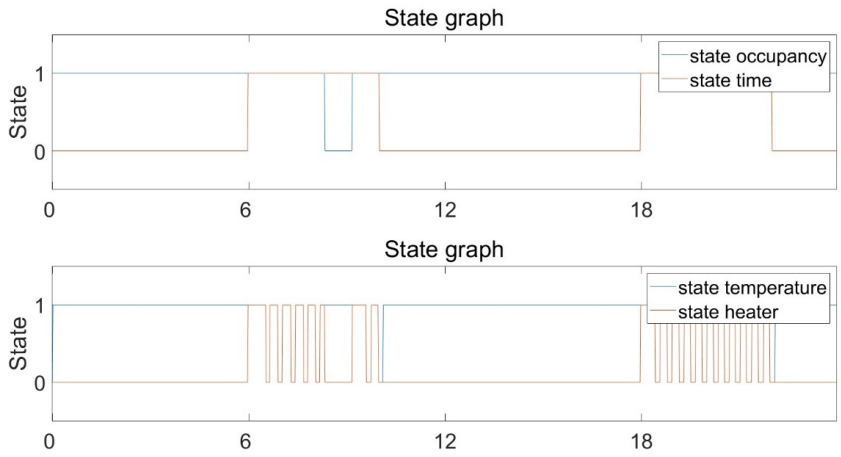


Figure 6.6.1: State graph for occupancy and room heating

upper graph, the blue curve is for the occupancy, while the orange curve is for limited heating time. 1 means allowing the heating is on. These two states are impacted by local conditions and inhabitants' behaviour. In the lower graph, the state of the temperature and the on/off state of the heater are shown. The state of the temperature means that, based on the indoor air temperature, the room requires heating or not. The state of the heater is the real condition of the electrical heater, as well as the final decision of the control system. For this single day, the inhabitant is not at home at about 9.00 a.m. Hence, even if it is the heating period, the heater would be turned off as the host is not at home. For the rest of the heating period, the heater is intermittently switched on for about 20 minutes and off for about 10 minutes and the pattern repeats, which is reasonable according to the real situation. Apart from heating periods, the heater would not be turned on for the rest of the day, regardless of the temperature or whether the occupant is at home or not.

6.7 Analysis and Comparison of Different Domestic Heating Systems

6.7.1 Introduction

Accounting for more than 40% of total energy consumption, buildings are also one of the largest carbon dioxide emitters in the world [282]. This energy consumption and carbon emission have already led to a real threat of climate change. The utilization of fossil fuels to generate power for homes and businesses exacerbates this risk [283]. Hence, most countries have policies to promote the increased concentration of renewable energy resources. Establishment of these policies not only have focused on the method of power generation, but also have paid attention to the way of energy consumption. A significant portion of energy is used for space heating and cooling in both developed and developing countries. As a result, researchers are focusing on developing new technologies to reduce energy consumption to meet heating and cooling needs [284].

In terms of analysis of energy consumption, construction factors, household size, occupation and age are the main factors that affect the energy consumption [285]. The major dominant factors that impact on consumers' choice of energy resources of are analysed in [286]. Various literatures have conducted in-depth studies on the characteristics of electrical and thermal loads and their impact on power systems.

In terms of comprehensive analysis and research, the economic profit, and environmental benefits of several types of electric heating were analysed in previous literatures. The energy saved by new energy electrical heating can lead to about 10 million dollar fuel costs, and 1 million environmental

protection costs each year in one province by [1]. With an energy storage system, the electricity consumption of electrical heating can save more energy than a traditional gas boiler [287]. In view of the life cycle of electric appliances, energy efficiency and pollution emissions of various types of heating system are compared in [288] based on full life cycle theory. Among all the systems, a much cleaner system is gas boiler heating considering all primary energy sources. At the same time, the heat pump and combined heating and power generation have the highest energy efficiency.

6.7.2 Methodology

In this chapter, based on the operation of thermal model for the domestic environment, the energy consumption based on gas boiler, electrical heater and GSHP would be simulated individually. Moreover, based on the energy consumption, the economic cost as well as GHG emissions would be compared.

The energy balance of domestic heating was proposed in previous sections. At the same time, there is a comprehensive simulation model for electric heater with hysteresis control, while the model of GSHP was also proposed. Based on these methods, the models can simulate for operation condition for the entire year, obtaining the corresponding energy consumption of different appliance. Moreover, the energy consumption of gas for room heating can be also estimated, based on heat demand (Q_{demand}) of domestic environment and efficiency of gas heating.

$$Q_{gas} = Q_{demand}/\eta_{gas} \tag{6.7.1}$$

Where η_{gas} is the efficiency of gas heating in the domestic environment, which is about 89% [289]. The result is the energy consumption when the room is heating based on central gas heating.

Additionally, the investment and operation cost of heating system could be calculated as:

$$Total\ cost = \ Cost_{investment} + \sum_{i=1}^{years} Cost_{operation} \times (1 + r\%)^{i} \tag{6.7.2}$$

The parameter r represents the inflation rate. The NPV, is the value of cash flow over different periods, which depends on the time interval and discount rate – the assumed equivalent value of interest obtained if an equivalent financial investment had been made.

$$NPV = \sum_{Yr=1}^{Yr} \frac{Cash_t}{(1\ +\ i\ )^{Yr}} - Cash_0 \tag{6.7.3}$$

Where $Cash_t$ is the net cash inflow during the period Yr. The cash flow can be calculated as the savings due to applying other appliances compared to gas boiler. Yr is the number of time periods which unit is year. $Cash_0$ is the initial cost. In this section, it is the combination of investment of heating appliances and related auxiliary equipment.

Understanding the costs associated with various heating methods, as well as their environmental impacts, is crucial for making informed decisions. The following table outlines the investment costs of different heating systems, the prices of electricity and gas, and the Global Warming Potential (GWP) of these energy sources. In order to analysis the economic benefit and environmental impact of various heating systems, the corresponding cost

are summarized in Table 6.7.1.

Table 6.7.1: Costs and GWP of different domestic heating methods

Parameter	Value	Source
Investment of electrical heater (£)	2100	[290]
Investment of GSHP (£)	24000	[291]
Investment of gas boiler (£)	4000	[292]
Electricity price (£/kWh)	0.135	[293]
Gas price (£/kWh)	0.0737	[293], [294]
GWP of electricity (kgCO2e/kWh)	0.233	[295], [296]
GWP of gas (kgCO2e/kWh)	0.184	[296]

For instance, as can be seen in the table, the initial investment for a GSHP is significantly higher than other methods, however, its long-term efficiencies and benefits might offset this initial cost. Similarly, while the price of electricity per kWh is higher than gas, its GWP is also slightly higher, indicating its greater environmental impact. Global Warming Potential (GWP) is the amount of heat absorbed by any greenhouse gas in the atmosphere and is a multiple of the amount of heat absorbed by the same mass of carbon dioxide (CO_2). CO_2 has a GWP of 1.

6.7.3 Results of Heating System Comparison

In order to compare energy consumption, and investigate on further economic analysis and emission reduction, several key values are exported from simulation. Basing on a one-year simulation, the heat demand, heat supply and energy consumption of electrical heater and GSHP in heating season are shown in Table 6.7.2.

In this table, based on the difference between indoor air and external com-

Table 6.7.2: Annual heat demand and energy consumption of different heating appliances (unit: kWh)

	Heat demand	Heat supply	Energy consumption
Electrical heater	2180.4	1763.3	1763.3
GSHP	2276.0	1675.4	391.9

ponents, the heat demand is not only supplied by heating appliances, but also by human activities, solar radiation, and other factors. As the heating appliances are freely used in heating season to maintain the indoor temperature, the value of demand for the heater and GSHP is close to each other. This numerical approximation also takes place on value of heat supply, while the distinguish heating mechanism of two appliances leads to slight difference. The heating mechanism, however, result in the dramatic difference in energy consumption of power in the electricity system. The electric heater consumes 1763 kWh of power. In contrast, the GSHP would only use 391.9 kWh of power to produce a similar amount of heat as a heater. When it comes to gas heating, 2519.1 kWh of gas would be consumed for heat, calculated based on efficiency equation.

Based on the annual energy consumption on different appliances, as well as the average unit energy cost from official statistics, the annual cost and global warming potential could be summarized as Figure 6.7.1.

Three primary heating methods are compared: electrical heaters, GSHP (Ground Source Heat Pumps), and gas boilers. For each heating method, there are two bars. The blue bar represents the cost associated with that particular heating method, while the orange bar depicts the GHG (Greenhouse Gas) emissions. This visual comparison offers a clear overview of the economic and environmental impacts of each heating system, allowing for a direct comparison of costs and emissions side by side. The type of energy required for the operation of a GSHP is the same as an electrical

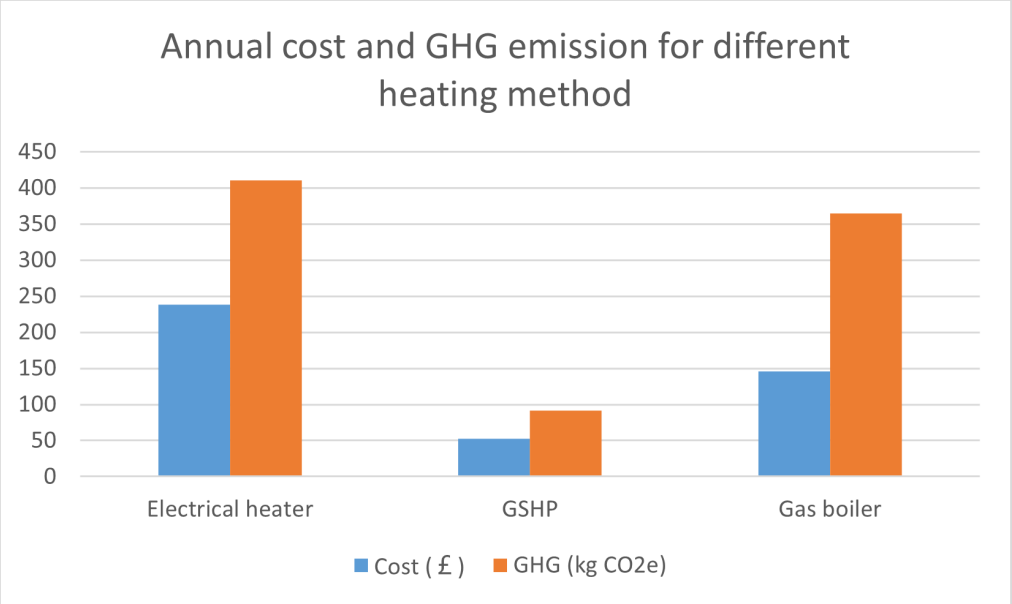


Figure 6.7.1: Annual cost and GWP for different heating method

heater, using the electricity from the national grid with same unit cost and emission. The annual electricity tariff of the electric heater is £238, while its GHG emission is 410kgCO2e. The total annual energy consumption, however, has a significant difference. As a result, the electricity tariff and GHG emission of GSHP are only about one-sixth of that of electrical heater for room heating. At the same time, the unit cost and GHG emission are both less than that of electricity. Owing to this, although the energy consumption by gas is lower than that of electricity, the annual cost and GHG emission is only £146 and 364kgCO2e. Comparing to the consumption by an electric heater, the tariff cost of gas is less, while its carbon emission is already closed to that of electric heater. In the future, along with the technique improvement of renewable generation, electrification of domestic heating has more potential to gain advantages in both economic and environmental impacts.

In conclusion, the analysis of various domestic heating systems offers valuable insights into both economic and environmental implications. While electrical heaters present a cost-effective option, GSHPs, despite their higher

initial investment, showcase potential for long-term benefits, especially when considering their low GHG emissions. Gas boilers, on the other hand, while economically competitive, have notable environmental concerns. The provided bar chart further underscores these findings, emphasizing the importance of considering both cost and GHG emissions when evaluating domestic heating options. As global efforts shift towards sustainability and carbon neutrality, such comparative analyses become crucial in guiding residential heating choices for a greener future.

It should also be noted that a low and fixed price for gas has been assumed for this analysis. Gas prices are certain to increase significantly in future years, encouraging the case for GSHPs for domestic heating.

6.8 Conclusion

In this chapter, a comprehensive exploration of thermal demands in domestic electricity systems was undertaken:

- Thermal Room Heating Model: A detailed thermal room heating model was presented, illustrating the dynamics of heating in a domestic setting. Factors like hysteresis control, parameter estimation, and model performance were thoroughly discussed.
- Ground Source Heat Pump (GSHP): An introduction and comprehensive modeling of the GSHP were provided. The GSHP model performance was evaluated, showing its efficiency and effectiveness in supplying thermal needs.
- Hot Water Usage Model: A deep dive into hot water usage patterns was conducted. The combination of hot water demand, the water

tank model, and their collective performance was meticulously evaluated.

- Electrical Cooking Model: A simulation of electrical cooking consumption in homes was established. This model captures typical cooking times, aligning them with common meal periods, thereby making it highly relevant for real-world scenarios.

- Analysis of Domestic Heating Systems: A critical comparison of electrical heaters, GSHPs, and gas boilers was presented. Economic implications, greenhouse gas emissions, and future potential of each system were analyzed. It was highlighted that while electrical heaters offer cost-effectiveness, GSHPs present significant long-term benefits, especially in terms of reduced greenhouse gas emissions.

Chapter 7

Results and Discussion: Integrated Models, LCC and LCA of Electrification, and Community Level Application

7.1 Model Integration and Comparison

7.1.1 Introduction to Models, Integration, and Comparisons

The growing global concern over climate change and the continuous advancement of new energy technologies have catalysed a profound transformation in modern residential energy systems [297]. Unlike the traditional models reliant on centralized power supplies such as non-renewable resources like coal and natural gas, these models are no longer tenable in

the face of future energy and environmental requirements. This thematic exploration, "Home Energy Models: Integrating Future Energy Technologies," seeks to delve into the strategies for achieving a more efficient, ecologically sound, and intelligent residential energy framework through the avenues of technological innovation and management strategies.

The intensifying global issues of climate change and environmental pollution have propelled the urgency to discover green, renewable energy solutions. As the basic unit of society, households' energy usage patterns wield considerable influence over overall energy consumption and carbon emissions. Concurrent with technological advancements, numerous emerging energy technologies, such as solar power, wind energy, and battery storage, are penetrating daily life, thus offering innovative opportunities for enhancing household energy systems [4]. This is further compounded by the gradually diminishing costs of new energy technologies, enabling households to access electricity more economically, fostering a heightened demand for household energy management and optimization.

The conventional household energy systems, characterized by isolation and static attributes, are ill-equipped to cope with the rapidly shifting energy markets and environmental dynamics [298]. In stark contrast, contemporary models emphasize the pivotal role of integrating multiple technologies and adopting dynamic management. This implies that the consideration should encompass not only the implementation of diverse new energy technologies within households, but also the art of seamlessly intertwining them into a cohesive and collaborative system.

This perspective underscores the necessity for a holistic and interconnected network for future residential energy systems, whereby each component mutually supports and synergize with others. This intricate network en-

compasses not only energy production and consumption but also extends to encompass energy storage, distribution, and comprehensive management. Moreover, the design and management of household energy systems should pivot around the unique demands and habits of the users [299]. This includes provisioning personalized energy services to guarantee an unwavering, economically viable power supply under any circumstances.

The ultimate aspiration of the home energy model lies in provisioning households with energy solutions that are not only environmentally responsible but also financially judicious. Such an arrangement is not merely confined to the domain of reducing electricity bills; it encompasses a larger purpose of contributing to the mitigation of carbon emissions, thus playing a pivotal role in the global effort to counteract climate change.

Simultaneously, as these novel models gain traction, they hold the potential to incite broader societal transformations towards a low-carbon, sustainable future. Households cease to be passive energy consumers, transitioning into active participants, intricately engaged in energy production and management. This transformation is expected to culminate in a decentralized, pliable, and resilient energy system, adeptly poised to navigate the challenges that lie ahead.

To achieve these environmentally and financially sensible solutions, the proposed model integrates several important sub-models, each of which addresses a different aspect of home energy management, as shown in Figure 7.1.1. The model carefully blends local household load data, photovoltaic (PV) forecasts, occupational models, electric vehicle (EV) usage, thermal simulation, and battery and home energy management system (HEMS) strategies to provide a comprehensive and realistic depiction of household energy dynamics. The model runs on a minute-by-minute basis,

facilitating seamless information exchange and decision-making between all sub-models, each of which is detailed in the corresponding subsequent section. This integration not only ensures synchronization and cohesion in managing different energy aspects, but also fine-tunes the predictive and adaptive capabilities of the entire model.

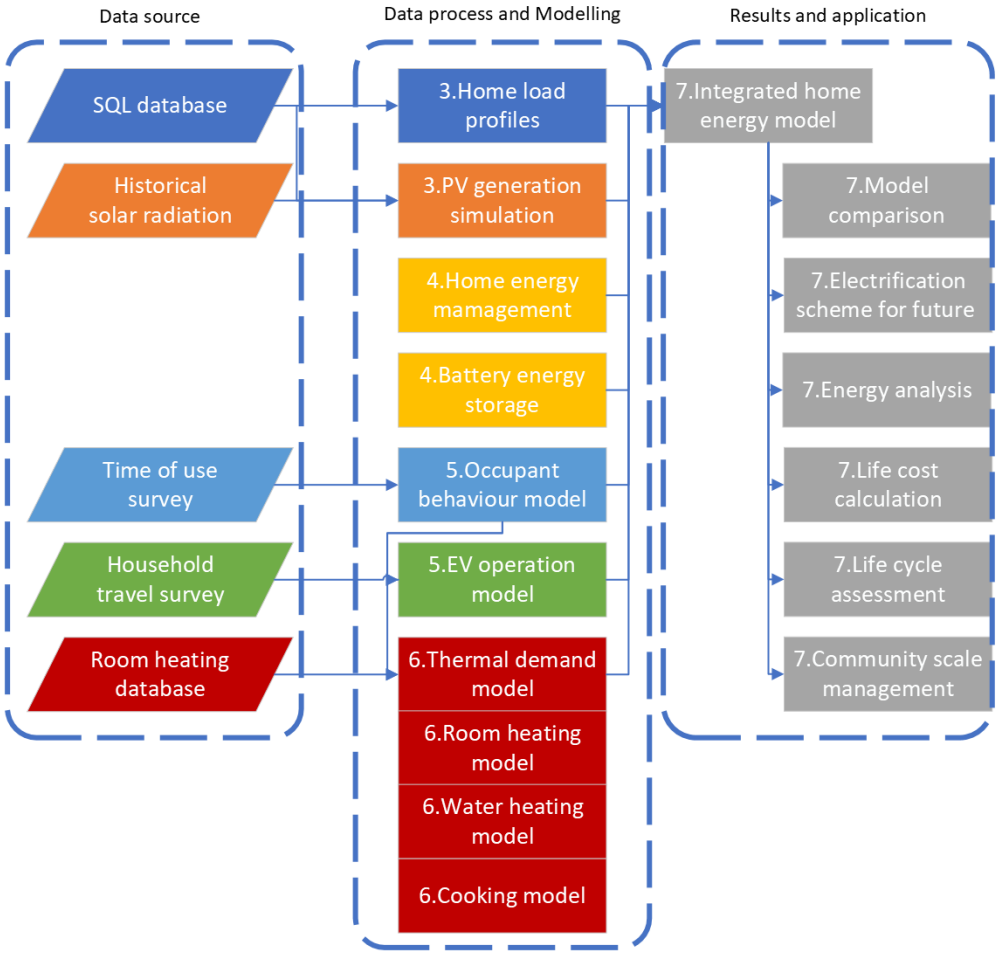


Figure 7.1.1: Structure diagram of modelling

Furthermore, the model is not just a static representation, but dynamically adapts to various internal and external factors, ensuring that proposed strategies and predictions are consistent with real-world scenarios. By ensuring coherent interaction between sub-models, the model not only ensures optimal energy management for individual households, but also contributes to the establishment of sustainable and efficient energy net-

works at the macro level.

Developed in 2010 at the Centre for Renewable Energy Systems Technology (CREST) in Loughborough University, the CREST model offers a probabilistic framework to estimate the electricity consumption of individual households [271]. This is predicated on key parameters: the number of residents, their occupancy patterns, and the household's appliance content.

The CREST model has the capability to generate electricity load profiles for individual households, extrapolated from the simulated use of distinct appliances. By amalgamating the approach of implementing Markov chain models based on time-use data with the strategy of generating electric appliance switch-on events, the CREST model has garnered widespread recognition and application in numerous scholarly publications.

7.1.2 Simulation Results and Comparison

A careful understanding of the model setup and methodology is critical to dissecting simulation results and making relevant comparisons. The following analysis is based on the simulation operation of the model proposed in the study and setup details of the CREST model.

For the CREST model, simulations were performed for 20 households located in Nottingham, specified at a latitude of 52.8° and a longitude of -1.2°. The model was used to simulate the energy profile of 20 different households. The CREST model inherently supports single-day simulations, so individual daily results need to be combined to build an aggregate representation. Due to the one-day simulation limit of the CREST model (which is an xlsx file), a Python program is used to systematically call the model every day and change the date and store the results. After daily simu-

lations, the results are combined to calculate average results to present a comprehensive view of the model's performance.

Unlike the CREST model, the proposed model possesses the capability to directly simulate the energy dynamics of a single household across an entire year, yielding a detailed and continuous dataset.

Key factors, namely house size and number of residents, are pivotal in the model. Data from the English Housing Survey (Floor Space in English Homes) [300], the average UK house size resides at 96 m^2, with a common range between 56 and 151.7 m^2. Consequently, house sizes are randomly selected between 56 and 152 m^2 during simulations to maintain a realistic representation.

Regarding the number of residents per household, information derived from "Families and households in the UK: 2022" [301] reveals an average of 2.36 residents per household. For the sake of simplicity in the model, households with more than four residents are categorized as four-resident households. Thus, the distribution of residents per household in the simulations is configured as follows: 45.2% with one resident, 29.6% with two residents, 11.8% with three residents, and 13.4% with four residents.

Through these settings, the model, characterized by dynamic adaptation and integration of various sub-models, aims to simulate the energy consumption for 20 households, and compare its average performance to the CREST model.

Based on the simulation of 20 households for one year, the Table 7.1.1 presents the simulated results of the CREST model and the models in the thesis across various energy-related aspects. These aspects include photovoltaic (PV) electricity generation, the total electricity consumption

of a household over a year (residential electricity demand), the portion of electricity used by the household, not returned to the grid (total self-consumption), the total electricity demand from the grid by the household (net electricity demand, calculated as total demand minus PV generation), thermal energy used for residential space heating (electrical heating energy), thermal energy used for water heating (e.g., showers, dishwashing) (water heating energy), thermal energy used for cooking (cooking energy), the capacity of household batteries used for energy storage (home battery), and the capacity of electric vehicle (EV) batteries (EV battery).

Table 7.1.1: Annual simulation results in CREST model and proposed model

Energy Section	**CREST Model**	**Proposed Model**
PV	916.4	742.5
Dwelling Elec. Demand	4032.9	2088.7
Total Self-Consumption	419.2	368.2
Net Demand	3116.5	4934.0
Room Heating	5553.9	2647.6
Water Heating	1870.0	606.9
Thermal Energy (cooking)	No (separated) calculation	497.5
Home Battery	No calculation	640.0
EV Battery	No calculation	514.1
EV Drivers	No calculation	1862.4

In terms of model characteristics, the CREST model simulates data for a day, with parameters like PV and whose attributes being randomly chosen from an index. This introduces a level of randomness in simulation results, especially in PV output. On the other hand, the proposed model's PV output is more data-driven and closely linked to historical data and technical parameters, potentially reflecting real-world conditions more accurately.

Regarding PV output, the CREST model predicts 916.4 kWh, while the proposed model estimates 742.5 kWh. Both values are within a reasonable range considering the corresponding peak power of PVs, as average 3200

kWh electricity with 4.3 kWp peak power is for the UK home [302], but the CREST model's prediction is slightly higher. This could be attributed to the PV systems chosen from the index having higher efficiency or larger capacity. Conversely, the proposed model might rely on average or typical solar radiation conditions, leading to outputs closer to long-term averages.

In terms of energy consumption, the CREST model employs a bottom-up approach by simulating individual household appliances' electricity use and summing them to estimate total household consumption (4032.9 kWh), matching UK average consumption (around 3600 kWh) [303]. In contrast, the proposed model's estimate is much lower at 2088.7 kWh. This difference might stem from the proposed model relying on localized data, influenced by specific region or dataset characteristics.

For self-consumption, the CREST model estimates self-consumption at 419.2 kWh, accounting for 45% of its total PV generation. This implies that 45% of the PV output is used by the household, while the remaining 55% is sent back to the grid. The proposed model's self-consumption is 368.2 kWh, constituting 49% of its total PV generation. This suggests that the proposed model's household better utilizes its PV generation, reducing grid dependency.

In terms of net demand, the CREST model's net electricity demand is 3116.5 kWh, indicating the electricity purchased from the grid minus the electricity sold back. Notably, the CREST model treats electrical and thermal energy distinctly. The proposed model's net demand is 4934.0 kWh, much higher than CREST due to considering thermal energy requirements, as well as that of EV charging. Hence, these two values cannot be directly compared. The one of the proposed model provides a more comprehensive view of energy demand, encompassing heating, water heating, cooking

electricity demand, and EV charging.

In the context of thermal energy consumption, specifically related to space heating, the two models, namely the CREST model and the proposed model, exhibit notable differences in their predictions. The CREST model anticipates a space heating demand of 5553.9 kWh, employing a gas supply-based simulation. Conversely, the proposed model projects a substantially lower space heating demand of 2647.6 kWh. Comparing these predictions to established reference values provides further insight. The reference values indicate that gas heating corresponds to 5249 kWh, while electric heating entails 2135 kWh [278]. Evidently, the CREST model's prediction aligns more closely with the reference value for gas heating, while the proposed model's prediction exceeds the reference value for electric heating. This discrepancy in the proposed model's prediction could potentially be attributed to the integration of time and occupancy-based control systems within the modelling framework, as well as the reference room area in the simulation. The difference between electric heating and gas heating for both models value and reference value, is due to the energy efficiency for different heating methods.

Moving into the domain of thermal energy allocation for water heating, distinct variations in the predictions of the CREST model and the proposed model emerge. The CREST model foresees a water heating demand of 1870.0 kWh, whereas the proposed model's projection is considerably lower at 606.9 kWh [278]. Consideration of established reference values supplements this analysis. The reference value for water heating stands at 945 kWh. This hot water demand is seriously affected by user behaviour and number of residents. The user parameters of the proposed model are closer to the average, but due to the limitation of the number of daily water uses in the hot water usage sub-model, this potentially reduces the energy

demand of the simulation results.

Shifting focus to the realm of thermal energy consumption associated with cooking activities, a comparison between the CREST model and the proposed model elucidates distinct methodologies. The CREST model does not incorporate calculations for thermal energy demand linked to cooking tasks. In contrast, the proposed model derives an estimate of 497.5 kWh for cooking energy demand. For contextualization, the reference value for cooking energy demand is 414 kWh [278]. The proposed model's prediction slightly exceeds this reference value. This variance could potentially be attributed to the nuances of the proposed model's underlying data and assumptions pertaining to cooking activities.

This section mainly analyses and verifies the performance of the model based on the comparison of the two models. Since the CREST model does not involve technical applications such as batteries and electric vehicles and energy control, no comparative analysis is performed here. In the following sections, more simulation analysis and considerations are carried out for the proposed model.

7.1.3 Conclusion of the Proposed Integrated Home Model

The proposed model exhibits unique characteristics in the field of energy modelling, with the integration of thermal energy, comprehensive heating control, and the consolidation of household energy systems being its key facets. These aspects not only set the model apart but also bring forth significant potential for future development.

Primarily, the model expands the horizon of household energy systems into

the realm of thermal energy through a more comprehensive integration. Unlike traditional electricity demand modelling, the proposed model incorporates heating, hot water, and cooking-related thermal energy requirements, offering a more holistic and accurate energy management approach. This integration not only reflects real-world household energy consumption but also presents opportunities for enhanced energy utilization.

Secondly, the model integrates comprehensive heating control strategies that optimize heating demand through time-based and occupant activity-based controls. This approach enables intelligent heating management, mitigates energy wastage, and enhances energy utilization efficiency. By dynamically adjusting heating requirements, the model enables households to reduce energy consumption while maintaining comfort levels.

Furthermore, the model holds the potential to consolidate household energy systems. It transcends discrete modelling of individual energy components and undertakes a comprehensive analysis of solar photovoltaic output, household consumption, self-consumption, and more. This systemic modelling approach streamlines household energy management, facilitating the formulation of integrated energy strategies to enhance overall energy efficiency.

In addition to aforementioned attributes and potential, the proposed model also addresses the future trend of household electrification and energy demand. As technology advances and society evolves, household energy demand is transitioning towards intelligent, efficient, and sustainable directions. In this context, the model emerges as a valuable tool to tackle forthcoming challenges in household energy management.

7.2 Models in the Traditional and the "all electric" Schemes

The structure diagram which integrated utilized models into the simulation of a traditional scheme and an electrified domestic environment is shown in Figure 7.2.1.

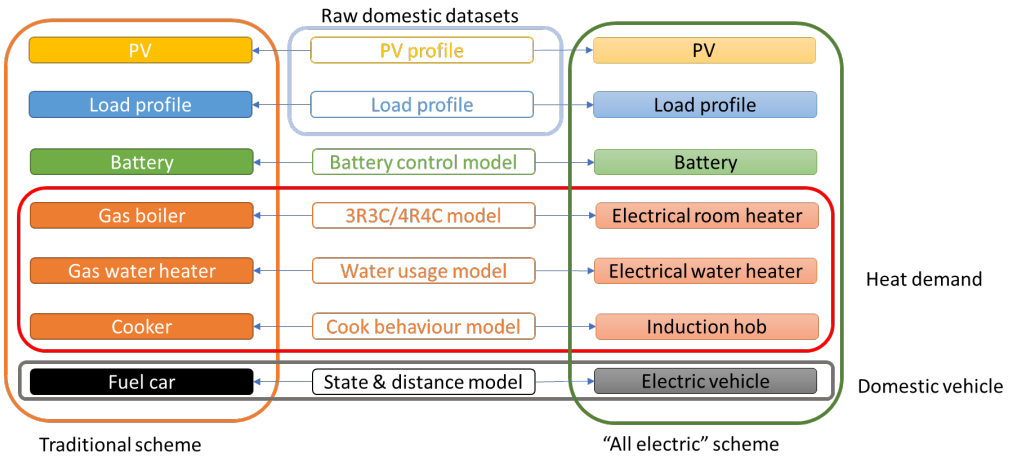


Figure 7.2.1: Structure diagram of integration of the load, PV, battery, heat and EV models in both schemes

Figure 7.2.1 shows the schemes aimed at utilizing various energy sources in a home energy system, as well as the related models for calculating energy consumption. In this section, two schemes are presented based on the power profiles and models. The first one is a traditional arrangement, based on common load profiles. Battery management and PV generation are integrated into the scheme. The second scheme is defined as the "all electric" scheme, which is aimed at simulation of the energy demand in future homes which are eco-friendly and "green".

In the previous chapters, energy databases which contain load and PV power profiles have been described and these can be used as datasets for the schemes to improve the efficiency of home energy utilization. These datasets can be utilized as the common load and for PV generation in typ-

ical homes. Additionally, a battery control algorithm is required by the research as both schemes require a home battery system to move energy consumption for further energy savings. There are also some other models that were put forward in previous chapters and are used in this section. The thermal capacitance/resistance grey box model can be used with either environments, which use gas or electricity for room heating described in section 6.2, (they are slightly different in their each of the models). The water usage model described in section 6.4, which also considers the temperature of used water, can simulate the hot water supply and its energy consumption. Based on the same heating requirements, the energy requirement from the two different energy sources may be different. A model of the cooking actions of UK inhabitants in a domestic dwelling, i.e., the real-time energy consumption used for cooking is also taken into account in the comparison of schemes. Furthermore, domestic vehicle usage is incorporated into the daily activities. Status and trip distance being simulated in the model. The traditional fuel cars consume fossil fuels, whereas EVs could have a strong influence on home energy use due to the V2G technique.

7.2.1 Power Profiles in Future Schemes

The load profiles come from the database and are used to indicate the real time power consumption of a typical house. The load consumption includes the commonly used electrical appliances in modern households, covering basic household needs which do not require gas. It is therefore used as the foundation of the energy consumption patterns for both schemes.

The PV generated power data sourced from PV profiles that were collected in the datasets, is modified slightly based on the specific location, solar radiation and the size of the area of the solar panels. As both schemes are

analysed for the same typical house, the PV generation profiles would have the same impact on the simulation for both of the houses.

7.2.2 Battery Control Algorithms in Future Schemes

The battery control algorithms are proposed to manage the energy storage in the battery, as well as control the input/output power rate of the battery in this system. Based on this control algorithm, the whole system would reduce energy consumption during high tariff periods and attempt to replace the imported power from grid by that from battery storage. In the traditional house, the whole home system only contains the fixed home battery.

For the "all electric" scheme, in addition to the home battery, the electric vehicle also has a battery which provides energy for the trip. Nowadays, the V2G technique is widely discussed, and it is applied in the algorithms. Hence, in the "all electric" scheme, two batteries are operated in the simulation at the same time. For the battery of the electric vehicle, it is mainly used to provide energy for driving, but can be also used to partly store excess energy in the system and supply energy to the home when needed. It is not connected to the home system for the whole day. It is connected only when the vehicle state is 'parking at home'. Otherwise, the electric vehicle would be 'offline' for the house if the vehicle is driven on the road or parked at other places. The control algorithms would properly arrange priorities to ensure that the battery is used effectively.

7.2.3 Heat Demand in Future Schemes

The heat demand in home system has three main sources, which are all simulated in the separated sub models in the project. The heat demand for room heating is the dominant energy consumption, followed by water heating and cooking.

For room heating, the proposed 3R3C model and 4R4C model are a good fit for the different types of energy consumption. For traditional heating in households, the gas would be burnt in gas boiler, and then the heated fluid would enter the radiators in each room through tubes. The heating of the room relies on the heat exchange between the room air and the heat exchangers. The 3R3C model matches the transfer of heat exchange. In the future "all electric" home, the room heating is more decentralized. Comparing the gas or heated fluid, electricity is an energy source which is easier to be migrated. Hence, the phenomenon of transferring electricity into heat energy can take place in different rooms individually, which is reflected by the 4R4C model.

The water usage model does not only simulate the water consumption based on the water use events of the inhabitants, but also simulates the changing state of the water tank to obtain the heat energy demand from using water. For hot water usage, people's behaviour plays an important role, deciding the trigger when using a sink or shower and their duration. For the water supply, low-temperature water is input from the water pipe, and the heating devices will be used to maintain the temperature of the water tank. The difference in the two schemes is that the electric water heater requires pre-heating of hot water as it has poor instant heating capability, whereas the gas water heater provides a large amount of hot water in a short time.

Cooking behaviours do not change with the energy type of the appliance. The gas cooker in the traditional scheme, and the induction hob in the "all electric" scheme, would not affect cooking needs and behaviours, as they are only a cooking utensil from the view of users. Their efficiency, however, would be influenced by the efficiency of the energy sources.

7.2.4 Vehicles in Future Schemes

In domestic environments, vehicles are commonly used for daily demand, including going to work, school, daily purchases, outings, etc. In the traditional scheme, a fossil fuel vehicle is taken into consideration, which is most widely used nowadays. The fossil fuel car is assumed to use petrol or diesel for driving, and it would not have a connection to other components in the home energy system. The only factor to judge the energy consumption is the driving distance, which can be obtained from the vehicle driving model. In addition to the driving distance, the model also gives the real time state of the vehicle. In the "all electric" scheme, three states of the electric vehicle are used to assist the home energy system. The battery of the EV is connected to the home energy system and can be utilized by the system. In addition to charging from low tariff electricity and the excess PV energy, the battery can also discharge to supply the home load when required. This change will not only bring more challenges to the power consumption side, but also provide more opportunities for intelligent management of household energy.

7.2.5 Traditional Scheme and the "all electric" Scheme

In summary, based on the power profiles and the proposed models, two household energy schemes can be presented, simulated and compared in the following sections. The traditional scheme, based on the basis of existing household equipment, shows the common reconstructions of integrating PVs and batteries. The traditional scheme contains a normal house electrical load, and the heat demand is satisfied by a gas boiler, gas cooker. Petrol vehicles are used for driving in this scheme. This scheme matches many existing housing schemes. In addition to the integration of PVs and batteries, the "all electric" scheme reflects a future which is highly electrified, and high energy consuming devices are electrified. The room heat demand is satisfied by an electric room heater, while hot water demand is satisfied by an electric water heater. Moreover, a GSHP could be also considered for room heating as a replacement. An induction hob is used for cooking, and electric cars are incorporated into a home energy system.

7.3 Energy Analysis of the Traditional and the "all electric" Schemes

7.3.1 Performance of Battery Management Schemes

Compared to the households where the raw datasets come from, the traditional scheme has a battery for home energy management, and these datasets have been supplemented with additional heating demand and petrol vehicle models. Of course, these types of energy demand are not reflected in the consumption of electricity. The traditional scheme also has a PV generation system. Hence, in the view of electricity, the main

difference from obtaining datasets of households and the traditional home scheme, is the existence of a battery system. The first thing to do is to identify the performance and role of the battery in the system. In the case study of this section, the applied home battery is Tesla Powerwall 2, which has a 13.5 kWh capacity and 5 kW power rating [304]. A comparison graph of the energy consumption for the traditional scheme and the original energy profiles for different tariff periods is shown in Figure 7.3.1 for a period of 1 year.

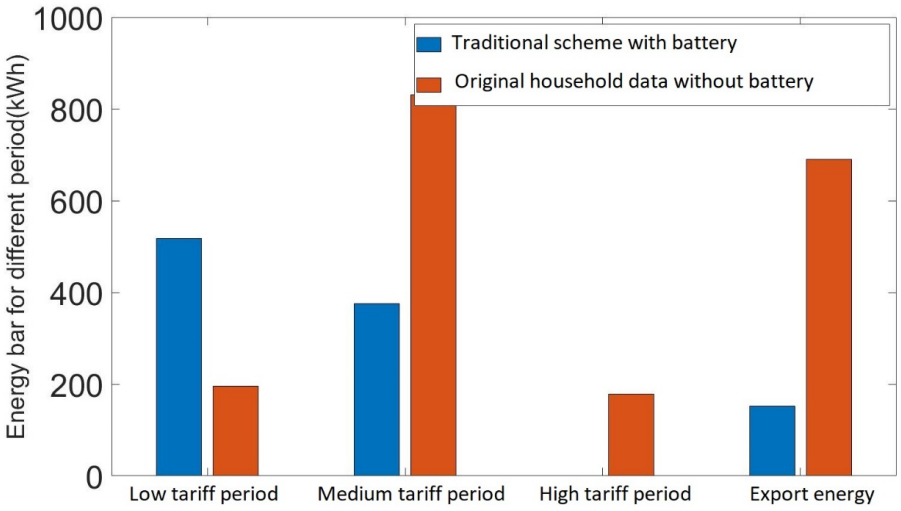


Figure 7.3.1: Bar graph of traditional scheme and original consumption profiles for different tariff periods

In Figure 7.3.1, based on the simulation with and without battery storage, the energy consumption for different tariff periods and export is calculated and shown. Four series of bars are shown in this graph, indicating the amount of electricity consumed during the different tariff periods using a TOU (time-of-use) tariff pricing strategy. There are low tariff periods, medium tariff periods and high tariff periods during the day. The low tariff period is from 0 to 7, the medium tariff period is from 7 to 16 and from 20 to 24, and the high tariff period is from 16 to 20. These three periods define the cost of the importing electricity from the grid. The last one is the exported

electricity from the home system to the grid, which is usually associated with a feed-in tariff. The two colours show the differences the schemes. The orange ones use the obtained datasets in a household without battery, while the blue bars are based on the simulation of the traditional scheme where the battery would make sense in the electricity system. When there is no home battery system, the electricity consumption in the low tariff period in this case is 156 kWh for one year. The highest electricity consumption takes place in the medium tariff period, (831 kWh). There is also some electricity demand in the high tariff period, as 196 kWh of electricity is consumed during this period. The medium tariff periods occupy about half of the day, leading to higher consumption and energy cost during this period. Although the high tariff period does not last for long, it is the most intense period for electricity consumption. Moreover, most PV energy generation occurs in the daytime, mainly the medium period, which can exceed the demand. The excess electricity consumption is exported to the grid (689 kWh). Considering the total PV generation over the year is 1100 kWh, the self-consumption rate is about 37%, i.e., close to the average value in the UK households which do not use 'enabling technologies' such as batteries or electric vehicles [91].

After the transformation of the traditional scheme with the battery, the electricity demand distribution of tariff periods has been greatly changed. For the low tariff periods, the electricity consumption climbs to 518 kWh, i.e., it is the highest in the traditional scheme. Because of the battery system, electricity can be imported from the grid during low tariff periods and consumed when required during the high tariff period. The electricity is imported and then stored in battery storage during the low tariff period. In the medium tariff period, the electricity consumption is still at a high level (375 kWh). Although the instantaneous demand is low, and it is

supplemented by solar energy generation. The most energy savings take place during the high tariff period. The imported energy is only 2 kWh, saving a great amount of money. In addition to self-consumption, the excess electricity from PV generation is also stored in the battery system, hence the exported energy is only 152 kWh in the traditional scheme.

Comparing the traditional scheme simulation results to the original datasets, it avoids direct electricity import during high tariff periods, and decreases the exported electricity by 78% for the whole year. This is due to the existence of the battery system, which could shift the demand, save the cost and increase local use of energy. The energy demand is 'shifted' to lower tariff periods, a period of less electricity demand and lower electricity prices within the grid. In addition to the battery system, the simulation of the traditional scheme also contains the heat demand of room heating, hot water and cooking, as well as the energy pattern for car driving, which is not in the original database. These parts of the energy consumption will be discussed in the following subsections.

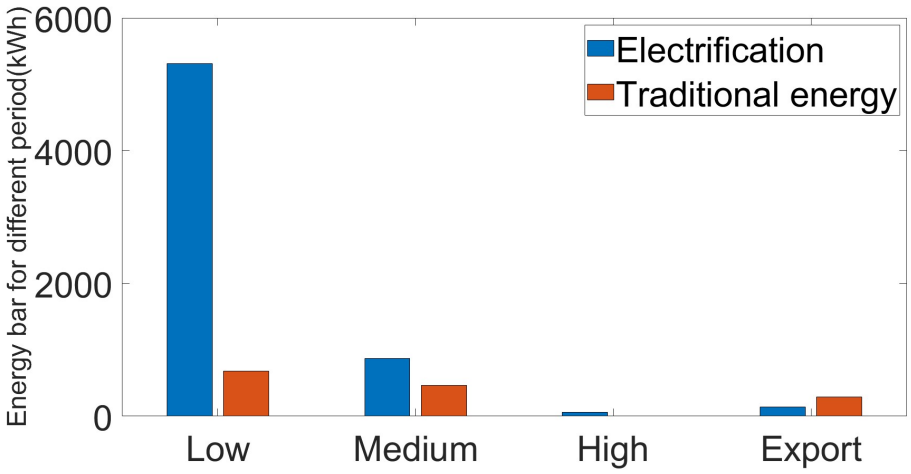
7.3.2 Energy Demand in Traditional and the "all electric" Schemes

Two models are considered in this section. The first is the traditional one, i.e., electricity for typical home appliances, with the gas used for all heat demand, including room heating, water heating, as well as cooking. The vehicle for user driving is assumed to be. The second is the "all electric" home where all thermal demand is satisfied by electrical heating appliances, such as an electrical heater or hob. The petrol car is replaced by an electrical vehicle In this section, the capacity is 60 kWh and charge power rating is 7 kW for the simulated EV [305]. Both schemes have PV

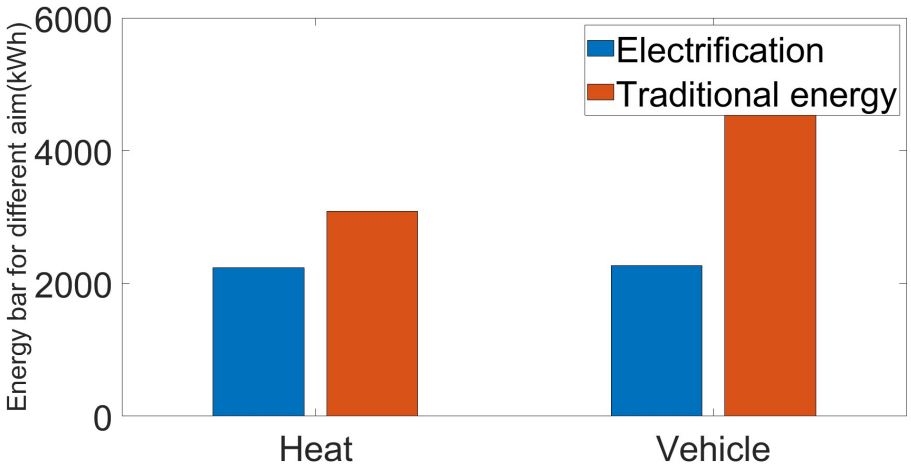
generation and a home battery, which has 13.5 kWh of capacity and 5 kW of power rating as the previous section [304].

In Figure 7.3.2, based on a one-year simulation for one house, the energy consumption patterns are classified by different tariff periods. The electricity import and export in the view of the whole system are shown in (a). The energy consumption of traditional heating and vehicles patterns is also compared with the electric appliances in (b). Time of use tariff pricing is applied in the simulation. During this simulation, the total PV generation for one year is 1100 kWh, while the total home load from raw database, is only 894 kWh in this case. The control algorithm for both houses follows the rule-based algorithm that proposed in HEMS chapter.

In the Figure 7.3.2a), the blue bars show the electricity consumption from the grid after electrification, while the orange bars indicate the consumption before electrification in different tariff periods. Due to the charging and discharging strategy, 5314 kWh of electricity is imported from the grid to the home during the low tariff period, to obtain energy at the cheapest price. For the medium tariff periods, 873 kWh of electricity is utilized, which is mainly to supply energy for direct use during the day. Only 56 kWh electricity is used during the high tariff period. For all of the year, the exported energy to the grid is 140 kWh. For the traditional scheme, when the heat demand and vehicle are not supplied by electricity but by fossil fuels, there is a huge decrease in electricity consumption. During the low tariff periods, 676 kWh of electricity is consumed. When the solar radiation achieves the highest and producing much energy to the system, only 465 kWh of electricity is imported for energy balance, while 289 kWh of electricity exports for all of the year. The electricity consumption is 1.4 kWh for high tariff periods.



(a) Energy consumption for the different tariff periods



(b) Energy consumption for different types of energy use

Figure 7.3.2: Energy bar of two schemes with different periods and usage

Due to the home battery, some energy is imported from grid in both schemes. For the exported energy, which basically excess solar generation 149 kWh more electricity is exported for the traditional scheme, compared to the "all electric" scheme. This difference is due to the existence of the new heating demand and EV charging during the PV generation. During this PV generation time, the inhabitants are not always at home. When they have left home, room heating is not required and the EV is not connected to the home system, hence there is only a little increase in the utilization of PV generation energy. Compared to the high tariff and export, energy figures which are close to each other. There is a huge dif-

ference in the electricity consumption during the low and medium periods, but the consumption of the "all electric" scheme is about 8 times the traditional scheme. This is led by the extra energy demand of the thermal heating and vehicles. As shown in Figure 7.3.2b, a total of 3088 kWh of energy would be consumed when using gas boilers and traditional stoves to provide heat energy in this case. When electrical heater and induction hobs are used, only 2239 kWh of electricity is required in replacement of gas, saving about half of the value of the energy. In the view of the vehicles, when the petrol car is used for driving demand, 5262 kWh of petrol is used considering the engine efficiency. When the electric vehicle is used, the energy consumption decreased to 2270 kWh. The energy consumption for heat and trip demand after electrification is only 74% and 43% of those using traditional energy. The change of fuel energy to electricity energy led to the increasing demand in system load, and thus dramatically increases the imported electricity from the grid. It is worth emphasizing, that the annual energy total for the EV is the energy for driving, being a part of the energy that flows through EV battery, as the rest energy is charged and discharged due to V2H.

Based on the detailed energy profiles for the one-year simulation, the energy consumption of the whole system can be classified by different types of energy. The stacked consumption charts of different home schemes are shown in Figure 7.3.3.

The first stacked bars of Figure 7.3.3 indicate the energy consumption in the system which using traditional energy. The green, blue and dark green bars represent the electricity consumption in low, medium and high tariff periods separately, nothing that the black bar is the exported energy during all the days. For heating demand, three types of heating demand are supplied by gas. The red one is for cooking, and the orange bar shows the

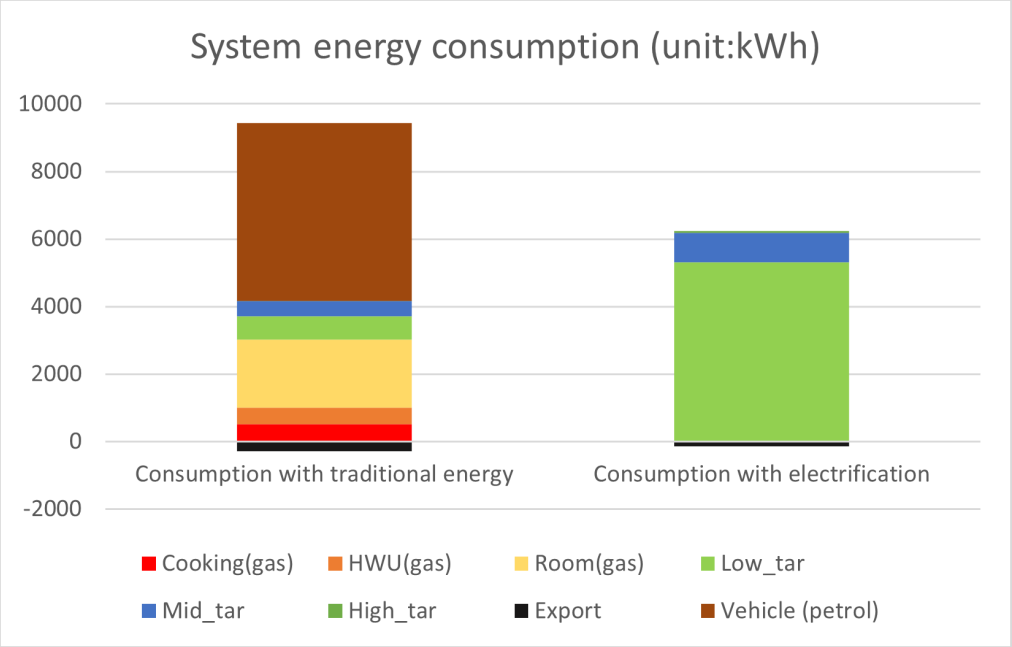


Figure 7.3.3: Detailed energy diagram of the composition of system energy

gas consumption for providing hot water, while room heating consumption is the yellow bar. Additionally, the brown bar shows the energy consumption when using petrol for inhabitants' driving. In the other stacked bar, traditional fossil fuels are abandoned, and electrical appliances are used to replace heating and trip demand. Hence, only electricity consumption in different periods is shown in this bar.

When using fuel energy in traditional scheme, 9144 kWh of energy consumed to satisfy the need of household appliances, heat as well as vehicle driving. It is a huge amount while the heat demand is above half of it. Compared with small household appliances, heating in winter requires a lot of heat energy. The consumption of a petrol vehicle is about 57%, which plays another important role. These two sections are not only the significant uses of energy, but also occupy a huge proportion of the home bills. After the electrification of the appliances, the total energy consumption for one-year decreases to 6103 kWh, dropping by 33%. The electricity consumed on heating is 33% of the total electricity consumption, while

that of EV is 37% of the total. Compared to the traditional scheme, the proportion decreases a lot, as the use of electrical energy is more effective.

7.3.3 Analysis of the Battery Charging and Discharging

In this system, in addition to provide energy for driving, the battery of the vehicle also discharges to supply the demand in peak hours. Based on the simulation results, the total energy demand and consumption can be calculated from the power matrix, such as charging, discharging and home load. The key values, which were not shown in the previous results, are shown in Table 7.3.1, to indicate the quantitative relationship between different parts of the direct energy supply to this house of case study.

Table 7.3.1: Calculated energy results of two schemes

Scheme/ Unit	EV battery	Home battery	PV	Load	Grid
All electric (kWh)	689 (17.5%)	624 (15.8%)	1100	3958	6243
Traditional (kWh)		619 (39.1%)	1100	1584	1142

Based on calculated results in Table 7.3.1, the battery discharge energy of the EV for the "all electric" scheme is 2989 kWh, which includes the energy for driving and for aiding the system load. Considering the energy for driving is 2270 kWh, as a result, the energy that is discharged by the EV battery for the home load is 691 kWh. The discharged value of the home battery is 624 kWh. The total electrical load, integrating electrical, heating and EV is 3958 kWh. Hence, the energy supplied by the EV and the home battery is 17.5% and 15.8% of the total load demand. For reference, the PV generation for the year is 1100 kWh and energy imported from the grid is 6243 kWh. These two values cannot directly take into calculations, as the excess PV generation does not supply load but is exported to the

grid. The value of the grid is influenced by different components of the system of energy balance in real time. When it comes to the traditional scheme, the vehicles and heat demand are not included in the electrical load, hence the load is only 1546 kWh for the year. In this scheme, the energy discharged from the home battery is 619 kWh, 39.1% of total load. The energy imported from the grid is only 894 kWh, as much of the demand is supplied by PV generation. In both schemes, the home battery provides about 620 kWh of energy. The battery, which is a common household battery on the market designed for modern demand, has been fully used even in the traditional scheme. Therefore, in the "all electric" scheme, the discharged energy of the home battery did not increase too much. Even if the capacity of the EV battery is much larger than the one for the home, but the energy provided by the EV battery is at the same level as the home battery. For the whole year, 2270 kWh of energy discharged by the EV battery is for driving, which is in the first priority. As the PV generation does not change after electrification, the increasing load demand is mainly satisfied by the grid, leading the energy value imported from the grid increasing dramatically.

7.3.4 Conclusion of the Energy Analysis

In summary, this section investigates the energy difference between traditional and "all electric" schemes, especially when integrating battery systems and navigating through different tariff periods. The key results are listed below:

- The introduction of a battery system (specifically, Tesla Powerwall 2) altered energy consumption across various tariff periods.

- The battery system facilitated the strategic import and storage of electricity during low tariff periods, for use during high tariff intervals, enhancing cost-efficiency and local energy consumption.

- The adoption of the "all electric" scheme significantly escalated electricity consumption across low and medium tariff periods, specifically.

- Conversion of electrical heating and EV use resulted in efficient energy use, evidenced by a dramatically reduction in energy consumption for heating and transportation respectively, relative to the scheme simulates on traditional energy sources.

- The EV battery discharged a cumulative 2707 kWh, with 2016 kWh allocated for driving and 691 kWh supporting a home energy load.

- The home battery discharged approximately 620 kWh, providing 39.1% and 15.8% of the total load in the traditional and "all electric" schemes, respectively.

- The electrification process notably heightened grid demand, with the additional load primarily satisfied through grid imports.

Overall, according to the analysis in this section, some detailed exploration of results can be summarized as follow:

- The integration and strategic management of battery systems are pivotal in modulating electricity demand across varying tariff periods, thus enhancing economic and energy efficiency.

- Electrification, despite increasing electricity demand in "all electric" schemes, substantively enhances energy efficiency by reducing overall energy usage when efficiently applied.

- The functionality of battery discharge, from both home batteries and EVs, provides a substantial contribution to meeting total load demand, while also influencing grid interaction and real-time energy balance.

7.4 Comparative Economic Analysis of the Traditional and the "all electric" Schemes

7.4.1 Analysis of Economic Benefits

In the simulation of combined model for one year, the energy consumption in different types is listed and calculated. For electricity, the influence of tariff periods is considered, and the real time results in different tariff periods are calculated in previous sections. The 24 hours in each day are classified into four parts, as three types of tariff periods. The tariff periods are shown in Table 7.4.1 [197].

Table 7.4.1: Electricity tariff of Time-of-Use (TOU)

Electricity rates (prices per kWh inc. VAT)	**Time Period**	**Rate**
Low tide	Midnight - 7am	7.5p
Tide	7am - 4pm	17.54p
High tide	4pm - 8pm	32.55p
Tide	8pm - midnight	17.54p

In time of use tariff, consumers are encouraged to use electricity in low tariff periods, to get better economic benefit. For most people, most electricity consumption takes place in the high tariff period, when people are at home. This difference is where battery storage can supply energy during demand peak and home energy management system makes sense.

The lowest tariff period is from 0 to 7 am, when 1 kWh of electricity from the grid costs 7.5 p. From 7 am to 4 pm, as well as 8 pm to midnight, are the periods for medium tariff, which price is 17.54p. The rest time, from 4pm to 8pm, cost 32.55 p per one kWh of electricity consumption. Additionally, considering the PV generation, the home system would export energy to the grid, and feed-in tariff is 7.5p. In spite of electricity consumption, the home system would also consume gas for heating, including providing heat for the room, maintaining hot water supply and cooking food. Due to various market reasons which causing volatility in fossil fuel prices, the price of gas has achieved 7.37 p. The average price of petrol for driving household vehicles is 1.482 pounds per litre.

In addition to the price of electricity and fuels used in a domestic environment, the electrification of households also leads to the change of equipment, as well as the price of these appliances. Before electrification, the boiler to supply hot water, the cooker, and the traditional heater all used gas to supply energy, which is burnt to provide heat for a home system. At the same time, the traditional vehicles which used by the inhabitants are commonly diesel cars or petrol cars. On the other hand, after electrification, the gas boiler is replaced by the electric water heater, while the induction hob is instead of the gas cooker. The room heating is also used electricity instead of community gas supply in the modern households. For vehicles, the penetration rate of electric vehicles in the domestic environment is increasing owing to technique improvement and incentive policy.

The investment on household equipment and related accessories are various. For the gas boiler, the investment fee is about 2500 pounds, while 5250 pounds should be paid for the gas room heater [306]. And the cost of the cooker is about 200 pounds [307]. In additional to consume gas, the cost of petrol car can be estimated as 26800 pounds [308]. After elec-

trification of households, all the mentioned equipment would be replaced by those consuming electricity. The electric water heater requires 4300 pounds [276], while electric room heater costs 4090 pounds [1]. The investment of replacing cooker costs 400 pounds [309]. Nowadays, the investment of electric car, which has similar performance to the mentioned petrol one, costs 29700 pounds [308]. Since both schemes utilize the same solar power system, the solar system does not impact the economic comparison. Additionally, it is assumed that there are no maintenance costs. Additionally, the investment and operation cost of the whole system could be calculated as Equation 7.4.1:

$$\text{Total cost} = Cost_{\text{investment}} + \sum_{i=1}^{\text{years}} Cost_{\text{operation}} \times (1 + r\%)^i \tag{7.4.1}$$

The parameter r represents the inflation rate. The NPV, is the value of cash flow over different periods, which depends on the time interval and discount rate – the assumed equivalent value of interest obtained if an equivalent financial investment had been made. It can be calculated as Equation 7.4.2.

$$NPV = \sum_{Yr=1}^{Yr} \frac{Cash_{Yr}}{(1+i)^{Yr}} - Cash_0 \tag{7.4.2}$$

Where $Cash_{Yr}$ Is the net cash inflow during the period Yr. The cash flow can be calculated as the savings due to applying other appliances compared to gas boiler. Yr is the number of time periods which unit is year. $Cash_0$ Is the initial cost. In this section, it is the combination of investment of electric appliances and related auxiliary equipment.

Considering the difference between investment and annual tariffs, the NPV graph is shown in Figure 7.4.1.

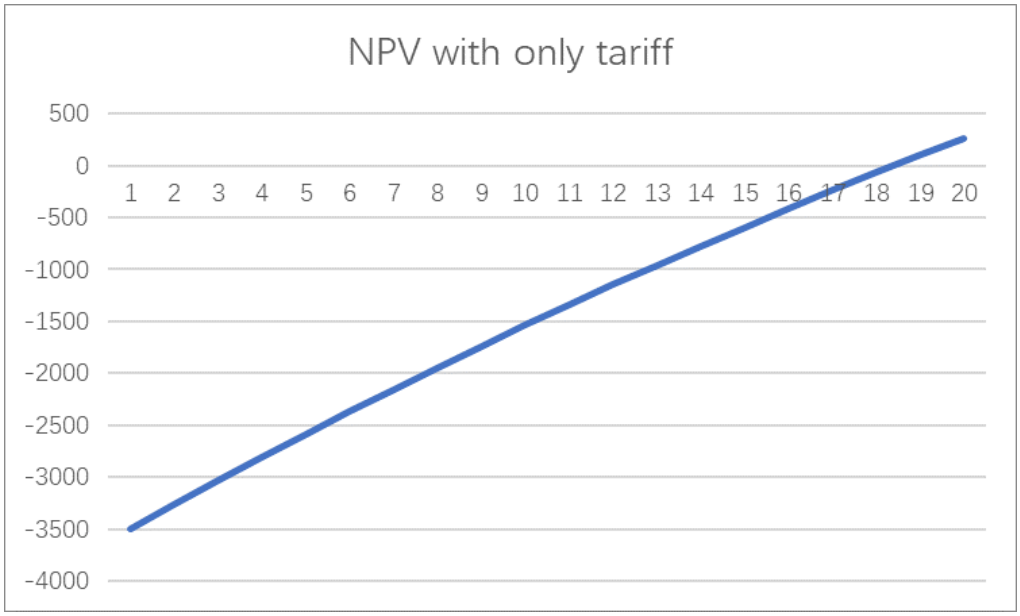


Figure 7.4.1: NPV graph with only electricity tariff (unit: £)

In Figure 7.4.1, the cost savings in the first year are about 240.23 pounds, with a flow rate of 2% and depreciation rate of 1%. In the view of investment, the investment on the "all electric" system costs 3740 pounds more than the one using a gas supply. If depreciation rate and inflation are not considered, the investment requires 15.6 years to get the benefit back. According to the NPV graph, this investment could not be got back for several years, until the 19^{th} year, when NPV equals to 101.9 pounds. For the whole system, the payback period is 19 years, and the total savings in 20 years is 266.8 pounds. Moreover, for both systems, the update and replacement of appliances are assumed close in frequency.

To investigation of the potential of the home electrical system should not only focus on direct economic benefit, should also pay attention to the hidden value that can be transformed into benefits. For instance, the environmental effect of various energy resources is different, as many governments and scholars are focusing on carbon emissions and related market policies. Some places impose additional taxes on heavy pollution or adjust prices to affect the proportion of energy use. According to the UK official statistics,

the equivalent carbon dioxide emissions of the mentioned sources in this chapter are listed in Table 7.4.2.

Table 7.4.2: Global warming potential of different energy sources

Type	Gas (kg/kWh)	Petrol (kg/L)	Electricity (kg/kWh)
CO2e	0.183	2.31	0.193

In Table 7.4.2, the values of CO2e are for the energy consumption for resident use, where gas is 0.183 kg CO2e/kWh and that of electricity is 0.193 kg CO2e/kWh. This difference is due to that gas has a good performance among traditional fossil fuels when it is fully burnt. Additionally, the electricity in grid comes from various sources, including fossil fuels, renewable energy or nuclear. Complex sources and processes lead to this higher CO2e value. However, in a home system, to achieve the same effect, the amount of gas consumption would be much bigger than using electricity. Hence, considering both the unit emission and energy consumption value, the way of consuming electricity would save many emissions than using gas and petrol. The annual emission before electrification is 2282.1 kg CO2e, and the one after electrification is 1641.4 kWh. The annual emission saving is 640.7 kg CO2e. In 2023 the carbon trade price in the UK market is 78 pounds/T.

Taking carbon emissions and the cost of carbon trading into account, the net present value of home energy systems in 20 years is shown in Figure 7.4.2.

In Figure 7.4.2, the initial cost savings are about 290.22 pounds in the first, which contains the cost of 49.98 pounds for carbon emissions. In the view of investment, the investment on the "all electric" system also costs 3740 pounds more than the one using gas supply. The investment requires 11.8 years to get benefit back, when the discount rate is not considered.

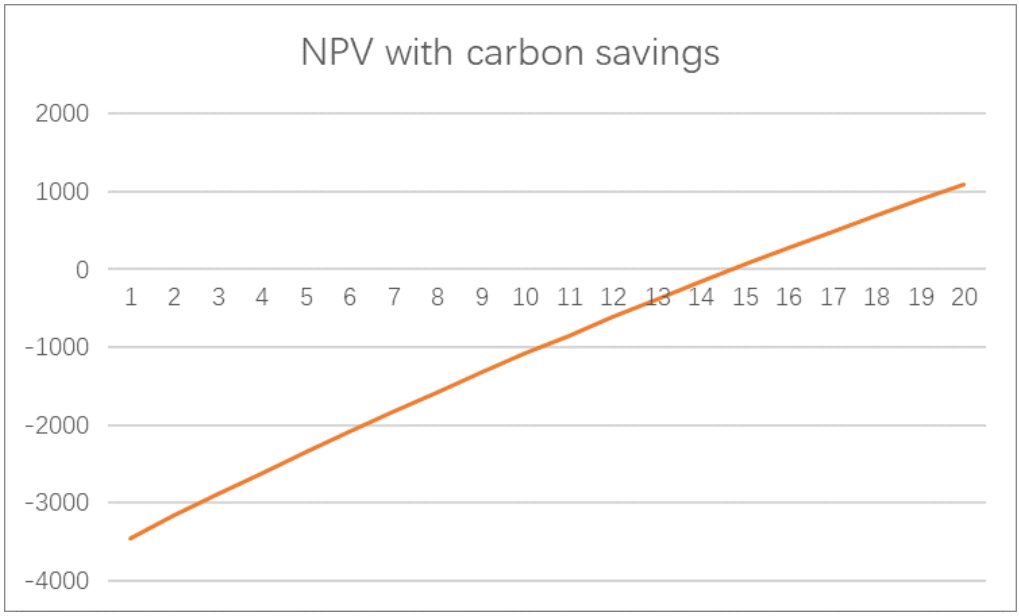


Figure 7.4.2: NPV graph with carbon savings benefit

According to the NPV graph, this investment could get back in 15 years, when NPV equals to 63.62 pounds. For the whole system, the payback period is 15 years, and the total savings in 20 years is 1100.34 pounds. Owing to the consideration of carbon emissions, the investment could get back a in a shorter period, comparing to only calculating economic benefits.

7.4.2 Sensitivity Analysis

A sensitivity analysis of a home energy system can be conducted by analysing the impact of changes in different economic parameters on the system's performance. Specifically, the considered factors include energy storage system, energy price and equipment costs.

The energy storage system is an essential component of a home energy system that allows excess energy generated by solar panels to be stored and used later when the sun is not shining [310]. The performance of the energy storage system can be evaluated based on its capacity, efficiency, and other characteristics. A larger capacity storage system will allow for more energy

to be stored, while a more efficient system will result in less energy loss during the charging and discharging process. A sensitivity analysis of the energy storage system can help identify the optimal size and specifications that can maximize the system's performance and economic benefits.

Energy prices, including electricity and fuel prices, can have a significant impact on the economic benefits of a home energy system [311]. For example, when electricity prices are high, the economic benefits of a home energy system that generates and stores its own electricity become more significant. Similarly, when fuel prices are high, a home energy system that uses renewable energy sources can offer cost savings compared to traditional fossil fuel-based energy sources. Sensitivity analysis of energy prices can help determine the level of price changes required for a home energy system to become economically viable and identify opportunities for cost savings.

The cost of equipment, including solar panels, energy storage systems, and other components, is a major factor that affects the economic feasibility of a home energy system [312]. The initial investment cost for a home energy system can be substantial, but over time, the system can generate significant cost savings. Sensitivity analysis of the equipment costs can help identify the optimal balance between initial investment cost and long-term cost savings to maximize the system's economic benefits. This analysis can help determine the most cost-effective equipment specifications and identify opportunities for cost reduction through technological advancements and economies of scale.

A sensitivity analysis of a home energy system can be conducted using various methods, such as single-factor analysis or multi-factor analysis. Single-factor analysis involves varying one parameter at a time while keeping the others constant, while multi-factor analysis involves varying multiple pa-

rameters simultaneously. By analysing the impact of different parameters, it is possible to optimize the design and operation of a home energy system and maximize its economic benefits.

Internal rate of return (IRR) is an indicator that measures the potential rate of return of an investment project and is commonly used to evaluate the economic benefits of an investment project [313]. IRR reflects the relationship between cash flow generated by the investment project and the investment cost and is also considered as the discount rate that makes the net present value zero.

In a sensitivity analysis, different investment schemes can be compared with their IRR values to evaluate their sensitivity to changes in input parameters. Typically, the higher the IRR value, the quicker the investment returns and the better the economic benefits of the investment project. Therefore, by conducting sensitivity analysis on IRR values, it is possible to determine which factors most affect the economic benefits of the investment project, and which factors have the greatest impact on IRR values.

It is important to note that IRR is a relative indicator and is only meaningful when comparing IRR values of similar projects. When conducting a sensitivity analysis, the investment schemes being compared should be kept consistent to ensure comparability of IRR values. In addition, the IRR has some limitations, such as ignoring the scale effect and time value of money on a project, so other economic indicators such as NPV and payback period should also be considered in order to comprehensively evaluate the economic benefits of the investment project.

7.4.2.1 Energy Storage

Energy storage devices, including batteries, play a crucial role in a home energy system. They enable excess energy generated by solar panels or other renewable sources to be stored and used later when energy demand exceeds supply. When selecting a battery for a home energy system, two important factors that need to be considered are its capacity and power rating.

Capacity refers to the amount of energy that can be stored in the battery. The battery's capacity determines how long it can provide power to the home during a power outage or when the primary energy source is unavailable. A higher-capacity battery can store more energy, and therefore, provide longer backup power. Capacity is usually measured in kilowatt-hours (kWh), and the ideal capacity depends on the energy needs of the household.

Power rating, on the other hand, refers to the maximum rate at which energy can be charged or discharged from the battery. This is usually measured in kilowatts (kW) and is an important consideration when selecting a battery for a home energy system. The power rating of the battery determines the maximum amount of power that can be delivered at any given time. A higher power rating means that the battery can deliver more power at a faster rate, which is essential when the energy demand suddenly increases.

In summary, both capacity and power rating are crucial considerations when selecting a battery for a home energy system. A battery with a high capacity can store more energy and provide longer backup power, while a battery with a high-power rating can deliver more power at a faster rate,

which is essential for meeting sudden increases in energy demand.

Based on the unit of energy storage, an IRR mesh can be obtained based on simulation, where battery capacity and power rating limitation are changed in a reasonable range.

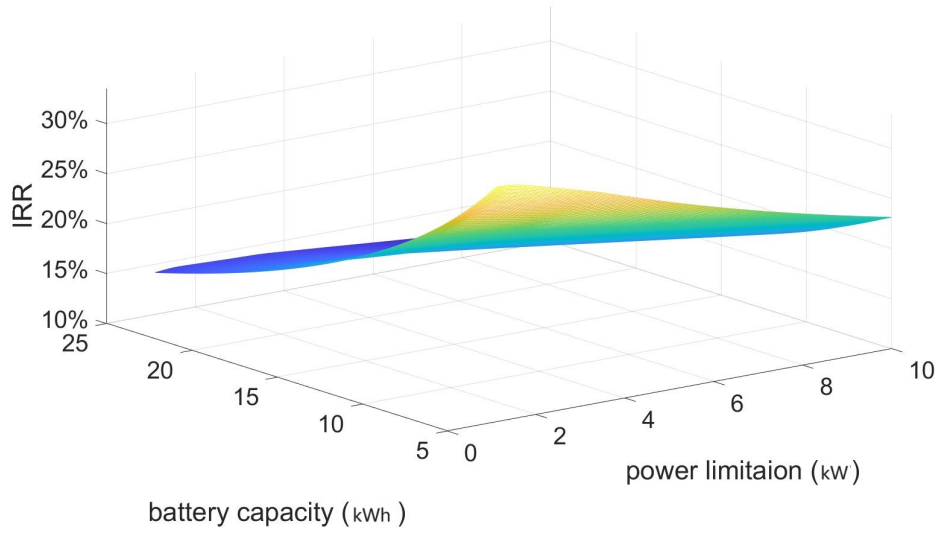


Figure 7.4.3: IRR results based on battery capacity and power rating limitation

In Figure 7.4.3, the X-axis is battery capacity, which unit is kWh, reflecting the size of home battery storage for energy management. The Y-axis is power limitation, which unit is kW, means the limitation of power rating of electricity transfer appliances of energy storage. The remaining axis is Z-axis of IRR, which indicates the general economic performance of the chosen system size. The colour of mesh can reflect the IRR value. Generally, when the battery capacity and power rating is extremely small, the system has an IRR around 30%, showing with orange. When both battery capacity and power rating increase, the global peak of the mesh takes place at the battery capacity of 5 kWh and power rating of 1.1 kW, being 33.48%. In this mesh graph, the points in yellow are those results closed to the peak point. After the peak point, when the battery capacity or power rating

keeps increasing, the corresponding result would decrease instead. The points in green have a less IRR than the orange ones, followed by blue ones. In this mesh graph, when the battery capacity and power rating is extremely high, the IRR drops to 11.72% instead. When the battery capacity is fixed as 5kWh, the minimum IRR result is 23.04% when the power rating limitation achieves its upper boundary in the simulation. On the other hand, if the power rating is fixed as 1.1 kW, the IRR result is only 14% as the power capacity achieves 25 kWh. The IRR results drop with increasing battery capacity are being more dramatic than the drop with power rating. In fact, when the battery capacity increased, the savings on tariff also grow. Due to the marginal effect, however, the growths in savings can not afford the increase of investment, lead to the low IRR results.

7.4.2.2 Investment Cost & Tariff

Conducting sensitivity analysis on both investment costs and energy prices simultaneously is important because both factors can have a significant impact on the economic benefits of a home energy system.

Investment costs represent the initial upfront costs of installing a home energy system, such as purchasing equipment and installation fees. These costs are typically substantial and can significantly impact the overall cost-effectiveness of the system. By analysing the sensitivity of the system's economic performance to investment costs, homeowners can identify ways to optimize the cost-benefit trade-off and determine the most cost-effective financing options, such as leasing or purchasing the equipment.

Energy prices, on the other hand, represent the ongoing costs of operating a home energy system, such as the cost of electricity, natural gas, or other fuels used to power the system. These costs can vary significantly

over time, and sensitivity analysis can help homeowners understand the potential impact of different energy price scenarios on the performance and economic benefits of the system. For example, a sudden increase in energy prices could significantly impact the payback period of the system, reducing its overall cost-effectiveness.

By considering investment costs and energy prices simultaneously in sensitivity analysis, homeowners can evaluate the overall financial feasibility of a home energy system and identify strategies for optimizing the system's performance and economic benefits. This can help ensure that the system provides a satisfactory return on investment and helps reduce overall energy costs over the long term.

To analyse the influence of investment and tariff cost in the system, a sensitivity analysis based on change of investment and annual cost would be calculated. The corresponding results are shown in Figure 7.4.4.

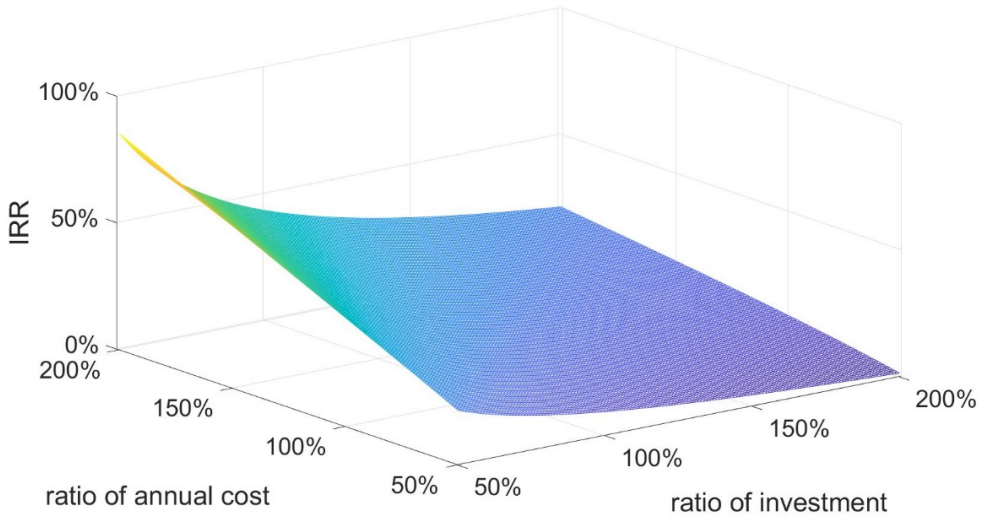


Figure 7.4.4: IRR results based on a ratio of annual cost and investment

In Figure 7.4.4, the X-axis is the ratio between initial investment and the changed investment for simulation, while the Y-axis is the difference be-

tween changed and initial annual savings, The initial annual savings are based on the difference between tariff cost before and after the "all electric" scheme. Along with the increase of ratio of investment, the IRR would be decreased due to high cost. The savings on annual cost, however, can save money and lead to higher IRR result if the ratio of savings is increased. The highest IRR takes place when the ratio of investment is 50% and the ratio of annual cost is 200% in this simulation. The corresponding IRR is 78%, comply with the principle of calculation and the macro trend in the graph.

According to the energy calculation results in previous chapters, before electrification, the traditional scheme contains large gas consumption and small electricity demand, the annual cost is mainly dominant by fossil fuel consumption. After electrification, all the energy demand is satisfied by electricity from energy storage, PV generation and the national grid. The annual cost, hence, is decided by change of electricity tariff. And the change of fossil fuel price is not always the same as electricity tariff price. Therefore, their impact ought to be considered separately.

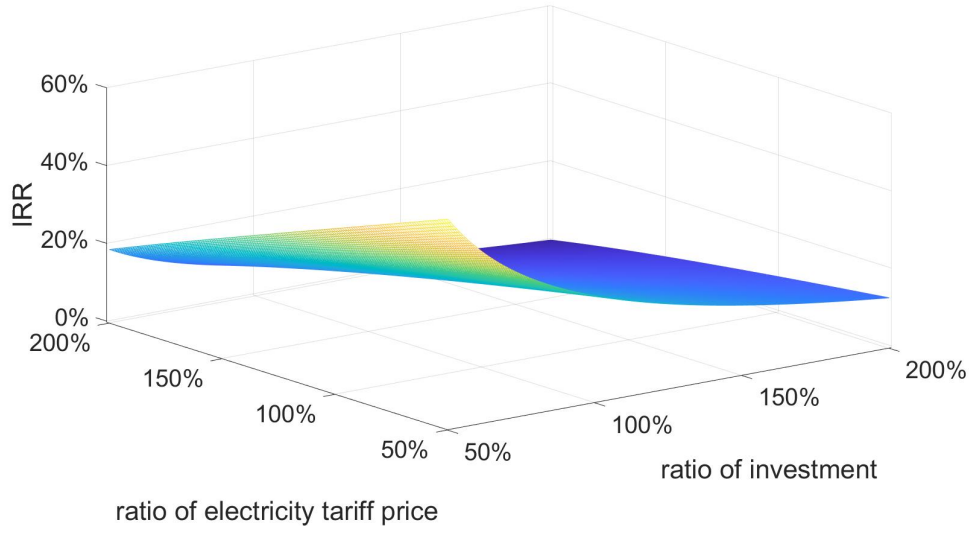


Figure 7.4.5: IRR results based on ratio of electricity tariff price and investment

In Figure 7.4.5, The X-axis is the ratio between initial investment and the changed investment for simulation, while the Y-axis is the difference between changed and initial electricity tariff. The initial electricity tariff is based on the difference between tariff cost before and after the "all electric" scheme. Along with the increase of ratio of investment, the IRR would be decreased due to high cost. The change of ratio of electricity tariff, however, has the similar trend. When the electricity tariff increases, the IRR decreases instead. The highest IRR takes place when the ratio of investment is 50% and the ratio of annual cost is 50% in this simulation. The corresponding IRR is 53%. The highest point in this graph is different from the previous one, this is due to the electricity tariff is one part of the annual cost. The electricity demand after electrification is higher than that before electrification, hence the increase of electricity money would reduce the annual savings.

In the first mesh graph which reflects the impact of annual cost and investment, the ratio of annual cost has more influence that led to IRR change. On the contrary, in the second mesh graph which reflects the impact of electricity tariff and investment, the ratio of investment has more influence that led to IRR change. This is due to the complex composition of annual savings, which contains electricity tariff in different periods, as well as price of different types of fossil fuels. A detailed analysis of energy prices is the next step in order to dig deeper into the economic impact.

7.4.2.3 Energy Price

Energy prices, such as electricity prices and natural gas prices, are important factors that can affect the economic benefits of a home energy system. The sensitivity analysis of a home energy system should consider variations

in energy prices to determine how changes in these prices can impact the system's performance and economic benefits.

Electricity prices are an essential factor when evaluating the economic benefits of a home energy system. The sensitivity analysis of electricity prices involves varying the electricity rates over a range of values and evaluating the impact of these changes on the system's performance and economic benefits. Higher electricity rates generally result in more significant economic benefits of the system since the electricity generated by the renewable energy source becomes more valuable.

Natural gas is a primary energy source for heating and cooking in many homes and is not solely used as a backup energy source. In a home energy system, natural gas can be used as a primary fuel source in addition to renewable energy sources such as solar panels or wind turbines. In recent years, there have been instances of natural gas price volatility due to unexpected events such as extreme weather events, pipeline disruptions, and supply shortages. These events have resulted in rapid price increases in some regions, which can have significant impacts on the economic benefits of a home energy system that uses natural gas as a primary or backup fuel source. Therefore, it is important to conduct sensitivity analysis on natural gas prices to understand the potential impact of sudden price increases on the performance and economic benefits of the home energy system.

Therefore, conducting sensitivity analysis on both electricity and natural gas prices can help identify the optimal combination of renewable energy generation and backup energy sources to maximize the economic benefits of a home energy system. Sensitivity analysis can be conducted by varying the energy prices over a range of values and evaluating the impact of these changes on the system's performance and economic benefits. The results

of the sensitivity analysis can be used to determine the most cost-effective energy strategy for the home energy system.

When conducting sensitivity analysis based on the changes in electricity and natural gas prices, the range and proportion of the changes are firstly required to be determined. For example, it can set the change proportion of electricity and natural gas prices to 5%, 10%, and 15% respectively, and then calculate the IRR or other economic indicators for each proportion. In analysis, the range of the changing ratio of prices changes from 0.1 to 2 (10% to 200%), to calculate the IRR results based on changing tariffs. As the electricity tariff includes TOU values and export tariff, the ratio is for general change of tariff prices. In fact, the tariff in different periods and for sell would not always change at the same range. This ratio only reflects general changes due to technology or policy. For fossil fuels, in the home energy system, gas for domestic use and petrol used in vehicles are included. Geopolitical stability, global market supply and demand, production costs, technological advancements, taxes and policies are those factors that influence on both gas and petrol prices. The ratio of fossil fuel price, hence, reflects the general trend of fossil fuels.

In Figure 7.4.6, the X-axis is a ratio of fossil fuel price, while the Y-axis is the ratio of electricity tariff price. When the ratio of fossil fuels increases, the IRR would also increase. On the contrary, when the ratio of electricity tariff price increases, the total IRR would drop. In this mesh graph, the colour with orange has the highest IRR, followed by green. When the colour is closer to the dark blue, the IRR result is smaller. According to the energy calculation results in previous chapters, before electrification, the traditional scheme contains large gas consumption and small electricity demand, the annual cost is mainly dominant by fossil fuel consumption. After electrification, all the energy demand is satisfied by electricity from

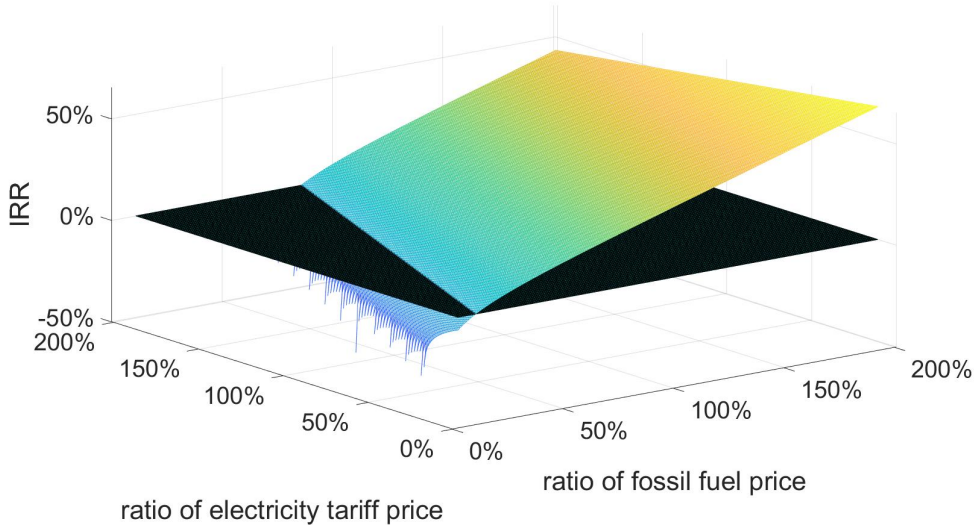


Figure 7.4.6: IRR results based on the ratio of the price of electricity and fossil fuel

energy storage, PV generation and the national grid. The annual cost, hence, is decided by change of electricity tariff. These two points determine the unidirectional change trend of the mesh graph.

In addition to mesh grid, there is a black cross section which indicates the Z-axis (IRR) equals to zero. When IRR is less than 0, means the investment would not get enough benefit back, as the points under the black cross section, indicates the combination of ratios would not get a good payback. Both ends of the intersection of two planes, are (0.19, 0.11, 0) and (0.86, 2, 0). They can be also defined as (19%, 11%, 0) and (86%, 200%, 0). The fitted tangent of X and Y axis is y= 2.82x -0.42. This is a watershed for the economic benefit of changing the ratio. When the ratio of electricity tariff is less than the result based on this formula, the IRR would be larger than 0, indicating the benefit. Based on this equation, two key points in the planes are (0.503, 1, 0) and (1, 2.4, 0). They can be also defined as (50.3%, 100%, 0) and (100%, 240%, 0). In a practical sense, when the electricity tariff is fixed, even the fossil fuel prices are only 50.3% of that in nowadays, the system could still get payback in the long-term.

On the contrary, if the price of fossil fuel is kept, the system can still benefit, even the electricity tariff is 2.4 times of today. In the long-term, the fossil fuel prices would be kept high, while the electricity tariff can benefit from technical improvement and promotion policy. Therefore, the electrification of system has a great potential in the economic view.

7.4.3 Conclusion of the Economic Analysis

This section provides a multifaceted analysis of the economic aspects between traditional and "all electric" residential schemes, emphasizing the potential and challenges posed by electrical and energy management.

- Battery Deployment: The implementation of battery systems, especially in variable tariff contexts (e.g., Tesla Powerwall 2), has proven crucial for modulating electricity demand and improving cost-effectiveness across diverse tariff periods.
- Investment and Operational Costs: The economic analysis delineated the nuanced interplay between initial investment and operational costs, highlighted through detailed NPV and IRR analyses. It's imperative to note that the investment recovery and economic feasibility are significantly influenced by these financial metrics.
- Parameter Sensitivity: The outcomes from the sensitivity analysis underline that the system's economic performance is particularly susceptible to fluctuations in energy storage characteristics and energy prices. This insight is vital for formulating strategies that safeguard against economic perturbations in the energy market.

7.5 Life Cycle Assessment of the Traditional and the "all electric" Schemes

7.5.1 Introduction of LCA Study

The life cycle assessment (LCA) method is widely applied nowadays in order to assist the optimization of eco-friendly options and quantification of environmental Impact [314]. In addition to the assessment of the environmental impact of energy, the materials, lifespan maintenance and final disposal are all taken into consideration. In order to operate the quantification of environmental Impact, a definition which is named as "carbon equivalent" is always applied to quantify and analyse the overall global warming potential impact of different emissions. The influence of various greenhouse gas emissions for the whole life cycle stages can be quantified and compared with the carbon equivalent [315]. The unit for this quantification of carbon equivalent is kg CO2e, as for a given mixture and amount of greenhouse gas, the amount of CO2 that would have the same global warming potential (GWP), when measured over a specified timescale [316]. The LCA methodology consists of four main steps, including definition of the goals and scopes of the assessment study, collection of the sources of parts of the system in different lifecycle stages, assessment of the environment impacts, as well as interpretation of LCA results. In the view of the LCA of energy utilization in the domestic environment, environmental impact of the home system from raw material acquisition, as well as processing, daily usage and final disposal would be reviewed.

In addition to the LCA literature which focused on the environmental impact of whole households in a domestic environment, novel records, chapters and reports also provided the assessment of single household ap-

pliances, including ovens, cooking hobs, boiler, dishwasher, cleaner, etc. [317, 318, 319, 320]. In this study of traditional schemes and the "all electric" schemes of households, the investigation results of separated appliances could be the parts of general schemes, when one-time emissions and continuous consumption are calculated separately. On the basis of life stage classification, appliance types or category is also classified. A bottom-up structure would be applied to approach to the final results of the system's potential impact. This effect not only concerns the environmental impact, but also economic benefits.

The energy consumption in the home with different schemes is still the dominant factor that impacts the energy efficiency and eco-friendly performance. Half of the environmental impact in a home energy management system takes place on the use stage, while most of the other half is for the assembly phase [321]. The energy consumption of communication and automation devices, however, ought to be decreased so that the home energy management system can become economically and environmentally profitable [322]. However, if a proper life cycle cost analysis is performed, it can be a beneficial and environmentally friendly solution.

7.5.2 Goal and Scope

Since both traditional and the "all electric" schemes are operated under real-time simulation, the evaluation of the home system must be a dynamic assessment. The results of life cycle assessment rely on the assumed boundaries of the case study, as well as the applied methodology for overall influence. In this section, the assessment is not focused on one specific phase of each component. Considering the integration of different components and electric appliances, the calculated results of different phases of

the components which match the unit of the domestic environment can be utilized. As this section is a comparative study of two schemes which are used as a replacement, the differences between two components which cater to the same role and function, is more important than the detailed investigation on one appliance itself. In the domestic environment, however, there is much comparative study focused on the aimed appliances. In this section, the integrated components including room heating (gas boiler VS. electric heater), hot water supply (gas heater VS. electric water heater), cooking (cooker VS. induction hob), domestic driving vehicles (fuel car VS. EV). In addition to the materials and manufacture of these components, the energy generation and distribution of the local area should be considered.

7.5.3 System Boundary

In the domestic environment, the collected components are listed and analysed in [323], while the phases of the integrated multiple components are summarized in [324]. Therefore, the life cycle phases and detailed options for each component in this research can be shown as Figure 7.5.1.

In Figure 7.5.1, this is a 'cradle to grave' work which considers the full life cycle of appliances. It is gathered into three main stages, as production, use and end of use (end-of-life). The system boundary of the LCA study should consider the resources used for appliance production, as well as the energy imported into the domestic system, such as the electricity from the national grid, and the fossil fuels supplied to this system. On the other hand, in the view of the output from the system to the outside, the waste after end-of-life should be taken into account, and the emissions also play a role.

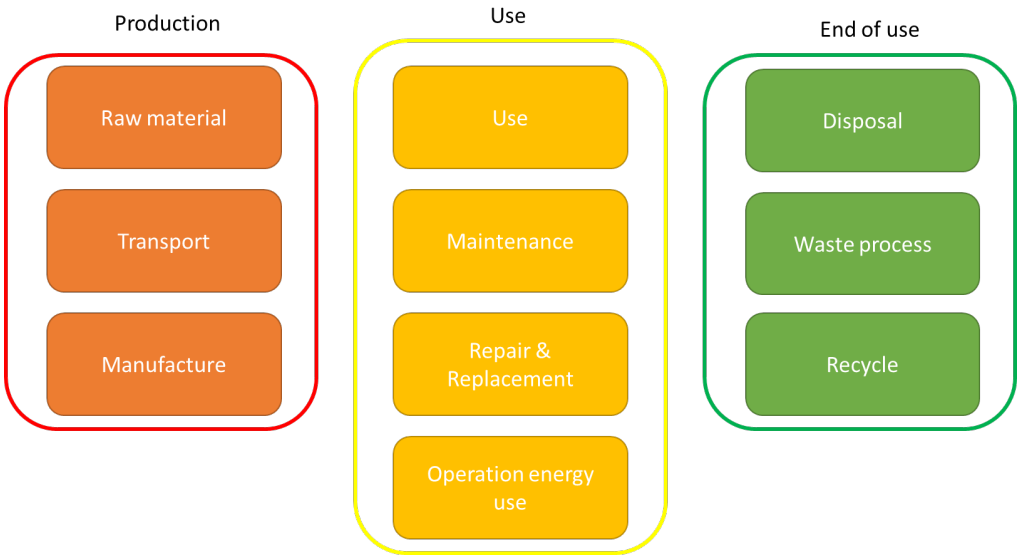


Figure 7.5.1: Phase graph of life cycle assessment of integrated energy system

For the production stage, the raw materials are the first-line thing to be considered, followed by the manufacture and transportation steps. These are all one-time calculations, as the returns and repairs are calculated elsewhere. The most important stage is the use phase in the LCA study. For the appliances in the domestic environment, not only the direct use is considered at this stage, but also the regular maintenance, as well as the possible repair is calculated at this stage in many investigations. As a meeting point of the general life cycle study and specific simulation in this research, the energy that's used by each component is the top priority. For instance, the electricity consumption of different electric appliances can be obtained from simulation, which is more specific and suitable for simulated situations, compared to the general energy consumption in the referred LCA studies. Similarly, the amount of gas consumption of a gas boiler is also obtained from the simulation, as well as the petrol and trip distance in the sub simulation of vehicles. Additionally, the energy source supplied for electricity generation changed by every year and different areas, while the global warming potential for electricity and fossil fuels would

be updated every year based on raw material changes and technological progress. Therefore, in the integral LCA study in this section, other one-time calculation stages are more reliant on referenced data, while the data on the use stage which repeatedly counts for each year, is replaced by the results which are based on the simulation in this project. The remaining last stage is the end of life, where disposal, recycle and waste process make sense. This stage is also calculated once.

7.5.4 Data Acquisition

A life cycle assessment and life cost calculation based on building information modelling are presented in [325]. In the LCA results of the general assessment, the retrofit stage and use stage is a detailed analysed, including material, transport, use, maintenance, repair, replacement and optional energy use. At the same time, the end-of-life results of boilers can be obtained from another investigation in [326], and a correction needs to be made according to the size. The results are summarized in Table 7.5.1

Table 7.5.1: LCA results of boilers of different phases (unit: kg CO_2e)

	Gas Boiler	**Electric Boiler**
Production Material & Transport	552	549
Maintenance	591	591
Repair	148	148
Replacement	1055	1647
End of Life	-19.1	5.3

In the view of cooking appliances, the traditional gas hob has a huge difference with the induction one. Hence, a comparative assessment ought to be applied. And the key focus of this section is on the climate change part. An analysis of life cycle phases of different hobs is presented in [317]. There are two scenarios in that research, being 3 times cooking per week

and 5 times cooking per week. In the cooking model in this project, a cooking behaviour model which is more in line with family data records and usage habits surveys is set up. Therefore, based on the analysis with fixed cooking times, the energy consumption due to cooking behaviour can be replaced by the unfixed cooking times from model simulation. And the key value of two scenarios with different hobs is shown in Table 7.5.2

Table 7.5.2: LCA results of hobs of different phases (unit: kg CO_2e)

	Gas Hob	**Induction Hob**
Production	60.6	95.9
Use (3 times per week)	592	894
Use (5 times per week)	986	1490
End of Life	0.109	1.33

In Table 7.5.2, three main stages are all listed, where the one-time production and end of life stages are same for different scenarios. And for two scenarios, the GHG emissions in the use stage have a huge difference. On use stage, the emissions of gas hob of scenario one is 60.04% of that of scenario two, while that of induction hob of scenario one is 60% of scenario two. This 60% is directly the ratio between the times (3/5). Therefore, compared to direct energy consumption, other factors in the use stage of cooking appliances accounts for only a negligibly small proportion. Using a simulated cooking energy consumption pattern takes the place of the corresponding data obtained in the literature.

For the life cycle assessment of vehicles, compared to fixed results of specific appliances, the related investigations more tend to acquire the results with the unit of g CO2e/km. In addition to the duplicate driving section of use stage, other stages such as manufacturing, and end of use are also related to the driving distance. Therefore, two values corresponding to distance should be emphasised. One is the distance for the whole lifespan of vehicles. The principle of engines in fuel cars and batteries in electric

vehicles are different, as internal engine always has a better maximum life trip distance than electric ones. However, 200,000 miles of car longevity is a reasonable value for both internal engine vehicles and electric vehicles [327], being 320,000 km. The other distance is the vehicle trip distance for every year, which is based on the simulation of vehicle model. For the simulation of one year period, the trip distance of domestic vehicles is 8106 km. And the relating energy consumption by electricity and petrol would be calculated separately. [328] Compared the LCA results of vehicles in different areas including China, the US, Germany and Italy, while [329] focused on the detailed stages of life cycle, as well as the difference between internal combustion engine vehicles, electric vehicles and hybrid vehicles. For the production stages, the petrol cars have a global warming potential of 83 g CO2e/km, while that value for EVs is 101. The unit here means that the value should be timed by distance and divided by 1000g/kg to have the same scale with other parts of the assessment. Moreover, for the end-of-life phase, 0.76 g CO2e/km and 0.22 g CO2e/km if for EVs and engine cars separately.

In spite of the fixed consumption on GHG emissions in both schemes, there is an annual difference due to the result of the simulation of two schemes. And this difference leads to the annual savings in GHG emissions.

7.5.5 LCA Results and Economic Benefits

Based on the simulation of two schemes and the calculation of the LCA study. For traditional scheme, the GHG emissions for those one-time stages in spite of energy consumption in use stage is 29018 kg CO2e, the GHG emissions for annual energy consumption is 2282 kg CO2e. For the "all electric" scheme, the GHG emissions for those one-time stages is 35600 kg

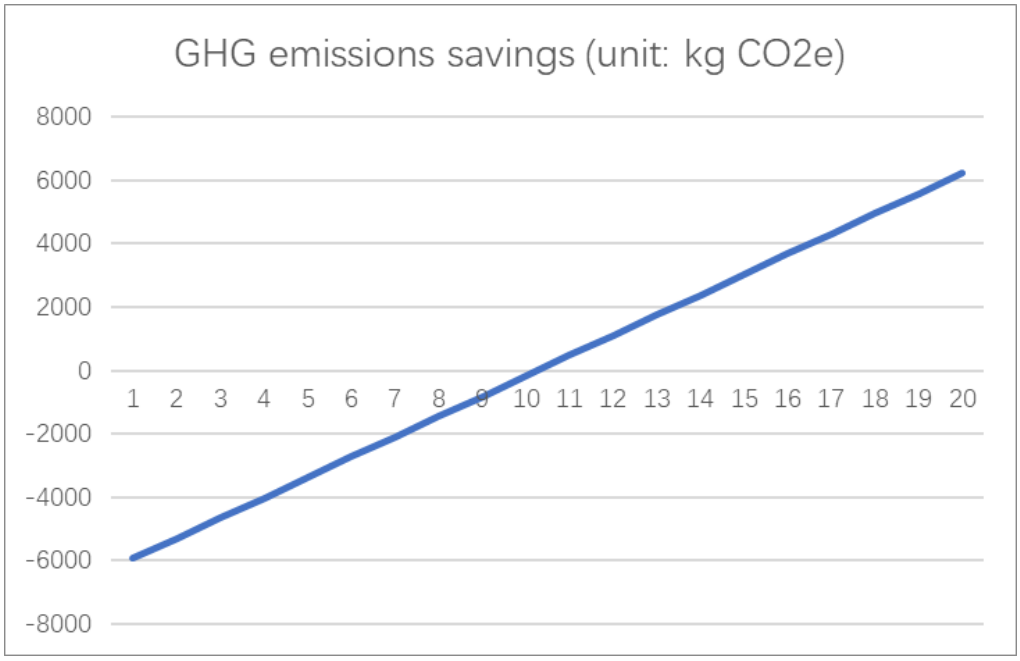


Figure 7.5.2: GHG emissions savings in 20 years by using the "all electric" scheme instead of the traditional scheme

CO2e, the GHG emissions for annual energy consumption is 1641 kg CO2e. Therefore, the total difference in the 'investment' of one-time emissions of GHG is 6582 kg CO2e (all electric scheme higher), and the annual saving in GHG emissions is 640 kg CO2e (all electric scheme lower).

For both schemes, the most dominant factor in one-time stages is the production of vehicles, followed by boilers. The production of both internal engine vehicle and electric vehicle would lead to huge GHG emissions. On the contrary, when it comes to daily energy consumption, the heating demand is the first-line thing, leading to a large amount of carbon dioxide emissions every year. This phenomenon is reasonable as vehicles have huge consumables and numerous processes, while producing heat requires a large amount of energy in daily life.

Based on the previous results, the relationship between annual saving on GHG emissions and the emission in other procedures is shown Figure 7.5.2, where using electricity heater and gas boiler are compared.

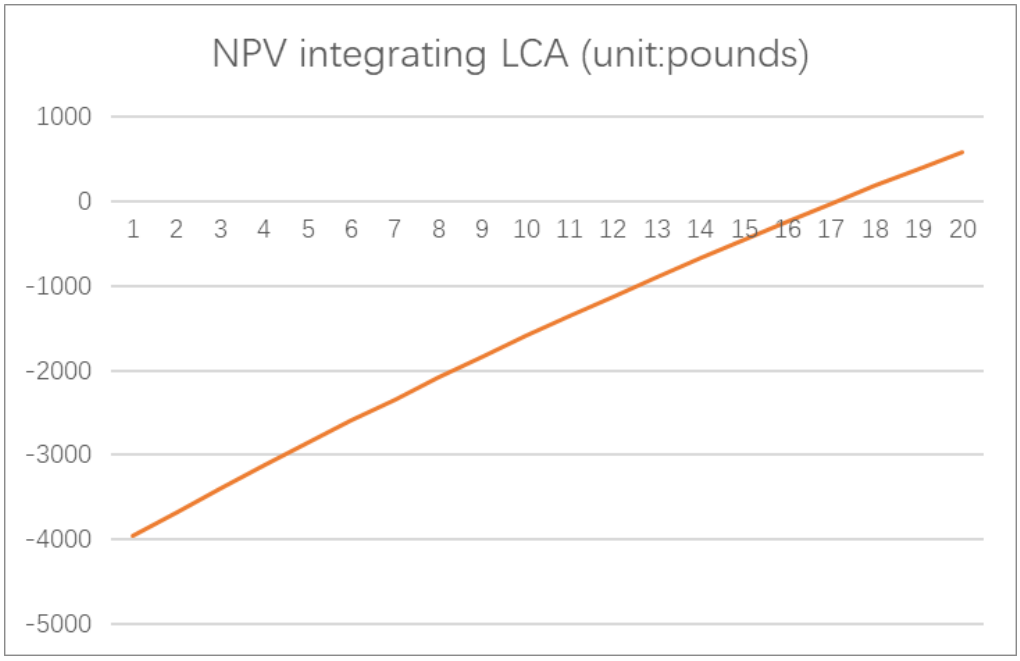


Figure 7.5.3: NPV in 20 years by using the "all electric" scheme instead of the traditional scheme considering LCA study

In Figure 7.5.2, there is a straight line instead of the curve, as the value of GHG emissions is decided when it is produced but not be reduced. In the 11th year, the GHG savings value is above 0, which means the emission of GHG due to production, maintenance and end of use can be compensated in 11 years. This is a positive sign that there is not much hidden environmental burden for the new system retrofit of the house. In the 20 years of lifespan of the domestic energy system, the total GHG saving is 6231 kg CO2e. The general saving in 20 years is about 2 times (1.94) of the GHG emissions cost of inputs.

Moreover, combined with the economic analysis of comparison of two schemes, the GHG emissions results can be quantified to the economic level, based on the principle of carbon trading. The NPV results can be shown in Figure 7.5.3.

In the Figure 7.5.3, both the investment and annual savings not only contains the economic ones as previous subsections, but also integrated the

GHG emissions lead by the life cycle of domestic appliances and the related energy consumption. After combination, the new initial annual saving is 290.2 pounds, as that of the pure economic analysis is 240.2 pounds. The GHG emissions savings occupy about 17.2% of total annual savings. In the view of general investment, the new value is 4253.5 pounds, 12% of which is results from the GHG emissions of the one-time life cycle stages.

The direct payback period is 14.7 years for the system. When inflation rate and the discount rate are taken into account, the investment from the traditional one in the "all electric" scheme can get back in the 18^{th} year, and the general NPV in 20 years is 586.9 pounds. Therefore, the "all electric" scheme of the domestic energy system can also save money, GHG emissions in addition to energy saving. As technology improves and energy prices rise, the advantages of electrification become more apparent in all these aspects.

However, comparing the NPV only based on economic investment and tariff savings with payback in 19 years, the integration of green environmental demands and the economic benefits of carbon emissions, cannot significantly improve the payback cycle. This is due to the fact that much new electrical equipment is not only costly but also does have a significant environmental impact when manufactured.

7.5.6 Conclusion of the LCA

The Life Cycle Assessment (LCA) of traditional and "all-electric" household schemes highlights critical aspects in the management of domestic energy systems:

- Manufacturing Impact: The production of vehicles and boilers emerges

as a significant source of one-time GHG emissions.

- Energy Usage: Notable yearly GHG emissions originate from heating, indicating a need for adept energy management.
- "All-electric" Scheme: While initially contributing higher GHG emissions, this scheme eventually offers an annual reduction in GHG emissions over a certain period.
- Technological Evolution: Advancements and changes in energy prices accentuate the merits of electrification in domestic environments.
- Environmental and Economic Intersection: Merging ecological demands and economic gains from carbon emission savings does not markedly quicken the payback period.
- Longevity Considerations: Over a 20-year framework, net GHG savings are achievable, recognizing that major emissions occur during the production and disposal phases of appliances.

In general, strategies aimed at optimizing domestic energy systems should intertwine technological, economic, and environmental considerations, propelling further research and adaption of alternative solutions for a sustainable future in household energy management.

7.6 Analysis and Comparison of Different Domestic Heating System

7.6.1 Introduction

Electric heating studies often compare various systems to understand their cost and environmental impacts better. Specifically, using new electric heating methods has shown to save on fuel and environmental costs, making a real-world economic difference [1]. The gradual shift towards electrification of household heating systems has triggered a clear shift in energy use patterns, opening the way for various technological interventions to sustainably meet heating needs. In particular, previous sections examine in detail the economic and environmental impacts of "all-electric" options featuring electric heaters. While electric heaters stand out for their simplicity of installation and operation, exploring alternative technologies within the same electrification scenario is crucial to fully understand the available options and their multifaceted implications. This section seeks to delve into a comparative analysis between two prevalent electric heating methods utilized in home electrification schemes: the electric heater and the Ground Source Heat Pump (GSHP).

Research that looks at the whole life of heating systems tries to understand their energy use and pollution [288]. For instance, gas boiler heating is seen as a particularly clean method, aligning well with primary energy sources. However, there are some concern about NO_x in urban areas. At the same time, heat pumps and combined heating and power generation stand out for their high energy efficiency.

The proposed model provides the ability to compare the energy consump-

tion of gas boilers, electric heaters, and GSHPs through distinct simulations based on the operation of a thermal model for the domestic environment. An "all electric" scheme simulation is employed to analyse the economic cost and GHG emissions changing from these heating systems in this section, and the GSHP is supposed to be used instead of electric heating for domestic electrification. Key parameters such as investment costs, energy prices, and the GWP of energy sources are investigated to afford a multi-faceted understanding of the economic and environmental implications of employing these heating methods in domestic settings.

7.6.2 Methodology

In this chapter, based on the operation of thermal model for the domestic environment, the energy consumed based on gas boiler, electrical heater and GSHP would be simulated individually. Moreover, based on the energy consumption, the economic cost as well as GHG emissions would be compared.

The energy balance of domestic heating was proposed in previous sections. At the same time, there is a comprehensive simulation model for electric heater with hysteresis control, while the model of GSHP was also proposed. Based on these methods, the models can simulate for operation for the entire year, obtaining the corresponding energy consumption of different appliances. Moreover, the energy consumption of gas for room heating can be also estimated, based on heat demand (Q_{demand}) of domestic environment and efficiency of gas heating.

$$Q_{\text{gas}} = \frac{Q_{\text{demand}}}{\eta_{\text{gas}}} \tag{7.6.1}$$

Where η_{gas} is the efficiency of gas heating in the domestic environment, which is about 70%. The result is the energy consumption when the room is heated based on gas central heating.

Additionally, the investment and operation cost of heating system, as well as NPV could be calculated as shown in the previous sections.

Understanding the costs associated with various heating methods, as well as their environmental impacts, is crucial for making informed decisions. The following table outlines the investment costs of different heating systems, the prices of electricity and gas, and the Global Warming Potential (GWP) of these energy sources. In order to analysis the economic benefit and environmental impact of various heating systems, the corresponding cost and global warming potential (GWP) are summarized in Table 7.6.1 .

Table 7.6.1: Supplement costs and GWP of different domestic heating methods

Parameter	**Value**	**Source**
Investment of GSHP (£)	18000	[291]
Total GWP (CO_2e)	2260	[330]

For instance, as can be seen in the table, the initial investment for a GSHP is significantly higher than other methods, however, its long-term efficiencies and benefits might offset this initial cost. Similarly, while the price of electricity per kWh is higher than gas, its GWP is also slightly higher, indicating its greater environmental impact. Global Warming Potential (GWP) is the amount of heat absorbed by any greenhouse gas in the atmosphere and is a multiple of the amount of heat absorbed by the same mass of carbon dioxide (CO_2). CO_2 has a GWP of 1.

7.6.3 Comparative Results of Energy System with Different Heating Appliances

In the simulation, the GSHP demonstrates a remarkable ability to generate a heat output of 1475 kWh while only consuming 391 kWh of electrical energy. This translates to a Coefficient of Performance (COP) of approximately 3.77, implying that for every unit of electricity consumed, about 3.77 units of heat are produced. This value is high for a GSHP and may be influenced by the assumption of an absolutely isolated underground system, as well as the dominant heat demand in cold seasons. Such a high COP not only indicates impressive energy efficiency but also underscores the potential for significant energy savings and reduced GHG emissions in the long term.

Examining the energy consumption between an electric heater and a GSHP under different tariff scenarios provides noteworthy findings. Figure 7.6.1 illustrates an annual simulation of energy consumption across varied tariff bands along with respective export values.

The electric heater exhibits higher energy consumption across all tariff bands, which could result in escalated operational costs, particularly during periods of high tariffs. Conversely, the GSHP, while demonstrating reduced energy usage, also exports more energy back to the grid, which might be financially beneficial depending on grid feedback incentives.

From an environmental perspective, the GSHP, which consistently utilizes less energy across all tariff bands, might be considered the eco-friendlier option. However, a holistic analysis should also factor in the source of electricity and operational efficiency of the GSHP under various external conditions.

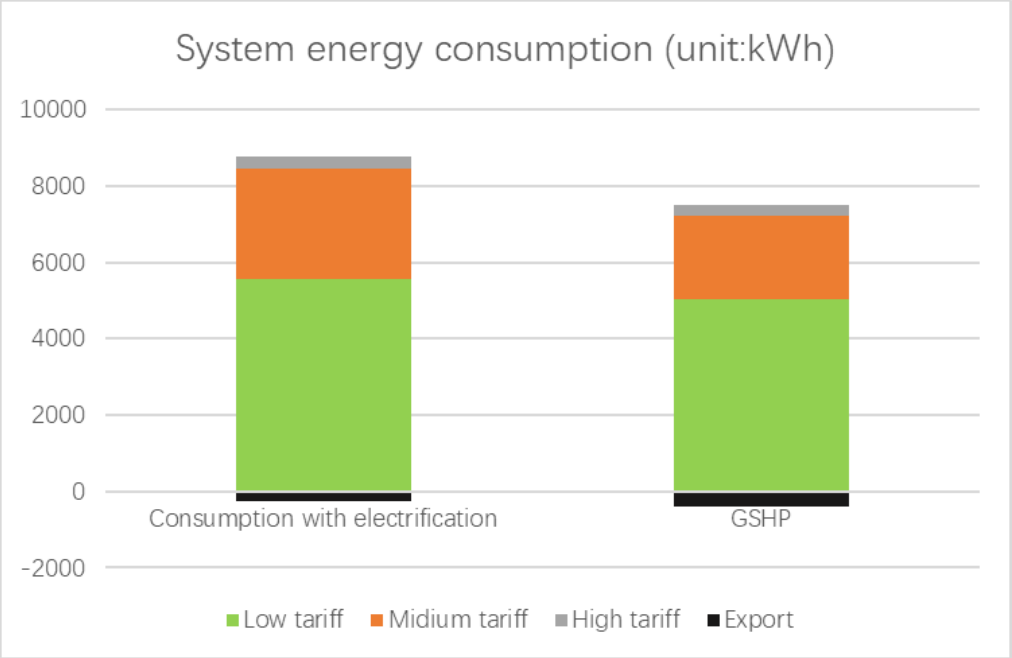


Figure 7.6.1: Annual Energy Consumption (kWh)

While the GSHP seemingly offers advantages in terms of reduced energy usage, the larger export values from the electric heater introduce a nuanced aspect of this comparison. With technological advancements and an increasing emphasis on renewables within domestic heating, continuous analyses are imperative to navigate the evolving landscape of energy markets.

The GSHP yields an annual saving of £384.47, while the electric heater provides a saving of £240.24. This indicates that the GSHP is more economical in terms of operational costs on an annual basis. The GSHP, therefore, provides an additional annual saving of £144.23 over the heater. The GSHP appears to be the more environmentally friendly option, offering a GWP saving of 911.18 kgCO2e, as opposed to the 640.71 kgCO2e saved by the heater. This indicates that the GSHP prevents an additional 270.47 kgCO2e from being emitted into the atmosphere annually, compared to the heater.

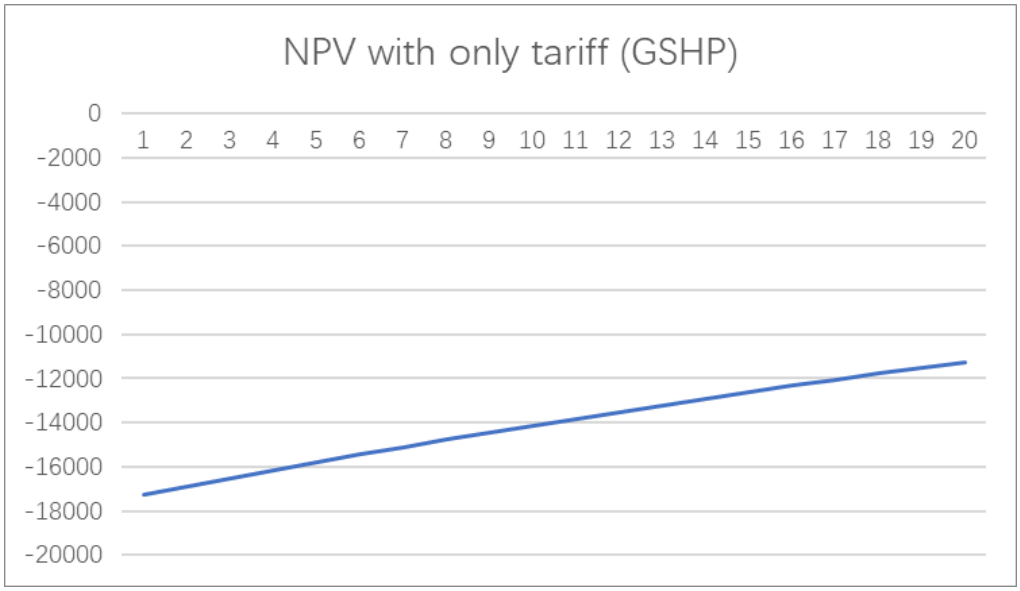


Figure 7.6.2: The NPV value of using GSHP in "all electric" scheme in twenty years (unit:£)

Analysing the NPV, considering an inflation rate (r) of 0.02, provides a detailed perspective on the economic viability of implementing the GSHP system over a 20-year period. The results are shown in Figure 7.6.2.

In Figure 7.6.2, the significant initial investment required for the GSHP system is observable through the initial negative NPV of £17,650, indicating a substantial upfront cost. Over the 20-year period, the NPV moves towards a less negative value, but does not reach a positive value within this analysed timeframe, highlighting a slow financial recuperation from the initial investment. Given the GSHP's ability to provide year-round water supply and the underground loop system's lifespan exceeding 50 years, a longer-term economic analysis may present varied insights.

Figure 7.6.3 shows the 20-year NPV of the Global Warming Potential for the GSHP. The graph starts with negative values and moves to positive ones, indicating a change from initial carbon costs to long-term savings. The GSHP begins with a high GWP, likely due to the energy and emissions from making and setting up the system. Each year, the GSHP reduces its

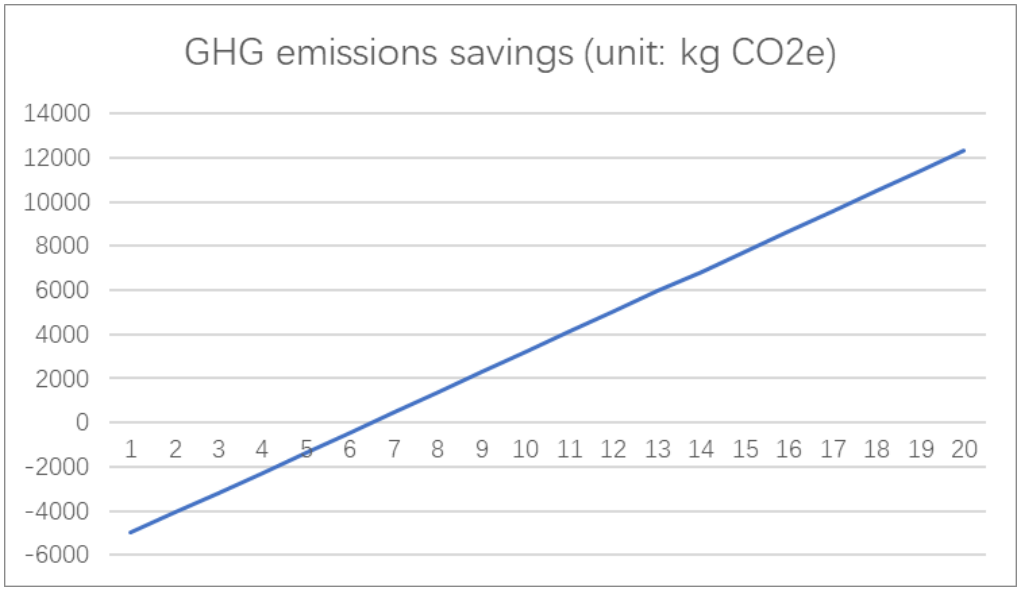


Figure 7.6.3: 20-year Net Present Value (NPV) of the GWP for the GSHP in "all electric" scheme

GWP, meaning it uses less energy and causes fewer emissions as it runs. In only 6 years, the GSHP can lower its total GWP. This means that even though it starts with high emissions, it can make up for this over time.

The general NPV which considers the carbon trade market based on the LCA is shown in Figure 7.6.4.

Figure 7.6.4 represents the trajectory of the comprehensive NPV for the GSHP system over a span of 20 years. Negative values represent net costs, while positive values indicate net savings or gains. The initial investment in GSHP is represented as an initial negative spike in NPV, which gradually rises over time due to operational cost and carbon emission savings. The GSHP demands a substantial initial investment, reflected as an initial negative value in the NPV. However, lower energy consumption and reduced carbon emissions during operation manifest as long-term gains. The negative NPV indicates it cannot be paid back in only 20 years when applying GSHP in the case of the "all electric" scheme.

The evident economic barrier presented by the GSHP, as indicated by the

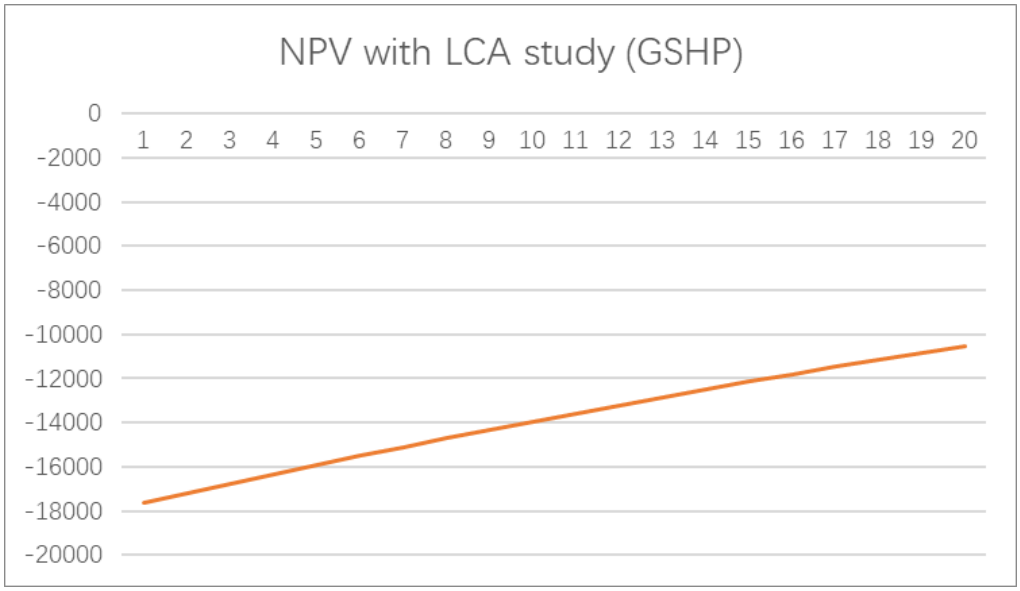


Figure 7.6.4: The NPV value of using GSHP in "all electric" scheme in twenty years with LCA study (unit: £)

NPV, presents its limitation about its accessibility and immediate applicability to all domestic environments. While the GSHP leads in annual GWP savings, the initial carbon cost (emerging from its manufacturing and installation) decreases its immediate environmental efficacy. The electric heater, presumably with a lower initial carbon cost, offers a more immediate, although smaller, positive impact. Even though the GSHP has a remarkable COP of 3.77, its implications, particularly concerning its installation, maintenance, and long-term economic return, remain discussion points. On the contrary, the electric heater, despite its lower operational efficiency, presents fewer technological and logistical barriers to implementation and maintenance.

7.6.4 Conclusion

The comparison between the GSHP and the electric heater shows a challenging decision-making situation, where both short-term and long-term economic and environmental factors need to be considered.

The GSHP, with its strong energy and GWP savings, stands out as a promising option for future home heating, aligning well with worldwide sustainability goals. However, the large initial cost and the long time needed to see its economic and environmental benefits require a careful and context-dependent adoption approach.

On the other hand, the electric heater comes forward as a practical and immediately helpful choice, both in terms of economics and the environment, even though its impacts are not as strong as the GSHP. Its clear and easy-to-see the benefits, both in cost savings and GWP reductions, highlight it as a reasonable and responsible option, especially where immediate economic factors are key.

In conclusion, it is clear that while the GSHP holds a lot of potential for future home heating solutions, the electric heater provides a practical and useful alternative right now, offering noticeable economic and environmental benefits without needing a big initial investment. Also, the assertion of economic benefits is critically dependent on electricity costs.

Looking ahead, a balanced approach that recognizes the immediate effectiveness of electric heaters while also strategically adding GSHPs—possibly through policy changes, subsidies, and new financing methods—could create a path towards sustainable, economically sound, and environmentally friendly home heating. This method ensures the quick realization of economic and environmental benefits while gradually making use of the broad potential of GSHPs in future home energy situations.

7.7 Applying Community Strategies Based on the Proposed Home Energy Management Models

7.7.1 Introduction

In the modern era, energy management at a community level has evolved to become an intricate system, leveraging advanced technologies and strategies to optimize energy use, reduce costs, and minimize environmental impacts. The method addressed in this section offers a comprehensive approach to applying community management strategies grounded in integrated home energy models, focusing particularly on the incorporation of battery storage and Photovoltaic (PV) system features.

Beginning with a simulation setup and a system model rooted in preceding research, this methodological framework employs an integrated home energy model that cohesively amalgamates features of battery storage and PV systems. The model enables a thorough assessment of the household energy needs and output, considering real-world specifications and performance predictions across varied conditions. This approach enables a nuanced consideration of household features and a strategic integration of a household energy management algorithm, which systematically optimizes energy usage while factoring in grid electricity prices and the technical constraints of devices.

The foundation of the approach is to ensure that every household energy needs are addressed. Each household, using its specific energy strategy, evaluates its energy demands, considering storage capabilities and potential renewable energy outputs. This framework then leads to the next phase:

energy sharing at the community level. Energy transactions, central to this strategy, rely on a set of complex decisions. These decisions are based not only on the current energy situation but also on future projections. Moving beyond a static approach, the community energy sharing method is dynamic and operates in defined time intervals. At each time interval, an energy management simulation runs for every household. After this analysis, once a household's energy balance is clear, the process moves to the next phase. This involves coordinating energy pairing and transactions, leading to inter-household energy exchanges.

The intricate economic models in place—including the Time of Use (TOU) model for electricity pricing and detailed economic analyses considering net present value (NPV) —provide a robust framework for ensuring the financial viability and profitability of the implemented energy management strategies. The practical applicability of the strategy is demonstrated through a detailed case study, focusing on UK-based residential houses, which are adeptly equipped with PV generation systems and a battery energy storage system. This case study navigates through various electricity tariff schemes, including the Time of Use (TOU) and fixed feed-in tariff schemes, providing a pragmatic view of the strategy's operation in a real-world context.

Through a detailed four-step approach, the method navigates through community-wide PV and battery sizing, distributing savings and NPV among households, individual household sizing, and a comparative analysis of distributed and individual sizing strategies. Each step is designed to ensure that both the community and individual households are accorded optimal PV and battery system sizes, ensuring a balanced and equitable distribution of energy and economic benefits across the board.

7.7.2 Method of Applying Community Management Strategies Based on Home Energy Models

7.7.2.1 Simulation Setup and System Model

An integrated home energy model from prior research serves as the foundation for this investigation. This model combines battery storage and PV system features, providing a framework to assess household energy needs and output.

Both the battery and photovoltaic systems are simulated based on real-world specifications. Performance predictions use device parameters and typical usage patterns across varied conditions. Various household features, such as the number of residents and living space, are considered. These parameters are essential for estimating PV output and load demands, which influence battery storage usage and interactions with the grid.

Furthermore, a household energy management algorithm from earlier research has been integrated. This algorithm optimizes household energy use, taking into account grid electricity prices and the technical constraints of household devices.

Electricity pricing adopts the Time of Use (TOU) model, segmented into low, medium, and high periods, which is mentioned in the life cost calculation in previous sections. This structure incorporates both grid electricity selling prices and intra-community transaction prices. The model assumes no energy losses during inter-household trades. This encompasses the notion that energy remains constant during exchanges, with no price deductions, and potential effects of distance on trades aren't considered.

The year-long simulation includes 20 households engaged in energy ex-

changes based on the proposed integration model in this project. The corresponding household parameters including size and number of inhabitants are automatically obtained based on the probability distribution, as mentioned in the section of model integration. The simulation updates decisions and data in one-minute intervals. All systems, such as energy management, battery storage, and PV, respond immediately to energy demands or trade requests.

For evaluation, several key metrics have been identified. The electricity cost-saving rate gauges financial benefits against a baseline. The self-sufficiency rate measures the community's reliance on its generated and stored energy, excluding external grid use. For each household, there are several equations to present the energy in home system and the corresponding cost.

$$PG_{\text{import}}(t) - PG_{\text{export}}(t) + P_{\text{BESS}}(t) = P_{\text{load}}(t) - P_{\text{PV_gen}}(t) \qquad (7.7.1)$$

The equation illustrates the power flow dynamics within the system, where $PG_{import}(t)$, $PG_{export}(t)$, $P_{load}(t)$ denote the power imported from the main electricity grid, exported to the main electricity grid, the demand of the home load energy during time interval t (in kW), $P_{PV_gen}(t)$ represents the electrical power generated by the PV system installed at the residence during time interval t (in kW), and $P_{BESS}(t)$represents the net electrical power discharged or charged by the battery energy storage system (BESS) during time interval t (in kW).

The simplified model utilized for the BESS in this research is expressed as:

$$E(t) = E(t-1) - \frac{\Delta T \times P_{\text{bat disch}}(t)}{\eta_d \times \eta_{\text{Conv}}} - \Delta T \times \eta_c \times \eta_{\text{Conv}} \times P_{\text{bat charge}} \quad (7.7.2)$$

$$SOC(t) = \frac{E(t)}{C_B} \quad (7.7.3)$$

The power discharged by the battery during time interval t is denoted as $P_{bat\ disch}(t)$, and $P_{bat\ charge}(t)$ are measured in kilowatts (kW). They represents the electrical power released from the battery to meet the system's demand and the power charged by the battery during time Additionally, the energy stored in the battery at time intervals t and t-1 is represented by $E(t)$ and $E(t-1)$, respectively, and is measured in kilowatt-hours (kWh). To account for the efficiency of the battery system, η_d and η_c are used to represent the discharging and charging efficiencies, respectively.

The state of charge (SOC) of the battery at time interval t is denoted by $SOC(t)$. Binary constraints Equation 7.7.4 to Equation 7.7.6 are included to prevent simultaneous charging and discharging of the battery energy storage system.

$$0 \leq P_{\text{bat disch}}(t) \leq \phi(t) \times P_{\text{BESS}}^{\text{rated}} \quad (7.7.4)$$

$$0 \leq P_{\text{bat charge}} \leq (1 - \phi(t)) \times P_{\text{BESS}}^{\text{rated}} \quad (7.7.5)$$

$$\phi(t) = \begin{cases} 1 & \text{if discharge} \\ 0 & \text{if charge} \end{cases} \quad (7.7.6)$$

where $\phi(t)$ is a binary variable.

Constraint represents the maximum power limit for charging or discharging sets an upper bound on the electrical power that can be charged or discharged from the battery energy storage system (BESS) at time interval t.

$$-P_{\text{BESS max}} \leq P_{\text{BESS}}(t) \leq P_{\text{BESS max}} \tag{7.7.7}$$

Constraint establishes the upper and lower limits of the state of charge of the battery energy storage system.

$$SOC_{\min} \leq SOC(t) \leq SOC_{\max} \tag{7.7.8}$$

where $SOC_{\max}$ and $SOC_{\min}$ represent the upper and lower limits, respectively, for the state of charge of the battery energy storage system in percentage (%).

Incorporating the PV system investment cost into the economic analysis is pivotal for a comprehensive assessment. The capital cost and operational cost of the PV system, coupled with the Battery Energy Storage System (BESS), from the total investment and operational costs.

$$\begin{aligned} C_{\text{investment}} = \Big(& IC_{\text{energy}} \times C_B \\ & + IC_{\text{power}} \times P_{\text{BESS}}^{\text{rated}} \\ & + C_{\text{Installation, BESS}} \Big) \\ & + \Big(IC_{\text{PV}} \times A_{\text{PV}} \\ & + C_{\text{Installation, PV}} \Big) \end{aligned} \tag{7.7.9}$$

Where:

IC_{PV} represents the investment cost per unit area of the PV system (£/m^2). A_{PV} denotes the area of the PV panels (m^2).

$C_{\text{Installation, PV}}$ and $C_{\text{Installation, BESS}}$ are the installation costs for the PV system and BESS, respectively.

The operational cost now encapsulates the costs related to both the PV system and the BESS:

$$\begin{aligned} C_{\text{operation}} = \sum_{\text{day 1}}^{\text{day 365}} \Big[& F_{\text{buy}}(t) \times \Delta T \times PG_{\text{import}}(t) \\ & - F_{\text{sell}}(t) \times \Delta T \times PG_{\text{export}}(t) \Big] \\ & + C_{\text{O\&M, PV}} + C_{\text{O\&M, BESS}} \end{aligned} \tag{7.7.10}$$

Where $C_{\text{O\&M, PV}}$ and $C_{\text{O\&M, BESS}}$ are the annual operation and maintenance costs for the PV system and BESS, respectively.

The total cost, considering the lifespan of the system, integrates the investment and annual operational costs, factoring in an inflation rate:

$$\text{Total cost} = C_{\text{investment}} + \sum_{i=1}^{\text{years}} C_{\text{operation}} \times (1+r)^i \tag{7.7.11}$$

7.7.2.2 Community Level Energy Pairing Strategies

The energy management strategy is a two-tiered system. A energy pairing strategy can balance community-wide considerations with individual microgrid/household management for effective overall operation [331, 332]. The

flow chart of the main objectives in the algorithm is shown in Figure 7.7.1

.

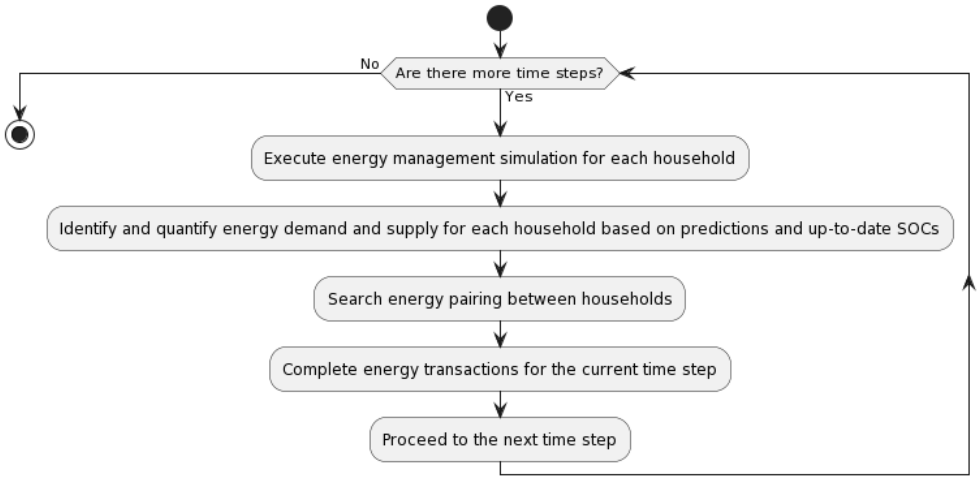


Figure 7.7.1: Flow chart of algorithms for pairing energy supply in community scale

For individual households, the energy management system activates at the beginning of each time step. This system determines each household's energy needs and potential contributions. The system considers factors like energy consumption patterns, potential renewable energy generation (e.g., solar panels), and battery storage status. Each household's unique economic and energy priorities influence these calculations.

After assessing household energy dynamics, the strategy then focuses on the entire community. The strategy aggregates predicted energy surpluses or deficits from all households after individual simulations, giving a comprehensive view of the community's energy dynamics for that time step.

Having a comprehensive understanding of the community's energy landscape, the strategy enters the energy pairing phase. Households with expected energy surpluses are paired with those anticipated to have deficits. This pairing mechanism is essential as it facilitates the efficient distribution of energy within the community, potentially reducing dependency on

external grids. The detailed pairing strategy and constraints is presented in the following context.

Once pairings are finalized, the process naturally progresses to the execution of energy transactions between matched households. These transactions are bound by several constraints, such as limits on battery storage, power system capacities, and real-time energy production and consumption rates. The goal is to complete each transaction within its time step, ensuring real-time energy balance in the community.

The entire process, from individual simulations to community transactions, repeats for each time step during the simulation. This iterative method allows energy management to adapt and respond to changing energy patterns and needs throughout the day.

The energy pairing strategy at the community level begins by delving into the energy status of each household.

A thorough examination of the energy needs of each household is initiated. By scrutinizing both historical and real-time data, the current and anticipated load requirements of each household are delineated. This involves an analytical process where the energy consumption patterns of households or buildings are studied, followed by forecasting any potential future variations.

Parallelly, the storage status of each household is assessed. This involves examining the battery storage capacity, its current charge state, and its discharge and charging capabilities. With this information, it becomes clear which households can provide energy to others in the short term and which ones might be in need of additional energy.

Lastly, the renewable energy output of each household is assessed. The

real-time and expected outputs of photovoltaic and other renewable energy systems within each household are analysed. This assessment aids in predicting which households might be in a position to generate and provide additional electricity in the upcoming time periods.

In the proposed energy pairing strategy, a deep understanding of the energy status of each household is crucial. This begins by analysing the predicted future energy demand of every household or household i. Defined as $E_{\text{prediction},i}$, it is calculated using the formula:

$$E_{\text{prediction},i} = \sum_{t=1}^{T} (L_{t,i} - R_{t,i}) \tag{7.7.12}$$

Where $L_{t,i}$ is the load demand at time t and $R_{t,i}$ Represents the photovoltaic output at that moment. Essentially, this equation captures the cumulative difference between the household's anticipated load and photovoltaic output throughout the day.

Moving on to battery operations, the state of charge (SOC) plays a pivotal role. For any battery i, its SOC, SOC, has to be within certain boundaries:

$$SOC_{\min} \leq SOC_i \leq SOC_{\max} \tag{7.7.13}$$

Here, $SOC_{\min}$ represents the minimum permissible state of charge, often zero but occasionally a non-zero value, depending on the battery type and manufacturer's guidelines. Conversely, $SOC_{\max}$ denotes the battery's maximum storage capacity.

Furthermore, when considering energy exchanges involving batteries, it is essential to understand the power rate limitations. For a given home bat-

tery i, its exchange power P_i Is subject to specific constraints:

$$-P_{\text{discharge,max}} \leq P_i \leq P_{\text{charge,max}} \tag{7.7.14}$$

With $P_{\text{discharge, max}}$ being the maximum power at which the battery can discharge and $P_{\text{charge, max}}$ Representing the maximum charging power. It is worth noting that while negative values suggest the battery is discharged, positive values indicate it is charging.

To optimize the energy sharing process, the pairing strategy is formulated to maximize the utilization of extra energy in each household. Initially, based on the identified energy demands, households are ranked in descending order of their energy needs, enabling prioritization of those with the most pressing requirements. Concurrently, the households are sorted in terms of the volume of energy they can provide, ensuring those with abundant supply are readily identified.

Pairing begins by establishing links between the household with the highest energy demand and the one capable of supplying the most energy. Throughout this pairing, it is vital to factor in the specific energy needs and supplies of each household, as well as any potential energy exchange constraints.

The essence of this pairing search lies in matching homes with the highest energy demands to those with abundant supplies. The main objective is to enhance the efficiency of energy sharing within the community. To structure this process, several equations and constraints are considered:

For a given household i, its energy demand D_i Is described by:

$$D_i = \max\left(E_{\text{prediction},i}, 0\right) \tag{7.7.15}$$

This representation focuses solely on positive demand, indicating the energy a household seeks to acquire from others.

Meanwhile, the energy supply S_i Of the household is:

$$S_i = \max\left(-E_{\text{prediction},i}, 0\right) \tag{7.7.16}$$

Here, the only positive supply is considered, representing the energy a household can offer to others.

When pairing household i with j, the energy exchanged should not exceed the demand or supply of either. Therefore:

$$E_{ij} \leq \min\left(D_i, S_j\right) \tag{7.7.17}$$

Additionally, this exchanged energy is bound by the battery's exchange power and state constraints.

Regarding the battery's exchange power, for a battery i, the exchanged power P_{ij} Adheres to:

$$-P_{\text{discharge,max},i} \leq P_{ij} \leq P_{\text{charge,max},i} \tag{7.7.18}$$

The change in the state of battery i, denoted ΔSOC_i, is given by:

$$\Delta SOC_i = \int P_{ij}\, dt \tag{7.7.19}$$

Where $\int P_{ij}\, dt$ Encapsulates the total energy over the exchange duration.

Finally, post-exchange, the SOC of battery i must remain within its bounds:

$$SOC_{\min} \leq SOC_i + \Delta SOC_i \leq SOC_{\max} \tag{7.7.20}$$

These equations and constraints provide a mathematical framework for the pairing search, ensuring maximized energy sharing efficiency within the community while adhering to various constraints.

In the settlement execution stage, the primary focus is the actual implementation of the energy exchange determined from the previous pairing phase. The goal is to ensure that the quantities of energy being exchanged adhere to the pre-established constraints. Furthermore, it is imperative that all participating households maintain a safe and efficient operation range throughout the entire exchange process.

For any two households, denoted as i and j, the actual energy exchange $E_{\text{actual},ij}$ is influenced by the previously determined E_{ij} And the constraints of energy demand and supply for the households:

$$E_{\text{actual},ij} = \min\left(E_{ij}, D_i, S_j\right) \tag{7.7.21}$$

As energy is exchanged, the state of charge (SOC) of the battery into household i is updated based on the actual exchanged energy, represented as:

$$\Delta SOC_{\text{actual},i} = \int P_{\text{actual},ij}\, dt \tag{7.7.22}$$

Subsequently, the actual energy demand and supply for each household are updated to reflect the energy exchange. Specifically, the energy demand

for household i becomes:

$$D_{\text{actual},i} = D_i - E_{\text{actual},ij} \tag{7.7.23}$$

And the energy supply for household j adjusts to:

$$S_{\text{actual},j} = S_j - E_{\text{actual},ij} \tag{7.7.24}$$

This approach ensures that during the entirety of the exchange, all batteries and household systems operate within their safe and efficient boundaries, satisfying all physical and technical constraints.

7.7.2.3 Case Study of Households

This subsection aims to apply the energy management strategy in a practical context, focusing on UK-based residential houses. These dwellings are equipped with a PV generation system and a battery energy storage system, providing a robust foundation for implementing the energy management strategy. Simultaneously, its connection to the main electricity grid facilitates additional energy imports when the PV system falls short, and allows the export of surplus PV energy back to the grid.

Two specific schemes are taken into account in the research regarding electricity tariff schemes. Firstly, there is the Time of Use (TOU) tariff scheme, which determines the cost of purchasing electric energy from the utility. Secondly, there is a fixed feed-in tariff scheme, which determines the revenue obtained from exporting electricity to the main grid. Table 7.7.1 is used in the research to provide tariff values for purchased electricity for the TOU tariff scheme. These values are sourced from the Green Energy

Company in the UK [194]. The research employs a value of 5.24 pence per kWh for the fixed feed-in tariff scheme. This value is obtained from an up-to-date website that provides information on feed-in tariffs in the UK [195].

Table 7.7.1: Unit cost values for TOU purchasing tariff scheme at each time period.

Time (h)	**Tariff**	**Unit cost (pence/kWh)**
23:00 to 06:00	Off-peak	7.5
06:00 to 16:00	Mid-peak	16.44
16:00 to 19:00	Peak	32.55
19:00 to 23:00	Mid-peak	16.44

After the simulation, an in-depth economic analysis is carried out. This analysis took into account the simulation results, as well as other important parameters like system specifications and tariff values. The specific system parameters and tariff values utilized in the simulation can be found in Table 7.7.2, sourced from reputable references [196, 197, 333, 198]. A comprehensive understanding of the optimal BESS and PV size and its economic viability was achieved by taking into account these factors.

Table 7.7.2: System parameters of case study

Parameter	**Value**
IC_{energy}	£135 /kWh
IC_{power}	£95 /kW
Battery Capacity C_B	13.5 kWh
Battery power limitation P_{BESS}^{Rated}	5 kW
IC_{PV} (PV system with 10 solar panels)	£5,000 (£250 per m^2)
PV system peak power	3.5 kWp (1.75 kWp/m^2)
PV system area A_{PV}	20 m^2
$SOC_{\min}$ - $SOC_{\max}$	20% - 90%
Converter efficiency η_{Conv}	98%
Battery charging & discharging efficiency (η_d, η_c)	90%
Inflation rate	2%

The value of cash flow over various periods can be assessed through the net present value (NPV), which takes into account the time interval and discount rate. It quantifies the equivalent interest value that would have

been earned if the same amount of money had been invested in more conventional investment accounts.

$$NPV = \sum_{Yr=1}^{Yr} \frac{Cash_{Yr}}{(1\ +\ r\ )^{Yr}} - Cash_0 \tag{7.7.25}$$

In Equation 7.7.25, the NPV is calculated by summing the net cash inflows $Cash_{Yr}$ for each period (Yr) and discounting them using the factor of $(1\ +\ r\ )^{Yr}$. The discount rate is set as 2% for the home system [199]. The resulting sum is then reduced by the initial investment cost ($Cash_0$).

Assessing profitability is done through the internal rate of return (IRR), which is the anticipated rate of return on the investment in future years. The discount rate at which the present value of future cash flows matches the initial investment is what determines it. A higher IRR value signifies a more favourable return on investment.

$$IRR = a + \left[\frac{NPV_a}{NPV_a - NPV_b}\ (b - a)\right] \tag{7.7.26}$$

Equation 7.7.26 outlines the calculation of the IRR. It involves determining the discount rate (a) at which the NPV is positive and (b) at which the NPV is negative. The IRR is then calculated as the value of a plus the ratio of NPV at a rate to the difference between NPV at rates a and b, multiplied by the difference between rates b and a.

The financial viability and profitability of the investment can be assessed by analysing the NPV and IRR. The long-term economic prospects of the investment are provided with valuable insights by these metrics.

7.7.2.4 Community & Households Sizing

Step 1: Community-wide PV and Battery Sizing

The starting point involves determining the optimal sizes for PV and battery systems for the entire community, treating it as a single entity. Here, an optimization model, which seeks to maximize the Net Present Value (NPV), is employed considering all households' cumulative energy demands and potential PV outputs. The combination of 20 households can be treated as a giant whole to run battery control algorithms and sizing, design, which power profiles are summed up.

Step 2: Distributing Savings and NPV Among Households

In the context of this step, it is pivotal to articulate the rationale behind the formulas used to compute each household's savings and NPV share. The formulas:

$$\text{NPV}_i = \left(\frac{E_i}{E_T}\right) \times \text{Total NPV} \tag{7.7.27}$$

Here, E_i represents the annual energy consumption of household i, and E_T is the cumulative energy consumption of the entire community. Their ratio thus symbolizes the proportion of the total community energy consumed by household i. It serves as a representative metric to distribute the total savings and investment of the community to each household fairly, aligning with their respective energy usages. Therefore, the division of total NPV based on an energy ratio make sense.

In simpler terms, if a household is responsible for a larger portion of the community's total energy consumption, it will accordingly receive a larger share of the total investment and savings. This approach ensures that households contributing more towards energy consumption (and poten-

tially, towards the overall community energy strategy) bear greater costs and incentives, thereby maintaining a fair and balanced incentive system across the community.

Step 3: Sizing and Simulation for Each Household

The third step is dedicated to individualized sizing the PV and battery systems for each household. The same optimization model from Step 1 is utilized but adapted to the specific energy demands and potential PV outputs of each household. Furthermore, a simulation involving pairing and energy transaction algorithms is run to calculate the NPV and savings for each household, considering internal energy transactions.

Step 4: Comparative Analysis of Distributed and Individual Sizing Strategies

In the final step, a comprehensive comparative analysis between the results from Step 2 and Step 3 is performed. The aim here is to evaluate the efficacy and efficiency of the community-wide sizing strategy against the individually tailored strategies for each household. Metrics such as total NPV, total savings, and individual household costs under both scenarios are analysed to discern the most economically viable and energy-efficient approach. The differences in outcomes under these two strategies are meticulously analysed to derive insights into how energy and economic benefits are distributed across the community under each scenario. This step is crucial to ascertain the pragmatic applicability and advantages of adopting a unified community energy strategy as opposed to individualized household strategies, thereby informing policy and decision-making at the community level.

There are several assumptions that should be made for the sizing, pairing

and consumption, as:

- Upon profiling energy generation, each household is attributed a specific photovoltaic (PV) peak power. Therefore, during system sizing, whether at a collective community level or individual household design, proportional adjustments can be effectively implemented based on the area and peak power parameters of installed PV systems/panels.
- All energy transfers within the community undergo a process devoid of energy losses, ensuring that energy exchanges between households are perfectly efficient.
- In the simulation of each household, due to the absence of a comprehensive internal pricing system in the strategy, the internal trading electricity cost is stipulated as the real-time electricity cost minus half of the selling electricity cost.
- Battery performance and lifespan adhere to the benchmarks and standards elucidated in previous chapters, ensuring a consistent basis for all related calculations and predictions.
- All residents are presumed to participate in the community's energy trading, thereby ensuring a consistent and reliable trading environment within the community.
- The community is assumed to be equipped with sufficient technological infrastructure to adeptly support the generation, storage, and distribution of energy amongst its residents.
- Throughout the analysis, the reliability and stability of the main power grid are considered to be constant, thereby providing a stable external power source for the community.

- The maintenance and operational costs of the photovoltaic (PV) systems and battery storage systems are either known or predictable, and these systems do not require significant repairs throughout their lifespan.

- All households are presumed to operate in compliance with the energy management strategy proposed by the model, ensuring homogeneity in energy management practices across the community.

7.7.3 Results of Community Simulation

7.7.3.1 Energy Analysis of the Separated Households and the Proposed Community Pairing Strategy

In order to compare the performance of the energy management in community scales, the energy bar of different TOU periods based on the one-year simulation of 20 households in one community is shown in Figure 7.7.2. In the simulation, the parameters of houses are set in the preset range. The home batteries for each household are set as Tesla Powerwall 2, with 13.5 kWh of capacity and 5 kW of power rating, while the PV peak power is 1.4 kept [304]. The simulation results for households without community electricity trading are named as the old community schemes, while the results under both domestic energy management and community pairing strategy are named as the new community schemes.

Figure 7.7.2 showcases the energy procurement from the grid during different tariff periods, comparing the results from the traditional strategy with the new community sharing strategy. Significant differences can be observed across the three tariff periods, emphasizing the influence of the community sharing approach on energy purchase behaviour.

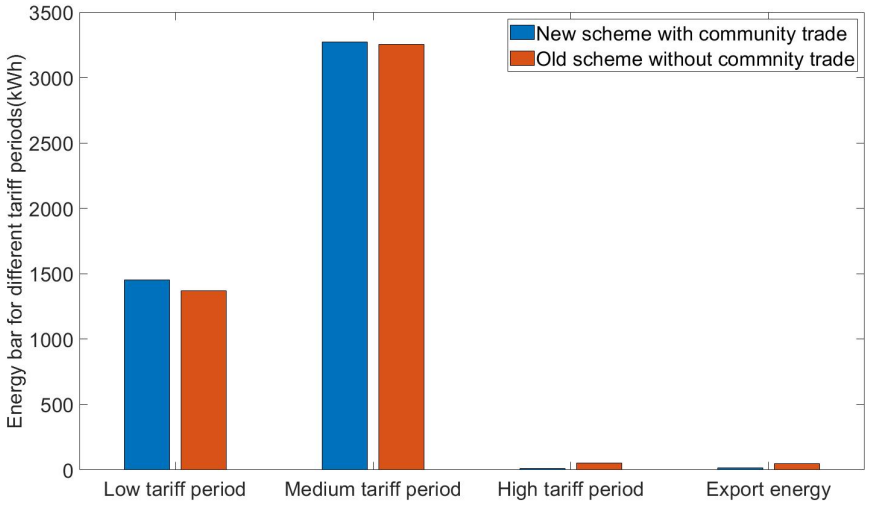


Figure 7.7.2: Energy bar of two schemes for different tariff periods

Under the new sharing strategy, there is an increase of 82.59 kWh during low tariff periods. This surge can be attributed to the enhanced utilization of batteries within homes due to the community exchange strategy. Households procure more energy when tariffs are low, preparing for peak tariff periods. In the medium tariff period, the increase is only 16.44 kWh, suggesting that most energy demands might be satisfied through internal community sharing. During high tariff periods, there is a reduction of 43.99 kWh, indicating a reduced dependency on the grid during peak tariff times, thanks to internal community sharing. The savings of export energy to the grid decreased with the pairing strategy. The value of energy, however, is less. Owing to the installation of battery systems in both community schemes, there is only little energy that required to be exported according to the control algorithm.

The data suggests that the new sharing strategy facilitates a more efficient use and distribution of energy within the community. This sharing might reduce energy burdens during high demand periods and maximize the internal usage of generated energy, rendering it more economically and

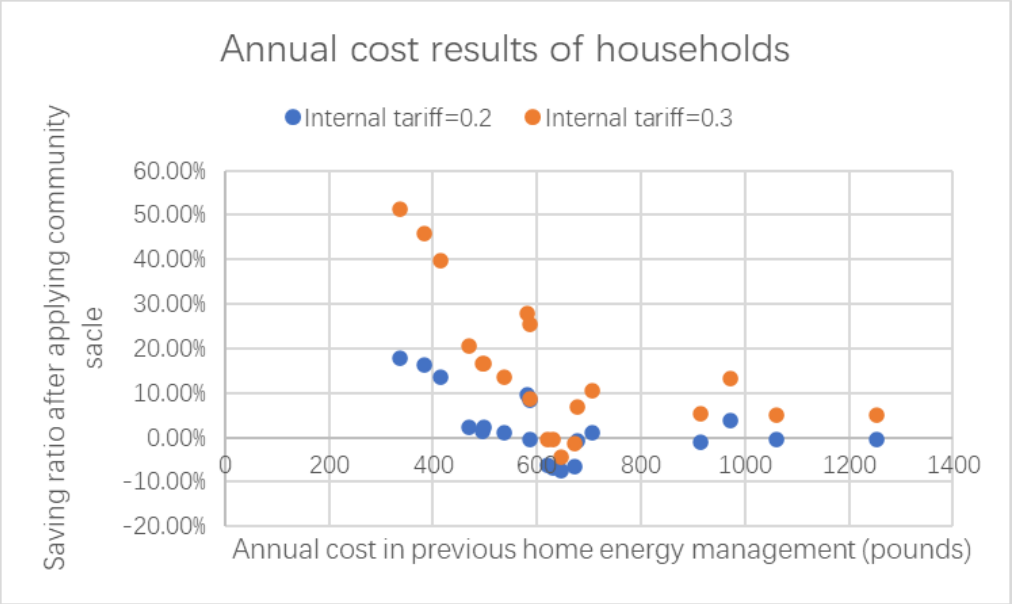


Figure 7.7.3: Initial annual cost of households versus the savings ratio

ecologically beneficial.

The community energy sharing strategy could redefine traditional power supply and distribution models. By optimizing energy distribution within the community, there is a potential to reduce dependence on external grids, lower total energy costs, and enhance system stability.

7.7.3.2 Internal Trade Tariff in Energy Community

Based on the simulation energy results of the community, the economic analysis utilizing TOU tariffs is applied and shown in Figure 7.7.3.

The Figure 7.7.3 provides a comprehensive insight into the economic impacts of implementing the community energy sharing strategy. The internal tariff defines the tariff for households to trade when pairing with each other. It visually represents the cost saving ratios across various households under the proposed strategy compared to the raw annual tariff, when there is no pairing strategy and the households only trade with national grid.

From the chart, a clear trend emerges regarding the relationship between initial costs and the corresponding savings percentage. Households with smaller raw annual tariff tend to achieve a substantial percentage of savings. For example, a specific household with a raw annual tariff of 382.94 pounds sees savings of up to 16.36%. Conversely, higher initial cost households sometimes experience a decline in their savings percentages, occasionally registering negative values. This implies that for these households, the new strategy might occasionally be more expensive than the conventional approach.

This significant variation in savings can be attributed to several factors. Households with relatively lower annual electricity bills often showcase smaller annual loads, translating to lower daily electricity consumption patterns. This low consumption combined with their existing photovoltaic systems and domestic batteries results in a surplus of energy. In the simulated environment, the photovoltaic system's size generally increases with the household size and occupancy. However, this proportional increase might not always align with the growth rate of the household's load, leading to potential mismatches in energy production and consumption.

Another consistent observation is the uniform storage capacity across households due to the standardized use of Tesla Powerwalls. This consistent storage solution means that low-load households frequently have a surplus of energy, which becomes available for sharing within the community. This energy redistribution proves beneficial for them as they can sell this surplus, while high-load households might find themselves purchasing additional energy to cater to their demands.

The complexity of internal trade pricing also play a pivotal role. Even though the community's internal energy trades are driven by surplus energy

availability rather than the trade price, fluctuations in this price can significantly impact the economic benefits for households. A notable instance is when the internal trading price shifts from 0.2 to 0.3 pounds/kWh, which results in a dramatic increase in benefits for certain households.

Although community energy trading lacks official regulatory design, agreements and self-regulation within the community can ensure fair and efficient energy distribution. These self-regulation measures help manage surplus energy and maintain transparent pricing, establishing trust among participants.

In conclusion, the community energy sharing strategy offers distinct advantages, especially for smaller households that frequently emerge as net energy providers within the community. Their combination of their photovoltaics and battery storage, becomes a valuable asset in this shared energy landscape. This analysis underscores the importance of tailoring energy-sharing strategies to the specific needs and configurations of individual households.

7.7.3.3 Sizing Battery and PV Systems for Community Energy Management

Building upon the community and household design methodologies introduced earlier, sizing designs for PV and batteries were conducted for the 20 households involved in the simulation. Within the context, it was additionally assumed that the community battery power is held constant at 5 kW. Simultaneously, the annual maintenance cost is 2% of the installation costs [334]. A comparative analysis was set forth, juxtaposing the energy usage results without a PV/battery system against a system investment plan boasting the optimal 20-year NPV.

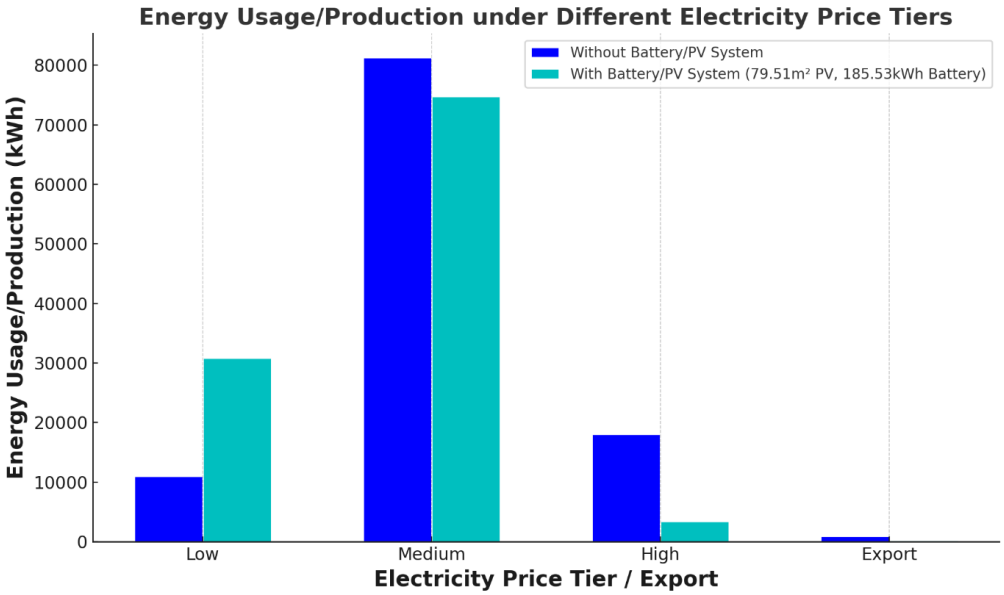


Figure 7.7.4: Energy utilization across different tariff periods for scenarios with and without a battery/PV system

Figure 7.7.4 contrasts energy utilization in kWh across different tariff periods (Low, Medium, High, and Export) for scenarios with and without a Battery/PV system. The right bars represent the scenario with a Battery/PV system of 79.51 m^2 and 185.53 kWh, while the left bars depict the scenario without these installations.

In the Low tariff period, the integration of the Battery/PV system (with 79.51 m^2 PV area and 185.53 kWh battery capacity) leads to a remarkable surge in energy utilization, insinuating an enhanced capacity to harness and utilize solar energy, thereby reducing dependency on grid energy. The Battery/PV system curtails energy use during medium and especially high tariff periods, indicating a strategy to minimize cost by relying on stored energy during peak price times. Lower energy exports with the Battery/PV system suggest a higher internal utilization of generated energy, optimizing its value by avoiding low export tariffs.

The Battery/PV system optimizes energy usage across different tariff periods, significantly impacting energy costs and reducing reliance on the grid,

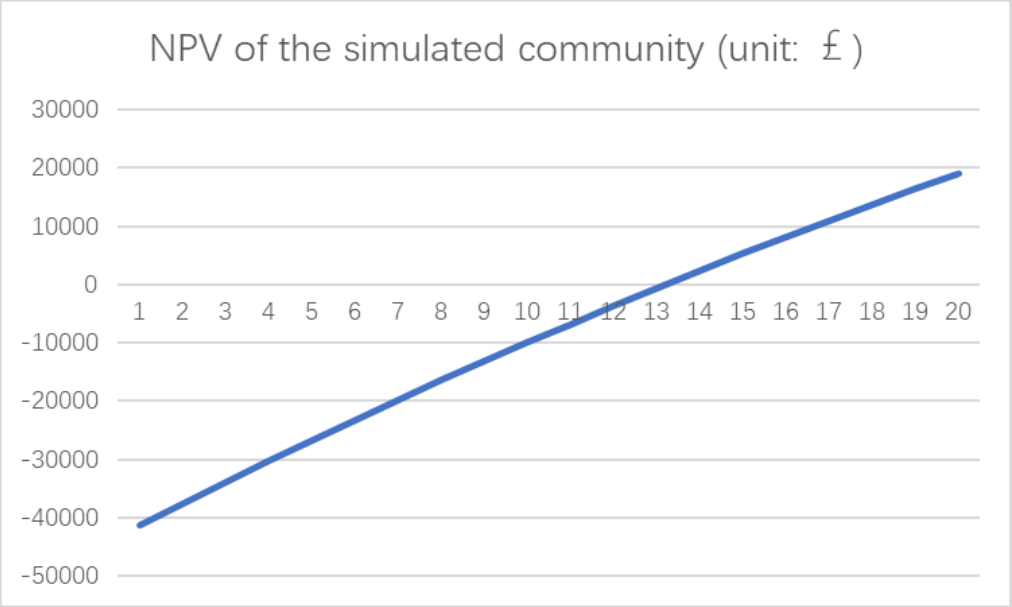


Figure 7.7.5: NPV graph for the optimal sizing of community

especially during high-tariff periods. With the identified PV and battery capacities (79.51 m^2 and 185.53 kWh), the system demonstrates a tangible impact on energy management and cost-saving, underlining the justification for the investment.

The corresponding NPV graph is shown in In Figure 7.7.5, the observed decline in electricity costs, from £20,014.94 pre-investment to £15,702.96 post-investment, underscores the immediate fiscal benefits of adopting Battery/PV technologies. This drop not only signifies considerable savings but also showcases the technologies' capability to efficiently produce and utilize energy in a financially advantageous manner.

Examining the 20-year NPV period, which begins at -£41,399.96 and gradually ascends to £19,109.24, several insights are unveiled. Initially, the NPV is negative, indicating that the initial and operational costs overshadow the savings achieved. However, the transition to a positive NPV around year 13 implies that the cumulative benefits begin to surpass the cumulative costs from this point onwards. A consistent rise in NPV thereafter signals

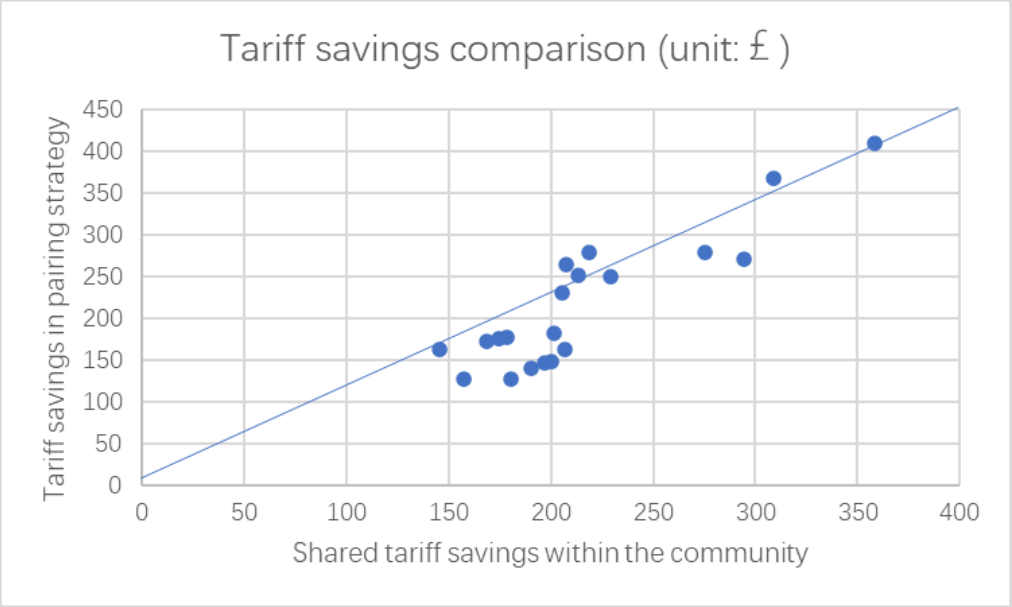


Figure 7.7.6: Tariff savings comparison of community sizing and pairing strategy

the long-term economic feasibility of the system.

The incorporation of the Battery/PV system delivers immediate electricity cost savings, despite substantial initial and operational costs, as reflected in the short-term NPV. The long-term economic outlook, demonstrated by the NPV curve, is optimistic, with tangible financial benefits becoming apparent after roughly 13 years. Hence, the overall investment in the Battery/PV system proves to be justified in the long run, presenting a strong case for its adoption, considering both the immediate and long-term economic and energy advantages. This analysis requires that decision-makers weigh the initial financial expenditure against the extended economic and energy gains, considering both the immediate and long-term impact of integrating such technologies.

The next step of comparing community design and household pairing savings is shown in Figure 7.7.6. Figure 7.7.6 shows the shared tariff savings within the community based on ratio of electricity consumption and the tariff savings with pairing strategy based on local NPV optimal solution for

each household. The line indicates the condition for the two saving values equal to each others.

In terms of total annual electricity cost savings across all 20 households, the shared tariff strategy yields about £4311.98, while the pairing strategy results in slightly higher savings of about £4323.19. Though the discrepancy is marginal, it highlights the pairing strategy's slight edge in optimizing total community-wide savings.

When comparing households, ansplit is observed: 10 households have greater savings with the shared tariff strategy, while the other 10 save more with the pairing strategy. This indicates that the best tariff strategy might vary for each household, depending on their energy consumption, PV production, and battery use.

These findings suggest that while there are general strategies for community energy management and cost savings, a more tailored approach based on each household's energy profile might be more efficient. Both the shared tariff and pairing strategies can reduce electricity costs after investing in PV and batteries, but choosing the best one requires a deeper understanding of each household's energy characteristics.

The pairing strategy shows variable savings, ranging from -25 % to 27 % compared to the shared tariff strategy. Some households experience up to 27 % more savings, proving the strategy 's effectiveness. However, for those facing a 25 % decrease, the strategy is not the best choice. This highlights the strategy's double-sided nature: it can be beneficial for some but not ideal for others.

A trend is observed where households with lower electricity consumption save more, particularly with the pairing strategy. This trend might be

due to the algorithm favoring households with less storage and electricity capacity. These households are more flexible in large scale level, changing how energy is traded and savings are distributed. This trend aligns with previous findings about the savings ratio, adding consistency to the analysis.

Both strategies offer insights. The pairing strategy can be effective despite its varied outcomes, providing a more tailored approach for community energy management. In contrast, the shared tariff strategy is simpler and applies uniformly, making it a practical choice for broad community energy savings. Both strategies' strengths and weaknesses need more research to determine their best application in different community energy settings.

In summary, both strategies can enhance community energy savings after PV and battery investments. Their success depends on specific household energy consumption, storage ability, and trading behavior. Combining the simplicity of the shared tariff strategy with the tailored approach of the pairing strategy might be the way forward for more fair and efficient community energy management.

7.7.4 Conclusion of Applying Model at Community Scale

According to the community pairing strategy and sizing, the results of this section can be summarized as:

- Achieved energy utilization efficiency across diverse TOU periods, reducing peak-period grid dependency through community energy sharing and optimized battery use.

- Evident influence on energy procurement behaviour with the community sharing approach, particularly during different tariff periods.
- Demonstrated the capability of properly sized PV and battery systems to optimize energy usage across tariff periods and deliver tangible economic benefits in the long run despite an initial negative NPV.
- Offered immediate and consistent electricity cost savings, with a shift towards positive NPV approximately 13 years into the 20-year analysis period.
- Identified variable outcomes with both shared tariff and pairing strategies, indicating potential benefits and shortcomings of each, and emphasizing a possible necessity for strategy customization per household energy profile.
- Noted an apparent bias towards smaller electricity usage households in savings, especially under the pairing strategy, suggesting a potential inherent algorithmic bias that may require further investigation and adjustment.

Chapter 8

Overall Conclusion

8.1 Summary

- Data Enhancement and Model Validation

  Through diligent data management and application of algorithms, such as KNN (K-Nearest Neighbors) and SVM-GMM (Support Vector Machine and Gaussian Mixture Model), the study has secured a robust, reliable, and validated dataset. This underpins the research, ensuring subsequent analyses and simulations are founded upon a stable and accurate base of information.

- Advanced Energy Systems Modelling and Simulation

  The research has successfully developed and validated models for various energy systems, including electric heater, GSHP, water heating, and electric cooking, ensuring a nuanced understanding and simulation capability of these specific energy subsystems. Furthermore, the utilization of the Markov Chain method has enabled a sophisticated simulation and prediction of EV operations, considering their

inherent randomness and variability.

- Strategic Application and Optimization in Energy Management

  The incorporation of HEMS has been explored in hybrid houses with gas heating, highlighting significant strides in optimizing energy consumption and enhancing cost-efficiency. Additionally, the study has comprehensively explored the electrification of household appliances and EVs, revealing its various implications on domestic electricity consumption and management.

- Economic and Environmental Impact Analysis

  An in-depth economic analysis, including calculations for NPV and IRR, has shed light on the economic feasibility and payback periods of both traditional and "all-electric" residential schemes. Concurrently, the research has dived into the environmental impacts, especially concerning GHG emissions, elucidating the long-term environmental ramifications and potential of these systems.

- Community-Level Energy Strategy Exploration

  The study has ventured into the realm of community energy management, examining strategies that leverage community energy sharing and optimized battery use to enhance energy utilization and economic efficiency across various Time of Use (TOU) periods.

- Addressing Challenges and Paving Future Directions

  The research has unveiled several challenges, particularly in algorithm implementation and model prediction, providing a springboard for further research and refinement in the realm of household energy management. Moreover, the findings and models presented set a robust foundation for future investigations, innovations, and practical

applications in domestic energy management, aligning with global sustainability goals and future energy trends.

8.2 Main Achievements

Navigating through the field of household energy management, this research has successfully delved into the intricate dynamics, challenges, and potentials ingrained within various energy components, models, and strategies, achieving the aims in Section 1.3.

- Exploration and Detailed Analysis of Diverse Energy Components

  Conducted an in-depth examination of PV systems (Section 3.3), EVs (Section 5.3), and HEMS (Section 4.3), elucidating their operational dynamics, technological challenges, and potential in systemic household energy management.

  Investigated the operational and energy dynamics of various subsystems, including GSHPs, electric cooking, and room heating, providing analytical insights into their energy behaviors and implications in Chapter 6.

- Formulation and Validation of Energy Optimization Strategies

  Developed and validated algorithmic strategies to optimize energy use, minimizing environmental footprint while ensuring economic and operational efficiency in Section 4.3.

  Implemented intelligent heating control algorithms and smart grid interactions to enhance energy utilization efficiency and reduce energy wastage in household settings in Section 6.2.

- Enhancement of Predictive Accuracy in Models and Simulations

Developed and validated several energy models, including GSHP, electric cooking, and room heating, ensuring their predictive capabilities are aligned with empirical data and real-world scenarios in Chapter 6.

Employed KNN and SVM-GMM algorithms for data integrity management, ensuring robust and accurate predictive modeling, especially in PV generation simulations in Chapter 3.

- Comparative Analysis and Integration of Energy Sub-Models

  Integrated and contrasted various energy sub-models, developing a holistic model that encapsulates comprehensive household energy management in Chapter 7.

  Ensured the consolidated model effectively simulates and predicts household energy dynamics, providing a foundation for strategic energy management at both individual and community levels.

- Economic and Environmental Impact Assessment

  Conducted a quantitative analysis on the economic and environmental impact of traditional and "all-electric" residential schemes in Section 7.3, Section 7.4 and Section 7.5.

  Provided a balanced perspective on the immediate and long-term impacts of different energy management approaches, ensuring both economic viability and environmental responsibility are considered in strategy formulation and practical application.

- Strategic Application at a Community Level

  Explored and demonstrated the potential of implementing developed energy management strategies at a community level in Section 7.7.

  Showcased the possibilities and implications of community energy

sharing, providing insights into the potential benefits and challenges of broadening the application of energy management strategies beyond individual households.

8.3 Contributions

Navigating through the complexities of home energy management, this research has made several key contributions by combining detailed engineering studies with practical applications in the field. The following points highlight these contributions:

- Creating a Unified Model: Developed a comprehensive model by bringing together different energy sub-models in Section 7.2. This allows for accurate predictions and representations of household energy use and needs.
- Developing and Testing Algorithms: Introduced and validated new algorithms, specifically designed to optimize how batteries operate, manage thermal energy, and control Electric Vehicle (EV) functionalities in Chapter 4 and Chapter 7.
- Analysing Energy Management Strategies: Thoroughly evaluated various energy management strategies, considering their technical, economic, and environmental aspects to provide a complete view of their real-world implications in Chapter 7.
- Enhancing Predictive Accuracy: Improved the reliability and accuracy of models and simulations to ensure they can be trusted to predict real-world household energy behaviours effectively in Section 5.2.

- Comparing Different Energy Schemes: Conducted an in-depth comparison of traditional and electrification schemes, providing clear insights into the strengths and weaknesses of each approach in Section 7.3, Section 7.4 and Section 7.5.

- Ensuring Wide Applicability of Models: Made sure that the models and strategies developed can be applied to a wide range of scenarios and scales, from individual households to larger communities in Chapter 7.

- Exploring Community-Level Applications: Expanded the research to a community level, exploring how the developed models and strategies can be applied to manage and share energy across larger groups of households in Section 7.7.

8.4 Proposals for Future Work

Future investigations could delve into enhancing energy models through the incorporation of smart home technologies and Internet of Things (IoT) devices, ensuring real-time data acquisition and precise control over home energy usage. The application of novel algorithms could enable models to continuously adapt and be more accurate, optimizing predictions and decision-making processes based on ongoing data accumulation.

Testing and applying the developed energy models across various geographical and climatic conditions stand as a pivotal future exploration area. Adjusting models to account for distinct local weather conditions, cultural habits, and energy usage patterns is essential to ascertain their universal applicability and accuracy. This ensures that the models and strategies are not confined to the initial test locations but are adaptable and efficient in

diverse environments and user scenarios.

A thorough evaluation of the larger-scale impacts resulting from the widespread application of the devised energy models and strategies is paramount. This encompasses understanding how these strategies influence the overarching power grid, fluctuate energy pricing, and impact total greenhouse gas emissions. A comprehensive analysis of the entire lifecycle of the deployed technologies ensures that they remain not only immediately beneficial but also sustainably viable and environmentally responsible in a long-term perspective.

In summary, future investigations anchored in these focal points can assure that advancements in household energy management remain technologically adept, geographically adaptable, and broadly impactful, balancing immediate efficacy with long-term sustainability and environmental responsibility.

Bibliography

[1] W. Wang and F. Li, "Study on substitutable value of electric heating instead of coal heating in northern China under carbon constraints," *Journal of Cleaner Production*, vol. 260, p. 121155, Jul. 2020.

[2] B. Mahapatra and A. Nayyar, "Home energy management system (HEMS): Concept, architecture, infrastructure, challenges and energy management schemes," *Energy Systems*, vol. 13, no. 3, pp. 643–669, Aug. 2022.

[3] Y. Ma, X. Chen, L. Wang, and J. Yang, "Study on Smart Home Energy Management System Based on Artificial Intelligence," *Journal of Sensors*, vol. 2021, p. e9101453, Oct. 2021.

[4] A. N. Abdalla, M. S. Nazir, H. Tao, S. Cao, R. Ji, M. Jiang, and L. Yao, "Integration of energy storage system and renewable energy sources based on artificial intelligence: An overview," *Journal of Energy Storage*, vol. 40, p. 102811, Aug. 2021.

[5] S. Sharda, M. Singh, and K. Sharma, "Demand side management through load shifting in IoT based HEMS: Overview, challenges and opportunities," *Sustainable Cities and Society*, vol. 65, p. 102517, 2021.

[6] M. Yousefi, A. Hajizadeh, M. N. Soltani, and B. Hredzak, "Predictive Home Energy Management System With Photovoltaic Array, Heat Pump, and Plug-In Electric Vehicle," *IEEE Transactions on Industrial Informatics*, vol. 17, no. 1, pp. 430–440, Jan. 2021.

[7] A.-R. Al-Ali, I. A. Zualkernan, M. Rashid, R. Gupta, and M. AliKarar, "A smart home energy management system using IoT and big data analytics approach," *IEEE Transactions on Consumer Electronics*, vol. 63, no. 4, pp. 426–434, 2017.

[8] A. Al-Wakeel, J. Wu, and N. Jenkins, "K-means based load estimation of domestic smart meter measurements," *Applied Energy*, vol. 194, pp. 333–342, May 2017.

[9] A. Ahmad, A. Khan, N. Javaid, H. M. Hussain, W. Abdul, A. Almogren, A. Alamri, and I. Azim Niaz, "An Optimized Home Energy Management System with Integrated Renewable Energy and Storage Resources," *Energies*, vol. 10, no. 4, p. 549, Apr. 2017.

[10] G. P. Hammond and P. J. Pearson, "Challenges of the transition to a low carbon, more electric future: From here to 2050," *Energy Policy*, vol. 52, no. 0, pp. 1–9, 2013.

[11] J. Keirstead, M. Jennings, and A. Sivakumar, "A review of urban energy system models: Approaches, challenges and opportunities," *Renewable and Sustainable Energy Reviews*, vol. 16, no. 6, pp. 3847–3866, 2012.

[12] R. Ma, H.-H. Chen, Y.-R. Huang, and W. Meng, "Smart grid communication: Its challenges and opportunities," *IEEE transactions on Smart Grid*, vol. 4, no. 1, pp. 36–46, 2013.

[13] B. Zafar and S. A. B. Slama, "PV-EV integrated home energy management using vehicle-to-home (V2H) technology and household occupant behaviors," *Energy Strategy Reviews*, vol. 44, p. 101001, Nov. 2022.

[14] M. A. A. Abdalla, W. Min, and O. A. A. Mohammed, "Two-Stage Energy Management Strategy of EV and PV Integrated Smart Home to Minimize Electricity Cost and Flatten Power Load Profile," *Energies*, vol. 13, no. 23, p. 6387, Jan. 2020.

[15] S. A. Aleem, S. S. Hussain, and T. S. Ustun, "A review of strategies to increase PV penetration level in smart grids," *Energies*, vol. 13, no. 3, p. 636, 2020.

[16] F. Massa Gray and M. Schmidt, "Thermal building modelling using Gaussian processes," *Energy and Buildings*, vol. 119, pp. 119–128, May 2016.

[17] X. Zhang, M. Pipattanasomporn, T. Chen, and S. Rahman, "An IoT-Based Thermal Model Learning Framework for Smart Buildings," *IEEE Internet of Things Journal*, vol. 7, no. 1, pp. 518–527, Jan. 2020.

[18] A. Seeam, D. Laurenson, and A. Usmani, "Evaluating the potential of simulation assisted energy management systems: A case for electrical heating optimisation," *Energy and Buildings*, vol. 174, pp. 579–586, Sep. 2018.

[19] A. Shabani, D. Dhamo, D. Panxhi, and O. Zavalani, "Domestic electrical appliance simulation for energy management: Application to real case study," in *2019 International IEEE Conference and Workshop in Óbuda on Electrical and Power Engineering (CANDO-EPE)*, Nov. 2019, pp. 73–78.

[20] C. Wang, D. Yan, and Y. Jiang, "A novel approach for building occupancy simulation," in *Building Simulation*, vol. 4. Springer, 2011, pp. 149–167.

[21] S. Amra, "Modelling Home Appliances of DC House Based on Rooftop Photovoltaic Power Supply," *Jurnal Litek : Jurnal Listrik Telekomunikasi Elektronika*, vol. 18, no. 1, pp. 7–12, Mar. 2021.

[22] C. Behm, L. Nolting, and A. Praktiknjo, "How to model European electricity load profiles using artificial neural networks," *Applied Energy*, vol. 277, p. 115564, Nov. 2020.

[23] G. Happle, J. A. Fonseca, and A. Schlueter, "A review on occupant behavior in urban building energy models," *Energy and Buildings*, vol. 174, pp. 276–292, Sep. 2018.

[24] M. Devi, M. S, E. R, and M. M, "Design and Implementation of a Smart Home Energy Management System Using IoT and Machine Learning," *E3S Web of Conferences*, vol. 387, p. 04005, 2023.

[25] E.Mallikarjuna, "Smart Home Energy Management Based on Zigbee," *J. of Advancement in Engineering and Technology*, vol. Volume 3, no. Issue 3, Sep. 2015.

[26] D. Chioran and H. Valean, "Design and Performance Evaluation of a Home Energy Management System for Power Saving," *Energies*, vol. 14, no. 6, p. 1668, Jan. 2021.

[27] S. Berry, D. Whaley, W. Saman, and K. Davidson, "Finding faults and influencing consumption: The role of in-home energy feedback displays in managing high-tech homes," *Energy Efficiency*, vol. 10, no. 4, pp. 787–807, Aug. 2017.

[28] M. Elkazaz, M. Sumner, E. Naghiyev, S. Pholboon, R. Davies, and D. Thomas, "A hierarchical two-stage energy management for a home microgrid using model predictive and real-time controllers," *Applied Energy*, vol. 269, p. 115118, Jul. 2020.

[29] I. Gomes, K. Bot, M. G. Ruano, and A. Ruano, "Recent Techniques Used in Home Energy Management Systems: A Review," *Energies*, vol. 15, no. 8, p. 2866, Jan. 2022.

[30] Y. Wang and Y. Xiang, "Photovoltaic-storage energy system management considering wireless data communication," *Energy Reports*, vol. 8, pp. 267–273, Nov. 2022.

[31] C. McIlvennie, A. Sanguinetti, and M. Pritoni, "Of impacts, agents, and functions: An interdisciplinary meta-review of smart home energy management systems research," *Energy Research & Social Science*, vol. 68, p. 101555, Oct. 2020.

[32] Z. M. Azizi*, N. S. M. Azizi, S. A. Samikon, and N. M. Nasir, "Raising Energy-Saving Awareness With The Home Energy Report," *European Proceedings of Multidisciplinary Sciences*, vol. Carving The Future Built Environment: Environmental, Economic And Social Resilience, Dec. 2017.

[33] C.-f. Chen, G. Zarazua de Rubens, X. Xu, and J. Li, "Coronavirus comes home? Energy use, home energy management, and the social-psychological factors of COVID-19," *Energy Research & Social Science*, vol. 68, p. 101688, Oct. 2020.

[34] D. V. Keyson, A. A. Mahmud, M. de Hoogh, and R. Luxen, "Designing a Portable and Low Cost Home Energy Management Toolkit," *Procedia Computer Science*, vol. 19, pp. 646–653, Jan. 2013.

[35] J.-S. Chou and N.-S. Truong, "Cloud forecasting system for monitoring and alerting of energy use by home appliances," *Applied Energy*, vol. 249, pp. 166–177, Sep. 2019.

[36] T. Malatesta, C. Eon, J. K. Breadsell, A. Law, J. Byrne, and G. M. Morrison, "Systems of social practice and automation in an energy efficient home," *Building and Environment*, vol. 224, p. 109543, Oct. 2022.

[37] A. Nilsson, M. Wester, D. Lazarevic, and N. Brandt, "Smart homes, home energy management systems and real-time feedback: Lessons for influencing household energy consumption from a Swedish field study," *Energy and Buildings*, vol. 179, pp. 15–25, Nov. 2018.

[38] S. Kallio and M. Siroux, "A Review – Home Renewable Energy Management Systems in Smart Grids," *IOP Conference Series: Earth and Environmental Science*, vol. 1050, no. 1, p. 012001, Jul. 2022.

[39] S. Oliveira, L. Badarnah, M. Barakat, A. Chatzimichali, and E. Atkins, "Beyond energy services: A multidimensional and cross-disciplinary agenda for home energy management research," *Energy Research & Social Science*, vol. 85, p. 102347, Mar. 2022.

[40] A. Q. H. Badar and A. Anvari-Moghaddam, "Smart home energy management system – a review," *Advances in Building Energy Research*, vol. 16, no. 1, pp. 118–143, Jan. 2022.

[41] K. Ellsworth-Krebs, L. Reid, and C. J. Hunter, "Home Comfort and "Peak Household": Implications for Energy Demand," *Housing, Theory and Society*, vol. 38, no. 1, pp. 1–20, Jan. 2021.

[42] L. M. Carrasco, L. Narvarte, F. Martínez-Moreno, and R. Moretón, "In-field assessment of batteries and PV modules in a large photo-

voltaic rural electrification programme," *Energy*, vol. 75, pp. 281–288, Oct. 2014.

[43] S. K. Hobbis, "Beyond electrification for development: Solar home systems and social reproduction in rural Solomon Islands," *Asia Pacific Viewpoint*, vol. 62, no. 2, pp. 151–163, 2021.

[44] N. Koltsaklis, I. Panapakidis, G. Christoforidis, and J. Knápek, "Smart home energy management processes support through machine learning algorithms," *Energy Reports*, vol. 8, pp. 1–6, Jun. 2022.

[45] E. L. Meyer and O. K. Overen, "Towards a sustainable rural electrification scheme in South Africa: Analysis of the Status quo," *Energy Reports*, vol. 7, pp. 4273–4287, Nov. 2021.

[46] I. Nygaard and T. Dafrallah, "Utility led rural electrification in Morocco: Combining grid extension, mini-grids, and solar home systems," *WIREs Energy and Environment*, vol. 5, no. 2, pp. 155–168, 2016.

[47] Y. Li, Y. Gu, and T. C. Green, "Revisiting Grid-Forming and Grid-Following Inverters: A Duality Theory," *IEEE Transactions on Power Systems*, vol. 37, no. 6, pp. 4541–4554, Nov. 2022.

[48] A. Washizu, S. Nakano, H. Ishii, and Y. Hayashi, "Willingness to Pay for Home Energy Management Systems: A Survey in New York and Tokyo," *Sustainability*, vol. 11, no. 17, p. 4790, Jan. 2019.

[49] M. De Simón-Martín, A.-M. Diez-Suárez, L. Álvarez-de Prado, A. González-Martínez, Á. De la Puente-Gil, and J. Blanes-Peiró, "Development of a GIS Tool for High Precision PV Degradation Monitoring and Supervision: Feasibility Analysis in Large and Small PV Plants," *Sustainability*, vol. 9, no. 6, p. 965, Jun. 2017.

[50] N. Munzke, B. Schwarz, F. Büchle, and M. Hiller, "Evaluation of the efficiency and resulting electrical and economic losses of photovoltaic home storage systems," *Journal of Energy Storage*, vol. 33, p. 101724, Jan. 2021.

[51] A. Nur and A. Buğutekin, "SOLAR PV SYSTEM COST ANALYSIS FOR A SMART HOME," *International Journal of Energy Applications and Technologies*, vol. 4, no. 4, pp. 152–163, Dec. 2017.

[52] K. S. K. Sari, W. Wati, and S. Syafii, "Home Industry Powered Grid-Connected PV System an Economic Feasibility Study," *Andalas Journal of Electrical and Electronic Engineering Technology*, vol. 1, no. 2, pp. 58–61, Dec. 2021.

[53] J. von Appen, T. Stetz, B. Idlbi, and M. Braun, "Enabling high amounts of PV systems in low voltage grids using storage systems," 2014.

[54] G. Zubi, R. S. Adhikari, N. E. Sánchez, and W. Acuña-Bravo, "Lithium-ion battery-packs for solar home systems: Layout, cost and implementation perspectives," *Journal of Energy Storage*, vol. 32, p. 101985, Dec. 2020.

[55] Y. Yu, N. Narayan, V. Vega-Garita, J. Popovic-Gerber, Z. Qin, M. Wagemaker, P. Bauer, and M. Zeman, "Constructing Accurate Equivalent Electrical Circuit Models of Lithium Iron Phosphate and Lead–Acid Battery Cells for Solar Home System Applications," *Energies*, vol. 11, no. 9, p. 2305, Sep. 2018.

[56] V. Stepaniuk, J. Pillai, and B. Bak-Jensen, "Battery Energy Storage Management for Smart Residential Buildings," in *2018 53rd International Universities Power Engineering Conference (UPEC)*, Sep. 2018, pp. 1–6.

[57] F. Keskin Arabul, A. Y. Arabul, C. F. Kumru, and A. R. Boynuegri, "Providing energy management of a fuel cell–battery–wind turbine–solar panel hybrid off grid smart home system," *International Journal of Hydrogen Energy*, vol. 42, no. 43, pp. 26 906–26 913, Oct. 2017.

[58] X. Wu, X. Hu, Y. Teng, S. Qian, and R. Cheng, "Optimal integration of a hybrid solar-battery power source into smart home nanogrid with plug-in electric vehicle," *Journal of Power Sources*, vol. 363, pp. 277–283, Sep. 2017.

[59] B. Zakeri, G. C. Gissey, P. E. Dodds, and D. Subkhankulova, "Centralized vs. distributed energy storage – Benefits for residential users," *Energy*, vol. 236, p. 121443, Dec. 2021.

[60] N. Narayan, T. Papakosta, V. Vega-Garita, Z. Qin, J. Popovic-Gerber, P. Bauer, and M. Zeman, "Estimating battery lifetimes in Solar Home System design using a practical modelling methodology," *Applied Energy*, vol. 228, pp. 1629–1639, Oct. 2018.

[61] P. Wang, "Life prediction and matching test of decommissioned power battery based on energy storage system," *Chemical Engineering Transactions*, vol. 67, pp. 853–858, Sep. 2018.

[62] T. Terlouw, X. Zhang, C. Bauer, and T. Alskaif, "Towards the determination of metal criticality in home-based battery systems using a Life Cycle Assessment approach," *Journal of Cleaner Production*, vol. 221, pp. 667–677, Jun. 2019.

[63] L. Noel, G. Zarazua de Rubens, J. Kester, and B. K. Sovacool, "Beyond emissions and economics: Rethinking the co-benefits of electric vehicles (EVs) and vehicle-to-grid (V2G)," *Transport Policy*, vol. 71, pp. 130–137, Nov. 2018.

[64] K. Alfaverh, F. Alfaverh, and L. Szamel, "Plugged-in electric vehicle-assisted demand response strategy for residential energy management," *Energy Informatics*, vol. 6, no. 1, p. 6, Mar. 2023.

[65] H. Li, P. Zeng, C. Zang, H. Yu, and S. Li, "An Integrative DR Study for Optimal Home Energy Management Based on Approximate Dynamic Programming," *Sustainability*, vol. 9, no. 7, p. 1248, Jul. 2017.

[66] O. Almughram, S. Ben Slama, and B. Zafar, "Model for Managing the Integration of a Vehicle-to-Home Unit into an Intelligent Home Energy Management System," *Sensors*, vol. 22, no. 21, p. 8142, Jan. 2022.

[67] A. R. Abul'Wafa, A. El'Garably, and W. A. Mohamed, "Electric Vehicle-to-Home Concept Including Home Energy Management," *International Journal of Engineering and Information Systems*, vol. 1, no. 6, pp. 20–28, 2017.

[68] B. Zafar and S. A. B. Slama, "PV-EV integrated home energy management using vehicle-to-home (V2H) technology and household occupant behaviors," *Energy Strategy Reviews*, vol. 44, p. 101001, Nov. 2022.

[69] L. Serafini, E. Principi, S. Spinsante, and S. Squartini, "Multi-Household Energy Management in a Smart Neighborhood in the Presence of Uncertainties and Electric Vehicles," *Electronics*, vol. 10, no. 24, p. 3186, Jan. 2021.

[70] G. Vacheva, N. Hinov, H. Kanchev, R. Stanev, and O. Cornea, "Energy Flows Management of Multiple Electric Vehicles in Smart Grid," *Elektronika ir Elektrotechnika*, vol. 25, no. 1, pp. 14–17, Feb. 2019.

[71] S. Lee and D.-H. Choi, "Energy Management of Smart Home with Home Appliances, Energy Storage System and Electric Vehicle: A Hierarchical Deep Reinforcement Learning Approach," *Sensors*, vol. 20, no. 7, p. 2157, Jan. 2020.

[72] V. Turanjanin, B. S. Vučićević, and M. P. Jovanović, "Different Heating Systems for Single Family House Energy and Economic Analysis," *Thermal Science*, vol. 20, pp. S309–S320, 2016.

[73] J. Wang, J. Liu, C. Li, Y. Zhou, and J. Wu, "Optimal scheduling of gas and electricity consumption in a smart home with a hybrid gas boiler and electric heating system," *Energy*, vol. 204, p. 117951, Aug. 2020.

[74] A. Cimini and M. Moresi, "Energy efficiency and carbon footprint of home pasta cooking appliances," *Journal of Food Engineering*, vol. 204, pp. 8–17, Jul. 2017.

[75] B. Ciupek, W. Judt, and R. Urbaniak, "Tests of changes in the resistance of heating water flow in the home heating system," *E3S Web of Conferences*, vol. 128, p. 01010, 2019.

[76] S. P. Larsen and H. Johra, "User engagement with smart home technology for enabling building energy flexibility in a district heating system," *IOP Conference Series: Earth and Environmental Science*, vol. 352, no. 1, p. 012002, Oct. 2019.

[77] K. M. A. Revell and N. A. Stanton, "Mental model interface design: Putting users in control of home heating," *Building Research & Information*, vol. 46, no. 3, pp. 251–271, Apr. 2018.

[78] ——, "Mind the gap – Deriving a compatible user mental model of the home heating system to encourage sustainable behaviour," *Applied Ergonomics*, vol. 57, pp. 48–61, Nov. 2016.

[79] J. Curtis and G. Grilli, "Does moving home affect residential heating decisions? Exploring heating fuel switching in Ireland," *Energy and Buildings*, vol. 241, p. 110918, Jun. 2021.

[80] J. Curtis, D. McCoy, and C. Aravena, "Heating system upgrades: The role of knowledge, socio-demographics, building attributes and energy infrastructure," *Energy Policy*, vol. 120, pp. 183–196, Sep. 2018.

[81] B. K. Sovacool and M. Martiskainen, "Hot transformations: Governing rapid and deep household heating transitions in China, Denmark, Finland and the United Kingdom," *Energy Policy*, vol. 139, p. 111330, Apr. 2020.

[82] I. Gomes, K. Bot, M. G. Ruano, and A. Ruano, "Recent Techniques Used in Home Energy Management Systems: A Review," *Energies*, vol. 15, no. 8, p. 2866, Jan. 2022.

[83] M. Yousefi, A. Hajizadeh, and M. N. Soltani, "A Comparison Study on Stochastic Modeling Methods for Home Energy Management Systems," *IEEE Transactions on Industrial Informatics*, vol. 15, no. 8, pp. 4799–4808, Aug. 2019.

[84] H. Wu, A. Pratt, P. Munankarmi, M. Lunacek, S. P. Balamurugan, X. Liu, and P. Spitsen, "Impact of model predictive control-enabled home energy management on large-scale distribution systems with photovoltaics," *Advances in Applied Energy*, vol. 6, p. 100094, Jun. 2022.

[85] E. Sarker, M. Seyedmahmoudian, E. Jamei, B. Horan, and A. Stojcevski, "Optimal management of home loads with renewable energy integration and demand response strategy," *Energy*, vol. 210, p. 118602, Nov. 2020.

[86] S. Seal, B. Boulet, and V. R. Dehkordi, "Centralized model predictive control strategy for thermal comfort and residential energy management," *Energy*, vol. 212, p. 118456, Dec. 2020.

[87] Tuğba Sarikaya and Sibel Zorlu Partal, "A Case Study of Load Scheduling For Home Energy Management with Integrated Renewable Energy," *International Journal of Engineering and Management Research*, vol. 12, no. 5, pp. 27–34, Oct. 2022.

[88] T. H. Tran and T. B. T. Nguyen, "Minimizing Total Cost of Home Energy Consumption under Uncertainties," *Electric Power Components and Systems*, vol. 50, no. 19-20, pp. 1143–1160, Dec. 2022.

[89] R. McKenna, L. Hofmann, M. Kleinebrahm, and W. Fichtner, "A stochastic multi-energy simulation model for UK residential buildings," *Energy and Buildings*, vol. 168, pp. 470–489, Jun. 2018.

[90] E. McKenna and M. Thomson, "High-resolution stochastic integrated thermal–electrical domestic demand model," *Applied Energy*, vol. 165, pp. 445–461, Mar. 2016.

[91] E. McKenna, J. Pless, and S. J. Darby, "Solar photovoltaic self-consumption in the UK residential sector: New estimates from a smart grid demonstration project," *Energy Policy*, vol. 118, pp. 482–491, Jul. 2018.

[92] L. G. Marín, M. Sumner, D. Muñoz-Carpintero, D. Köbrich, S. Pholboon, D. Sáez, and A. Núñez, "Hierarchical Energy Management

System for Microgrid Operation Based on Robust Model Predictive Control," *Energies*, vol. 12, no. 23, p. 4453, Jan. 2019.

[93] M. Elkazaz, M. Sumner, and D. Thomas, "Energy management system for hybrid PV-wind-battery microgrid using convex programming, model predictive and rolling horizon predictive control with experimental validation," *International Journal of Electrical Power & Energy Systems*, vol. 115, p. 105483, Feb. 2020.

[94] A. Fazeli, M. Sumner, C. M. Johnson, and E. Christopher, "Investigating the impact of varying the number of distributed energy resources on controlling the power flow within a microgrid," in *2015 IEEE Power & Energy Society Innovative Smart Grid Technologies Conference (ISGT)*, Feb. 2015, pp. 1–5.

[95] M. Fathi and H. Bevrani, "Statistical cooperative power dispatching in interconnected microgrids," *IEEE Transactions on Sustainable Energy*, vol. 4, no. 3, pp. 586–593, 2013.

[96] F. Luo, G. Ranzi, C. Wan, Z. Xu, and Z. Y. Dong, "A multistage home energy management system with residential photovoltaic penetration," *IEEE Transactions on Industrial Informatics*, vol. 15, no. 1, pp. 116–126, 2018.

[97] F. Luo, G. Ranzi, S. Wang, and Z. Y. Dong, "Hierarchical energy management system for home microgrids," *IEEE Transactions on Smart Grid*, vol. 10, no. 5, pp. 5536–5546, 2018.

[98] B. Zhao, X. Wang, D. Lin, M. M. Calvin, J. C. Morgan, R. Qin, and C. Wang, "Energy management of multiple microgrids based on a system of systems architecture," *IEEE Transactions on Power Systems*, vol. 33, no. 6, pp. 6410–6421, 2018.

[99] N. Nikmehr and S. N. Ravadanegh, "Optimal power dispatch of multi-microgrids at future smart distribution grids," *IEEE transactions on smart grid*, vol. 6, no. 4, pp. 1648–1657, 2015.

[100] N. G. Paterakis, O. Erdinç, I. N. Pappi, A. G. Bakirtzis, and J. P. Catalão, "Coordinated operation of a neighborhood of smart households comprising electric vehicles, energy storage and distributed generation," *IEEE Transactions on smart grid*, vol. 7, no. 6, pp. 2736–2747, 2016.

[101] C. Zhang, Y. Xu, Z. Y. Dong, and K. P. Wong, "Robust coordination of distributed generation and price-based demand response in microgrids," *IEEE Transactions on Smart Grid*, vol. 9, no. 5, pp. 4236–4247, 2017.

[102] J. Li, Y. Liu, and L. Wu, "Optimal operation for community-based multi-party microgrid in grid-connected and islanded modes," *IEEE Transactions on Smart Grid*, vol. 9, no. 2, pp. 756–765, 2016.

[103] J. Ni and Q. Ai, "Economic power transaction using coalitional game strategy in micro-grids," *IET Generation, Transmission & Distribution*, vol. 10, no. 1, pp. 10–18, 2016.

[104] X. Zhao, W. Gao, F. Qian, and J. Ge, "Electricity cost comparison of dynamic pricing model based on load forecasting in home energy management system," *Energy*, vol. 229, p. 120538, Aug. 2021.

[105] D. W. van der Meer, M. Shepero, A. Svensson, J. Widén, and J. Munkhammar, "Probabilistic forecasting of electricity consumption, photovoltaic power generation and net demand of an individual building using Gaussian Processes," *Applied Energy*, vol. 213, pp. 195–207, Mar. 2018.

[106] N. Qi, L. Cheng, H. Xu, K. Wu, X. Li, Y. Wang, and R. Liu, "Smart meter data-driven evaluation of operational demand response potential of residential air conditioning loads," *Applied Energy*, vol. 279, p. 115708, Dec. 2020.

[107] SP. Mishra and PK. Dash, "Short term wind power forecasting using Chebyshev polynomial trained by ridge extreme learning machine," in *2015 IEEE Power, Communication and Information Technology Conference (PCITC)*. IEEE, 2015, pp. 173–177.

[108] S. Netsanet, J. Zhang, D. Zheng, R. K. Agrawal, and F. Muchahary, "An aggregative machine learning approach for output power prediction of wind turbines," in *2018 IEEE Texas Power and Energy Conference (TPEC)*. IEEE, 2018, pp. 1–6.

[109] T. Hiyama and E. Karatepe, "Investigation of ANN performance for tracking the optimum points of PV module under partially shaded conditions," in *2010 Conference Proceedings IPEC*. IEEE, 2010, pp. 1186–1191.

[110] D. O'Leary and J. Kubby, "Feature selection and ANN solar power prediction," *Journal of Renewable Energy*, vol. 2017, 2017.

[111] M. David, F. Ramahatana, P.-J. Trombe, and P. Lauret, "Probabilistic forecasting of the solar irradiance with recursive ARMA and GARCH models," *Solar Energy*, vol. 133, pp. 55–72, 2016.

[112] W. Liu and Y. Xu, "Randomised learning-based hybrid ensemble model for probabilistic forecasting of PV power generation," *IET Generation, Transmission & Distribution*, vol. 14, no. 24, pp. 5909–5917, 2020.

[113] H. Sheng, J. Xiao, Y. Cheng, Q. Ni, and S. Wang, "Short-term solar power forecasting based on weighted Gaussian process regression," *IEEE Transactions on Industrial Electronics*, vol. 65, no. 1, pp. 300–308, 2017.

[114] A. Khosravi, S. Nahavandi, D. Creighton, and A. F. Atiya, "Lower upper bound estimation method for construction of neural network-based prediction intervals," *IEEE transactions on neural networks*, vol. 22, no. 3, pp. 337–346, 2010.

[115] Y. Wang, D. Gan, M. Sun, N. Zhang, Z. Lu, and C. Kang, "Probabilistic individual load forecasting using pinball loss guided LSTM," *Applied Energy*, vol. 235, pp. 10–20, 2019.

[116] "Energy Consumption in the UK - How many kWh per day is the average?" Jul. 2022.

[117] "Save Energy with Solar, Powervault & Octopus Go," https://www.powervault.co.uk/article/an-ideal-threesome-for-your-home-solar-pv-powervault-and-octopus-go/, Apr. 2022.

[118] M. Farrugia, K. Scerri, and A. Sammut, "Imputation of Electrical Load Profile Data as Derived from Smart Meters," in *2022 IEEE 21st Mediterranean Electrotechnical Conference (MELECON)*, Jun. 2022, pp. 1067–1072.

[119] M. Trigo-González, FJ. Batlles, J. Alonso-Montesinos, P. Ferrada, J. Del Sagrado, M. Martínez-Durbán, M. Cortés, C. Portillo, and A. Marzo, "Hourly PV production estimation by means of an exportable multiple linear regression model," *Renewable energy*, vol. 135, pp. 303–312, 2019.

[120] S. Massucco, G. Mosaico, M. Saviozzi, and F. Silvestro, "A hybrid technique for day-ahead PV generation forecasting using clear-sky models or ensemble of artificial neural networks according to a decision tree approach," *Energies*, vol. 12, no. 7, p. 1298, 2019.

[121] K. Dhibi, R. Fezai, M. Mansouri, M. Trabelsi, A. Kouadri, K. Bouzara, H. Nounou, and M. Nounou, "Reduced kernel random forest technique for fault detection and classification in grid-tied PV systems," *IEEE Journal of Photovoltaics*, vol. 10, no. 6, pp. 1864–1871, 2020.

[122] M. Pan, C. Li, R. Gao, Y. Huang, H. You, T. Gu, and F. Qin, "Photovoltaic power forecasting based on a support vector machine with improved ant colony optimization," *Journal of Cleaner Production*, vol. 277, p. 123948, 2020.

[123] J. Ferrero Bermejo, J. F. Gómez Fernández, F. Olivencia Polo, and A. Crespo Márquez, "A review of the use of artificial neural network models for energy and reliability prediction. A study of the solar PV, hydraulic and wind energy sources," *Applied Sciences*, vol. 9, no. 9, p. 1844, 2019.

[124] W. Liu, X. Xu, and X. Zhou, "Daily load forecasting based on SVM for electric bus charging station," *Electric Power Automation Equipment*, vol. 34, no. 11, pp. 41–47, 2014.

[125] "POWER Data Access Viewer," https://power.larc.nasa.gov/data-access-viewer/.

[126] J. Han, C.-S. Choi, and I. Lee, "More efficient home energy management system based on ZigBee communication and infrared remote controls," *IEEE Transactions on Consumer Electronics*, vol. 57, no. 1, pp. 85–89, 2011.

[127] M. Kuzlu, M. Pipattanasomporn, and S. Rahman, "Hardware demonstration of a home energy management system for demand response applications," *IEEE Transactions on Smart grid*, vol. 3, no. 4, pp. 1704–1711, 2012.

[128] A. Dimeas, S. Drenkard, N. Hatziargyriou, S. Karnouskos, K. Kok, J. Ringelstein, and A. Weidlich, "Smart Houses in the Smart Grid: Developing an interactive network." *IEEE Electrification Magazine*, vol. 2, no. 1, pp. 81–93, 2014.

[129] Y. Zhang, P. Zeng, and C. Zang, "Review of home energy management system in smart grid," *Power system protection and control*, vol. 42, no. 18, pp. 144–154, 2014.

[130] A. Lopez, L. Sanchez, F. Doctor, H. Hagras, and V. Callaghan, "An evolutionary algorithm for the off-line data driven generation of fuzzy controllers for intelligent buildings," in *2004 IEEE International Conference on Systems, Man and Cybernetics (IEEE Cat. No. 04CH37583)*, vol. 1. IEEE, 2004, pp. 42–47.

[131] J. Wang, L. Li, and J. Zhang, "Deep reinforcement learning for energy trading and load scheduling in residential peer-to-peer energy trading market," *International Journal of Electrical Power & Energy Systems*, vol. 147, p. 108885, May 2023.

[132] S. Wang and X. Xu, "Optimal and robust control of outdoor ventilation airflow rate for improving energy efficiency and IAQ," *Building and Environment*, vol. 39, no. 7, pp. 763–773, 2004.

[133] X. Chen, T. Wei, and S. Hu, "Uncertainty-aware household appliance scheduling considering dynamic electricity pricing in smart home," *IEEE Transactions on Smart Grid*, vol. 4, no. 2, pp. 932–941, 2013.

[134] K. O. Oureilidis, E. A. Bakirtzis, and C. S. Demoulias, "Frequency-based control of islanded microgrid with renewable energy sources and energy storage," *Journal of Modern Power Systems and Clean Energy*, vol. 4, no. 1, pp. 54–62, 2016.

[135] E. Kabalci and Y. Kabalci, *Smart Grids and Their Communication Systems*. Springer, 2019, no. 1.

[136] E. Rodriguez-Diaz, E. J. Palacios-Garcia, M. Savaghebi, J. C. Vasquez, and J. M. Guerrero, "Development and integration of a HEMS with an advanced smart metering infrastructure," in *2016 IEEE International Conference on Consumer Electronics (ICCE)*. IEEE, 2016, pp. 544–545.

[137] M. Shakeri, M. Shayestegan, S. S. Reza, I. Yahya, B. Bais, M. Akhtaruzzaman, K. Sopian, and N. Amin, "Implementation of a novel home energy management system (HEMS) architecture with solar photovoltaic system as supplementary source," *Renewable energy*, vol. 125, pp. 108–120, 2018.

[138] M. Srikranjanapert, S. Junlakarn, and N. Hoonchareon, "How an Integration of Home Energy Management and Battery System Affects the Economic Benefits of Residential PV System Owners in Thailand," *Sustainability*, vol. 13, no. 5, p. 2681, 2021.

[139] A. Nacer, B. Marhic, and L. Delahoche, "Smart Home, Smart HEMS, Smart heating: An overview of the latest products and trends," in *2017 6th International Conference on Systems and Control (ICSC)*, May 2017, pp. 90–95.

[140] Y. Yoshimura, T. Kondo, M. Kawanishi, T. Narikiyo, and A. Sato, "Model predictive control of ev storage battery with hems based on

particle swarm optimization," in *2015 IEEE Innovative Smart Grid Technologies-Asia (ISGT ASIA)*. IEEE, 2015, pp. 1–5.

[141] E. Sarker, P. Halder, M. Seyedmahmoudian, E. Jamei, B. Horan, S. Mekhilef, and A. Stojcevski, "Progress on the demand side management in smart grid and optimization approaches," *International Journal of Energy Research*, vol. 45, no. 1, pp. 36–64, 2021.

[142] R. Banos, F. Manzano-Agugliaro, FG. Montoya, C. Gil, A. Alcayde, and J. Gómez, "Optimization methods applied to renewable and sustainable energy: A review," *Renewable and sustainable energy reviews*, vol. 15, no. 4, pp. 1753–1766, 2011.

[143] P. H. Shaikh, N. B. M. Nor, P. Nallagownden, I. Elamvazuthi, and T. Ibrahim, "A review on optimized control systems for building energy and comfort management of smart sustainable buildings," *Renewable and Sustainable Energy Reviews*, vol. 34, pp. 409–429, 2014.

[144] S. B. Wali, MA. Hannan, MS. Reza, P. J. Ker, RA. Begum, MS. Abd Rahman, and M. Mansor, "Battery storage systems integrated renewable energy sources: A biblio metric analysis towards future directions," *Journal of Energy Storage*, vol. 35, p. 102296, 2021.

[145] C. Guzman, L. Rueda, G. Romero, S. Biscans, K. Agbossou, and A. Cardenas, "Enabling winter behavior analysis on electrically heated residential buildings by smart sub-metering," in *2018 IEEE International Conference on Industrial Technology (ICIT)*. IEEE, 2018, pp. 1213–1218.

[146] A. O. Ali, M. R. Elmarghany, M. M. Abdelsalam, M. N. Sabry, and A. M. Hamed, "Closed-loop home energy management system with

renewable energy sources in a smart grid: A comprehensive review," *Journal of Energy Storage*, vol. 50, p. 104609, 2022.

[147] Y. Himeur, A. Alsalemi, A. Al-Kababji, F. Bensaali, A. Amira, C. Sardianos, G. Dimitrakopoulos, and I. Varlamis, "A survey of recommender systems for energy efficiency in buildings: Principles, challenges and prospects," *Information Fusion*, vol. 72, pp. 1–21, 2021.

[148] Y. Himeur, A. Alsalemi, F. Bensaali, A. Amira, I. Varlamis, G. Bravos, C. Sardianos, and G. Dimitrakopoulos, "Techno-economic assessment of building energy efficiency systems using behavioral change: A case study of an edge-based micro-moments solution," *Journal of Cleaner Production*, vol. 331, p. 129786, 2022.

[149] M. Ceraolo, G. Lutzemberger, and D. Poli, "Aging evaluation of high power lithium cells subjected to micro-cycles," *Journal of Energy Storage*, vol. 6, pp. 116–124, 2016.

[150] W. Diao, S. Saxena, and M. Pecht, "Accelerated cycle life testing and capacity degradation modeling of LiCoO2-graphite cells," *Journal of Power Sources*, vol. 435, p. 226830, 2019.

[151] I. Laresgoiti, S. Käbitz, M. Ecker, and D. U. Sauer, "Modeling mechanical degradation in lithium ion batteries during cycling: Solid electrolyte interphase fracture," *Journal of Power Sources*, vol. 300, pp. 112–122, 2015.

[152] M. Berecibar, I. Gandiaga, I. Villarreal, N. Omar, J. Van Mierlo, and P. Van den Bossche, "Critical review of state of health estimation methods of Li-ion batteries for real applications," *Renewable and Sustainable Energy Reviews*, vol. 56, pp. 572–587, 2016.

[153] X. Han, M. Ouyang, L. Lu, and J. Li, "A comparative study of commercial lithium ion battery cycle life in electric vehicle: Capacity loss estimation," *Journal of Power Sources*, vol. 268, pp. 658–669, 2014.

[154] B. Xu, A. Oudalov, A. Ulbig, G. Andersson, and D. S. Kirschen, "Modeling of Lithium-Ion Battery Degradation for Cell Life Assessment," *IEEE Transactions on Smart Grid*, vol. 9, no. 2, pp. 1131–1140, Mar. 2018.

[155] E. ASTM, "Standard practices for cycle counting in fatigue analysis," *E1049-85.*, 2011.

[156] C. A. Rosenkranz, U. Köhler, and J. L. Liska, "Modern battery systems for plug-in hybrid electric vehicles," in *Proceedings of the 23rd International Battery, Hybrid and Fuel Cell Electric Vehicle Symposium and Exhibition (EVS-23), Anaheim, CA, USA*, 2007, pp. 2–5.

[157] Z. Shahan, "38,000 Tesla Powerwall Reservations In Under A Week (Tesla / Elon Musk Transcript)," https://cleantechnica.com/2015/05/07/38000-tesla-powerwall-reservations-in-under-a-week-tesla-elon-musk-transcript/, May 2015.

[158] C. N. Truong, M. Naumann, R. C. Karl, M. Müller, A. Jossen, and H. C. Hesse, "Economics of Residential Photovoltaic Battery Systems in Germany: The Case of Tesla's Powerwall," *Batteries*, vol. 2, no. 2, p. 14, Jun. 2016.

[159] P. M. Attia, A. Grover, N. Jin, K. A. Severson, T. M. Markov, Y.-H. Liao, M. H. Chen, B. Cheong, N. Perkins, Z. Yang, P. K. Herring, M. Aykol, S. J. Harris, R. D. Braatz, S. Ermon, and W. C.

Chueh, "Closed-loop optimization of fast-charging protocols for batteries with machine learning," *Nature*, vol. 578, no. 7795, pp. 397–402, Feb. 2020.

[160] Z. Huang, Z. Xie, C. Zhang, S. H. Chan, J. Milewski, Y. Xie, Y. Yang, and X. Hu, "Modeling and multi-objective optimization of a standalone PV-hydrogen-retired EV battery hybrid energy system," *Energy conversion and management*, vol. 181, pp. 80–92, 2019.

[161] M. Kilic and AF. Altun, "Dynamic modelling and multi-objective optimization of off-grid hybrid energy systems by using battery or hydrogen storage for different climates," *International Journal of Hydrogen Energy*, 2022.

[162] S. D. Downing and DF. Socie, "Simple rainflow counting algorithms," *International journal of fatigue*, vol. 4, no. 1, pp. 31–40, 1982.

[163] D. Fioriti, L. Pellegrino, G. Lutzemberger, E. Micolano, and D. Poli, "Optimal sizing of residential battery systems with multi-year dynamics and a novel rainflow-based model of storage degradation: An extensive Italian case study," *Electric Power Systems Research*, vol. 203, p. 107675, Feb. 2022.

[164] P. Ayuso, H. Beltran, J. Segarra-Tamarit, and E. Pérez, "Optimized profitability of LFP and NMC Li-ion batteries in residential PV applications," *Mathematics and Computers in Simulation*, vol. 183, pp. 97–115, 2021.

[165] M. Kassem, J. Bernard, R. Revel, S. Pelissier, F. Duclaud, and C. Delacourt, "Calendar aging of a graphite/LiFePO4 cell," *Journal of Power Sources*, vol. 208, pp. 296–305, 2012.

[166] M. Chawla, R. Naik, R. Burra, and H. Wiegman, "Utility energy storage life degradation estimation method," in *2010 IEEE Conference on Innovative Technologies for an Efficient and Reliable Electricity Supply*. IEEE, 2010, pp. 302–308.

[167] S. Mishra, M. Pecht, T. Smith, I. McNee, and R. Harris, "Remaining life prediction of electronic products using life consumption monitoring approach," in *Proceedings of the European Microelectronics Packaging and Interconnection Symposium*. n. June, 2002, pp. 136–142.

[168] R. Dufo-Lopez and J. L. Bernal-Agustín, "Multi-objective design of PV–wind–diesel–hydrogen–battery systems," *Renewable energy*, vol. 33, no. 12, pp. 2559–2572, 2008.

[169] R. Spotnitz, "Simulation of capacity fade in lithium-ion batteries," *Journal of power sources*, vol. 113, no. 1, pp. 72–80, 2003.

[170] X. Han, M. Ouyang, L. Lu, J. Li, Y. Zheng, and Z. Li, "A comparative study of commercial lithium ion battery cycle life in electrical vehicle: Aging mechanism identification," *Journal of Power Sources*, vol. 251, pp. 38–54, 2014.

[171] HJ. Santner, K.-C. Möller, J. Ivančo, MG. Ramsey, F. P. Netzer, S. Yamaguchi, JO. Besenhard, and M. Winter, "Acrylic acid nitrile, a film-forming electrolyte component for lithium-ion batteries, which belongs to the family of additives containing vinyl groups," *Journal of power sources*, vol. 119, pp. 368–372, 2003.

[172] MC. Smart, BV. Ratnakumar, VS. Ryan-Mowrey, S. Surampudi, GKS. Prakash, J. Hu, and I. Cheung, "Improved performance of lithium-ion cells with the use of fluorinated carbonate-based electrolytes," *Journal of power sources*, vol. 119, pp. 359–367, 2003.

[173] S. S. Choi and H. S. Lim, "Factors that affect cycle-life and possible degradation mechanisms of a Li-ion cell based on LiCoO2," *Journal of Power Sources*, vol. 111, no. 1, pp. 130–136, 2002.

[174] P. Novák, F. Joho, M. Lanz, B. Rykart, J.-C. Panitz, D. Alliata, R. Kötz, and O. Haas, "The complex electrochemistry of graphite electrodes in lithium-ion batteries," *Journal of power sources*, vol. 97, pp. 39–46, 2001.

[175] I. Renewables, "Public Report 12 (Final Report) Lithium-ion Battery Testing."

[176] M. Rastegar, M. Fotuhi-Firuzabad, and H. Zareipour, "Home energy management incorporating operational priority of appliances," *International Journal of Electrical Power & Energy Systems*, vol. 74, pp. 286–292, 2016.

[177] G. Koutitas, "Control of flexible smart devices in the smart grid," *IEEE Transactions on Smart Grid*, vol. 3, no. 3, pp. 1333–1343, 2012.

[178] A. A. Khan, S. Razzaq, A. Khan, and F. Khursheed, "HEMSs and enabled demand response in electricity market: An overview," *Renewable and Sustainable Energy Reviews*, vol. 42, pp. 773–785, 2015.

[179] M. S. Ahmed, A. Mohamed, T. Khatib, H. Shareef, R. Z. Homod, and J. A. Ali, "Real time optimal schedule controller for home energy management system using new binary backtracking search algorithm," *Energy and Buildings*, vol. 138, pp. 215–227, Mar. 2017.

[180] T. AlSkaif, A. C. Luna, M. G. Zapata, J. M. Guerrero, and B. Bellalta, "Reputation-based joint scheduling of households appliances and storage in a microgrid with a shared battery," *Energy and Buildings*, vol. 138, pp. 228–239, Mar. 2017.

[181] E. Shirazi and S. Jadid, "Optimal residential appliance scheduling under dynamic pricing scheme via HEMDAS," *Energy and Buildings*, vol. 93, pp. 40–49, Apr. 2015.

[182] G. Carpinelli, F. Mottola, and D. Proto, "Probabilistic sizing of battery energy storage when time-of-use pricing is applied," *Electric Power Systems Research*, vol. 141, pp. 73–83, 2016.

[183] J. S. Anagnostopoulos and D. E. Papantonis, "Pumping station design for a pumped-storage wind-hydro power plant," *Energy Conversion and Management*, vol. 48, no. 11, pp. 3009–3017, 2007.

[184] O. Erdinc and M. Uzunoglu, "Optimum design of hybrid renewable energy systems: Overview of different approaches," *Renewable and Sustainable Energy Reviews*, vol. 16, no. 3, pp. 1412–1425, 2012.

[185] H. Yang, Z. Wei, and L. Chengzhi, "Optimal design and techno-economic analysis of a hybrid solar–wind power generation system," *Applied Energy*, vol. 86, no. 2, pp. 163–169, Feb. 2009.

[186] H. Shareef, E. Al-Hassan, and R. Sirjani, "Wireless Home Energy Management System with Smart Rule-Based Controller," *Applied Sciences*, vol. 10, no. 13, p. 4533, Jan. 2020.

[187] K. Garifi, K. Baker, B. Touri, and D. Christensen, "Stochastic Model Predictive Control for Demand Response in a Home Energy Management System," in *2018 IEEE Power & Energy Society General Meeting (PESGM)*, Aug. 2018, pp. 1–5.

[188] S.-Y. Chen and C.-H. Chang, "Optimal Power Flows Control for Home Energy Management With Renewable Energy and Energy Storage Systems," *IEEE Transactions on Energy Conversion*, vol. 38, no. 1, pp. 218–229, Mar. 2023.

[189] I. Hussain, M. Ullah, I. Ullah, A. Bibi, M. Naeem, M. Singh, and D. Singh, "Optimizing Energy Consumption in the Home Energy Management System via a Bio-Inspired Dragonfly Algorithm and the Genetic Algorithm," *Electronics*, vol. 9, no. 3, p. 406, Mar. 2020.

[190] M. Talha, M. S. Saeed, G. Mohiuddin, M. Ahmad, M. J. Nazar, and N. Javaid, "Energy Optimization in Home Energy Management System Using Artificial Fish Swarm Algorithm and Genetic Algorithm," in *Advances in Intelligent Networking and Collaborative Systems*, ser. Lecture Notes on Data Engineering and Communications Technologies, L. Barolli, I. Woungang, and O. K. Hussain, Eds. Cham: Springer International Publishing, 2018, pp. 203–213.

[191] I. Richardson and M. Thomson, "Domestic electricity demand model-simulation example," 2010.

[192] "Average Household Gas and Electricity Usage — UKPower," https://www.ukpower.co.uk/home_energy/average-household-gas-and-electricity-usage.

[193] "PVOutput," https://pvoutput.org/.

[194] G. Riley, "Time of Use Tariffs: Saving the UK Grid?" https://blog.spiritenergy.co.uk/homeowner/time-of-use-tariffs-uk.

[195] "Feed-in tariffs in the United Kingdom," *Wikipedia*, Aug. 2023.

[196] "Capacity Market auction parameters: Letters from BEIS to National Grid ESO, July 2019," https://www.gov.uk/government/publications/capacity-market-auction-parameters-letter-from-beis-to-national-grid-eso-july-2019.

[197] Facebook, Twitter, Print, Whatsapp, and Mailme, "Green Energy launches 'time-of-day' tariff – elec-

tricity savings available but gas remains pricey," https://www.moneysavingexpert.com/news/2017/01/green-energy-launches-time-of-day-tariff—electricity-savings-available-but-gas-remains-pricey/.

[198] "Limejump secures the majority of the fully Dynamic Volume awarded in the January month ahead tender, continuing their dominant trend in FFR Auctions," Jan. 2019.

[199] C. Heymans, S. B. Walker, S. B. Young, and M. Fowler, "Economic analysis of second use electric vehicle batteries for residential energy storage and load-levelling," *Energy Policy*, vol. 71, pp. 22–30, Aug. 2014.

[200] E. McKenna, M. Krawczynski, and M. Thomson, "Four-state domestic building occupancy model for energy demand simulations," *Energy and Buildings*, vol. 96, pp. 30–39, Jun. 2015.

[201] B. Abushakra, J. S. Haberl, and D. E. Claridge, "Overview of Existing Literature on Diversity Factors and Schedules for Energy and Cooling Load Calculations." *ASHRAE transactions*, vol. 110, no. 1, 2004.

[202] A. Andrew, S. Cattan, M. C. Dias, C. Farquharson, L. Kraftman, S. Krutikova, A. Phimister, and A. Sevilla, "The gendered division of paid and domestic work under lockdown," *Fiscal Studies*, vol. n/a, no. n/a.

[203] S. D'oca, V. Fabi, S. P. Corgnati, and R. K. Andersen, "Effect of thermostat and window opening occupant behavior models on energy use in homes," in *Building Simulation*, vol. 7. Springer, 2014, pp. 683–694.

[204] U. Wilke, F. Haldi, J.-L. Scartezzini, and D. Robinson, "A bottom-up stochastic model to predict building occupants' time-dependent activities," *Building and Environment*, vol. 60, pp. 254–264, 2013.

[205] M. A. Halverson, M. I. Rosenberg, P. R. Hart, E. E. Richman, R. A. Athalye, and D. W. Winiarski, "ANSI/ASHRAE/IES Standard 90.1-2013 Determination of Energy Savings: Qualitative Analysis," Pacific Northwest National Lab.(PNNL), Richland, WA (United States), Tech. Rep., 2014.

[206] P. Kräuchi, C. Dahinden, D. Jurt, V. Wouters, U.-P. Menti, and O. Steiger, "Electricity consumption of building automation," *Energy Procedia*, vol. 122, pp. 295–300, 2017.

[207] T. Buso, V. Fabi, R. K. Andersen, and S. P. Corgnati, "Occupant behaviour and robustness of building design," *Building and Environment*, vol. 94, pp. 694–703, 2015.

[208] A. Mahdavi and F. Tahmasebi, "Predicting people's presence in buildings: An empirically based model performance analysis," *Energy and Buildings*, vol. 86, pp. 349–355, 2015.

[209] MA. López-Rodríguez, I. Santiago, D. Trillo-Montero, J. Torriti, and A. Moreno-Munoz, "Analysis and modeling of active occupancy of the residential sector in Spain: An indicator of residential electricity consumption," *Energy Policy*, vol. 62, pp. 742–751, 2013.

[210] J. Widén, A. M. Nilsson, and E. Wäckelgård, "A combined Markov-chain and bottom-up approach to modelling of domestic lighting demand," *Energy and Buildings*, vol. 41, no. 10, pp. 1001–1012, 2009.

[211] J. Widén and E. Wäckelgård, "A high-resolution stochastic model of domestic activity patterns and electricity demand," *Applied energy*, vol. 87, no. 6, pp. 1880–1892, 2010.

[212] F. Tahmasebi and A. Mahdavi, "The sensitivity of building performance simulation results to the choice of occupants' presence models: A case study," *Journal of Building Performance Simulation*, vol. 10, no. 5-6, pp. 625–635, 2017.

[213] "CREST Demand Model," Sep. 2015.

[214] "UK Data Service Series," https://beta.ukdataservice.ac.uk/datacatalogue/series/serie

[215] H. H. Eldeeb, S. Faddel, and O. A. Mohammed, "Multi-objective optimization technique for the operation of grid tied PV powered EV charging station," *Electric Power Systems Research*, vol. 164, pp. 201–211, 2018.

[216] X. Hao, P. Wei, and K. Li, "Multi-objective optimization scheduling method for active distribution network with large scale electric vehicles," *Transactions of China Electrotechnical Society*, vol. 32, no. S2, pp. 179–189, 2017.

[217] S. Yang, M. Wu, X. Yao, and J. Jiang, "Load modeling and identification based on ant colony algorithms for EV charging stations," *IEEE Transactions on Power Systems*, vol. 30, no. 4, pp. 1997–2003, 2014.

[218] J. Zheng, X. Wang, K. Men, C. Zhu, and S. Zhu, "Aggregation model-based optimization for electric vehicle charging strategy," *IEEE Transactions on Smart Grid*, vol. 4, no. 2, pp. 1058–1066, 2013.

[219] C. Moreira, J. P. Lopes, P. R. Almeida, L. Seca, and F. J. Soares, "A STOCHASTIC MODEL TO SIMULATE ELECTRIC VEHICLES

MOTION AND QUANTIFY THE ENERGY REQUIRED FROM THE GRID," 2011.

[220] P. A. Gagniuc, *Markov Chains: From Theory to Implementation and Experimentation*. John Wiley & Sons, 2017.

[221] E. B. Iversen, J. K. Møller, J. M. Morales, and H. Madsen, "Inhomogeneous Markov Models for Describing Driving Patterns," *IEEE Transactions on Smart Grid*, vol. 8, no. 2, pp. 581–588, Mar. 2017.

[222] A. Lojowska, D. Kurowicka, G. Papaefthymiou, and L. van der Sluis, "Stochastic Modeling of Power Demand Due to EVs Using Copula," *IEEE Transactions on Power Systems*, vol. 27, no. 4, pp. 1960–1968, Nov. 2012.

[223] A. Santos, N. McGuckin, H. Y. Nakamoto, D. Gray, and S. Liss, "Summary of travel trends: 2009 national household travel survey," United States. Federal Highway Administration, Tech. Rep., 2011.

[224] "2021 Nissan LEAF Specs & Prices — Nissan USA," https://www.nissanusa.com/vehicles/electric-cars/leaf/specs/compare-specs.html.

[225] "How much electricity does a car use per mile?" https://www.mina.co.uk/ev-knowledge-hub/how-much-electricity-does-a-car-use-per-mile, Jul. 2023.

[226] WBC. WBCSD, "Energy efficiency in buildings: Transforming the market," 2009.

[227] S. Somasundaram, RG. Pratt, BA. Akyol, N. Fernandez, N. Foster, S. Katipamula, E. Mayhorn, A. Somani, A. Steckley, and Z. Taylor, "Reference guide for a transaction-based building controls framework," *Pacific Northwest National Laboratory*, 2014.

[228] R. V. Jones, A. Fuertes, C. Boomsma, and S. Pahl, "Space heating preferences in UK social housing: A socio-technical household survey combined with building audits," *Energy and Buildings*, vol. 127, pp. 382–398, Sep. 2016.

[229] H. Lund, S. Werner, R. Wiltshire, S. Svendsen, J. E. Thorsen, F. Hvelplund, and B. V. Mathiesen, "4th Generation District Heating (4GDH): Integrating smart thermal grids into future sustainable energy systems," *Energy*, vol. 68, pp. 1–11, Apr. 2014.

[230] D. Fischer and H. Madani, "On heat pumps in smart grids: A review," *Renewable and Sustainable Energy Reviews*, vol. 70, pp. 342–357, Apr. 2017.

[231] E. Atam and L. Helsen, "Ground-coupled heat pumps: Part 1 – Literature review and research challenges in modeling and optimal control," *Renewable and Sustainable Energy Reviews*, vol. 54, pp. 1653–1667, Feb. 2016.

[232] P. Carroll, M. Chesser, and P. Lyons, "Air Source Heat Pumps field studies: A systematic literature review," *Renewable and Sustainable Energy Reviews*, vol. 134, p. 110275, Dec. 2020.

[233] L. Pérez-Lombard, J. Ortiz, and C. Pout, "A review on buildings energy consumption information," *Energy and buildings*, vol. 40, no. 3, pp. 394–398, 2008.

[234] ES. Trust, "Measurement of domestic hot water consumption in dwellings," *Energy Sav Trust*, 2008.

[235] L. D. Harvey, *A Handbook on Low-Energy Buildings and District-Energy Systems: Fundamentals, Techniques and Examples*. Routledge, 2012.

[236] E. Fuentes, L. Arce, and J. Salom, "A review of domestic hot water consumption profiles for application in systems and buildings energy performance analysis," *Renewable and Sustainable Energy Reviews*, vol. 81, pp. 1530–1547, Jan. 2018.

[237] S. Kammila, J. F. Kappen, D. Rysankova, B. Hyseni, and V. R. Putti, "Clean and improved cooking in Sub-Saharan Africa: A landscape report," The World Bank, Tech. Rep., 2014.

[238] V. R. Putti, M. Tsan, S. Mehta, and S. Kammila, "The state of the global clean and improved cooking sector," 2015.

[239] Energy Sector Management Assistance Program, *The State of Access to Modern Energy Cooking Services*. World Bank, 2020.

[240] M. Shupler, M. O'Keefe, E. Puzzolo, E. Nix, R. A. de Cuevas, J. Mwitari, A. Gohole, E. Sang, I. Čukić, and D. Menya, "Pay-as-you-go liquefied petroleum gas supports sustainable clean cooking in Kenyan informal urban settlement during COVID-19 lockdown," *Applied energy*, vol. 292, p. 116769, 2021.

[241] X. Xu and S. Wang, "A simplified dynamic model for existing buildings using CTF and thermal network models," *International Journal of Thermal Sciences*, vol. 47, no. 9, pp. 1249–1262, 2008.

[242] X. Q. Li, Y. Chen, JD. Spitler, and D. Fisher, "Applicability of calculation methods for conduction transfer function of building constructions," *International Journal of Thermal Sciences*, vol. 48, no. 7, pp. 1441–1451, 2009.

[243] A. Aliberti, F. M. Ugliotti, L. Bottaccioli, G. Cirrincione, A. Osello, E. Macii, E. Patti, and A. Acquaviva, "Indoor air-temperature forecast for energy-efficient management in smart buildings," in *2018*

IEEE International Conference on Environment and Electrical Engineering and 2018 IEEE Industrial and Commercial Power Systems Europe (EEEIC/I&CPS Europe). IEEE, 2018, pp. 1–6.

[244] L. Mba, P. Meukam, and A. Kemajou, "Application of artificial neural network for predicting hourly indoor air temperature and relative humidity in modern building in humid region," *Energy and Buildings*, vol. 121, pp. 32–42, 2016.

[245] P. Bacher and H. Madsen, "Identifying suitable models for the heat dynamics of buildings," *Energy and Buildings*, vol. 43, no. 7, pp. 1511–1522, Jul. 2011.

[246] H. Harb, N. Boyanov, L. Hernandez, R. Streblow, and D. Müller, "Development and validation of grey-box models for forecasting the thermal response of occupied buildings," *Energy and Buildings*, vol. 117, pp. 199–207, Apr. 2016.

[247] M. Hu, F. Xiao, and L. Wang, "Investigation of demand response potentials of residential air conditioners in smart grids using grey-box room thermal model," *Applied Energy*, vol. 207, pp. 324–335, Dec. 2017.

[248] P. Bacher and H. Madsen, "Identifying suitable models for the heat dynamics of buildings," *Energy and Buildings*, vol. 43, no. 7, pp. 1511–1522, 2011.

[249] E. P. Del Barrio, G. Lefebvre, P. Behar, and N. Bailly, "Using model size reduction techniques for thermal control applications in buildings," *Energy and Buildings*, vol. 33, no. 1, pp. 1–14, 2000.

[250] S. F. Fux, A. Ashouri, M. J. Benz, and L. Guzzella, "EKF based self-adaptive thermal model for a passive house," *Energy and Buildings*, vol. 68, pp. 811–817, Jan. 2014.

[251] "Sie suchten nach FSR61VA Eltako."

[252] "FHEM for Debian," https://debian.fhem.de/.

[253] "EnOcean – Sustainable IoT Solutions," https://www.enocean.com/en/.

[254] "Parameter estimation for grey-box models of building thermal behaviour," *Energy and Buildings*, vol. 169, pp. 58–68, Jun. 2018.

[255] E. G. UK, "Appliance Running Costs UK - How Much Electricity Do You Use?" Sep. 2022.

[256] C. P. Underwood, "14 - Heat pump modelling," in *Advances in Ground-Source Heat Pump Systems*, S. J. Rees, Ed. Woodhead Publishing, Jan. 2016, pp. 387–421.

[257] I. Sarbu and C. Sebarchievici, "General review of ground-source heat pump systems for heating and cooling of buildings," *Energy and Buildings*, vol. 70, pp. 441–454, Feb. 2014.

[258] M. R. Ally, J. D. Munk, V. D. Baxter, and A. C. Gehl, "Exergy and energy analysis of a ground-source heat pump for domestic water heating under simulated occupancy conditions," *International Journal of Refrigeration*, vol. 36, no. 5, pp. 1417–1430, Aug. 2013.

[259] "Ground-source heat pumps systems and applications," *Renewable and Sustainable Energy Reviews*, vol. 12, no. 2, pp. 344–371, Feb. 2008.

[260] A. Priarone, F. Silenzi, and M. Fossa, "Modelling Heat Pumps with Variable EER and COP in EnergyPlus: A Case Study Applied to Ground Source and Heat Recovery Heat Pump Systems," *Energies*, vol. 13, no. 4, p. 794, Jan. 2020.

[261] A. R. Puttige, S. Andersson, R. Östin, and T. Olofsson, "Application of Regression and ANN Models for Heat Pumps with Field Measurements," *Energies*, vol. 14, no. 6, p. 1750, Jan. 2021.

[262] E. Wang, A. S. Fung, C. Qi, and W. H. Leong, "Performance prediction of a hybrid solar ground-source heat pump system," *Energy and Buildings*, vol. 47, pp. 600–611, Apr. 2012.

[263] "European High Performance Climate Solutions Expert — CIAT UK," https://www.ciat.com/en/uk/.

[264] "Handbook," https://www.ashrae.org/technical-resources/ashrae-handbook.

[265] US. DOE, "Uniform Test Method for Measuring the Energy Consumption of Electric Refrigerators and Electric Refrigerator-Freezers," *US Department of Energy, Washington, DC, Report*, no. 430, 2011.

[266] T. M. Mata and C. A. V. Costa, "Life cycle assessment of different reuse percentages for glass beer bottles," *The International Journal of Life Cycle Assessment*, vol. 6, no. 5, pp. 307–319, Sep. 2001.

[267] J. Widén, M. Lundh, I. Vassileva, E. Dahlquist, K. Ellegård, and E. Wäckelgård, "Constructing load profiles for household electricity and hot water from time-use data—Modelling approach and validation," *Energy and buildings*, vol. 41, no. 7, pp. 753–768, 2009.

[268] H. Benli, "Potential application of solar water heaters for hot water production in Turkey," *Renewable and Sustainable Energy Reviews*, vol. 54, pp. 99–109, Feb. 2016.

[269] L. Gelažanskas and K. A. Gamage, "Forecasting hot water consumption in residential houses," *Energies*, vol. 8, no. 11, pp. 12 702–12 717, 2015.

[270] C. Bennett, R. A. Stewart, and C. D. Beal, "ANN-based residential water end-use demand forecasting model," *Expert systems with applications*, vol. 40, no. 4, pp. 1014–1023, 2013.

[271] R. McKenna, L. Hofmann, M. Kleinebrahm, and W. Fichtner, "A stochastic multi-energy simulation model for UK residential buildings," *Energy and Buildings*, vol. 168, pp. 470–489, Jun. 2018.

[272] "Harmonised European Time Use Survey - Access to microdata - Eurostat," https://ec.europa.eu/eurostat/web/microdata/time-use-survey.

[273] U. Jordan and K. Vajen, "Realistic domestic hot-water profiles in different time scales," *Report for IEA-SHC Task*, vol. 26, 2001.

[274] B. Hendron, J. Burch, and G. Barker, "Tool for generating realistic residential hot water event schedules," National Renewable Energy Lab.(NREL), Golden, CO (United States), Tech. Rep., 2010.

[275] D. Fischer, T. Wolf, J. Scherer, and B. Wille-Haussmann, "A stochastic bottom-up model for space heating and domestic hot water load profiles for German households," *Energy and Buildings*, vol. 124, pp. 120–128, Jul. 2016.

[276] "Energy Use & Cost to Run an Electric Water Heater — Perch Energy," https://www.perchenergy.com/energy-calculators/water-heater-electricity-usage-cost.

[277] "Measurement of domestic hot water consumption in dwellings," https://www.gov.uk/government/publications/measurement-of-domestic-hot-water-consumption-in-dwellings.

[278] "Household Electricity Survey," https://www.gov.uk/government/publications/household-electricity-survey–2.

[279] "U.S. time spent cooking 2019," https://www.statista.com/statistics/1085305/time-spent-cooking-weeknight-in-the-us/.

[280] "Kitchen Appliance Lifespan," https://www.magnet.co.uk/news/kitchen-appliance-lifespan/.

[281] "Energy Follow Up Survey (EFUS) 2017 reports," https://www.gov.uk/government/publications/energy-follow-up-survey-efus-2017-reports.

[282] M. H. J. Weck, J. van Hooff, and W. G. J. H. M. van Sark, "Review of barriers to the introduction of residential demand response: A case study in the Netherlands," *International Journal of Energy Research*, vol. 41, no. 6, pp. 790–816, May 2017.

[283] A. Mustafa Omer, "Ground-source heat pumps systems and applications," *Renewable and Sustainable Energy Reviews*, vol. 12, no. 2, pp. 344–371, Feb. 2008.

[284] T. Sivasakthivel, K. Murugesan, and P. K. Sahoo, "A study on energy and CO2 saving potential of ground source heat pump system in

India," *Renewable and Sustainable Energy Reviews*, vol. 32, pp. 278–293, Apr. 2014.

[285] G. Besagni and M. Borgarello, "The determinants of residential energy expenditure in Italy," *Energy*, vol. 165, pp. 369–386, Dec. 2018.

[286] S. Copiello and C. Grillenzoni, "Is the cold the only reason why we heat our homes? Empirical evidence from spatial series data," *Applied Energy*, vol. 193, pp. 491–506, May 2017.

[287] J. Wang, J. Liu, C. Li, Y. Zhou, and J. Wu, "Optimal scheduling of gas and electricity consumption in a smart home with a hybrid gas boiler and electric heating system," *Energy*, vol. 204, p. 117951, Aug. 2020.

[288] J. Wu, L. Cheng, Y. Lu, and L. Song, "Life cycle inventory analysis of clean alternatives to scattered coal heating." *China Environmental Science*, vol. 38, no. 4, pp. 1570–1578, 2018.

[289] J. Wang, J. Liu, C. Li, Y. Zhou, and J. Wu, "Optimal scheduling of gas and electricity consumption in a smart home with a hybrid gas boiler and electric heating system," *Energy*, vol. 204, p. 117951, Aug. 2020.

[290] "Quarterly Energy Prices," https://www.gov.uk/government/collections/quarterly-energy-prices, Sep. 2023.

[291] G. Huttrer, "Geothermal Power Generation in the World 2015-2020 Update Report," p. 17.

[292] "Gas Boiler cost data," http://2050-calculator-tool-wiki.decc.gov.uk/cost_categories/82.

[293] "Average UK gas and electricity prices per kWh unit — usave.co.uk," https://usave.co.uk/energy/average-uk-gas-and-electricity-prices-per-unit/.

[294] "What is the average annual gas and electricity bill – British Gas," https://www.britishgas.co.uk/energy/guides/average-energy-bill.html.

[295] "Carbon tracker — Bulb," https://bulb.co.uk/carbon-tracker/.

[296] "Greenhouse gas reporting: Conversion factors 2021," https://www.gov.uk/government/publications/greenhouse-gas-reporting-conversion-factors-2021.

[297] C. Breyer, S. Khalili, D. Bogdanov, M. Ram, A. S. Oyewo, A. Aghahosseini, A. Gulagi, A. A. Solomon, D. Keiner, G. Lopez, P. A. Østergaard, H. Lund, B. V. Mathiesen, M. Z. Jacobson, M. Victoria, S. Teske, T. Pregger, V. Fthenakis, M. Raugei, H. Holttinen, U. Bardi, A. Hoekstra, and B. K. Sovacool, "On the History and Future of 100% Renewable Energy Systems Research," *IEEE Access*, vol. 10, pp. 78 176–78 218, 2022.

[298] M. McPherson, E. Rhodes, L. Stanislaw, R. Arjmand, M. Saffari, R. Xu, C. Hoicka, and M. Esfahlani, "Modeling the transition to a zero emission energy system: A cross-sectoral review of building, transportation, and electricity system models in Canada," *Energy Reports*, vol. 9, pp. 4380–4400, Dec. 2023.

[299] "Design Visions for Future Energy Systems: Towards Aligning Developers' Assumptions and Householders' Expectations — Nordic Human-Computer Interaction Conference," https://dl.acm.org/doi/abs/10.1145/3546155.3546655?casa_to-

ken=tErvhihtKIUAAAAA:NA_pl_10WLLyaRoeIQk0HYA9uzxpfw8JmloGnPKfCkt5r
FKkX6gAo9aAU79mCmbSMekoKKbV1RNQ.

[300] L. Donaldson, "Floor Space in English Homes – main report."

[301] "Families and households in the UK - Office for National Statistics," https://www.ons.gov.uk/peoplepopulationandcommunity/birthsdeathsandmarriages/

[302] "How much electricity do solar panels produce? [UK, 2024]," https://www.sunsave.energy/solar-panels-advice/system-size/output.

[303] "Average gas and electricity use explained," https://www.ofgem.gov.uk/information-consumers/energy-advice-households/average-gas-and-electricity-use-explained.

[304] "Powerwall," https://www.tesla.com/powerwall.

[305] "Electric vehicles — Battery — Capacity and Lifespan," https://www.eonenergy.com/electric-vehicle-charging/running-costs-and-benefits/battery-capacity-and-lifespan.html.

[306] G. Bennett, S. Watson, G. Wilson, and T. Oreszczyn, "Domestic heating with compact combination hybrids (gas boiler and heat pump): A simple English stock model of different heating system scenarios," *Building Services Engineering Research and Technology*, vol. 43, no. 2, pp. 143–159, Mar. 2022.

[307] "Installing a gas cooker or hob costs in your area," https://www.hamuch.com/cost/connect-gas-hob.

[308] "Electric vs petrol car comparison and costs — British Gas," https://www.britishgas.co.uk/smart-home/guides/electric-vehicles/electric-vs-petrol.html.

[309] "Can induction hobs save you money?" https://www.trustedreviews.com/explainer/can-induction-hobs-save-you-money-4230890, May 2022.

[310] M. Moser, H.-C. Gils, and G. Pivaro, "A sensitivity analysis on large-scale electrical energy storage requirements in Europe under consideration of innovative storage technologies," *Journal of Cleaner Production*, vol. 269, p. 122261, Oct. 2020.

[311] R. A. Biroon, Z. A. Biron, and R. Hadidi, "Commercial Load Profile Sensitivity Analysis to Electricity Tariffs and Battery Characteristics," *IEEE Transactions on Industry Applications*, vol. 56, no. 2, pp. 1021–1030, Mar. 2020.

[312] H. Ren, W. Gao, and Y. Ruan, "Economic optimization and sensitivity analysis of photovoltaic system in residential buildings," *Renewable Energy*, vol. 34, no. 3, pp. 883–889, Mar. 2009.

[313] "Internal rate of return," *Wikipedia*, Jun. 2023.

[314] E. Romano, P. Negro, and F. Taucer, "Seismic performance assessment addressing sustainability and energy efficiency," *JRC Scientific and Policy Reports*, 2014.

[315] A. Akbarnezhad and J. Xiao, "Estimation and minimization of embodied carbon of buildings: A review," *Buildings*, vol. 7, no. 1, p. 5, 2017.

[316] "Kilogram of carbon dioxide equivalent per kilogram," https://www.wikidata.org/wiki/Q57084968.

[317] C. Favi, M. Germani, D. Landi, M. Mengarelli, and M. Rossi, "Comparative life cycle assessment of cooking appliances in Italian kitchens," *Journal of Cleaner Production*, vol. 186, pp. 430–449, 2018.

[318] A. Gallego-Schmid, J. M. F. Mendoza, H. K. Jeswani, and A. Azapagic, "Life cycle environmental impacts of vacuum cleaners and the effects of European regulation," *Science of the Total Environment*, vol. 559, pp. 192–203, 2016.

[319] D. Landi, A. Consolini, M. Germani, and C. Favi, "Comparative life cycle assessment of electric and gas ovens in the Italian context: An environmental and technical evaluation," *Journal of Cleaner Production*, vol. 221, pp. 189–201, 2019.

[320] G. Vignali, "Environmental assessment of domestic boilers: A comparison of condensing and traditional technology using life cycle assessment methodology," *Journal of Cleaner Production*, vol. 142, pp. 2493–2508, 2017.

[321] M. Gangolells, M. Casals, N. Forcada, M. Macarulla, and A. Giretti, "Environmental impacts related to the commissioning and usage phase of an intelligent energy management system," *Applied energy*, vol. 138, pp. 216–223, 2015.

[322] SS. Van Dam, CA. Bakker, and JC. Buiter, "Do home energy management systems make sense? Assessing their overall lifecycle impact," *Energy Policy*, vol. 63, pp. 398–407, 2013.

[323] C. Spreafico and D. Russo, "Assessing domestic environmental impacts through LCA using data from the scientific literature," *Journal of Cleaner Production*, vol. 266, p. 121883, Sep. 2020.

[324] J.-N. Louis and E. Pongrácz, "Life cycle impact assessment of home energy management systems (HEMS) using dynamic emissions factors for electricity in Finland," *Environmental Impact Assessment Review*, vol. 67, pp. 109–116, Nov. 2017.

[325] N. Shibata, F. Sierra, and A. Hagras, "Integration of LCA and LCCA through BIM for optimized decision-making when switching from gas to electricity services in dwellings," *Energy and Buildings*, vol. 288, p. 113000, Jun. 2023.

[326] R. G. Raluy and A. C. Dias, "Life cycle assessment of a domestic gas-fired water heater: Influence of fuel used and its origin," *Journal of Environmental Management*, vol. 254, p. 109786, Jan. 2020.

[327] "Car longevity," *Wikipedia*, Mar. 2023.

[328] S. Franzò and A. Nasca, "The environmental impact of electric vehicles: A comparative LCA-based evaluation framework and its application to the Italian context," in *2020 Fifteenth International Conference on Ecological Vehicles and Renewable Energies (EVER)*, Sep. 2020, pp. 1–4.

[329] P. Wolfram and T. Wiedmann, "Electrifying Australian transport: Hybrid life cycle analysis of a transition to electric light-duty vehicles and renewable electricity," *Applied Energy*, vol. 206, pp. 531–540, Nov. 2017.

[330] M. Smith, A. Bevacqua, S. Tembe, and P. Lal, "Life cycle analysis (LCA) of residential ground source heat pump systems: A comparative analysis of energy efficiency in New Jersey," *Sustainable Energy Technologies and Assessments*, vol. 47, p. 101364, Oct. 2021.

[331] C. Ju, "Hierarchically Coordinated Energy Management for A Regional Multi-microgrid Community," Feb. 2021.

[332] M. Elkazaz, "Hierarchical energy management system for controlling distributed energy resources in a community microgrid," https://eprints.nottingham.ac.uk/66176/, Dec. 2021.

[333] "How Much Do Solar Panels Cost? UK Installation Prices 2023," https://heatable.co.uk/solar-advice/solar-panel-costs.

[334] "What would be the annual maintenance cost for a solar PV system?"